BOEM 2019-053

ANIMIDA III Boulder Patch and Other Kelp Communities in Development Area
Final Report

Prepared By:
Kenneth H. Dunton, Principal Investigator
University of Texas Marine Science Institute
750 Channel View Drive, Port Aransas, Texas 78373
e-mail of corresponding author: ken.dunton@utexas.edu

Authors:

Kenneth H. Dunton[1], Christina E. Bonsell[1], Katrin Iken[2], Brenda Konar[2], Arley F. Muth[1], and Susan V. Schonberg[1]
[1]University of Texas Marine Science Institute
[2]University of Alaska Fairbanks

Prepared For:

Cathy Coon
Chief, Environmental Sciences Management
Alaska Office Bureau of Ocean Energy Management
3801 Centerpoint Drive, Suite 500
Anchorage, Alaska 99503

Cooperative Agreement No. M12AC00007
15 January 2020

Table of Contents

Acknowledgements

This study was funded by the U.S. Department of Interior, Bureau of Ocean Energy and Management (BOEM), Alaska Outer Continental Shelf Region, Anchorage, Alaska under BOEM Cooperative Agreement No. M12AC00007. The studies of the Boulder Patch have benefited greatly from BOEM support. We are deeply grateful to Dick Prentki, our former Project Officer (PO) who launched the ANIMIDA III Boulder Patch program before his retirement in 2012. Cathy Coon followed as PO with the same level of enthusiasm and dedicated support. Despite her promotion to a leadership role at BOEM during this project, she always made time in her busy schedule to continue providing critical guidance. Cathy was especially receptive to our logistic requests and assisted with our outreach activities at Kaktovik. We thank John and Ted Dunton, the crew of the *R/V Proteus*, who in addition to providing a safe and reliable diving platform, helped design and fabricate equipment for deployment and assisted with every aspect of our field work. Tim Whiteaker (University of Texas at Austin) assisted with the creation and maintenance of a dedicated Boulder Patch web site that is linked to our BOEM work in the western Arctic. Finally, special thanks to Arley Muth and Susan V. Schonberg who handled the giant task of extracting chapters from all of us and organizing this eight-chapter final report.

Executive Summary

Arley F. Muth, Christina E. Bonsell and Kenneth H. Dunton

In the nearshore Alaskan Beaufort Sea, discrete, isolated rocky habitats harbor biological communities that are unusually diverse for the region, with markedly different fauna and flora than found in the surrounding soft sediment areas. The boulder fields also support tightly linked food webs, with connections to higher trophic levels such as fishes and seals. These systems are highly vulnerable to disturbances, including sedimentation from human activities and coastal erosion, fluctuations in salinity from seasonal river discharge, and temperature increases from heat influx originating at lower latitudes and from atmospheric warming. Spatial isolation of these boulder fields and the slow development of benthic communities, limit ecosystem recovery from disturbance. To assess the possible ecological effects of such environmental disturbances, this field program undertook an investigation of the biological communities and environmental conditions across the Boulder Patch, the largest of the Beaufort Sea nearshore boulder fields.

The overlying objectives of this program were to: 1) monitor incident and in situ photosynthetically active radiation (PAR), salinity, temperature, currents, and pH to define the spatial variability in annual kelp productivity and biomass; 2) characterize benthic community structure changes across environmental gradients in the Boulder Patch and 3) collect annual measurements of kelp growth in the Boulder Patch to provide a nearly continuous record of kelp growth since 1977. Within and in addition to these objectives, individual research projects were completed, using experimental approaches, genetic analysis and historical data to gain an in depth understanding of mechanisms (past and present) that resulted in the Boulder Patch community we see today and how this community may vary in future conditions. This report is composed of eight chapters. The first three chapters focus on the larger scale setting of the Boulder Patch, building on the earlier work conducted by Dunton, Iken, Konar and Schonberg. The second five chapters address specific and directed experimental and observational studies that were performed by UT-Austin Ph.D. students Christina Bonsell and Arley Muth. Our combined effort work reveals that the Boulder Patch remains a dynamic, productive, biologically diverse environment within Stefansson Sound well after its initial discovery over 50 years ago. Seasonal environmental fluctuations, particularly of salinity and light levels, create the current spatial species distributions. Through long-term observations, benthic monitoring and experimental work, we continue to better understand how environmental factors shape this ecosystem and it may respond to changes associated with regional climate warming.

BACKGROUND AND SETTING

1. Seasonality and change near the mouth of an Arctic river: Environmental variability in Stefansson Sound, Alaska

On Arctic inner shelves, seasonal spatial gradients in abiotic conditions caused by bathymetry and distance from freshwater inputs influence biological characteristics and biogeochemical processes. Spatial variations were examined in near-benthic temperature, salinity, currents, pH and light over seasonal and annual timescales (2011-2017) in Stefansson Sound, a shallow embayment (<15 m) at the mouth of the Sagavanirktok River on the North Slope of Alaska. Stable temperature and salinity conditions prevailed in the study area throughout the winter (-1.9 to -1.8^{o}C, salinity 33-35). However, spatial abiotic differences developed from May-October. During these months, temperature and salinity exhibited strong cross-shelf gradients, especially in June-September when nearshore sites reached 6^{o}C or more and exhibited salinities below 20, while offshore sites averaged 2^{o}C and salinities of 28-29. Under the cover of landfast ice and coincident with the spring freshet, coastal waters near the mouth of the Sagavanirktok River experienced salinities below 10 at 4 m depths in one of the sampled years. Currents are generally alongshore and bi-directional from November-May, but flow direction becomes wind-driven and variable following ice break-up. In all seasons, currents were faster and more variable at sites adjacent to deep, inter-island passes, reflecting influence by strong offshore currents. Underwater light levels were highest in July and August, but extremely variable in space and time (0.0-12.6 mol photon m^{-2} day^{-1}) in response to wind-driven resuspension events. The timing of ice break-up appears to determine mean annual conditions, as it separates the cold, dark, high salinity, low variance winter from the warmer, fresher, high variance summer. These measurements imply that a considerable portion of the benthos is regularly exposed to low salinity conditions before the beginning of ice break-up. Our results reinforce the estuarine nature of Arctic nearshore systems and provides the hydrographic setting that determines the strong seasonal nature of the coupled benthic and pelagic ecosystem of the Beaufort Sea.

2. Spatial and temporal trends in community composition in the Arctic Boulder Patch

Epilithic communities were investigated over four study years, 2005, 2006, 2013, and 2015, at seven locations across the Boulder Patch. Macroalgal biomass overwhelmed invertebrate biomass throughout all sampling years and locations. Macroalgal biomass was consistently dominated by four species: the kelp *Laminaria solidungula* and the red algae *Phycodrys* sp., *Coccotylus truncatus* and *Dilsea* sp. These species (along with *Rhodomela*, which is frequent but has low biomass owing to its filamentous morphology) are common in the Arctic and are prominent in the Boulder Patch (Dunton et al., 1982). A comparison of the biomass of these four genera between 1978-80 at site DS-11 and this study yielded similar patterns in abundance over a span of nearly 40 years. Biomass values in this study ranged from 162 g m^{-2} for *L. solidungula*, to 51 g m^{-2} for *Phycodrys*, 42 g m^{-2} for *C. truncates*, and

25 g m^{-2} for *Dilsea*. Dunton et al. (1982) reported biomass values for these same genera as 262 g m^{-2}, 45 g m^{-2}, 33 g m^{-2}, and 31 g m^{-2}, respectively. In this study, overall biomass varied greatly across sites and years, although relatively high biomass consistently occurred at sites DS11 and W3, indicating dependably favorable algal growth conditions. At DS-11, We observed overall slightly lower algal biomass and changes in composition in 2013, which was also reflected in higher dispersion in community structure in that year at some sites, possibly in response to a disturbance. Macroalgal biomass was positively correlated, although not significantly, with invertebrate biomass, which also varied across sites and years. Invertebrate biomass was consistently dominated by sponges, bryozoans, and hydrozoans, which matches patterns from the late 1970s. Bryozoans and hydroids are typical Arctic coastal community components, but sponges seem to be more unique to the Boulder Patch, where they act as dominant space competitors. Distinct differences in invertebrate community composition in 2013 matched observations for the macroalgal communities, emphasizing potential disturbances in that year. Temporal differences were driven by small and mobile species such as amphipods and polychaetes, which are fast to respond to changes in environmental conditions.

Patterns in epilithic communities were compared with those in Camden Bay to the east, sampled in 2005, 2007, and 2017. The main macroalgal taxa in Camden Bay were relatively like those in the Boulder Patch but invertebrate taxa differed considerably, with significant differences in both assemblage types between the two regions. Overall average algal biomass was higher in Camden Bay while overall average invertebrate biomass was higher in the Boulder Patch. Invertebrate composition in Camden Bay was dominated by a few highly abundant taxa within the crustaceans and mollusks, but some groups regularly occurring in the Boulder Patch, such as echinoderms, decapods, and chitons, were completely absent in Camden Bay. This could indicate environmental constraints in Camden Bay or distribution limits and bottlenecks to dispersal and recruitment.

3. Patterns and drivers of benthic community structure and early succession in an estuarine Arctic kelp bed

Benthic community structure in Arctic nearshore ecosystems may result from both seasonal abiotic variability and the processes of recruitment and succession, all of which could be mediated by physiographic and bathymetric characteristics. Spatial differences were compared in community structure to environmental conditions (temperature, salinity, current speed, underwater light), and to bathymetry and physiography (depth, distance from river inputs) in a shallow Arctic kelp bed. Additionally, because propagule delivery and recruitment can overcome strictly abiotic effects on ecosystem structure, we monitored spatial and temporal patterns of recruitment and community development to assess the timescale and trajectory of ecological succession. The benthic community varied among sites but was dominated by red algae (47-79% average cover at each site), prostrate kelps (2-19% average cover), and crustose coralline algae (0-19% average cover). Strong spatial distinctions among sites were particularly due to the positive correlation between distance to river inputs and cover by crustose coralline algae (ρ

= 1.0), and larger proportions of invertebrates at a high flow site. However, there were no significant relationships between any single environmental characteristic and any functional group. Recruitment patterns indicated that successional processes are important to structuring the community, with foliose red algae as a key early successional group (up to ~60% of recruits at shallow sites). Greater variance in successional trajectory at sites near deep passes compared to more sheltered sites indicated that differential flow patterns affect community development by altering the local propagule pool. Succession also occurred extremely slowly, which would hinder ecosystem recovery after catastrophic disturbances. These results suggest that community development in the nearshore Beaufort Sea occurs over many years and is influenced by combinations of abiotic and biotic factors. The benthic community, therefore, reflects an integration of abiotic conditions over timescales longer than most ecological studies. While seasonality exerts strong influence on Arctic systems, ecologically important environmental variability in the coastal zone can also occur over extended time periods. Climate-driven changes in Arctic Ocean wind dynamics, freshwater budgets, sea ice extent, and erosional inputs will alter the community structure and distribution of shallow kelp beds.

DIRECTED EXPERIMENTAL AND OBSERVATIONAL STUDIES

4. Within- and between-basin population connectivity in the Arctic endemic kelp Laminaria solidungula

Pathways of dispersal and post-glacial recolonization patterns across the Arctic Ocean may provide insight into climate-driven borealization of Arctic ecosystems. To assess connectivity and dispersal in this rapidly-changing region, we analyzed population genetic structure in the Arctic endemic kelp *Laminaria solidungula* at two scales: 1) among populations in the Alaskan Beaufort Sea using microsatellites, and 2) among populations from across the Arctic using ribosomal large sub-unit (LSU) sequence data. The Beaufort Sea populations appear to be largely panmictic (global F_{ST}: 0.01), though sampling stations as close as 6 km could exhibit significant pairwise differentiation. Apparent inbreeding was extremely low ($F_{IS}<0$) and genetic diversity was high ($H_e>0.5$) at all well-sampled stations, indicative of rare self-recruitment. These results suggest that sub-polar benthic species migrating into the Beaufort Sea will quickly spread across the U.S. Arctic coast, likely assisted by alongshore transport during fall storms. Conversely, LSU analysis revealed two genotypes that represent strong population differentiation between Beaufort Sea *L. solidungula* and those from the Canada and Svalbard, indicating that phylogeography of this species reflects Arctic recolonization after the Last Glacial Maximum. LSU topology within Laminariales demonstrates that this partition represents a significant subdivision within *L. solidungula*.

5. Long-term patterns of benthic irradiance and kelp production in the central Beaufort Sea reveal implications of warming for Arctic inner shelves

A multidecadal dataset of annual growth was synthetized of the Arctic endemic kelp *Laminaria solidungula* and corresponding measurements of in situ benthic irradiance from Stefansson Sound in the central Beaufort Sea. We incorporate long-term data on sea ice concentration (National Sea Ice Data Center) and wind (National Weather Service) to assess how ice extent and summer wind dynamics affect the benthic light environment and annual kelp production. We find evidence of significant changes in sea ice extent in Stefansson Sound, with an extension of the ice-free season by approximately 17 days since 1979. Although kelp elongation at 5-7 m depths varies significantly among sites and years (3.8 to 49.8 cm yr^{-1}), there is no evidence for increased production with either earlier ice break-up or a longer summer ice-free period. This is explained by very low light transmittance to the benthos during the summer season (mean daily percent surface irradiance ±SD: 1.7±3.6 to 4.5±6.6, depending on depth, with light attenuation values ranging from 0.5 to 0.8 m^{-1}), resulting in minimal potential for kelp production on most days. Additionally, on month-long timescales (35 days) in the ice-free summer, benthic light levels are negatively related to wind speed. The frequent, wind-driven resuspension of sediments following ice break-up significantly reduce light to the seabed, effectively nullifying the benefits of an increased ice-free season on annual kelp growth. Instead, benthic light and primary production may depend substantially on the 1-3-week period surrounding ice break-up when intermediate sea ice concentrations reduce wind-driven sediment resuspension. These results suggest that both benthic and water column primary production along the inner shelf of Arctic marginal seas may decrease, not increase, with reductions in sea ice extent.

6. Physiological responses of an Arctic crustose coralline alga (Leptophytum foecundum) within variations of salinity

Arctic crustose coralline algae (CCA) persist in an environment of high seasonal variability. In addition to anthropogenic seawater chemistry changes (ocean acidification), calcifying organisms in the Arctic face naturally low pH ocean water and high magnitude freshwater pulses in the spring. The effects of salinity on the CCA *Leptophytum foecundum* were observed through a series of laboratory and field experiments in Stefansson Sound, Alaska. Laboratory experiments demonstrated through varying parameters (photosynthetic yield, pigments, and calcium carbonate dissolution), that salinity (treatments of 10, 20 and 30), independent of pH, affected *L. foecundum* physiology and dissolution. These experiments also revealed that *L. foecundum* was resilient to salinity down to 20, as individuals in the 20 and 30 salinity treatments were not significantly different for any of the parameters tested. This result was driven by aragonite saturation ($\mathbf{\Omega}$ aragonite) levels of the culture media; the 20 and 30 salinity treatments had levels of equilibrium or saturation (precipitation favored), while the 10 salinity treatments were undersaturated in regard to aragonite (dissolution favored). Reciprocal transplants and recruitment patterns between areas dominated by CCA and areas where CCA were absent, illustrate that in-shore locations receiving large pulses of freshwater are not suitable for the persistence CCA. Ultimately, spatially and

temporally varying salinity regimes and the resultant **Ω** arag levels determine distribution of CCA in the near shore Arctic.

7. Carbonate chemistry of the nearshore Arctic: shifts and future implications

World-wide, oceans are threatened by increased atmospheric carbon dioxide (CO_2) levels that result in increased CO_2 levels absorbed into seawater. This process, known as ocean acidification, leads to physiological disruption of species processes and the dissolution of calcifying marine organisms. The Arctic Ocean is more susceptible to ocean acidification due to natural factors that lower pH in addition to anthropogenic climate change. In order to quantify pH and other calcium carbonate parameters, pH, salinity, and temperature sensors were deployed at inshore near the mouth of the Sagavanirktok River (E-1) and 6 km offshore (DS-11) in 2016 and 2017 for one year. In addition, invertebrate and algal assemblages were quantified and compared between sites. Aragonite (the most common calcium carbonate mineral) saturation levels (**Ω** arag) were also calculated, due to the direct impact on calcifying organisms. Levels above one favor precipitation, while saturation levels below one favor dissolution. Seasonal and annual variations were detected within and between sites. In general, the inshore site (E-1) experienced lower salinity levels during the spring freshet and the freshwater input resulted in lower **Ω** arag levels. However, pH was slightly higher at the inshore site, and this pH signal was associated with runoff from the Sagavanirktok River, with waters slightly more basic than ocean water. Likely associated with low **Ω** arag levels, crustose coralline algae were absent from the inshore site. Red algal biomass increased at the inshore site and inshore invertebrate communities were bryozoan-dominated. Salinity changes, total alkalinity, and runoff from the Sagavanirktok River strongly influenced ocean water carbonate chemistry and these values resulted in different benthic communities. The inshore communities have the potential to expand throughout the Boulder Patch as freshwater runoff increases and ocean acidification continue to decrease **Ω** arag levels.

8. Freshwater input effects on Laminaria solidungula microscopic stages

The Arctic endemic kelp species, *Laminaria solidungula*, is an important contributor to nearshore food webs of the Alaska Arctic. Population density differences among areas of the Stefansson Sound Boulder Patch led to questions of effects of abiotic factors on population persistence. Although many factors affect sporophyte densities, microscopic stages of the life history are known to be more susceptible to environmental conditions. *Laminaria solidungula* were cultured under varying light (10, 20 and 40 μmol photons m^2 s^{-1}) and salinity (10, 20, 30) treatments in order to explore how these factors interactively and separately affect microscopic sporophyte production. Ultimately, cultures in the low salinity treatment were not able to produce sporophytes regardless of light level, however, light levels did affect final densities. As freshwater influence from the Sagavanirktok River continues to increase, lower salinity levels and light reducing sediments may reach further offshore could decrease sporophyte production and *L. solidungula* population persistence.

BACKGROUND AND SETTING

1. Seasonality and change near the mouth of an Arctic river: Environmental variability in Stefansson Sound, Alaska

Christina E. Bonsell and Kenneth H. Dunton

INTRODUCTION

Shallow, predominantly soft sediment habitats, which characterize the benthic nearshore areas of the U.S. Arctic, are important settings for marine life and ecological processes. These ecosystems are also locations of ongoing and proposed industrial activity. Numerous river and stream inputs define the inner shelf area as an estuarine environment (Carmack and Wassman 2006). Benthic organisms on the inner shelf include key consumers that assimilate both autochthonous and allochthonous (mostly terrestrial) sources of carbon. Consumer dependence on terrestrial sources is now well documented by isotopic evidence and gut analyses of fauna collected in lagoon systems along the Beaufort Sea coast (Craig et al. 1984, Dunton et al. 2012, Harris et al. 2018). The high productivity within the linked barrier island lagoon environment allow migratory birds, marine and anadromous fishes, and marine mammals to take advantage of the food and habitat provided by these protected lagoon systems (Craig et al. 1984, Craig 1984, Dickovy 1984, Frost and Lowry 1984). In addition, the strong seasonality of Arctic coastal ecosystems defines the timing and magnitude of freshwater inflows, sea ice dynamics, and water exchange with the ocean, which in turn shapes their estuarine nature.

Seasonal changes in the physiochemical environment of these systems is largely event driven, dominated by annual cycles of river inputs and ice cover (Mcclelland et al. 2012, Weingartner et al. 2017). Rivers draining the North Slope of Alaska discharge over half of their annual flow in a short, two-week spring melt period between late May and early June (i.e. the "spring freshet"; McClelland et al. 2012, McClelland et al. 2014). This flow initially occurs above and beneath the sea ice, creating a relatively stable stratified layer of river water that can reach up to ~ 3 m deep (Reimnitz 2000, Alkire and Trefry 2006, Kasper and Weingartner 2015) until sea ice break-up commences and wind mixing strengthens (Weingartner et al. 2017). Depending on winds, currents, and flow conditions, ice break-up can occur over a period of days or weeks. In the Beaufort Sea, the ice free summer is then characterized by wind mixing and higher current speeds, especially late in the season (Weingartner et al. 2017). Ice formation begins as the amount solar energy that reaches Arctic latitudes decreases in the fall, further homogenizing the water column. Landfast ice forms along the shore, then spreads offshore, with freeze-up complete in nearshore areas by late-October (Barry et al. 1979, Mahoney et al. 2014). As ice formation continues, both salinity and inorganic nutrient levels increase within the underlying waters through the respective processes of brine

rejection and remineralization (Chapman and Lindley 1980, Matthews 1981, Dunton et al. 1982, Macdonald and Yu 2006).

In the marine realm of Arctic nearshore systems, bathymetry and proximity to river inputs mediate seasonal variation in abiotic conditions, and thereby impart "zones" of ecological characteristics and biogeochemical processes. For example, greater sediment resuspension at shallow depths due to summer wind mixing can reduce benthic primary productivity relative to deeper, more offshore areas (Aumack et al. 2007). Additionally, stratification in the spring and early summer exposes nearshore, near river benthos to a distinct, river derived water mass. Associated organic matter, freshwater, and heat inputs may result in profound differences between nearshore and offshore benthic diversity and biogeochemical processes (Bonsell 2019, sections 1.2 and 2.4.).

Understanding year round in situ conditions is a critical knowledge gap linking Arctic abiotic factors to biological characteristics and biogeochemical processes. As seasonal transitions can vary from year to year (e.g., Harris et al. 2017), multiple years of data are necessary to assess the magnitude and spatial extent of abiotic changes. Logistical constraints and ice risks discourage long-term mooring deployments in shallow areas, meaning that underwater conditions during the freshet and ice break-up are not well characterized for most Arctic estuaries. Recent technological advances have made affordable in situ instrumentation more readily available, and researchers more willing to risk equipment for the chance of acquiring valuable environmental data.

The goals of this study are to: 1) Define the seasonal cycle in temperature, salinity, currents, and underwater light in the nearshore environment of Stefansson Sound; 2) Determine the influence of bathymetric and physiogeographic characteristics (distance from river inputs and coastline orientation) on spatial differences in the marine environment; 3) Discuss the influence of regional wind patterns on temporal variability and current dynamics; and 4) Assess evidence for long-term change in temperature and salinity in Stefansson Sound. This work depicts the environmental setting for nearshore biological processes on Arctic inner shelves.

Weingartner et al. (2017) recently described seasonal abiotic conditions in the nearshore landfast ice zone of the central Beaufort Sea coast, with moorings as shallow as 7 m in Stefansson Sound. Their study provides important environmental context for ecological studies and proposed development scenarios related to oil and gas extraction. Our work extends shoreward to 4 m within Stefansson Sound, where stratified fluvial inputs interact with benthic processes that affect local production, diversity, and biogeochemical cycling. Observations of temperature, salinity, and currents collected in this study were compared to offshore measurements, as well as to data collected in previous decades (1970s and 1980s). Comparisons to historical datasets are important since the changes occurring over sub-decadal time scales can be masked by innate interannual variability. We

consider the effects of bathymetric and physiogeographic characteristics on the abiotic environment, and how those may impact marine life. Our dataloggers were within 60 cm of the benthos, providing an opportunity to describe how benthic biota experience seasonality adjacent to river inputs.

METHODS

Study Area

Stefansson Sound is a shallow (<10 m) embayment on the central Beaufort Sea coast, partially protected by barrier islands. The Sagavanirktok River, with headwaters in the Brooks Range, empties into the Stefansson Sound via numerous delta channels (Fig. 1.1). Like most of the Beaufort Sea coast, the benthos is primarily composed of silty sediments, but a large deposit of boulders and cobbles, termed the "Boulder Patch", gives rise to a unique benthic bed community in the eastern portion (Fig. 1.1; Dunton et al. 1982). The Endicott Causeway, completed in 1985, extends into the sound past the Sagavanirktok River delta. Development of the adjacent Prudhoe Bay oilfield resulted in intense study of Stefansson Sound relative to other Arctic inner shelf habitats. As a result, changes to the marine environment over time can be evaluated from historical in situ datasets.

Over the course of the study period (2011-2017), we occupied five long-term monitoring sites within the Boulder Patch area of Stefansson Sound. Sites differed in depth and distance from Sagavanirktok River channels (Fig. 1.1, Table 1.1). These included three nearshore sites (E1, L1, and W1), and two sites further offshore (DS11, W3).

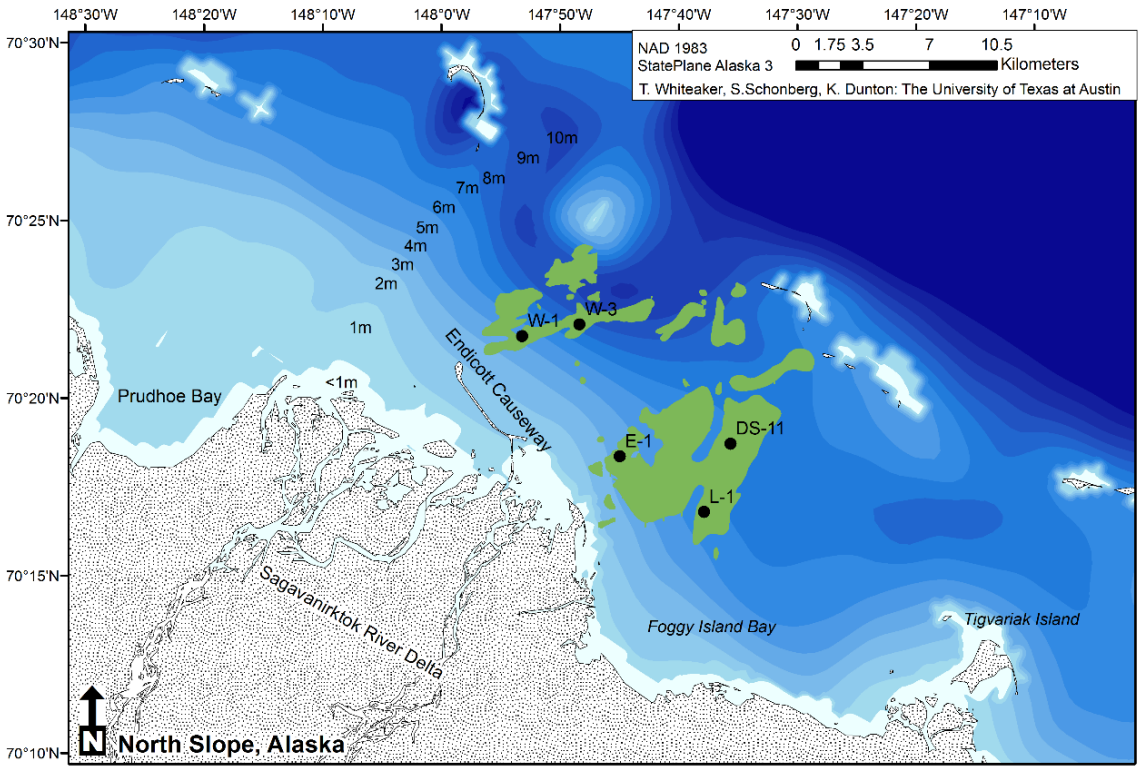

Figure 1.1. Map of the Stefansson Sound area, with the five long-term study sites used in this study: W1, W3, E1, L1, and DS11. The green area symbolizes the Boulder Patch.

Mooring description

Benthic moorings, composed of a variety of in situ data loggers (described below), collected continuous environmental data at each of our sites. These were retrieved each summer (July or August) and redeployed within two weeks after downloading the data. Photosynthetically active radiation (PAR) was recorded ~ 50 cm above the seabed using a LI-COR LI-193SA spherical quantum sensor (accuracy: ±5%) connected to LI-1000, LI-1400, or LI-1500 dataloggers. Some of these data have been incorporated in previous studies to examine multidecadal underwater light patterns in the Boulder Patch (Bonsell and Dunton 2018). Continuous in situ measurements of conductivity and temperature were collected with HOBO U24 Conductivity/Temperature Loggers (hourly sample interval) and Star Oddi DST loggers (30 min sample interval; accuracy for both loggers: ± 0.1 ^{o}C, ±1.0 salinity). Instantaneous measurements of temperature and conductivity were measured upon deployment and retrieval of loggers using a YSI Data Sonde to calibrate records at each site. Temperature and conductivity were used to calculate salinity using the 1983 UNESCO equation. Measurements of temperature, current velocity and current bearing within ~1.2 m of the bottom were collected using SeaHorse Tilt Current meter fitted with a MAT-1 accelerometer or with a Lowell MAT-1 Tilt Current Meter (30 min sample intervals, accuracy: ± 1^{o}).

In addition, Sea-bird (Satlantic) SeaFETs and SBE 37-SM MicroCATs C-T (P) were deployed July 2016-July 2018 at two sites within the Boulder Patch, Stefansson Sound, Alaska (Fig. 1.1); Site E1 (70°18.8665 N, 147°44.0413 W; 4 m depth) and site DS-11 (70°19.3248 N, 147°34.8816; 7 m depth).

Our mooring design placed conductivity cells within 30 cm of the benthos. This exposed them to fouling by resuspended sediments during fall storms, a known problem in these environments (Weingartner et al. 2017). As a result, conductivity data was removed for portions of the record at some sites. Additionally, some moorings were lost to damage by deep draft ice, though the large majority survived deployment (Fig. 1.2).

Data analyses

After undergoing quality control, summary statistics were generated for each data type at each site overall and separated by season: ice-covered winter (December through April), pre ice break-up spring (May through June), open water summer (July through September), and fall freeze-up (October through November). This definition corresponds with the timing of key hydrologic events: the spring freshet (late May to early June), landfast ice break-up (July), and sea ice freeze-up (early to mid-November). The four-season model has been used by others to describe Arctic annual cycles in connection to biological activity (Carmack & Macdonald, 2002). To directly assess how abiotic conditions differed among sites over time daily mean values for each continuous variable (temperature, salinity, PAR, current velocity) were calculated for each day where there was data for >1 site and compared using a blocked-ANOVA approach using time (day) as a block. Post-hoc pairwise comparisons assessed differences in least-squared means, with Tukey-adjusted p-values for multiple comparisons. Daily mean current direction and summary statistics were determined to the nearest degree using the R package 'circular' (Agostinelli and Lund 2013). Average daily wind speed and fastest five-minute wind direction from the Deadhorse Airport were downloaded from the National Climate Data Center (National Weather Service) and plotted against mean daily current conditions at each site. All data analysis was carried out using R v. 3.3.3 (R Core Team, 2016).

Table 1.1. Site locations, bathymetric, and physiographic information.

Site	Latitude (DD)	Longitude (DD)	Depth (m)	Dist. to river input (km)
DS11	70.32228	-147.579	6.1	9.03
E1	70.31495	-147.732	4.4	3.54
L1	70.28993	-147.613	5.5	7.20
W1	70.37003	-147.873	6.0	3.54
W3	70.37627	-147.794	6.6	7.31

RESULTS

Our data show the strong seasonal pattern of environmental conditions in the Arctic, with relatively consistent temperature, salinity, light, and currents during the winter and a much more variable environment during the rest of the year (Table 1.2, Figs. 1.2-1.5). Generally, sites experienced synchronous variations in all parameters except salinity, though the magnitude of change could vary significantly between sites (Figs. 1.2 and 1.5) Signatures of the annual sea ice cycle and the spring freshet are apparent in the underwater physiochemical record.

Salinity on the seabed reached its highest average (33-36) in the winter, and its lowest average in summer (below 30) at all sites (Table 1.2). Winter temperatures were stable at ~-1.9 to -1.8°C but reached upwards of 5°C in the summer (Table 1.2, Figs. 1.2-1.4). Shallow, inshore sites experienced the greatest range in salinities, with E1 and W1 fresher than the other sites in the spring and summer (Table 1.2, Figs. 1.2 and 1.3). The site closest to the river mouth (E1) also exhibited the greatest riverine influence: temperatures rose earlier and a springtime pulse of low salinity was noted in some years that was not seen at the offshore sites (Figs. 1.2 and 1.4). E1 also had significantly higher temperatures than the other sites during spring and summer and was the warmest site overall (Tables 1.2-1.3). While the freshet signal was strongest at E1, it could also be seen at other sites as a small (<1^{o}C) rise in temperature in the spring (Fig. 1.2). The subsequent onset of sea ice melt was marked by a rapid, large (> 2°C) increase in temperature and a decrease in salinity (>3) across Stefansson Sound (Fig. 1.2). Temperatures were maximal in August, then decreased gradually through the early fall until dropping rapidly by more than 2°C leading up to sea ice freeze-up (Fig. 1.2).

Photon flux was extremely variable across sites in the summer, but most notably at E1 (Table 1.2, Figs. 1.2 and 1.3). Underwater light levels hit their annual maximum in July (above 5 mol photons m^{-2} day^{-1}), with the rest of the summer characterized by smaller, sporadic spikes of measurable light levels (Fig. 1.2). In summer, DS11 and E1 tended to have higher underwater light levels than other sites (Table 1.3). PAR dropped to zero in the fall, then increased briefly in the spring in two of the four years (2014 and 2017), before dropping to zero again (Fig. 1.2).

At all sites, near bottom current velocities were much lower and less variable under ice cover during the winter and spring (<2 cm/s, Table 1.2, Figs. 1.2,1.3 and 1.5). Like temperature, current speeds accelerated slightly (<2 cm s^{-1}) with the freshet, then strengthened considerably as sea ice cover decreased in the Beaufort Sea during summer (Fig. 1.2). Average velocity at all sites was highest in the summer and fall (average >3 cm s^{-1}, Table 1.2, Figs. 1.2, 1.3 and 1.5). The shallow, within bay sites E1 and L1 experienced their maximum seasonal current velocity in the summer, while currents were fastest in the fall at the more exposed and deeper sites (DS11, W1, W3; Table 1.2, Figs. 1.2, 1.3 and 1.5). On average, velocity was greater at these three sites, while E1 and L1 had significantly lower velocities, and lower variability (as measured by standard deviation) across seasons (Tables 1.2

and 1.3, Fig. 1.3). The onset of sea ice freeze-up in October (2014-2015) or November (2016) caused current speed to plummet (Figs. 1.2 and 1.5).

Current direction data failed to meet the assumptions for statistical comparisons between sites and seasons as it was not Von Mises distributed (Watson test for continuous probability distribution on the circle, α=0.1). Currents were primarily bi-directional: east-west for W1 and W3, northwest-southeast for L1 and DS11 (Figs. 1.5-1.7). Unlike the other sites, currents at E1 were more unidirectional and tended to be toward the south (Figs. 1.5-1.7, Table 1.3). At all sites, the strongest currents typically had a northwest bearing (Figs. 1.5 and 1.7). During summer and fall, strong along-shore flows developed throughout the Boulder Patch (Fig. 1.6). Currents bearing south became more frequent during the winter and pre break-up spring (Figs. 1.5 and 1.6).

Table 1.2. Mean and standard deviation of daily benthic environmental conditions measured at each site, split by season, of entire data record (Fig. 1.2). Subscripts refer to number of observations (days). Superscripts indicate that there were significant differences between sites, with letter indicating group affinity within each season (α=0.05, Supp. Table 1.1). * Differences in mean current direction could not be analyzed statistically.

Season	Site	Temp. (°C)	Salinity	Current vel. (cm s^{-1})	Current direction (degrees)*	PAR (mol photons m^{-2} day^{-1})
Ice-covered (Dec-Apr)	DS11	-1.8±0.1 $^{a}_{908}$	34±1 $^{a}_{908}$	1.7±1.3 $^{a}_{151}$	180±83 $_{151}$	0.013±0.025 $_{605}$
	E1	-1.9±0.1 $^{b}_{605}$	34±2 $^{b}_{598}$	1.3±0.6 $^{bd}_{454}$	236±64 $_{454}$	0.014±0.034 $_{454}$
	L1	-1.8±0.1 $^{a}_{605}$	36±1 $^{c}_{240}$	0.7±0.4 $^{c}_{454}$	194±108 $_{454}$	0.012±0.025 $_{302}$
	W1	-1.9±0.1 $^{b}_{454}$	33±1 $^{d}_{151}$	1.3±1.0 $^{b}_{303}$	144±48 $_{303}$	Instrument failed
	W3	-1.8±0.1 $^{c}_{485}$	34±1 $^{ab}_{302}$	1.6±0.8 $^{ad}_{151}$	162±100 $_{302}$	0.017±0.024 $_{151}$
Pre-break-up spring (May-Jun)	DS11	-1.6±0.2 $^{a}_{366}$	33±1 $^{a}_{366}$	1.7±1.2 $^{a}_{61}$	96±83 $_{61}$	0.082±0.178 $_{244}$
	E1	-1.3±0.7 $^{b}_{244}$	31±6 $^{b}_{243}$	1.5±0.8 $^{b}_{183}$	199±69 $_{183}$	0.070±0.186 $_{183}$
	L1	-1.5±0.2 $^{c}_{244}$	35±1 $^{c}_{132}$	0.7±0.5 $^{c}_{183}$	198±91 $_{183}$	0.065±0.113 $_{122}$
	W1	-1.6±0.2 $^{ad}_{183}$	31±0 $^{b}_{77}$	1.4±0.9 $^{b}_{122}$	149±47 $_{122}$	Instrument failed
	W3	-1.7±0.2 $^{d}_{183}$	34±1 $^{a}_{122}$	1.6±0.7 $^{a}_{61}$	166±68 $_{122}$	0.082±0.103 $_{61}$
Open water summer (Jul-Sep)	DS11	2.0±2.2 $^{a}_{519}$	29±3 $^{a}_{519}$	7.3±4.9 $^{ab}_{108}$	353±97 $_{109}$	1.062±1.878 $^{a}_{336}$
	E1	3.2±2.5 $^{b}_{377}$	27±3 $^{b}_{377}$	5.3±3.7 $^{c}_{248}$	266±90 $_{248}$	0.812±1.789 $^{ab}_{247}$
	L1	2.0±2.1 $^{a}_{326}$	29±4 $^{c}_{246}$	3.9±2.6 $^{c}_{250}$	279±87 $_{250}$	0.620±1.314 $^{b}_{222}$
	W1	1.7±2.2 $^{a}_{232}$	26±4 $^{d}_{148}$	7.7±5.5 $^{a}_{215}$	193±75 $_{217}$	0.102±0.236 $^{b}_{27}$
	W3	1.6±2.1 $^{a}_{334}$	28±3 $^{a}_{270}$	6.5±4.0 $^{b}_{201}$	206±71 $_{219}$	0.534±1.188 $^{b}_{126}$
Fall freeze-up (Oct-Nov)	DS11	-1.4±1.0 $_{366}$	31±2 $^{ab}_{322}$	8.8±8.4 $^{a}_{61}$	235±80 $_{61}$	0.014±0.053 $_{244}$
	E1	-1.3±1.1 $_{244}$	31±2 $^{bc}_{221}$	4.3±4.8 $^{b}_{183}$	271±73 $_{183}$	0.013±0.040 $_{183}$
	L1	-1.4±0.9 $_{244}$	32±2 $^{c}_{124}$	3.5±4.3 $^{b}_{183}$	285±86 $_{183}$	0.002±0.005 $_{124}$
	W1	-1.4±0.9 $_{183}$	29±2 $^{a}_{49}$	7.7±7.5 $^{a}_{142}$	215±68 $_{142}$	Instrument failed
	W3	-1.4±0.9 $_{244}$	31±3 $^{abc}_{98}$	8.0±5.9 $^{a}_{108}$	228±97 $_{132}$	0.001±0.002 $_{70}$

Table 1.3. Daily, year-round mean (±SD) benthic environmental conditions at each site of entire data record (Fig. 1.2). Superscripts indicate that there were significant differences between sites, with letter indicating group affinity (α=0.05, Supp. Table 1.1). * Differences in mean current direction could not be analyzed statistically.

Site	Temperature (°C)	Salinity	Current velocity (cm s^{-1})	Current direction (degrees)*	PAR (mol photons m^{-2} day^{-1})
DS11	-0.78±1.96 $^{a}_{2159}$	32±3 $^{a}_{2115}$	4.4±5.3 $^{a}_{381}$	181±77 $_{382}$	0.271±1.013 $_{1429}$
E1	-0.41±2.50 $^{b}_{1470}$	31±4 $^{b}_{1439}$	2.8±3.2 $^{b}_{1068}$	239±66 $_{1068}$	0.208±0.925 $_{1067}$
L1	-0.82±1.89 $^{a}_{1419}$	33±4 $^{a}_{742}$	1.9±2.7 $^{c}_{1070}$	251±76 $_{1070}$	0.194±0.756 $_{772}$
W1	-0.95±1.84 $^{a}_{1052}$	30±4 $^{c}_{425}$	4.3±5.4 $^{d}_{782}$	164±61 $_{784}$	0.102±0.236 $_{27}$
W3	-0.80±1.88 $^{a}_{1246}$	32±3 $^{b}_{792}$	4.8±4.6 $^{a}_{521}$	189±71 $_{775}$	0.184±0.700 $_{408}$

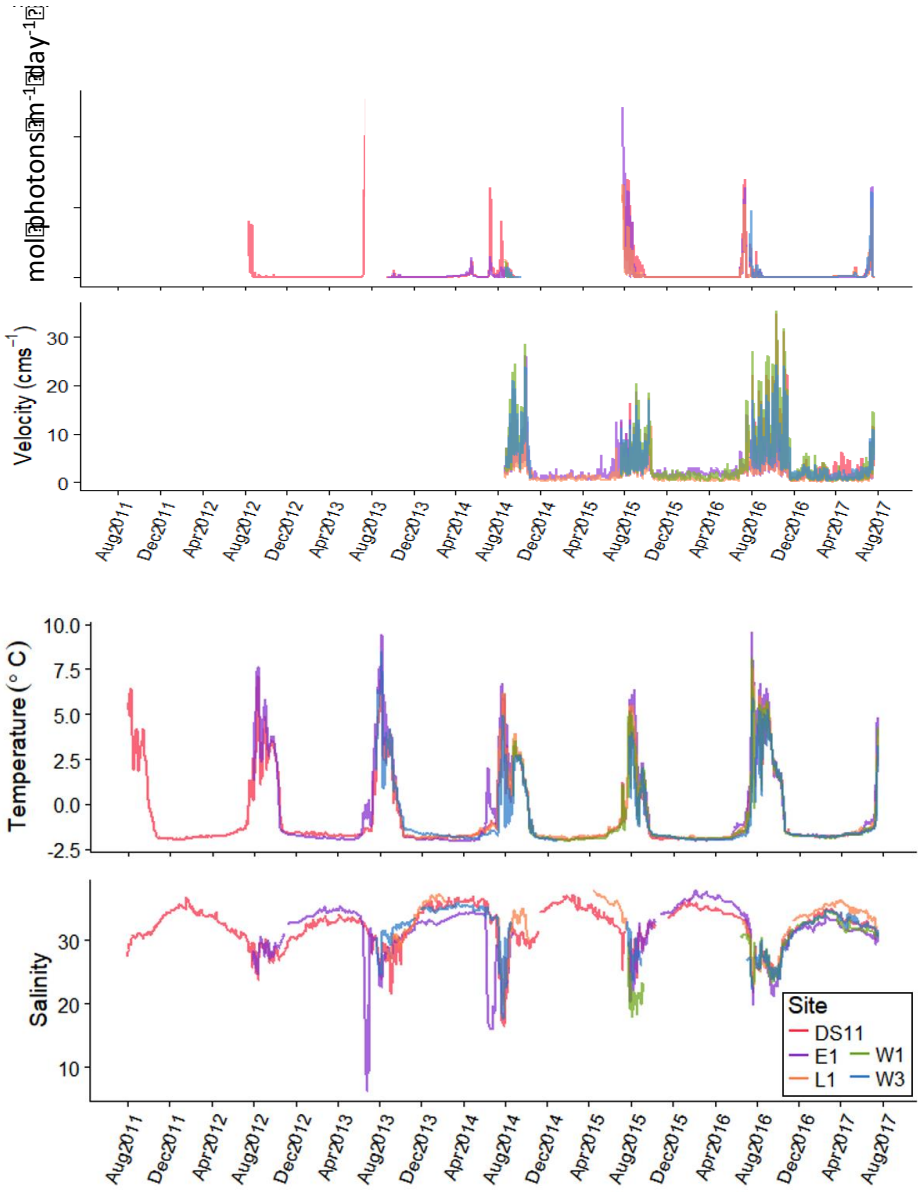

Figure 1.2. Timeseries of daily mean temperature, salinity, photon flux, and current velocity at each site.

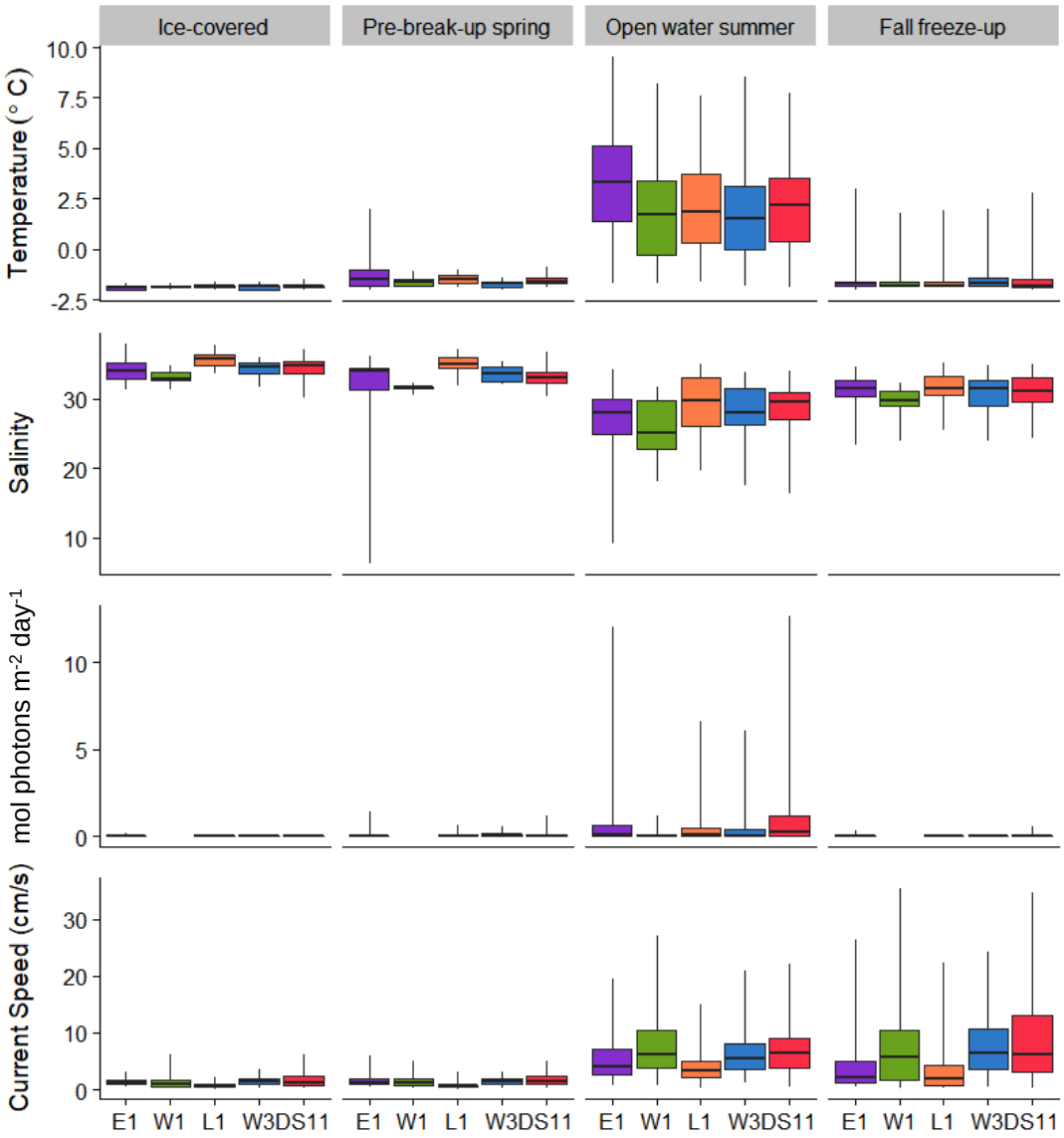

Figure 1.3. Distribution of measurements for each variable by site and season for entire data record (Fig. 1.2). Sites are ordered by increasing distance offshore. Central horizontal line indicates the median, upper and lower limits of the box indicate interquartile range; vertical lines indicate the overall range of values. See Table 1.2 for significant group affinities. This figure differs from Table 1.2 in that it shows median values, so less weight is given to rare observations at the edge of the range.

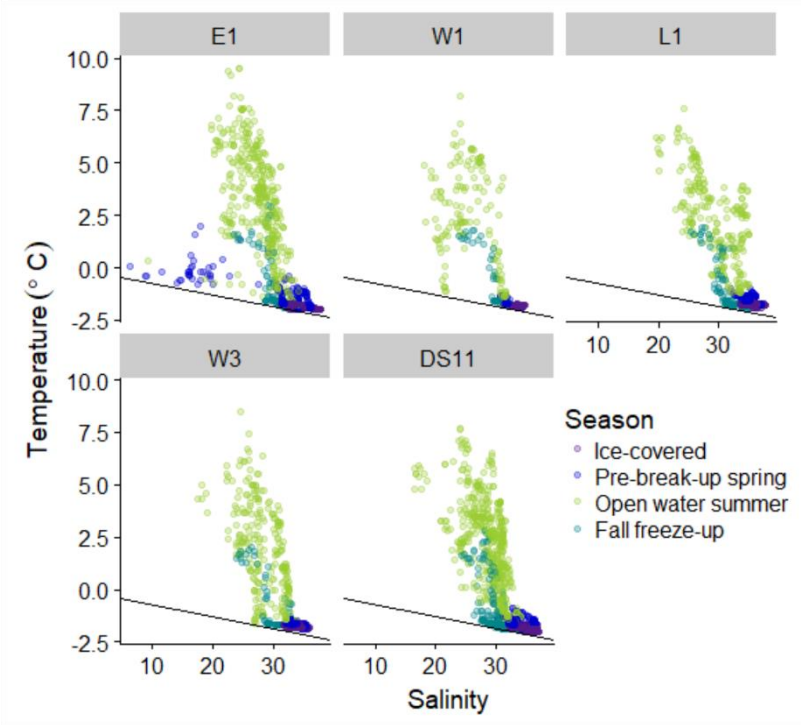

Figure 1.4. Temperature vs. salinity plots at each site for entire data record (Fig. 1.2), color-coded by season. Purple: ice-covered; blue: spring; green: summer; teal: fall. Black line indicates the freezing point of water.

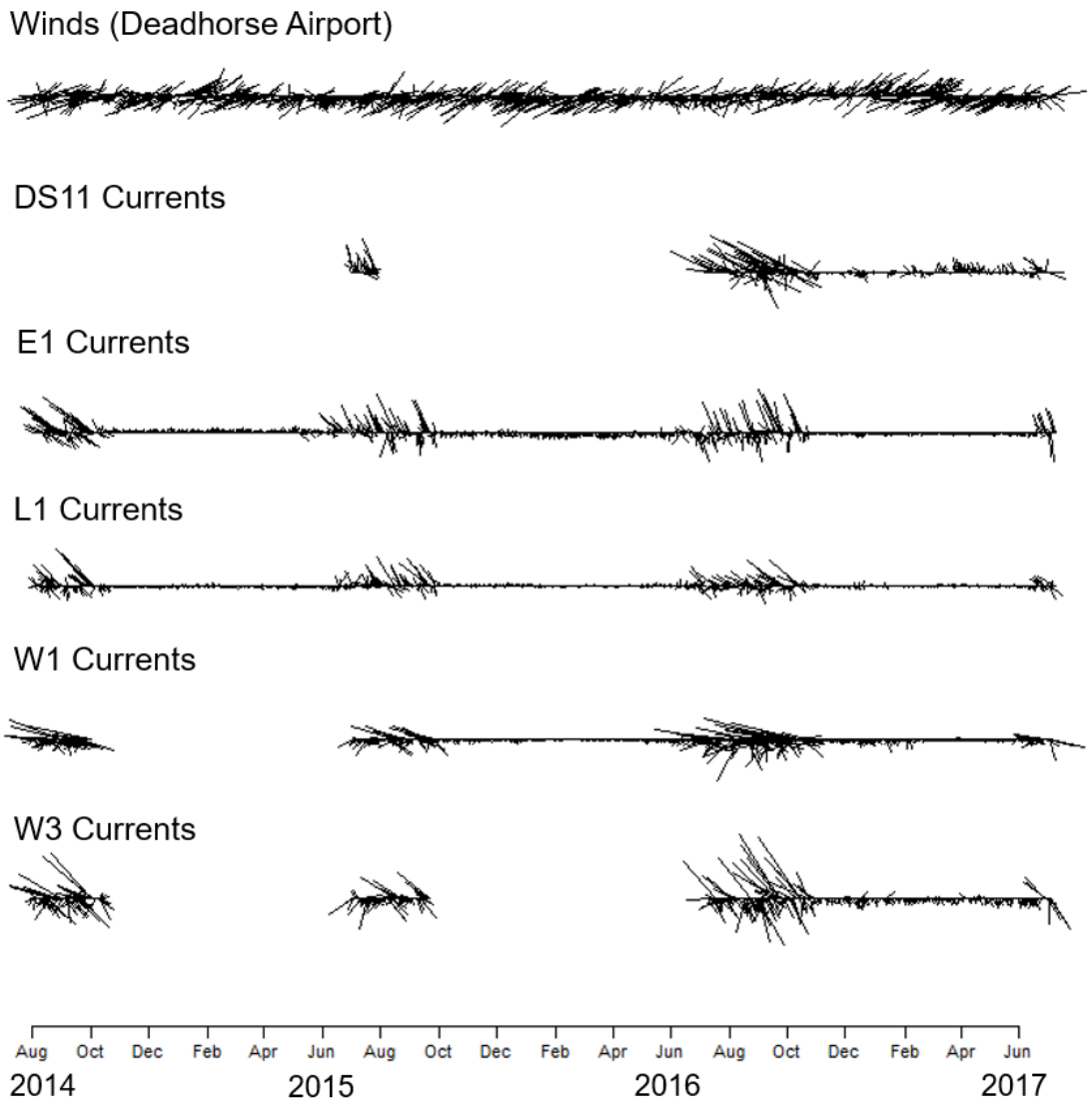

Figure 1.5. Timeseries of daily direction and relative speed of wind at Deadhorse Airport (NWS) and currents at each site. North is positive in the y-axis; east is positive in the x-axis.

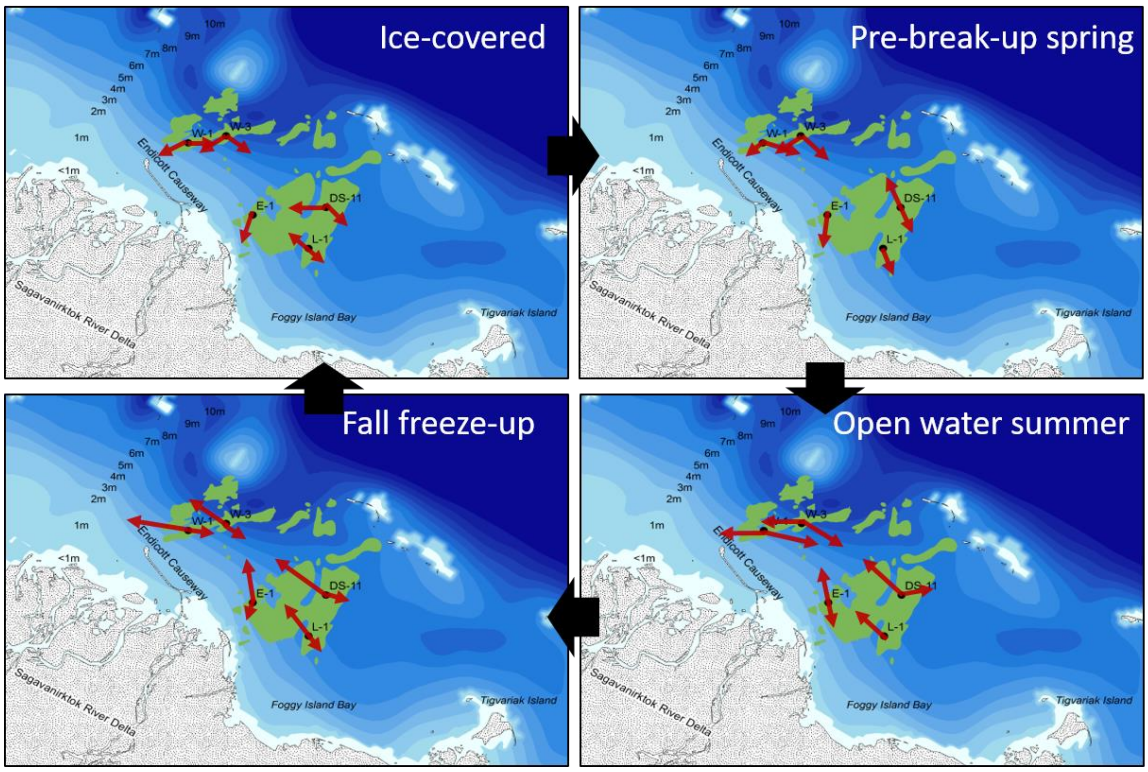

Figure 1.6. Seasonal flow patterns over the Boulder Patch. Vectors display the principal uni- or bi-directionality and relative velocity, based on circular histograms of current data.

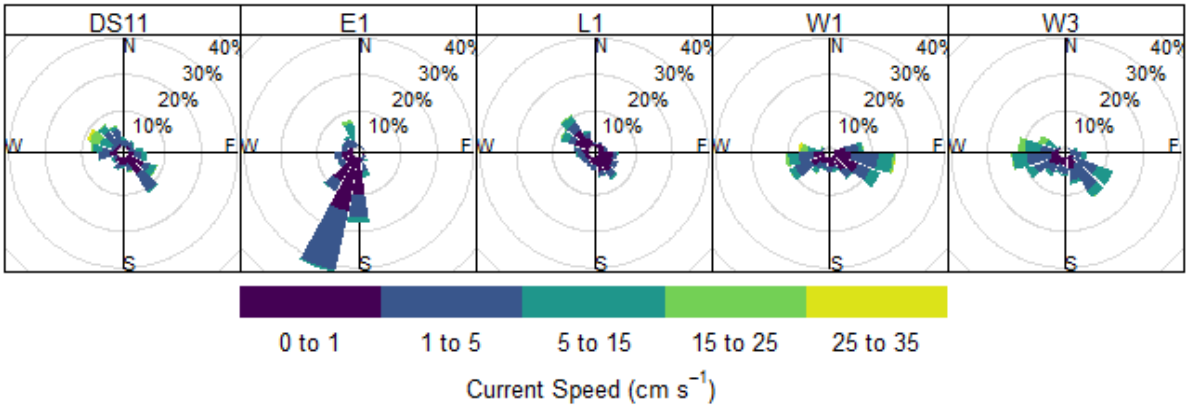

Figure 1.7. Distribution of mean daily current velocity and direction for each site for the entire dataset. Arc sections indicate the frequency of currents of a particular velocity and bearing, binned by 20^{o}

pH values

pH$_T$ values were recorded hourly for 2016 deployments, however, upon retrieval both pH sensors had failed (E-1: July 2016-June2017; DS-11: July 2016-February 2017). Sensors were reset for the 2017 deployments to record pH$_T$ every two hours and were actively recording when retrieved in July 2018. Values and trends were similar between sites for each year, but drastic variations were seen between years. For more detailed pH and carbonate chemistry results and discussion see section 2.4.

2016 Results

Coastal ocean pH$_T$ followed seasonally distinct transitions that relate to four main events: the summer open water, fall freeze-up, the winter ice covered season, and the spring freshet. For the 2016-2017 deployment, pH$_T$ during the freshet was not captured due to sensor failure. pH$_T$ varied from 7.83 – 8.70 at E1 (error 0.042) and 7.79 – 8.69 at DS-11 (0.046), both sites showed a unique pH spike during freeze-up (Fig. 1.8).

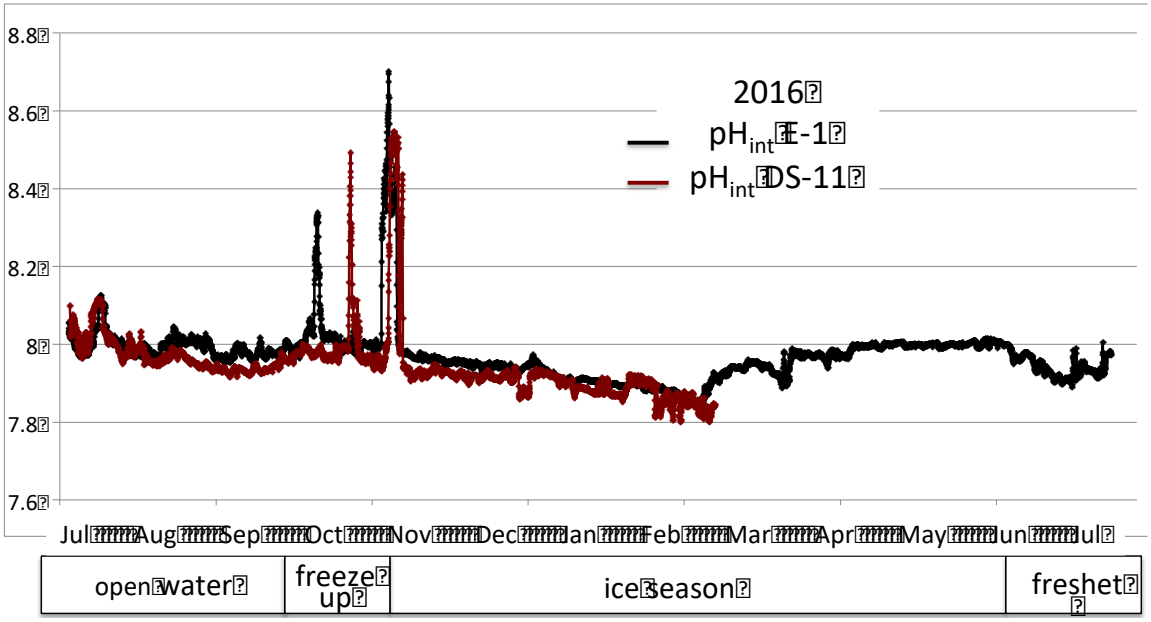

Figure 1.8. pH_T values for 2016 at E-1 (black) and DS-11 (red). Data can be observed in four distinct periods, based on ice formation and run-off from the adjacent Sagavanirktok River; open water, freeze-up, ice season, and freshet.

2017 results

pH_T varied from 7.67 – 8.67 at E1 (error 0.085) and 7.75 – 8.34 at DS-11 (0.028), both sites showed pH spikes when salinity declined due to run-off from the Sagavanirktok River; open water season (DS-11-July 2017) and the spring freshet (E1-July 2018), but spikes were not detected during freeze-up as they were in 2016 for both sites (Figs. 1.8 and 1.9). Heterotrophy during the ice season and low light season likely increased pCO_2 and caused a slight decrease in pH as seen in 2016-2017.

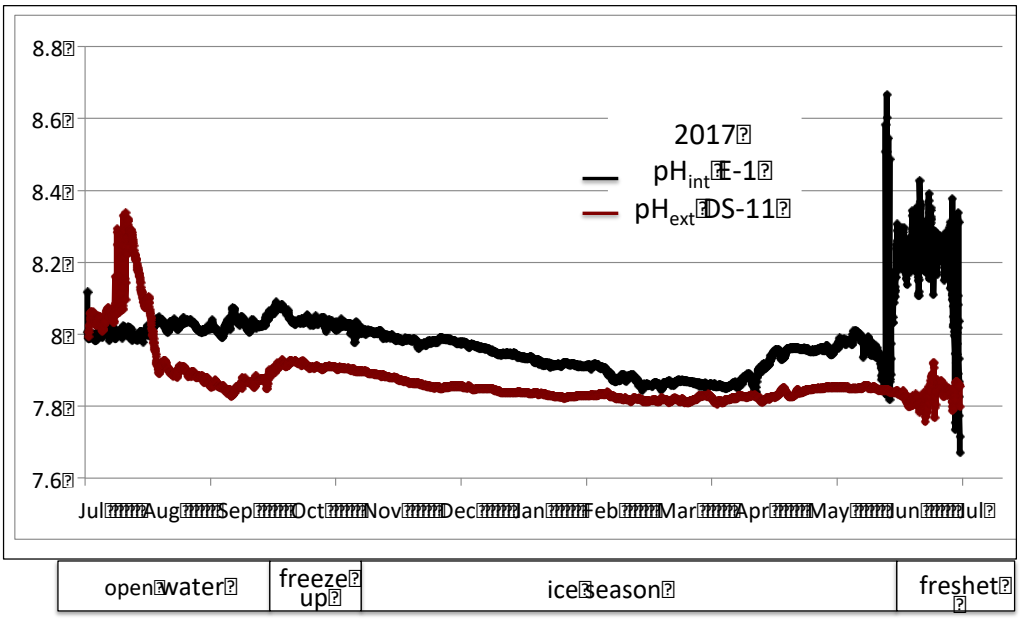

Figure 1.9. pH_T values for 2016 at E-1 (black) and DS-11 (red). Data can be observed in four distinct periods, based on ice formation and run-off from the adjacent Sagavanirktok River; open water, freeze-up, ice season, and freshet.

DISCUSSION

Spatiotemporal variability

Temporal abiotic variability in Stefansson Sound is primarily driven by sea-ice dynamics. On annual timescales, the timing of ice break-up and freeze-up determines the magnitude of current velocity, as well as temperature and salinity variation (Figs. 1.2 and 1.5). This timing also significantly influences underwater light levels (Dunton et al. 1992). Since tides along the Beaufort Sea coast are minimal, higher-frequency variations are caused by atmospheric forcing, which drives nearshore water mass movement (Dunton et al. 2006, Weingartner et al. 2017). In the absence of ice cover, this effect is amplified, leading to higher environmental variability in the summer. Much of the temperature and salinity variation at offshore sites (DS11 and W3) from July-October can be explained by upwelling due to easterly winds, which transports cold, saline shelf bottom waters further onto the inner shelf (Dunton et al. 2006). Westerly winds, on the other hand, entrain warm, fresh nearshore water into Stefansson Sound (Sellmann et al. 1992). These drivers are strengthened in the absence of sea ice, so most of the major spatial abiotic variability exists outside of the ice-covered winter months.

Spatial abiotic variation is linked to bathymetry and distance from the Sagavanirktok River. While our salinity record is inconsistent due to sediment fouling, some key trends emerge. By mid-November, after fall freeze-up, equivalent bottom temperature and salinity conditions prevail throughout Stefansson Sound.

Winter minimum temperatures of ~-1.9, just above the freezing point (Fig. 1.4), as reported by Matthews (1981) and Sellmann et al. (1992), persist until May. Salinity increases to above 33 through the beginning of winter as a result of ion exclusion by the growing sea ice (Matthews 1981). With the advancement of spring, river runoff and sea ice melt begin to influence salinity and temperature in shallow areas (Figs. 1.2-1.3). Low salinities (mean ≤ 32) at E1 and W1 suggest greater riverine influence at these sites through the spring and summer (Table 1.3, Figs. 1.3 and 1.4). This is especially evident at E1, where the freshet was documented each year in June (Figs. 1.2-1.4), as predicted by modelling studies which showed that stratified fluvial plumes are retrained in the nearshore during ice cover (Kasper and Weingartner 2015). Elevated bottom temperatures at the shallow, nearshore site (E1; annual mean -0.47 ^{o}C) indicate frequent position above the thermocline, and exposure to warmer, inshore waters throughout the summer, when the mean temperature at this site is ~ 1 ^{o}C above that of the other sites (Tables 1.2 and 1.3, Figs. 1.3 and 1.4; Sellmann et al. 1992). While the timing of these events corresponds to Weingartner et al. (2017), comparison of the two studies emphasizes the cross shore estuarine gradient in Stefansson Sound, with nearshore waters generally warmer by a few degrees and fresher than those further offshore.

pH was also linked to distance from the Sagavanirktok River, timing of ice formation and the spring freshet. This dataset marks the first, continuous dataset for the Arctic Ocean. Although previous studies have reported pH and associated carbonate chemistry parameters for this area (Mathis et al. 2015), the measurements were not continuous and represented specific time periods over multiple areas. Section 2.4 of this report discusses in depth pH values for the Boulder Patch and the associated carbonate chemistry parameters.

Underwater light levels in the Boulder Patch are negligible for most of the year. In the winter, ice cover and the polar night keep the benthos in darkness. Sediments in the sea ice, which become entrained during fall storms (Osterkamp and Gosnik 1984) can further attenuate light at the sea surface. In some years (2014 and 2017), underwater light briefly rose in the spring, likely due to the presence of an ice canopy relatively free of these sediments, which allows light to penetrate into the water column. In spring of 2014, the year with the highest under ice light levels, the return to darkness corresponded with the pulse of low salinity at E1 (Fig. 1.2), indicating that sediment and debris accompanying spring runoff either wash over or spread under the ice, causing light levels to drop again. Underwater light levels increase dramatically during ice break-up, the time when they reach their maximum annual value (Bonsell and Dunton 2018). After ice break-up, wind and runoff events suspend sediments in the water column and light levels decrease until the sediments settle (Aumack et al. 2007, Bonsell and Dunton, 2018). Comparisons between sites agree with past studies that showed daily underwater light levels are often elevated at the deep, offshore sites (Table 1.3) where concentrations of suspended sediment are reduced (Aumack et al. 2007, Bonsell and Dunton 2018).

Unlike other variables, current velocity and direction show large spatial variability in both summer and into winter, connected to the bathymetry and physiography of Stefansson Sound (Tables 1.2 and 1.3, Figs. 1.3, 1.5 and 1.6). In winter, currents are minimal at most shallow sites (E1, L1; <2 cm s^{-1}). Offshore circulation patterns may influence sites adjacent to deep areas (W1, DS11 and W3, Fig. 1.1), and result in larger variability in winter current velocities, though overall velocities remained low (<3 cm s^{-1}), similar to winter measurements made by Matthews (1981) at DS11. Without direct influence from surface winds, currents appear more tidally influenced during winter and spring (Figs. 1.5 and 1.6). After ice break-up, flow direction becomes much more variable, as water motion becomes influenced by surface winds (Weingartner et al., 2017). Alongshore currents dominate across the Boulder Patch (Figs. 1.5 and 1.6). Wind driven flows periodically reach above 15 cm s^{-1}, usually associated with easterly winds (Figs. 1.5 and 1.7). Spatial variability in current velocity and direction is related to geomorphology and bathymetry: W1, which is less protected and closer to a deep inter island pass than the other shallow sites (Fig. 1.1), has the highest mean current velocity in summer and fall (> 8 cm s^{-1}; Table 1.2, Fig. 1.3). The nearby deep site, W3, also experiences elevated flow velocity during summer and fall, as does DS11 (means >6 cm s^{-1}). Flow speeds are less than those measured north of Stefansson Sound at 17 m depth, which can reach above 50 cm s^{-1} in the fall (Weingartner et al. 2017), and the shallow sites closer to Foggy Island Bay have even lower mean current speeds (≤5 cm s^{-1}). Strong east wind events during late summer and fall result in elevated current velocity, often bearing northwest, until freeze-up is complete (Figs. 1.2 and 1.5). The W3 site mooring was lost to ice scour during one such fall storm in 2015. We were able to reconstruct the event to the day (11 October 2015) by a sudden increase in current speeds across Stefansson Sound leading up to instrument loss, which corresponded to a days-long easterly wind event (Figs. 1.2 and 1.5), which would have pushed drifting ice into and across Stefansson Sound (Fig. 1.6). This annual cycle of current velocity, driven by ice cover and wind, reflects previous studies in Stefansson Sound (Weingartner et al. 2017).

Long-term change

In Stefansson Sound, the ice free season has lengthened by ~17 days over the past four decades (Bonsell and Dunton 2018). Comparisons to previous studies suggest that Stefansson Sound is warming as well: the average temperature at DS11 for August 1987-August 1988 was -1.25±1.42°C (Sellmann et al. 1992), compared to our August 2011-July 2017 average of -0.76±1.97°C (Fig. 1.10). The spring freshet signal was also absent from the 1988 temperature record, leading to a difference of 0.3 degrees in average May-June temperature (2012-2017 mean±SD: -1.58±0.20, 1988 mean±SD: -1.82±0.08, Fig. 1.10). Long-term warming may be confined to the spring and summer months, since our winter measurements of benthic temperature and salinity at DS11 mirror those collected at midwater depths from November 1978- February 1979 (-1.98--1.80 °C, salinity 32.5-34.3; Matthews, 1981a). The longer open-water season in the landfast ice zone during the recent decade is a

result of temperatures increasing earlier and decreasing later in the year (Fig. 1.10; Mahoney et al. 2014). While the range of salinities appears similar, summertime salinities dropped later in the year in 1987 due to a later melt season.

A longer ice-free season would profoundly impact annual current dynamics. Of the variables we measured, currents responded most immediately to ice break-up and freeze-up, which confines the interaction between wind forcing and water motion (Figs. 1.2 and 1.5; Weingartner et al. 2017). Earlier melt and later freeze-up would raise annual mean current velocity. Additionally, strengthened easterly winds in the Beaufort Sea region (Wood et al. 2013, 2015) would intensify advection from Stefansson Sound. This would potentially increase summer salinities at the benthos by transporting buoyant freshwater offshore.

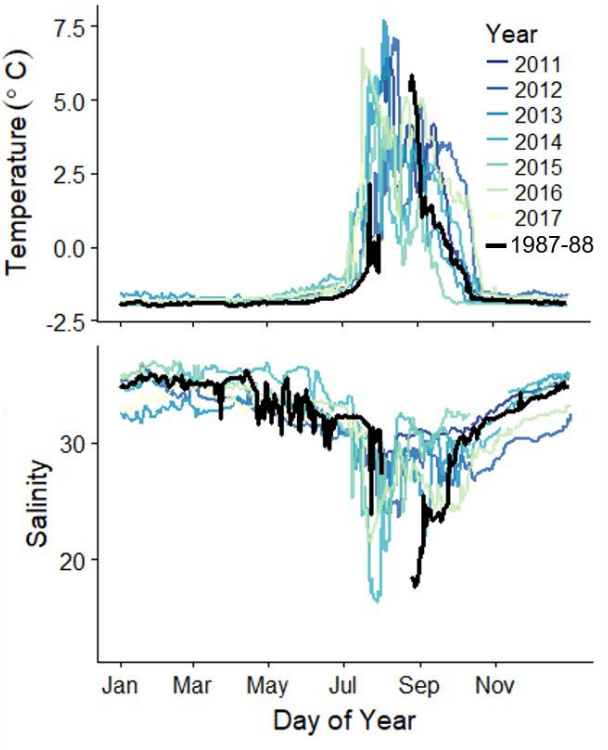

Figure 1.10. Temperature and salinity at DS11 for 2011-2017 (colored lines, this study) compared to 25 August 1987 to 11 August 1988 (black line, Sellmann et al. 1992).

Implications for the benthic ecosystem

In river fed estuaries, the flow of freshwater can create gradients that affect ecological and biogeochemical processes. The extent and character of these gradients impact the ecosystem function of the estuary. In this study, we have demonstrated that the freshwater plume associated with the freshet can bathe shallow portions of Stefansson Sound in low salinity water, reaching down to ~4 m in certain years (Figs. 1.2 and 1.3). Arctic river water differs from seawater not only in salinity, but in other chemical constituents, which could affect the physiology of

benthic organisms underlying the buoyant layer. Nutrient depleted river water displaces seawater high in inorganic nutrients, which have built up over the winter, which may result in significant nutrient stress for benthic autotrophs. Additionally, the organic composition of freshwater could create zones of differential biological activity and biogeochemical processes. For example, the dissolved organic matter associated with the freshet is highly labile (Holmes et al. 2008). If mixing is minimal (as it is under the ice), a nearshore zone with high concentrations of labile DOM could impact sediment microbial diversity and activity.

Current dynamics also influence the benthic realm by determining rates of sedimentation, as well as the delivery of food and nutrients to benthic organisms (e.g., Pequegnat 1964, Sebens 1984). High flow speeds can also mechanically stress or remove attached flora and fauna. Additionally, current dynamics determine the advection and transport of planktonic propagules, thereby impacting population connectivity and persistence within the region (e.g., Cowen and Sponaugle 2009, Coleman et al. 2011). The annual cycle of minimal currents in the winter and maximal currents in the fall imply that propagule transport for any given species greatly depends on the timing of its life cycle. Differences in current regime between the eastern Boulder Patch sites and the deep and western sites (Figs. 1.5-1.7) suggest that these locations may have differing rates of propagule advection and delivery, which could affect benthic community structure and genetic diversity. Intensified easterly winds (Wood et al. 2013, 2015) and a longer open-water season (Mahoney et al. 2014) in the Beaufort Sea would increase the advection of terrestrial material, nutrients, plankton, and propagules away from the coastal zone.

Studies that focus on estuarine processes within the Arctic are rare, and even fewer studies cover time periods outside of mid- to late summer (McClelland et al. 2012). However, as demonstrated here, environmental variability occurs during periods outside the summer months that could profoundly affect nearshore ecosystems. Knowledge of the range and spatial patterns of abiotic conditions provide the conceptual basis to evaluate and understand ecosystem processes and function on Arctic inner shelves.

APPENDIX

Supplementary Table S1.1. Results table for comparing each abiotic factor among sites via a blocked ANOVA (blocked by day) for the entire data record.

Season		**Variable**	**Sig diff. by site?**
All		Temperature	Yes
	Sum Sq.	**DF**	**F**
Intercept	153.0	1	37.08
Site	188.5	4	11.42
Day	210.3	1	50.95
Residuals	30295.3	7340	
Season		**Variable**	**Sig diff. by site?**
Ice covered winter		Temperature	Yes
	Sum Sq.	**DF**	**F**
Intercept	12.62	1	1326.85
Site	2.21	4	58.18
Day	0.15	1	15.77
Residuals	29.01	3051	
Season		**Variable**	**Sig diff. by site?**
Spring break-up		Temperature	Yes
	Sum Sq.	**DF**	**F**
Intercept	2.38	1	19.29
Site	18.51	4	37.57
Day	0.03	1	0.24
Residuals	149.55	1214	
Season		**Variable**	**Sig diff. by site?**
Open water summer		Temperature	Yes
	Sum Sq.	**DF**	**F**
Intercept	137.8	1	27.90
Site	486.5	4	24.62
Day	82.2	1	16.65
Residuals	8802.7	1782	
Season		**Variable**	**Sig diff. by site?**
Fall freeze-up		Temperature	No
	Sum Sq.	**DF**	**F**
Intercept	20.17	1	22.17
Site	2.72	4	0.75
Day	8.88	1	9.76

Residuals	1160.22	1275	
Season		**Variable**	**Sig diff. by site?**
All		Salinity	Yes
	Sum Sq.	**DF**	**F**
Intercept	4886	1	364.16
Site	3278	4	61.08
Day	171	1	12.72
Residuals	73888	5507	
Season		**Variable**	**Sig diff. by site?**
Ice covered winter		Salinity	Yes
	Sum Sq.	**DF**	**F**
Intercept	3738.8	1	2016.10
Site	609.3	4	82.14
Day	24.2	1	13.06
Residuals	4066.9	2193	
Season		**Variable**	**Sig diff. by site?**
Spring break-up		Salinity	Yes
	Sum Sq.	**DF**	**F**
Intercept	519.9	1	46.53
Site	1600.5	4	35.81
Day	116.6	1	10.43
Residuals	10437.6	934	
Season		**Variable**	**Sig diff. by site?**
Open water summer		Salinity	Yes
	Sum Sq.	**DF**	**F**
Intercept	2367.7	1	211.53
Site	1432.7	4	31.97
Day	133.8	1	11.94
Residuals	17408.8	1554	
Season		**Variable**	**Sig diff. by site?**
Fall freeze-up		Salinity	Yes
	Sum Sq.	**DF**	**F**
Intercept	2060.6	1	428.57
Site	131.2	4	6.82
Day	191.1	1	39.74
Residuals	3885.0	808	
Season		**Variable**	**Sig diff. by site?**
All		PAR	No
	Sum Sq.	**DF**	**F**
Intercept	0.01	1	0.01
Site	4.81	4	1.46
Day	0.27	1	0.33
Residuals	3000.75	3654	

Season		**Variable**	**Sig diff. by site?**
Ice covered winter		PAR	No
	Sum Sq.	**DF**	**F**
Intercept	0.0005	1	0.60
Site	0.0030	3	1.28
Day	0.0001	1	0.09
Residuals	1.1660	1507	
Season		**Variable**	**Sig diff. by site?**
Spring break-up		PAR	No
	Sum Sq.	**DF**	**F**
Intercept	0.04	1	1.37
Site	0.02	3	0.30
Day	0.02	1	0.70
Residuals	16.16	605	
Season		**Variable**	**Sig diff. by site?**
Open water summer		PAR	Yes
	Sum Sq.	**DF**	**F**
Intercept	9.29	1	3.40
Site	61.27	4	5.60
Day	15.10	1	5.52
Residuals	2491.96	911	
Season		**Variable**	**Sig diff. by site?**
Fall freeze-up		PAR	No
	Sum Sq.	**DF**	**F**
Intercept	0.045	1	29.19
Site	0.003	3	0.70
Day	0.460	1	26.60
Residuals	0.940	615	
Season		**Variable**	**Sig diff. by site?**
All		Current velocity	Yes
	Sum Sq.	**DF**	**F**
Intercept	3835	1	243.08
Site	6335	4	100.38
Day	3353	1	212.49
Residuals	54293	3441	
Season		**Variable**	**Sig diff. by site?**
Ice covered winter		Current velocity	Yes
	Sum Sq.	**DF**	**F**
Intercept	10.40	1	14.78
Site	198.55	4	70.58
Day	5.97	1	8.49
Residuals	953.65	1356	

Season		**Variable**	**Sig diff. by site?**
Spring break-up		Current velocity	Yes
	Sum Sq.	**DF**	**F**
Intercept	21.55	1	32.73
Site	91.89	4	34.90
Day	17.24	1	26.19
Residuals	357.47	543	
Season		**Variable**	**Sig diff. by site?**
Open water summer		Current velocity	Yes
	Sum Sq.	**DF**	**F**
Intercept	160.8	1	9.65
Site	2097.0	4	31.45
Day	78.8	1	4.72
Residuals	15235.2	914	
Season		**Variable**	**Sig diff. by site?**
Fall freeze-up		Current velocity	Yes
	Sum Sq.	**DF**	**F**
Intercept	2.8	1	0.08
Site	2680.2	4	18.81
Day	25.3	1	0.71
Residuals	21733.6	610	

2. Spatial and temporal trends in community composition in the Arctic Boulder Patch

Katrin Iken and Brenda Konar

INTRODUCTION

The Alaskan Beaufort Sea seafloor is, like most Arctic shelves, typically dominated by soft sediments (Carmack and MacDonald 2002). In isolated nearshore locations, however, sea ice deposited rocks create hard substratum that can be colonized by a markedly different fauna and flora than found in the surrounding low-diversity soft sediment areas (Dunton and Schell 1986). These rocky areas are biodiversity hotspots that support tightly linked food webs, based on benthic primary producers (macroalgae) that typically do not occur on Arctic shelves (Dunton et al. 1982). The high biodiversity associated with rocky areas lies primarily with the availability of hard substratum, providing structural habitat for an epilithic community, and with the presence of large macroalgae that serve as foundation species for associated organisms (Steneck et al. 2002, Christie et al. 2003, Filbee-Dexter et al. 2018). The communities inhabiting these nearshore rocky areas are structured by physical factors, e.g., sea ice, presence of substratum, light, and sedimentation (Dunton and Dayton 1995, Aumack et al. 2007, Konar 2007, Zacher et al. 2009, Bonsell and Dunton 2018) as well as by complex biological interactions, such as competition (Barnes 2002, Barnes and Kuklinski 2004, Konar and Iken 2005, Campana et al. 2009).

The Boulder Patch in Stefansson Sound is considered a regional biodiversity hotspot with higher macroalgal and invertebrate diversity than in the surrounding regions (Dunton and Schonberg 2000). While the overall area of the Boulder Patch is approximately 63 km^2, environmental conditions such as light availability can differ considerably among different locations within the Boulder Patch region. Given that biological communities are driven strongly by the physical environment (Bonsell and Dunton 2018), it would stand to reason that community composition and biodiversity of the epilithic community differs among the different locations within the Boulder Patch. We here explored whether epilithic community patterns differed among various sites in the Boulder Patch and if these spatial differences were consistent over time. In addition, we tested whether community patterns in a smaller boulder region in Camden Bay were like those in the Boulder Patch and how these regional differences compared to local spatial differences.

METHODS

Epilithic communities associated with deposited boulders were sampled at six sites (DS11, E1, E2, E3, W1, W2, W3) in the summers (early August) of 2005,

2006, 2013, and 2015. All sampling was done using SCUBA, following protocols established by the Census of Marine Life 'NaGISA' Project (Natural Geography in Shore Areas; Rigby et al. 2007). Macroalgal and invertebrate assemblages were sampled from 10 randomly placed 0.25 m^2 quadrats. All macroalgal and invertebrate samples were collected and placed in fine mesh bags *in situ*. All samples were carefully washed over 500 µ mesh and the retained fraction sorted under a compound microscope. Macroalgae were identified to species level where possible and wet weight determined to 1 g precision. Macroalgal identifications were assisted by taxonomic experts (Sandra Lindstrom, University of British Colombia, Canada; Robert Wilce, University of Massachusetts Amherst (emeritus), USA; Christian Wiencke, Alfred Wegener Institute, Germany). In several cases it was unclear if different species identifications were due to regional differences or to different specialists identifying algae from different regions. As to not overestimate regional differences in the algal community, we therefore performed these comparisons based on the genus level. Invertebrates were sorted and identified to species or higher taxonomic level in those cases where species identifications were impossible (taxonomic assistance by Susan Schonberg, University of Texas, USA). Invertebrate wet biomass was determined to 0.0001 g accuracy. All invertebrates were preserved in 10% buffered formalin and later transferred into 50% isopropanol for long-term storage at the University of Alaska Fairbanks.

In addition to collections in the Boulder Patch, we performed similar collections in Camden Bay in 2005 (macroalgae only), 2007, and 2017. Except for 2017, collections in Camden Bay were done on five replicate quadrats per site. Macroalgal samples were done at site DSE, DSC and DSW in 2005, and sites DSW and DS4 were sampled for macroalgae and invertebrates in 2007 and 2017. Samples were processed as described for those in the Boulder Patch.

Community data were analyzed using multivariate statistics in the software package PRIMER™ version 7 (Clarke et al. 2014). Macroalgal and invertebrate assemblages were analyzed separately to account for the vast differences (by >3-4 orders of magnitude) larger algal biomass than invertebrate biomass and to assess if the two groups showed similar patterns. Both datasets were first dispersion-weighted to account for the large variance in some of the taxa (e.g., kelp in macroalgal and sea stars in invertebrate datasets, respectively, could have very small or very large biomass in different replicates, leading to large variance). Distribution of taxa across replicates was then assessed via shade plots and both datasets square-root transformed, which reduced the weight of outlier values and led to comparable data ranges in both datasets. A resemblance matrix using Bray-Curtis similarities was created including a 0.1 dummy variable to account for the lack of variance because some replicates did not contain any biological material (all macroalgal and invertebrate biomass was zero). The effects of time (year) and location (site) was tested using PERMANOVA, with year as a random factor and site as fixed factor. A SIMPER analysis was conducted on both macroalgal and invertebrate datasets to identify taxa that contributed to differences in the assemblages among sites and/or years. Shannon's Diversity index [H' = SUM(Pi*ln(Pi))] and Pielou's Evenness index [J' = H'-Log(S)] were calculated, where Pi is the proportion of species *i* relative to the

total number of species, and S is the total number of species. The distance to centroids in the data matrix was used to assess dispersion of communities at the seven study sites over time, measuring the "spread" or heterogeneity of data within the assemblages. Differences in distance to centroid for each site across study years were statistically tested using ANOVA. A Euclidean distance matrix was applied to dispersion measures from a PERMDISP analysis to test for significant differences in a PERMANOVA design with year as a random factor and site as fixed factor.

We also sampled epilithic communities in Camden Bay during some of the study years (2005, 2007, 2017). Sampling protocols were like those employed in the Boulder Patch although replication was typically limited to 5 replicates instead of 10 but level of analysis was typically the same (except that in 2005, invertebrate assemblages were not identified for biomass in Camden Bay). Also, sampling site selection in Camden Bay was more haphazard than in the Boulder Patch and sites were not possible to consistently revisit over sampling years, making the assessment of temporal trends more difficult. Only one site (DSW) was sampled in all three years, and site DS4 was sampled in 2007 and 2017. Data for Camden Bay (macroalgae and invertebrates considered separately) were treated as described for the Boulder Patch data. Camden Bay assemblages were assessed via diversity measures (Pielou's and Shannon), hierarchical cluster analysis, and nMDS plots. Assemblage composition was compared between the two regions (Boulder Patch and Camden Bay) using Analysis of Similarity (ANOSIM) and by hierarchical cluster analysis. A SIMPROF test examined statistical differences ($p=0.05$) among clusters and a SIMPER analysis identified taxa that contributed most to differences in groupings.

Table 2.1. Macroalgal biomass (g wet weight 0.25 m^{-2}) at seven sites in the Boulder Patch over four study years.

Site	Year	*Phycodrys* sp.	*Coccotylus truncatus*	*Dilsea* sp.	*Odonthalia dentata*	*Rhodomela* sp.	*Chaetomorpha melagonium*	*Laminaria solidungula*	*Saccharina latissima*	*Alaria esculenta*	*Chaetopteris plumosa*	*Battersia arctica*	*Ahnfeltia plicata*
DS11	2005	13.7	10.6	6.3	0.5	0.5	0.0	40.6	0.0	0.0	0.0	0.0	0.0
E1	2005	30.3	29.8	4.5	1.1	0.5	0.0	2.6	0.0	0.0	0.3	0.0	0.0
E2	2005	26.6	17.0	0.5	0.5	0.2	0.0	7.4	0.0	0.0	0.1	0.0	0.0
E3	2005	4.0	7.8	1.1	0.1	0.0	0.0	7.5	0.0	0.0	0.0	0.0	0.0
W1	2005	9.6	4.8	0.2	1.1	0.0	0.0	6.3	0.0	0.0	0.0	0.0	0.0
W2	2005	13.1	11.5	0.0	0.0	0.0	0.0	8.6	0.0	0.0	0.0	0.0	0.0
W3	2005	22.9	17.7	16.0	3.5	5.5	0.0	23.3	0.0	0.0	0.0	0.0	0.0
DS11	2006	25.0	15.2	26.5	0.8	1.8	0.0	28.8	18.0	2.7	0.0	0.0	0.0
E1	2006	42.0	19.0	1.6	0.5	0.1	0.1	8.5	0.0	0.0	0.4	0.0	0.0
E2	2006	22.9	9.6	0.3	0.2	0.0	0.0	35.5	0.0	0.0	0.0	0.0	0.7
E3	2006	17.3	7.6	12.0	0.0	0.0	0.0	24.9	0.0	0.0	0.0	0.0	0.0
W1	2006	18.7	4.6	1.4	0.3	0.0	0.0	9.1	0.0	0.0	0.0	0.0	0.0
W2	2006	44.7	43.8	0.3	0.0	0.0	0.0	43.8	0.0	0.0	0.2	0.0	0.0
W3	2006	68.0	42.2	49.6	2.5	3.3	0.0	128.6	14.3	0.0	0.0	0.0	0.0
DS11	2013	15.4	7.2	16.7	0.3	0.4	0.0	14.9	19.6	0.0	0.0	0.0	0.2
E1	2013	13.5	6.8	3.0	0.5	0.5	0.0	19.6	4.4	0.0	3.4	1.1	0.0
E2	2013	54.5	14.5	1.4	1.0	0.1	0.0	11.3	0.4	0.0	0.3	0.3	0.0
E3	2013	14.7	7.9	16.2	0.1	0.4	0.0	18.4	0.0	0.0	0.0	0.0	0.0
W1	2013	12.6	5.0	15.1	0.2	2.3	0.0	7.7	0.2	0.0	0.0	0.0	0.0
W2	2013	4.0	4.3	0.1	0.0	0.1	0.0	7.0	0.0	0.0	0.0	0.0	0.0
W3	2013	14.4	15.9	8.6	0.0	3.4	0.0	15.6	0.2	0.0	0.0	0.0	0.0
DS11	2015	35.0	31.5	27.7	1.4	1.1	0.0	22.7	58.1	7.3	0.0	0.0	0.6
E1	2015	21.3	29.5	1.4	1.6	0.2	0.0	1.0	0.7	0.0	3.8	0.4	0.0
E2	2015	28.7	18.0	5.7	2.7	0.1	0.0	18.4	0.0	0.0	1.8	0.1	0.0
E3	2015	31.1	16.3	16.0	0.0	0.5	0.0	14.3	0.9	0.0	1.3	0.0	1.2
W1	2015	15.4	13.0	6.9	0.0	0.0	0.0	18.4	0.0	0.0	0.0	0.0	0.0
W2	2015	10.3	11.2	0.1	0.3	0.0	0.0	2.2	0.0	0.0	0.0	0.0	0.0
W3	2015	34.4	19.5	17.4	1.9	5.1	0.0	32.2	6.4	0.0	0.0	0.0	0.0

Table 2.2. Invertebrate biomass (g wet weight 0.25 m^{-2}) at seven sites in the Boulder Patch over four study years.

		ARTHROPODA				MOLLUSCA			ANNELIDA	ECHINODERMATA		CNIDARIA			ASCIDIACEA	BRYOZOA	PORIFERA	NEMERTEA
Site	Year	Amphipoda	Isopoda	Decapoda	Crustacea other	Pyrenogonida	Gastropoda	Polyplacophora	Bivalvia	Polychaeta	Asteroidea	Holothuroidea	Anthozoa	Hydrozoa	Cnidaria other	Ascidiacea	Bryozoa	Porifera	Nemertea
DS11	2005	0.00	0.00	0.00	0.00	0.00	0.07	0.52	0.00	0.13	0.04	0.00	0.00	0.49	0.00	0.00	0.20	0.56	0.00
E1	2005	0.00	0.31	0.00	0.03	0.00	0.00	0.00	0.10	0.01	0.00	0.00	0.00	0.01	0.00	0.00	2.44	0.17	0.00
E2	2005	0.00	0.08	0.00	0.00	0.00	0.01	0.00	0.01	0.02	0.00	0.00	0.00	0.53	0.00	0.00	0.54	0.29	0.00
E3	2005	0.01	0.00	0.00	0.00	0.00	0.02	0.00	0.00	0.03	0.00	0.00	0.00	0.50	0.00	0.00	0.07	1.88	0.00
W1	2005	0.00	0.00	0.00	0.00	0.00	0.02	0.01	0.00	0.01	0.00	0.00	0.03	1.60	0.00	0.00	0.19	1.71	0.00
W2	2005	0.02	0.39	0.00	0.00	0.00	1.13	0.11	0.00	0.05	8.40	0.00	0.34	0.86	0.00	0.00	0.60	4.88	0.00
W3	2005	0.00	0.00	0.00	0.00	0.00	0.01	0.24	0.00	0.00	0.01	0.00	0.71	0.17	0.00	0.01	0.18	0.24	0.00
DS11	2006	0.02	0.00	0.00	0.00	0.01	0.02	0.12	1.37	0.06	0.01	0.00	0.00	0.39	0.00	0.00	0.84	6.42	0.00
E1	2006	0.01	0.07	0.00	0.25	0.00	0.00	0.00	0.25	0.00	0.00	0.00	0.00	0.15	0.00	0.03	3.02	1.39	0.00
E2	2006	0.02	0.12	0.00	1.39	0.00	0.00	0.77	0.18	0.00	0.00	0.00	0.00	0.51	0.00	0.01	1.57	0.69	0.00
E3	2006	0.00	0.59	0.00	0.00	0.00	0.02	0.15	0.01	0.05	0.00	0.00	0.00	1.02	0.00	0.03	0.47	0.44	0.00
W1	2006	0.09	0.00	0.00	0.00	0.02	0.00	0.07	0.00	0.04	0.00	0.00	0.18	1.11	0.00	0.02	0.76	0.39	0.00
W2	2006	0.01	0.00	0.00	0.00	0.00	0.02	0.00	0.01	0.14	0.02	0.00	0.70	0.82	0.00	0.03	2.17	0.66	0.00
W3	2006	0.00	0.00	0.00	0.00	0.02	0.05	0.42	0.01	0.04	0.12	0.71	0.30	0.10	0.00	0.00	0.55	3.37	0.00
DS11	2013	0.01	0.00	0.31	0.00	0.00	0.06	0.38	0.57	0.05	0.01	0.00	0.02	0.67	0.01	0.00	0.11	1.38	0.00
E1	2013	0.04	0.41	0.00	0.06	0.00	0.03	0.00	0.11	0.00	0.00	0.00	0.58	0.36	0.00	0.00	0.17	0.55	0.00
E2	2013	0.07	0.69	0.00	0.00	0.01	0.00	0.00	0.10	0.02	0.00	0.00	0.00	0.12	0.00	0.00	1.10	1.11	0.00
E3	2013	0.03	0.00	0.83	0.00	0.01	0.03	0.36	0.03	0.02	0.01	0.00	0.00	0.19	0.00	0.00	0.05	0.24	0.00
W1	2013	0.00	0.00	0.00	0.00	0.03	0.20	0.42	0.00	0.02	0.20	0.00	1.45	0.34	0.00	0.33	0.08	0.33	0.00
W2	2013	0.01	0.36	0.00	0.00	0.02	0.03	0.67	0.00	0.06	0.09	0.00	1.99	0.06	0.00	0.00	0.16	0.63	0.00
W3	2013	0.00	0.00	0.00	0.00	0.01	1.17	0.16	0.20	0.04	0.00	1.22	0.04	0.12	0.00	0.05	0.45	0.05	0.00
DS11	2015	0.00	0.00	0.00	0.00	0.00	0.13	0.49	0.00	0.20	0.00	0.00	0.00	0.51	0.00	0.01	6.26	11.79	0.00
E1	2015	0.13	0.05	0.00	0.00	0.00	0.00	0.00	0.00	0.01	0.00	0.00	0.00	0.06	0.00	0.00	0.72	0.49	0.00
E2	2015	0.11	0.43	0.00	0.31	0.00	0.01	0.00	0.29	0.02	0.00	0.00	0.00	0.46	0.00	0.00	0.33	2.66	0.00
E3	2015	0.09	0.91	0.00	0.00	0.01	0.03	0.27	0.01	0.08	0.02	0.00	0.00	0.05	0.00	0.00	2.72	4.81	0.00
W1	2015	0.05	0.74	0.00	0.00	0.01	0.09	0.11	0.00	0.08	0.19	0.00	1.54	0.15	0.00	0.00	0.32	8.32	0.00
W2	2015	0.00	0.00	0.00	0.00	0.01	0.02	0.00	0.00	0.01	17.69	0.00	2.17	0.05	0.00	0.00	0.15	3.00	0.00
W3	2015	0.07	0.00	1.18	0.00	0.02	0.09	0.17	0.00	0.02	0.10	0.00	0.93	0.02	0.00	0.03	5.64	10.68	0.00

RESULTS

Boulder Patch

Over the four investigation years, we observed 12 macroalgal species and 249 invertebrate taxa across the Boulder Patch. Not all taxa occurred in collections in all years, but some taxa were common and typically dominated the community in terms of biomass (Tables 2.1 and 2.2). Macroalgal biomass ranged from 15.6 – 308.5 g wet weight 0.25 m^{-2} per sites and year (Fig. 2.1). Among the macroalgae, the kelp *Laminaria solidungula* and the red algae *Phycodrys* sp., *Coccotylus truncatus* and *Dilsea* sp. were typically the largest biomass contributors (Fig. 2.1). Kelps contributed much to the variability in total biomass at particular sites per year. Invertebrate biomass was an order of magnitude lower than that of macroalgae and ranged from 1.4 – 19.4 g wet weight 0.25 m^{-2} per sites and year (Fig. 2.1). Most invertebrate biomass was contributed by Porifera (39% of total invertebrate biomass), Bryozoa (18%), Echinodermata (esp. Asteroidea, 15%), Hydrozoa and Cnidaria (both 6%). Among those, biomass of Cnidaria and Asteroidea was highly clumped at some sites (Fig. 2.2).

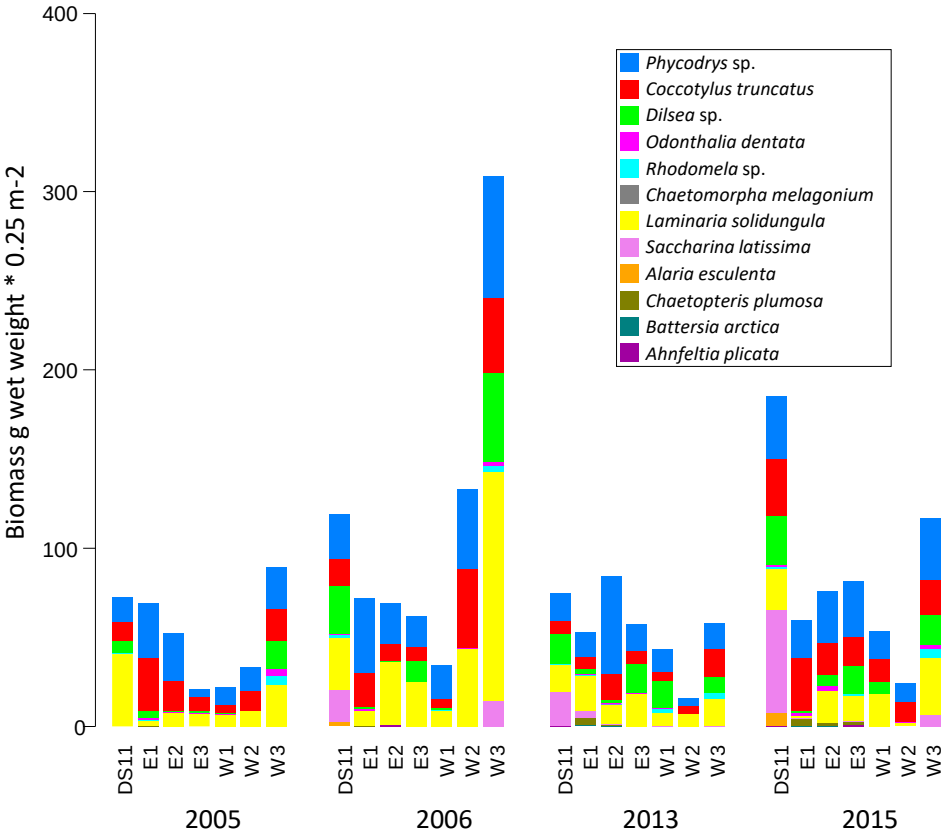

Figure 2.1. Macroalgal species biomass (g wet weight 0.25 m^{-2}) at seven sites in the Boulder Patch over four study years.

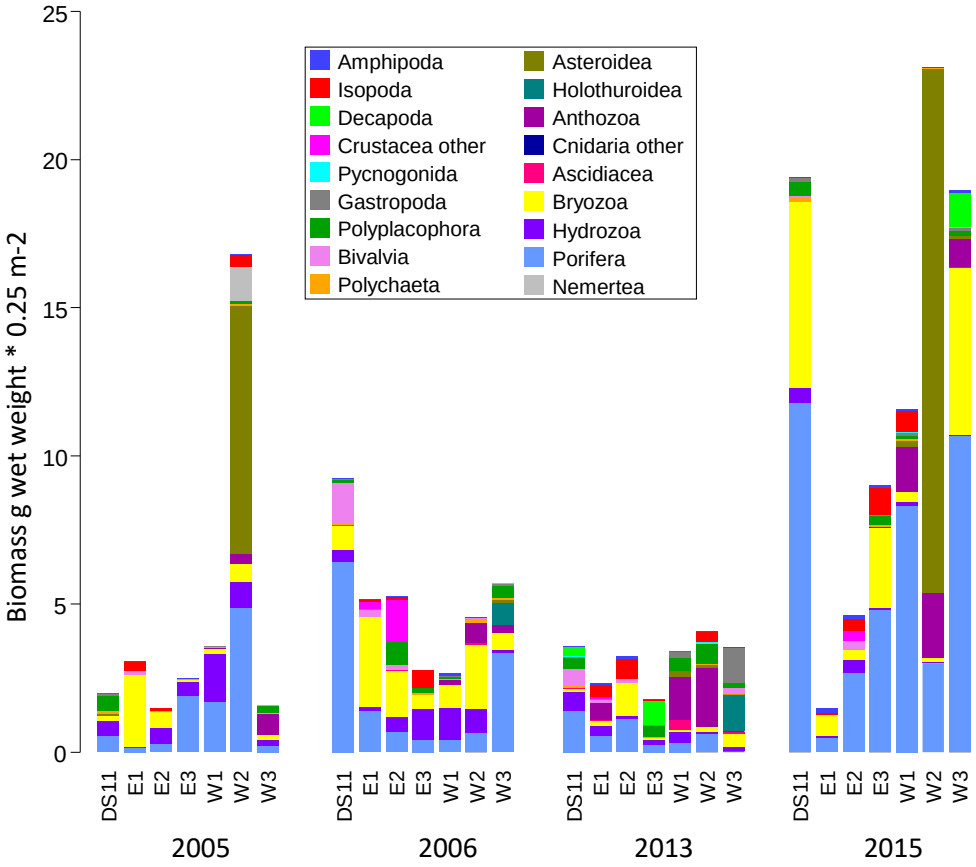

Figure 2.2. Invertebrate taxon biomass (g wet weight 0.25 m^{-2}) at seven sites in the Boulder Patch over four study years.

The interaction term year x site in the PERMANOVA of the macroalgal dataset was significant, indicating that the change in macroalgal assemblage among sites was dependent on the year of investigation, with the interaction term explaining about 14% of total variability (Table 2.3a). Site itself had a stronger effect on macroalgal assemblage composition than year in this analysis (15% versus 5% of the variance explained, respectively). The year x site effect (Table 2.3a) was also illustrated in the nMDS plot where especially the assemblage in 2013 was very different from the assemblages in other years for most sites (strong effects at DS11, E1, W2 and W3) while the 2013-year effect was less noticeable at the other sites (Fig. 2.3). The residual effect was large (65%), pointing towards other drivers of patterns in macroalgal assemblages, not explained by sites and years. Strong site differences were mostly driven by greater biomass of *Rhodomela* sp. at DS11 and W3, *Dilsea* sp. being generally higher at DS11, E3 and W3, and *Odonthalia dentata* particularly low at several sites in 2013 (Fig. 2.4). Shannon diversity was variable across sites and years but tended to be higher in later years (Fig. 2.5). Evenness also was variable, but generally slightly lower at sites E1 and E2. Similar to assemblage structure, dispersion within the assemblages was significantly affected by the year x site interaction (19% of variance), although the effect of "site" alone was negligible

in this analysis (Table 2.3b). Dispersion, measured as the distance to centroid, was significantly larger in 2013 at sites DS11, E1, and W2 (Fig. 2.6).

Table 2.3. PERMANOVA results of Boulder Patch macroalgal assemblage composition by year and site (a) and of dispersion of Boulder Patch macroalgal assemblages by year and site (b).

a

Source	df	SS	MS	Pseudo-F	P(perm)	Unique perms
year	3	21600	7200	6.4453	0.001	9905
site	6	84169	14028	3.9108	0.001	9913
year x site	18	64566	3587	3.211	0.001	9809
Residual	252	2.82E+05	1117.1			
Total	279	4.52E+05				

Estimates of components of variation

Source	Estimate	Sq.root	% Variance
V(year)	86.898	9.3219	5.1
S(site)	261.03	16.156	15.2
V(yexsi)	246.99	15.716	14.4
V(Res)	1117.1	33.423	65.3

b

Source	df	SS	MS	Pseudo-F	P(perm)	Unique perms
year	3	5707	1902.3	18.922	0.0001	9946
site	6	1335.1	222.51	0.58501	0.7393	9947
year x site	18	6846.4	380.36	3.7833	0.0001	9906
Residual	252	25335	100.54			
Total	279	39224				

Estimates of components of variation

Source	Estimate	Sq.root	% Variance
V(ye)	25.74	5.0734	17.1
S(si)	-3.9461	-1.9865	-2.6
V(yexsi)	27.982	5.2898	18.6
V(Res)	100.54	10.027	66.9

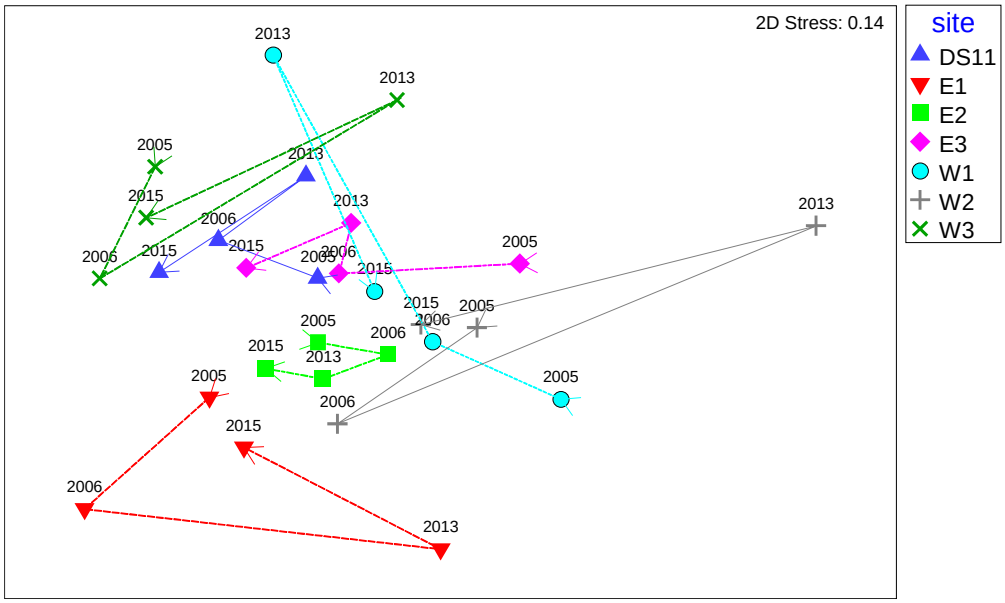

Figure 2.3. nMDS (non-metric Multidimensional Scaling) plot of macroalgal assemblages at seven sites in the Boulder Patch over four study years. Sites are represented as different symbols and years are indicated in the plot. Trajectories indicate direction of change in macroalgal assemblage structure over time per site.

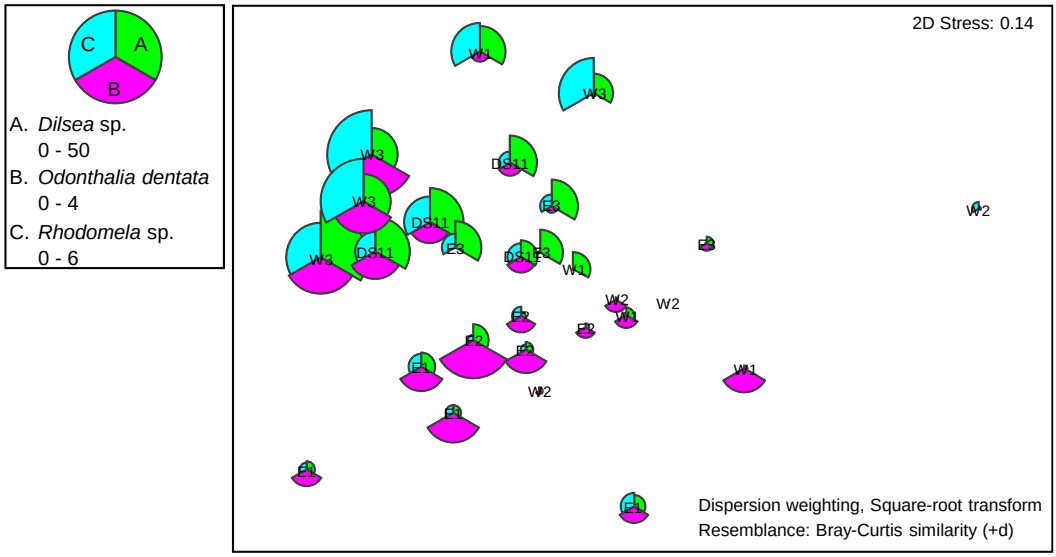

Figure 2.4. Macroalgal species contributing to the differences in assemblage structure among sites in the Boulder Patch. Species are indicated as pie slices (A-C) with pie pieces proportional to the range of biomass within each taxon.

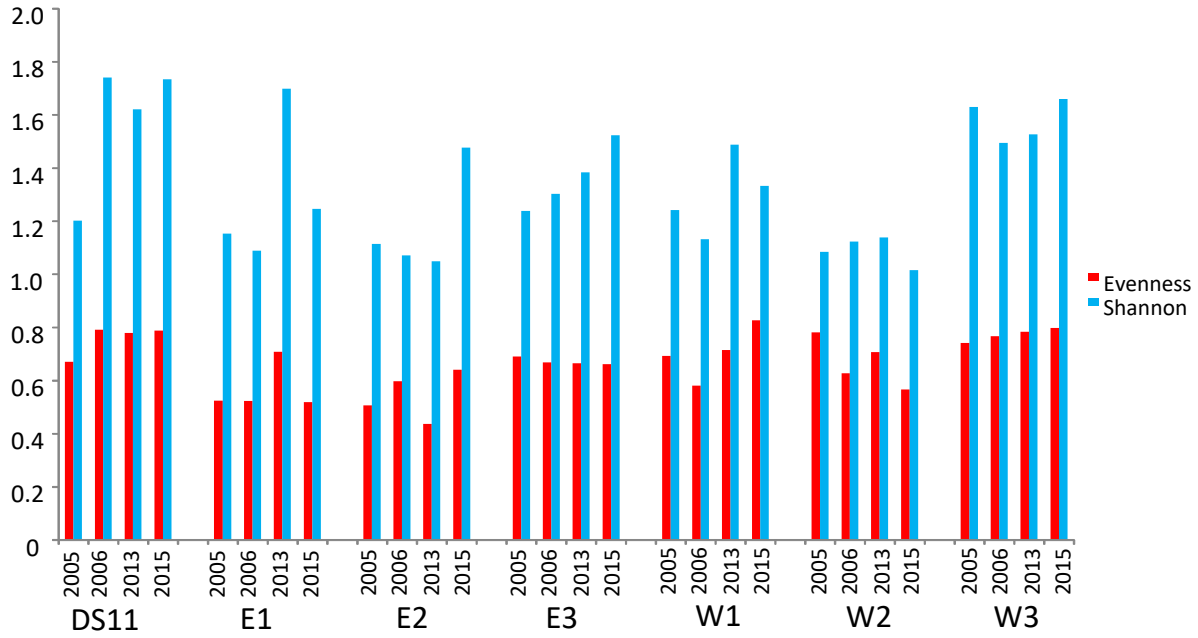

Figure 2.5. Shannon Wiener diversity index (H') and Pielou's evenness index (J') for macroalgal assemblages at seven sites in the Boulder Patch over four study years.

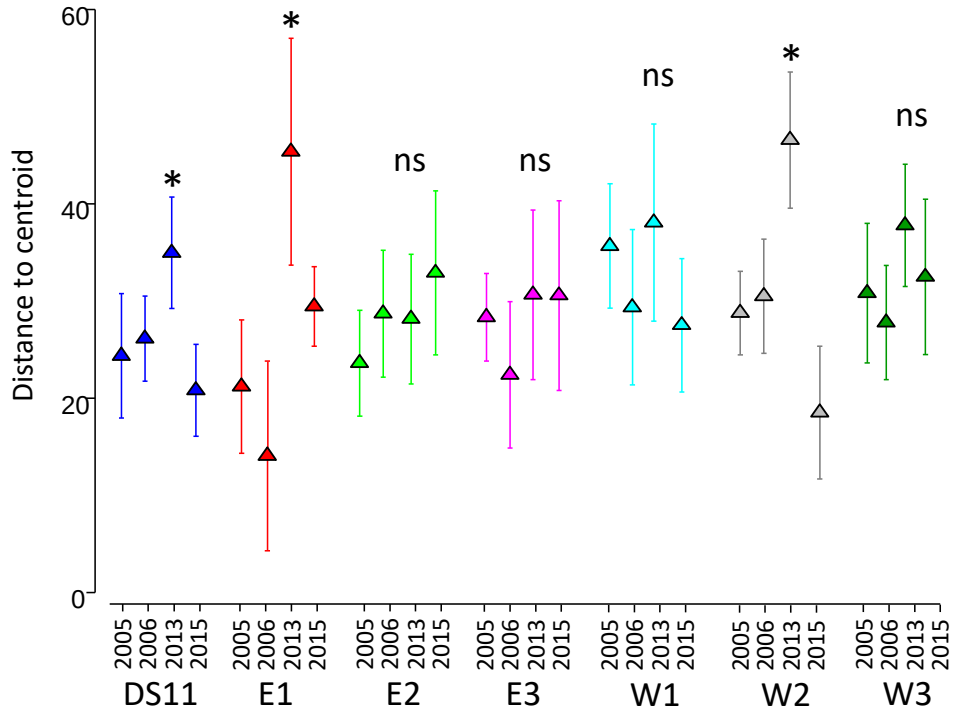

Figure 2.6. Mean dispersion, measured as the distance to centroid, for macroalgal assemblages at seven sites in the Boulder Patch over four study years. Dispersion is a measure of the scatter within the multivariate assemblage. Asterisks above means indicate significant (ANOVA, p≤0.05) differences among years within each site;

placement of asterisk in the graph identifies the years that are different within each respective site.

Invertebrate assemblages also were driven by a significant year x site interaction term in the PERMANOVA, explaining about 13% of the variance (Table 2.4a). Among the individual terms, year (16%) had a much larger effect than site (5%). While all sites clustered relatively closely in 2005 and 2006, invertebrate assemblage composition was distinctly different in 2013 and then again in 2015 (Fig. 2.7). Invertebrate assemblages in 2005 and 2006 were characterized by higher biomass of especially the chiton *Stenosemus albus*, the bryozoan *Eucratea loricata* and other Bryozoa, the hydroid *Sertularia cupressoides*, while assemblages in 2013 were particularly rich in the polychaete *Exogone* sp., and those in 2015 contained high biomass of Amphipoda (Fig. 2.8). Shannon diversity within sites and years was higher but much more variable than for macroalgae, with a general trend to lower values in 2015 (Fig. 2.9). Evenness was generally lower than for macroalgae with no discernable trend among sites or years. Like overall assemblage structure, the year x site interaction term and the individual year term were significant when assessing dispersion within sites across years, accounting for 16% and 19% of the variance, respectively (PERMANOVA, Table 2.4b). Dispersion, measured as the distance to centroid, was significantly greater at E1 and W3 in 2013 compared to other years, but was significantly lower in 2015 at DS11, in 2006 at W2, and in 2005 and 2006 at W1 compared with other years at those sites (Fig. 2.10). Total invertebrate biomass was positively correlated to total macroalgal biomass and different morphological groups of macroalgae (bushy morphology of red algae, erect blade morphology of kelps), but none of these relationships were significant (all $p>0.05$).

Table 2.4. PERMANOVA results of Boulder Patch invertebrate assemblage composition by year and site (a) and of dispersion of Boulder Patch invertebrate assemblages by year and site (b).

a

Source	df	SS	MS	Pseudo-F	P(perm)	Unique perms
si	6	1.07E+05	17822	2.1105	0.0002	9827
ye	3	1.52E+05	50593	17.463	0.0001	9804
sixye	18	1.52E+05	8444.4	2.9147	0.0001	9475
Res	252	7.30E+05	2897.2			
Total	279	1.14E+06				

Estimates of components of variation

Source	Estimate	Sq.root	% Variance
S(si)	234.44	15.311	5.4
V(ye)	681.37	26.103	15.6
V(sixye)	554.73	23.553	12.7
V(Res)	2897.2	53.825	66.3

b

Source	df	SS	MS	Pseudo-F	P(perm)	Unique perms
si	6	1072	178.66	0.79333	0.5944	9960
ye	3	4164.8	1388.3	20.529	0.0001	9947
sixye	18	4053.8	225.21	3.3303	0.0001	9898
Res	252	17041	67.623			
Total	279	26332				

Estimates of components of variation

Source	Estimate	Sq.root	% Variance
S(si)	-1.1636	-1.0787	-1.2
V(ye)	18.866	4.3435	18.7
V(sixye)	15.759	3.9697	15.6
V(Res)	67.623	8.2233	66.9

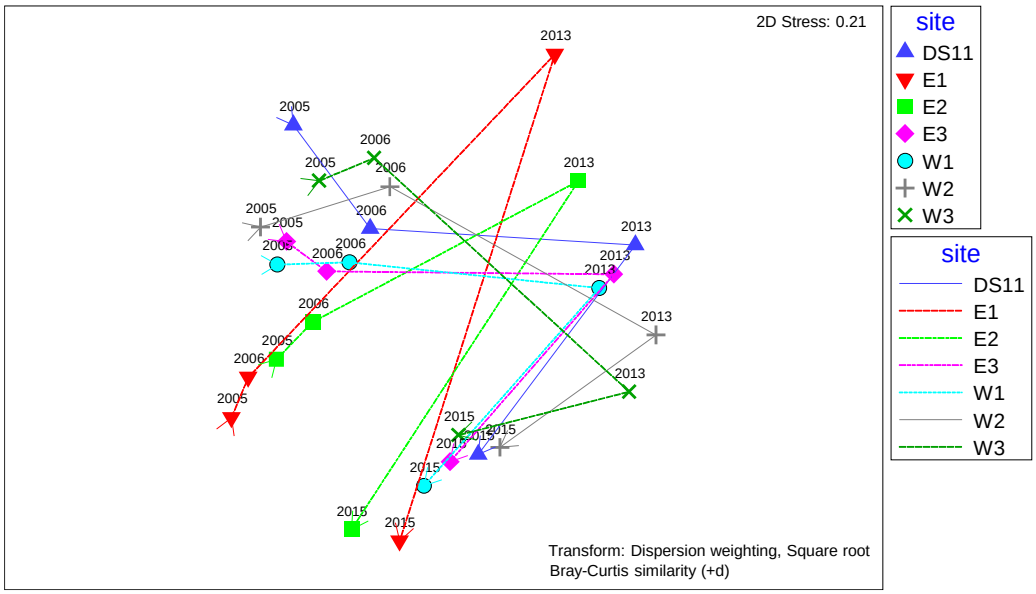

Figure 2.7. nMDS plot of invertebrate assemblages at seven sites in the Boulder Patch over four study years. Sites are represented as different symbols and years are indicated in the plot. Trajectories indicate direction of change in macroalgal assemblage structure over time per site.

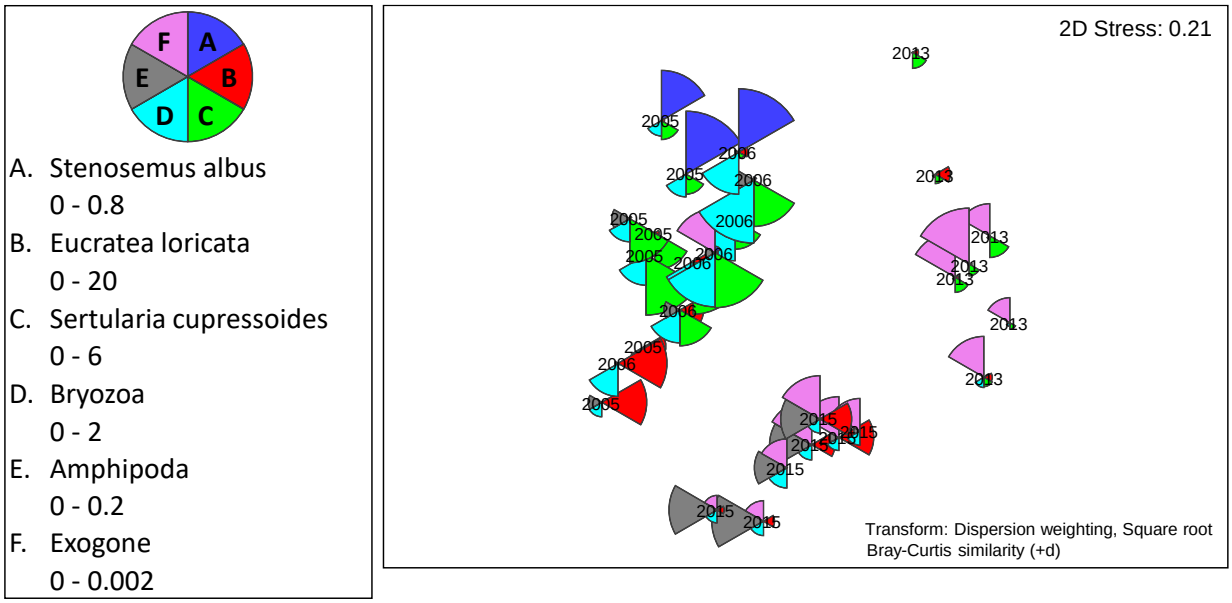

Figure 2.8. Invertebrate species contributing to the differences in assemblage structure among years in the Boulder Patch. Species are indicated as pie slices (A-F) with pie pieces proportional to the range of biomass within each taxon.

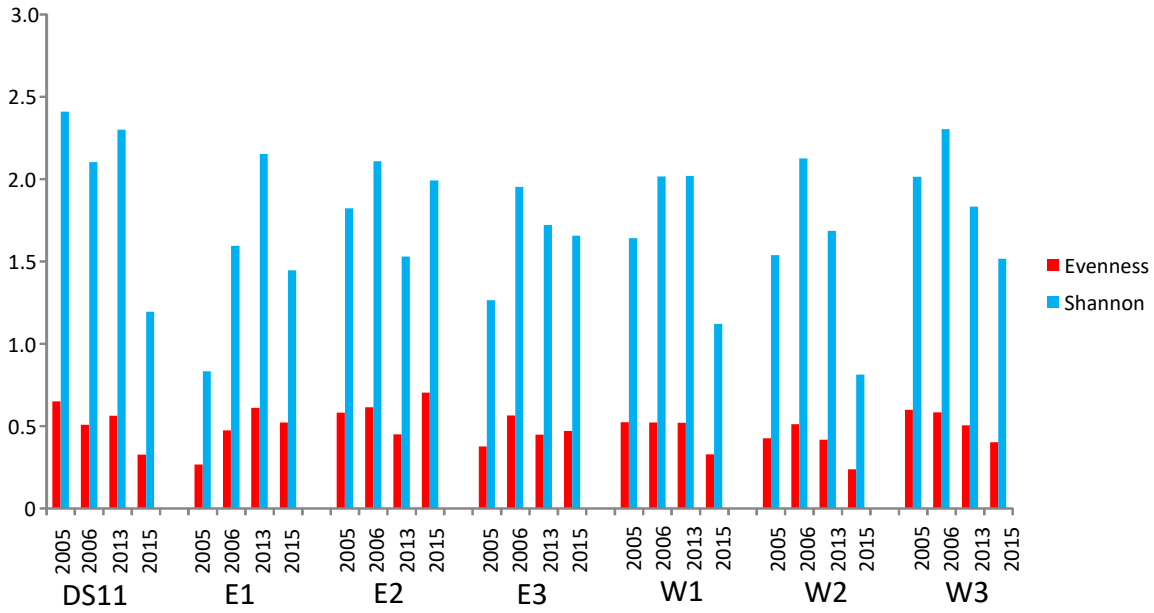

Figure 2.9. Shannon Wiener diversity index (H') and Pielou's evenness index (J') for invertebrate assemblages at seven sites in the Boulder Patch over four study years.

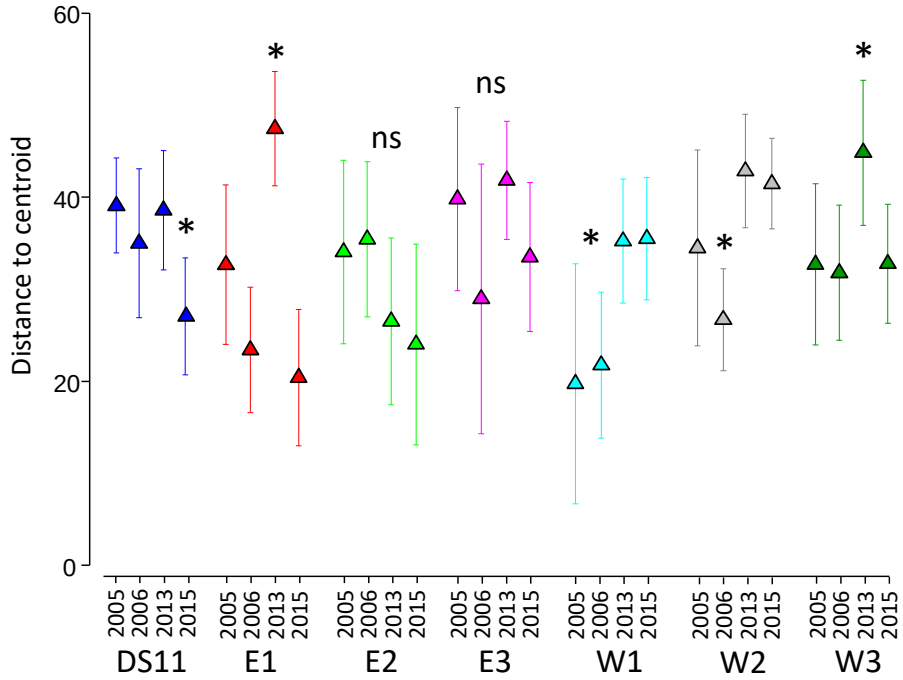

Figure 2.10. Mean dispersion, measured as the distance to centroid, for invertebrate assemblages at seven sites in the Boulder Patch over four study years. Dispersion is a measure of the scatter within the multivariate assemblage. Asterisks above means indicate significant (ANOVA, $p \leq 0.05$) differences among years within each site; placement of asterisk in the graph identifies the years that are different within each respective site.

Camden Bay (and comparison with Boulder Patch)

The most common macroalgal taxa in Camden Bay were *Coccotylus truncatus*, *Dilsea* sp., *Phycodrys* sp., and *Laminaria solidungula*, with *Saccharina latissima* and *Alaria esculenta* also common at some sites (Fig. 2.11, Table 2.5). Total biomass varied strongly among sites and years, with unusually high biomass at site DS4 in 2007.

Table 2.5. Macroalgal biomass (g wet weight 0.25 m^{-2}) in Camden Bay over three study years.

Sample	*Phycodrys* sp.	*Coccotylus truncatus*	*Dilsea* sp.	*Odonthalia dentata*	*Rhodomela* sp	*Chaetomorpha melagonium*	*L. solidungula*	*S. latissima*	*Alaria esculenta*	*Chaetopteris plumosa*	*Battersia arctica*	Rhodophyta
DSE2005	23.36	18.54	1.00	1.42	0.06	0.05	0.09	0.80	0.00	0.74	0.00	0.22
DSC2005	13.24	7.66	21.64	3.42	1.68	0.28	0.32	0.70	0.00	1.10	0.10	0.23
DSW2005	3.36	7.48	6.84	1.62	0.94	0.03	0.00	1.76	0.00	0.44	0.00	0.12
DSW2007	1.40	1.41	70.40	37.20	3.00	0.40	4.40	43.80	18.00	5.00	0.00	0.00
DS42007	59.40	45.80	15.80	45.00	0.21	0.01	115.20	87.00	11.20	2.80	0.00	0.00
DSW2017	9.97	18.19	13.25	3.63	1.29	0.15	0.10	0.23	39.57	6.58	0.16	0.14
DS42017	2.65	9.30	0.00	1.59	0.14	0.03	42.81	20.86	6.37	0.60	0.00	0.00

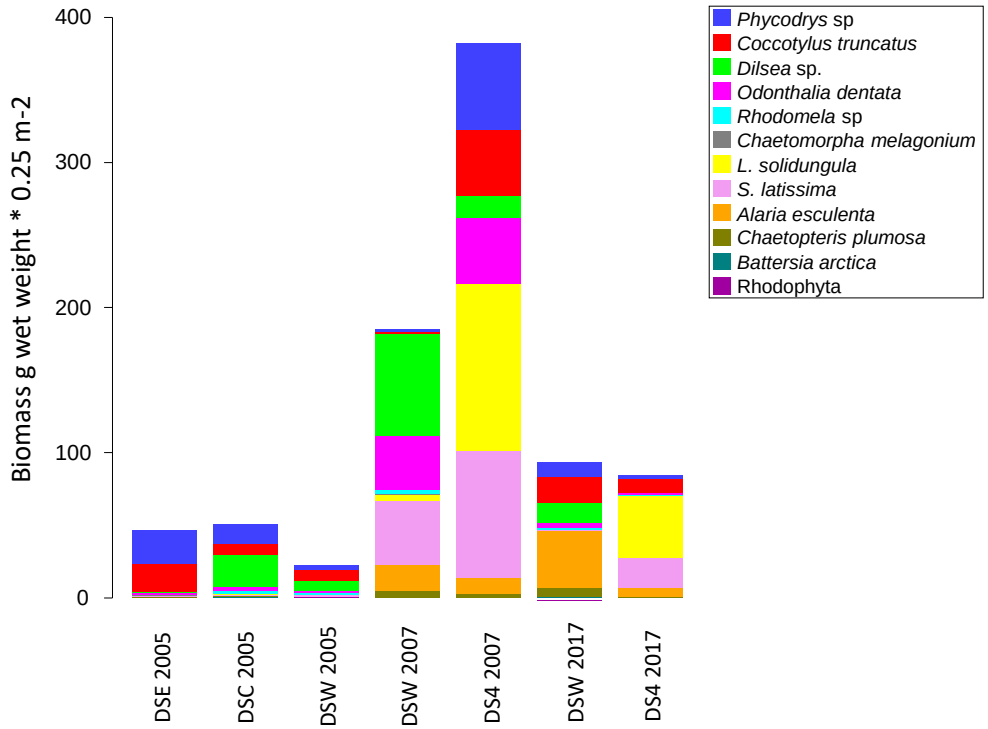

Figure 2.11. Macroalgal species biomass (g wet weight 0.25 m^{-2}) at four sites at Camden Bay over three study years. Not all sites were surveyed during each year.

Shannon diversity and Pielou's Evenness were slightly lower in 2017 compared with other years but there were no significant differences (ANOVA, $p>0.05$ for all comparisons; Fig. 2.12). Macroalgal assemblage composition fell into two distinct clusters on a 45% similarity level (Fig. 2.13). Among the taxa causing this separation were mostly the kelps *Laminaria solidungula* and *Saccharina latissima* (Fig. 2.14).

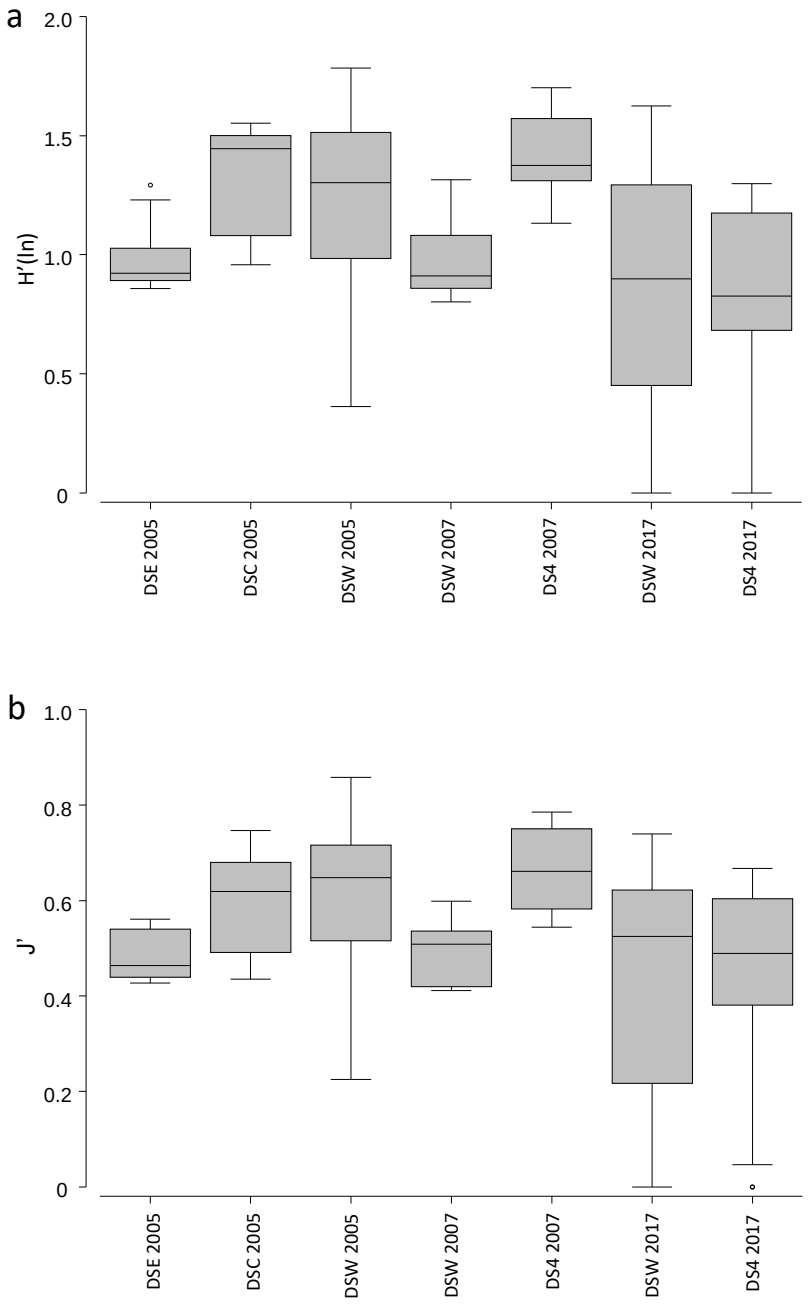

Figure 2.12. Box plots of macroalgal assemblage Shannon diversity (a) and Pielou's evenness (b) four sites at Camden Bay over three study years (not all sites were surveyed each year). There were no significant differences in any of the measures.

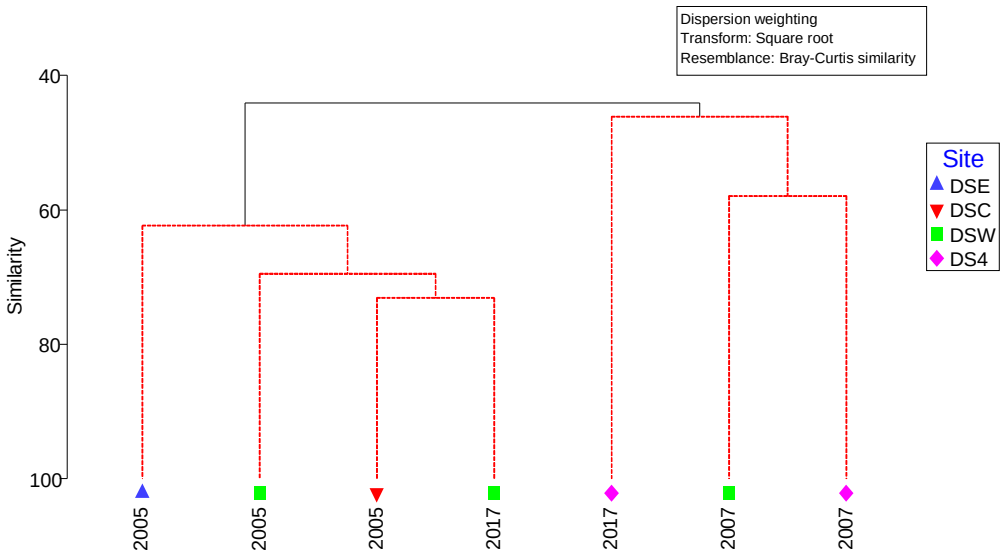

Figure 2.13. Hierarchical cluster analysis of the macroalgal assemblages at Camden Bay. Results of a SIMPROF test are displayed by colored histogram branches, where red branches signify no significant difference between connecting samples.

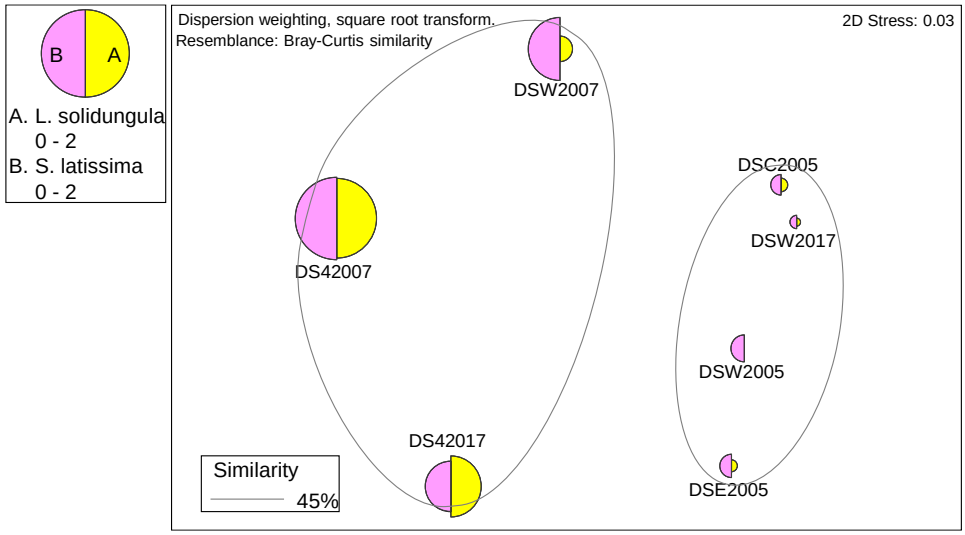

Figure 2.14. Macroalgal species contributing to the differences in assemblage structure among sites and years at Camden Bay. Species are indicated as pie slices (A-C) with pie pieces proportional to the range of biomass within each taxon. Green circles represent non-significant groupings from the cluster analysis (Fig. 2.13) at a 45% similarity level.

Overall average biomass at Camden Bay was higher than at the Boulder Patch, mostly driven my higher biomass of the kelps *Saccharina latissima* and *Alaria esculenta* (Fig. 2.15). Shannon diversity was higher in Camden Bay, although this difference was not statistically significant (t-test, p=0.093) and there also was no

regional statistical difference in Pielou's evenness (Fig. 2.16). Macroalgal assemblage structure in the two regions (combining sites and years within each region) was significantly different (AMOSIM test, global R = 0.445, p = 0.001) (Fig. 2.17). In addition to the differences in kelp mentioned above, these regional differences were also driven by the complete absence of *Ahnfeltia plicata* in Camden Bay.

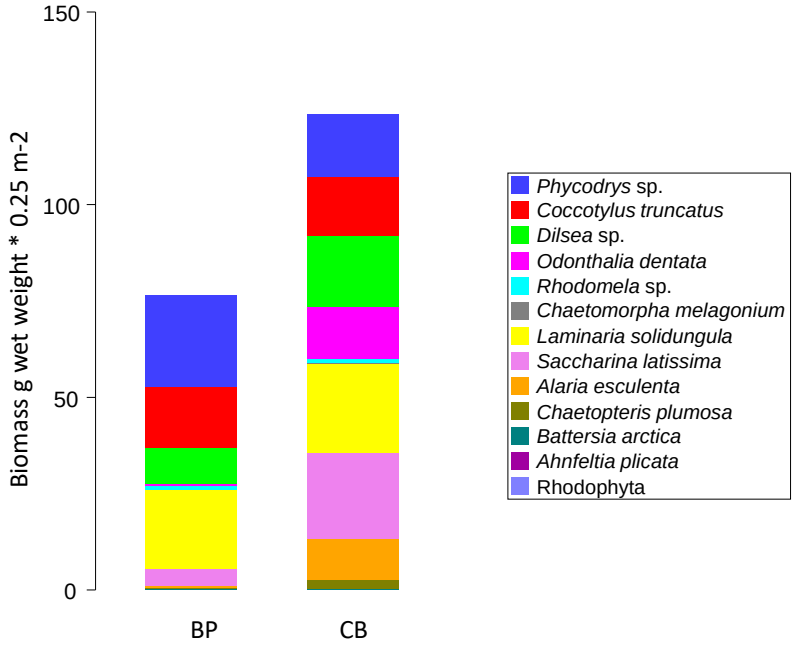

Figure 2.15. Overall average macroalgal biomass (g wet weight 0.25 m^{-2}) in the Boulder Patch and at Camden Bay. Overall biomass per region is separated by taxa indicated in the legend.

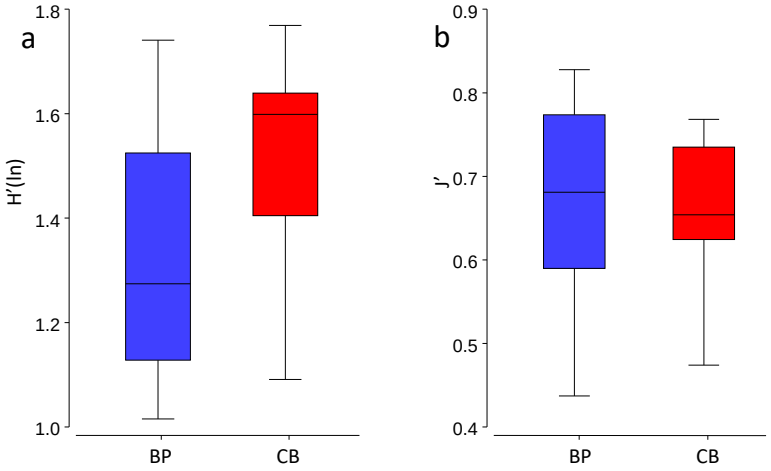

Figure 2.16. Box plots of macroalgal assemblage Shannon diversity (a) and Pielou's evenness (b) in the Boulder Patch and at Camden Bay. There were no significant differences in any of the measures.

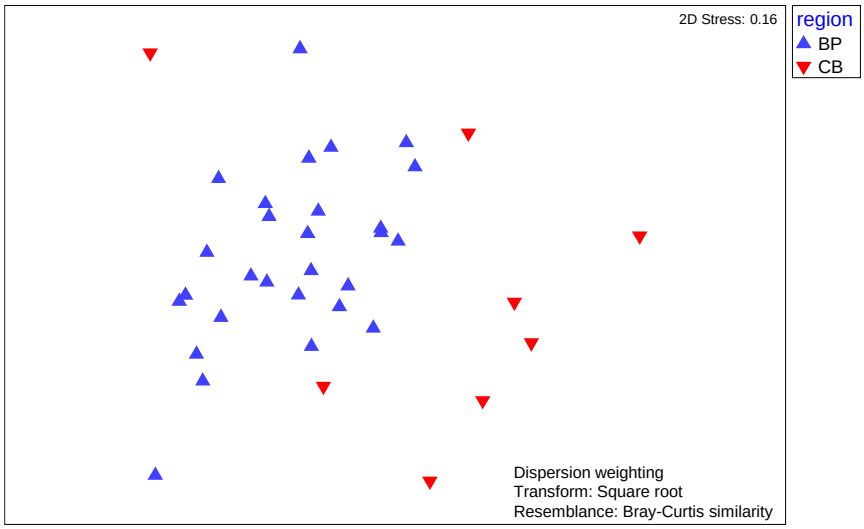

Figure 2.17. nMDS plot of macroalgal assemblages between the two regions. Each symbol represents the assemblage at a certain site and year.

Invertebrate assemblages in Camden Bay were mostly composed of amphipods, bivalves, and polychaetes (Fig. 2.18, Table 2.6). Overall, invertebrate assemblages were less taxon rich than in the Boulder Patch, although the more limited sampling in Camden Bay could contribute to some of those differences. Camden Bay invertebrate assemblages differed strongly between the two sampling years (only about 10% similarity between years, ANOSIM global R for year effect: 0.725, p=0.001), but also between the two sites sampled in both years (ANOSIM global R for site effect: 0.477, p=0.001). Differences in invertebrate assemblages in Camden Bay between sampling years were mostly driven by the gastropods Rissoidae, the amphipods *Atylus carinatus* and *Apherusa megalops*, and differences between sites were influenced mostly by the bivalve *Musculus discors* and the barnacle *Balanus crenatus* (Fig. 2.19). Shannon diversity and Pielou's evenness were higher in 2007 than 2017 but only the 2007 to 2017 evenness comparison for DSW was statistically significant (Fig. 2.20; ANOVA, Tukey post-hoc comparison p=0.046).

Table 2.6. Invertebrate biomass (g wet weight 0.25 m^{-2}) in Camden Bay over three study years.

Sample	Amphipoda	Isopoda	Crustacea oth	Gastropoda	Bivalvia	Polychaeta	Ascidiacea	Bryozoa	Hydrozoa	Porifera	Nemertea
DS42017	1.907	0.100	0.816	1.159	2.050	1.368	0.167	0.166	0.135	0.200	0.243
DSW2017	5.161	0.000	0.470	1.359	0.079	0.314	0.000	0.216	0.200	0.000	0.000
DS42007	1.667	0.000	1.236	0.746	2.150	2.579	0.000	1.013	0.807	0.748	0.199
DSW2007	1.288	0.200	0.471	0.679	0.898	0.276	0.200	0.985	0.200	0.227	0.000

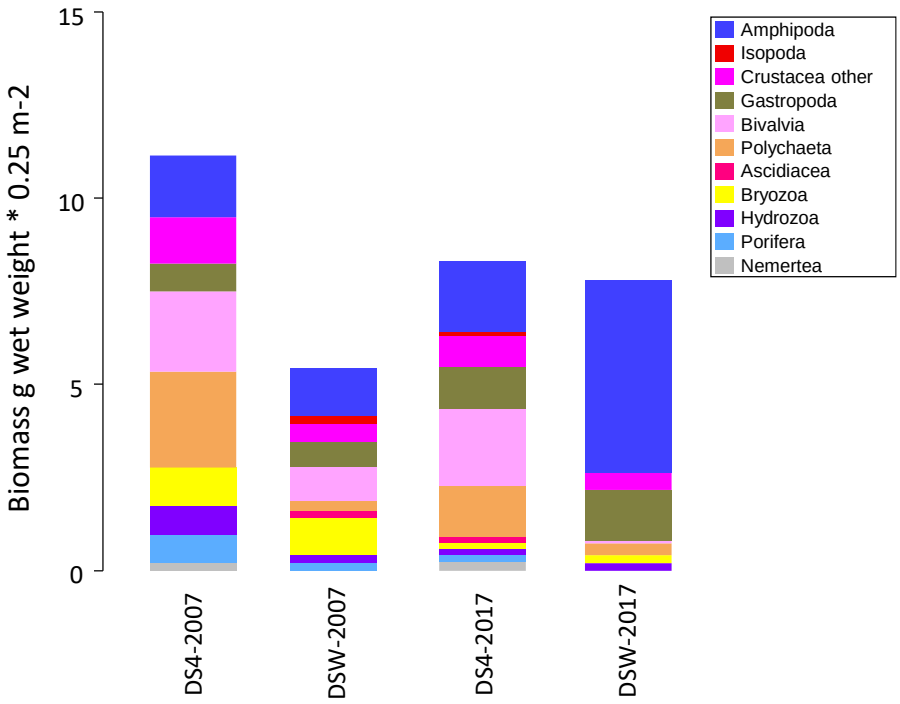

Figure 2.18. Invertebrate taxon biomass (g wet weight · 0.25 m^{-2}) by taxa at two sites and two years.

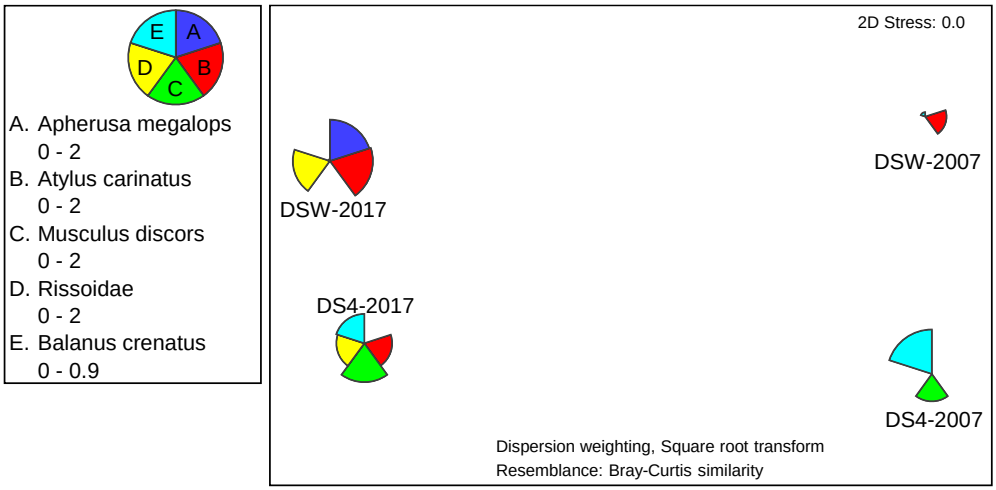

Figure 2.19. Invertebrate species contributing to the differences in assemblage structure among sites and years at Camden Bay. Species are indicated as pie slices (A-E) with pie pieces proportional to the range of biomass within each taxon.

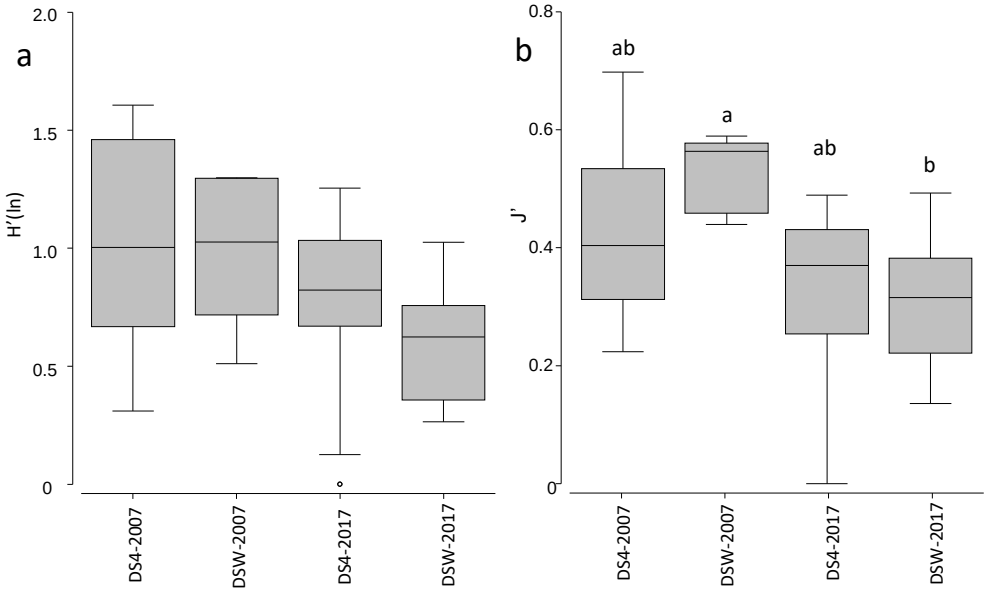

Figure 2.20. Box plots of invertebrate assemblage Shannon diversity (a) and Pielou's evenness (b) at Camden Bay. There were no significant differences in Shannon diversity; statistical differences (ANOVA, $p<0.05$) in Pielou's evenness are indicated by different letters above boxes.

The invertebrate assemblages between the two regions separated significantly (ANOSIM global R = 0.557, p = 0.01; Fig. 2.21). There were much fewer Porifera, Bryozoa, and Cnidaria in Camden Bay than in the Boulder Patch, and Echinodermata were missing completely in Camden Bay. In contrast, Arthropoda (mostly based on Amphipoda) were much more prominent in Camden Bay (Fig. 2.22). Overall, invertebrate assemblages were less taxon rich than in the Boulder Patch, with significantly lower Shannon diversity in Camden Bay (Fig. 2.23; t-test, p=0.046), although the more limited sampling in Camden Bay could contribute to some of those differences.

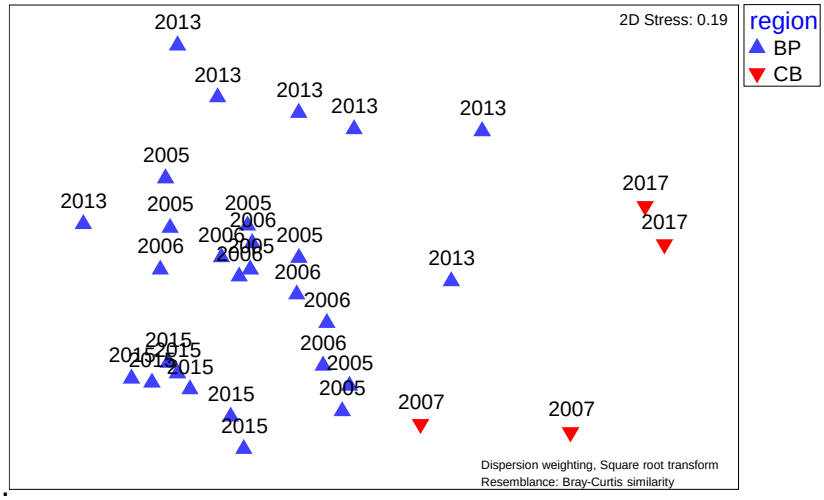

Figure 2.21. nMDS plot of invertebrate assemblages between the two regions. Each symbol represents the assemblage at a certain site and year.

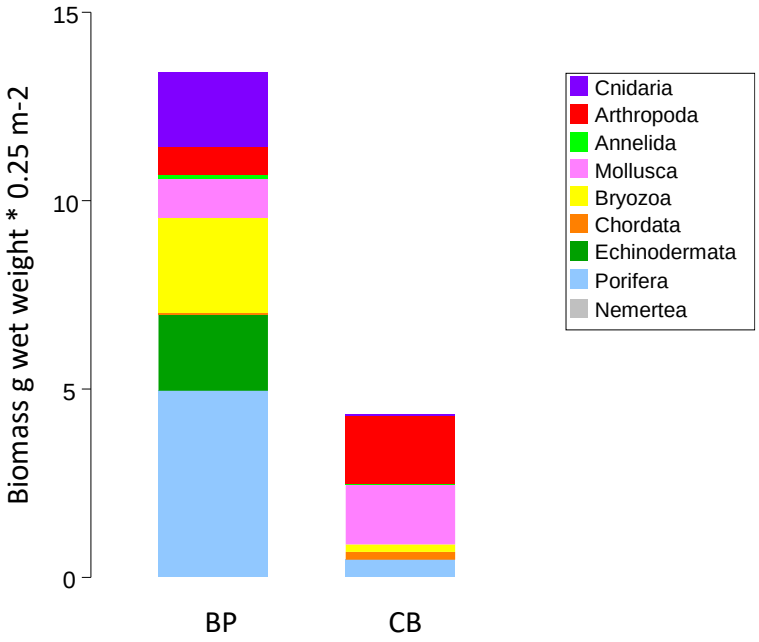

Figure 2.22. Overall average invertebrate biomass (g wet weight · 0.25 m^{-2}) in the Boulder Patch and at Camden Bay. Overall biomass per region is separated by taxa indicated in the legend.

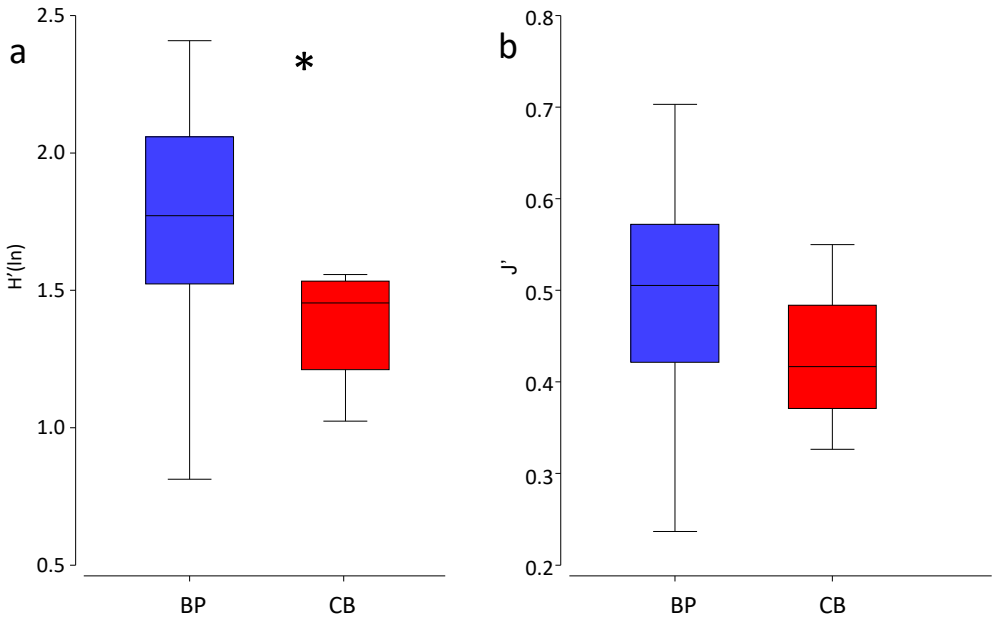

Figure 2.23. Box plots of invertebrate assemblage Shannon diversity (a) and Pielou's evenness (b) in the Boulder Patch and at Camden Bay. Shannon diversity was statistically different (ANOVA, $p<0.05$) between regions but not Pielou's evenness.

DISCUSSION

Epilithic assemblage patterns in the Boulder Patch

The Boulder Patch is considered a high biodiversity environment in the Beaufort Sea, dominated by macroalgal biomass and supporting a rich invertebrate assemblage (Dunton et al. 1982, Dunton and Schonberg 2000). Our investigations support these earlier assessments despite large interannual variability in overall biological biomass and differences in community composition. A comparison with adjacent boulder regions in Camden Bay establishes that these also may serve as biodiversity hotspots in the region, while being distinct in their macroalgal and invertebrate assemblage structures compared with the Boulder Patch.

Macroalgae growing on the rock deposits form the foundation of the epilithic communities, forming habitat as well as provide a food source for the system, either via direct grazing or through particulate organic matter (POM; Dunton and Schell 1987, Christie et al. 2007, Renaud et al. 2015, Filbee-Dexter et al. 2019). Macroalgal assemblages are dominated by red and brown algae, specifically kelp, with 12 common taxa. This number of species was much lower than a recent compilation of algae in the Boulder Patch (Wilce and Dunton 2014) but included all biomass dominant taxa. Average algal biomass was highly variable among sites and years with little overall consistency, although sites DS11 and W3 had among the highest biomass in most study years, indicating consistently favorable algal growth

conditions. Both these sites had high rock cover (unpublished data), which may favor algal recruitment and subsequent growth.

The prominent species across sites and years were very consistent with the red algae *Phycodrys* sp., *Coccotylus truncatus* and *Dilsea* sp. as well as the kelp *Laminaria solidungula*. Spatial consistency of prominent species was also a characteristic of coastal ecosystems the European Arctic (Włodarska-Kowalczuk et al. 2009) and likely reflects the competitive advantage of some key species in each environment (Konar and Iken 2005). Among the red algae, *Phycodrys* sp. and *Coccotylus truncatus* were the most abundant and regularly occurring species. These two taxa alone comprised between 34-89% of the average macroalgal biomass across sites and years. Both taxa have been the most abundant rhodophytes in the Boulder Patch since early studies in the area (Martin and Gallaway 1994). A red alga reported as very common in the Boulder Patch in the past are encrusting coralline red algae (e.g., Martin and Gallaway 1994), which we also observed but were not quantified using epilithic scrapes. However, their distribution among sites was assessed in a different portion of this study (see section 1.3). The two fleshy red algal genera are also known from other Arctic regions, including several transarctic exchanges (van Oppen et al. 1995), confirming the species' adaptation to a wide range of arctic temperature, nutrient, and light conditions for growth and reproduction (Schoschina 1996), likely rendering these taxa as relatively resilient to environmental variation. Other red algal species were less abundant, yet with *Dilsea* sp. contributing noticeable biomass. This is different from slightly higher biomass of *O. dentata* over *Dilsea* sp. found in biomass scrapes in the Boulder Patch in the late 1970s (Dunton and Schonberg 2000); in addition, although methods cannot be directly compared, our finding is also distinctly different from the frequency of occurrence in photo quadrats established in the Boulder Patch between 1984 and 1991 (Martin and Gallaway 1994), where *O. dentata* was about 3-5 times more frequent than *Dilsea* sp. The distinct morphology of the two species makes misidentifications as a cause for these differences unlikely. Rather, the consistency of higher *Dilsea* sp. biomass in our study since at least 2005 may indicate that a shift in the relative abundance of these two species may have occurred sometime in the late 1990s or early 2000s. This shift may have been location specific as *Dilsea* sp. biomass was highest in most years at sites DS11, E3 and W3 but only marginally present at some other sites (e.g., E2, W2).

The most abundant brown alga in the Boulder Patch was the kelp *Laminaria solidungula*, comprising between 2 – 56% of the average macroalgal biomass. The kelp *Saccharina latissima*, was occasionally abundant at some sites and years, especially DS11 and W3, but not as consistent as *L. solidungula*. Lowest kelp abundance consistently over the years, except in 2013, was at site E1. The Arctic kelp *L. solidungula* is particularly well adapted to the arctic light and nutrient conditions as it is able to photosynthesize in the summer under good light conditions but not use the stored photosynthate for actual growth until winter time, when nutrient concentrations are replenished (Henley and Dunton 1995, Bartsch et al. 2008). In contrast, growth of *S. latissima* is more closely tied to photosynthesis in the summer, which may explain its lesser abundance in the highly seasonal light and

nutrient conditions in the Boulder Patch (Henley and Dunton 1995, Bonsell and Dunton 2018), although it has been found to also be able to mobilize storage laminarin into mannitol for metabolic processes in the winter (Scheschonk et al. 2019). The seasonally adaptive growth strategy in *L. solidungula* is likely beneficial under the typical low temperature regimes of the Arctic based on reduced respiration rates (Borum et al. 2002) but may not be a competitive strategy should water temperatures increase in the coastal Arctic. Warmer water temperatures may favor physiological processes (e.g., growth) in *S. latissima* (Scheschonk et al. 2019), although the continued prolonged darkness of the polar night, and possibly even further reduced light availability from increasing sediment load in the water column with increased fetch at reduced sea ice cover (Bonsell and Dunton 2018) may offset any positive effect on *S. latissima*. Hence, the combined trajectories of temperature and light will be instrumental in determining the performance and possible resilience of these two main kelp species to future environmental conditions.

The macroalgal assemblage structure was specific to the different sites although there was a significant interaction with the factor year in the analysis, meaning that within each site, macroalgal assemblages also changed among study years. The year that had the greatest influence at the macroalgal assemblages at several of the sites was 2013. This difference in macroalgal assemblage structure in 2013 was also evident from the dispersion, basically a measure of the homogeneity of community assemblage, which was significantly higher in 2013 at several sites. This increased dispersion indicates that the assemblages responded to some disturbance that created higher variability in the distribution and biomass of macroalgae within the affected sites. In most cases, algal assemblages returned closer to previous assemblage structures in 2015, indicating some recovery from the 2013 disturbance. This suggests that the 2013 disturbance was not catastrophic as full recovery of the assemblages takes years, probably decades in the Boulder Patch (Konar 2013).

Macroalgae create habitat for associated invertebrate assemblages. This association can in part be driven by algal morphology, where a bushy thallus morphology close to the substrate like in *Phycodrys* sp. and *Coccolytus truncatus* provides good habitat structure for associated invertebrates, as found in other arctic and subarctic systems (Lippert et al. 2001, Christie et al. 2007). Similarly, erect kelp blades provide suitable habitat for an increased abundance of invertebrates, although distinct from those associated with bushy growth forms (Lippert et al. 2001, Christie et al. 2007), although studies in other systems found that general landscape features rather than individual algal morphologies may influence associated invertebrates (Cacabelos et al. 2010, Torres et al. 2015). We did not investigate relationships between invertebrate biomass and individual algal species or algal morphologies but the generally positive relationship (albeit not significant) between macroalgal and invertebrate biomass suggests that in the Boulder Patch, macroalgae are important habitat providers.

Invertebrate biomass was most consistently dominated by three groups of sessile taxa: sponges, bryozoans, and followed by hydrozoans. All three taxa also

have been the dominant epilithic fauna in the late 1970s, even in the species being represented such as *Halichondria panicea, Choanites lutkenii* , and *Semisuberites cribrosa* within Porifera, *Eucratea loricata* within Bryozoa, and *Sertularia cupressoides* within Hydrozoa (Dunton et al. 1982, Martin and Gallaway 1994, Dunton and Schonberg 2000). This temporal consistency indicates that the overall dominance structure of the assemblage on the phylum or class level has remained for several decades. Among these taxa, bryozoans and hydrozoans are typical members of Arctic and other high latitude hard substrate assemblages, often dominating frequency of occurrence or biomass (Lippert et al. 2001, Kuklinski and Barnes 2008, Włodarska-Kowalczuk et al. 2009). Bryozoan biomass in the Boulder Patch is contributed by both, those associated with rocky substrate (Kuklinski et al. 2006) but also those encrusting on blades of the red alga *Coccotylus truncates*. In contrast, sponges are often present but not dominant in other Arctic boulder or hard substrate regions (e.g., Beuchel and Gullikson 2008). Yet, in the Boulder Patch, persistence of sponges may be supported by the fast-vegetative regrowth of sponges after biomass removal through a disturbance (Konar 2013) and their competitive advantage over other space occupiers (Konar and Iken 2005). It is unclear why sponges are so successful in the Boulder Patch because of the high inorganic sedimentation rates there but their dominance may make the Boulder fields unique even within the Arctic. But similarly to some of the bryozoans and hydrozoans, sponges may be a rather unusual Arctic K-strategist that thrives in the Boulder Patch environment.

Invertebrate assemblages were more strongly influenced by study year than macroalgal assemblages, and distinct assemblage changes were observed at all sites from the earlier study years (2005 and 2006) to 2013, before assemblages changed again to a yet different structure in 2015. Some of these temporal differences were driven by small and mobile species that contribute much to diversity and assemblage structure but do not contribute much to overall biomass (e.g., amphipods, polychaetes). Those species are often highly adaptable and quickly respond to environmental changes, and may be a result of the possible increase in disturbance in the later study years already discussed above for macroalgal assemblage structure. The effect in 2013 was also noticeable as a general decline of invertebrate biomass compared with other study years. The concurrent reduction in biomass in some of the sessile key bryozoans (*Eucratea loricata*) or hydroids (*Sertularia cupressoides*) in later years supports the idea that disturbance took place that changed some of the character taxa from earlier study years. The overall effect of this presumed higher disturbance on the homogeneity of the invertebrate assemblage was less unified than in the macroalgal assemblage but at most sites manifested as higher dispersion in 2013 (or 2013 and 2015) compared with other study years (note that DS11 was an exception in this trend).

Comparisons with Camden Bay boulder fields

Overall, the main macroalgal taxa in Camden Bay were relatively similar to those in the Boulder Patch but invertebrate taxa differed considerably, and both assemblage compositions were significantly different between the two regions.

Camden Bay had higher average biomass and diversity in macroalgae but overall lower average invertebrate biomass and diversity. Hence, it seems that while the overall species present in the two regions may derive from a regional species pool, that local conditions in either region then drive the specific assemblage compositions.

Macroalgal biomass in Camden Bay differed greatly among years, with very low biomass in 2005, highest biomass in 2007, and intermediate biomass in 2017. Much of this difference was driven by differences in kelp biomass, possibly reflecting better and worse growth years for kelps in Camden Bay. Kelp growth is especially dependent on light availability (Dunton and Schell 1986, Dunton 1990), and like the situation in the Boulder Patch, summer light availability can be extremely low based on suspended sediment load (Bonsell and Dunton 2018). Since sampling years in Camden Bay were not the same as in the Boulder Patch, we cannot compare if 2007 may have been a particularly prosperous year for kelps across both regions. If sampling years and sites are averaged for each region, Camden Bay had about a third higher macroalgal biomass than the Boulder Patch, although these comparisons have to be interpreted with caution as differences in sampling (number of replicates, sites, and years) will contribute to differences in average biomass. Other than different biomass proportions in macroalgal species between the two regions, a noteworthy observation was that *Ahnfeltia plicata* was absent in all years in Camden Bay. While this distinct red algal species is not a large biomass contributor in the Boulder Patch either, it is a regular member of the macroalgal assemblage there. *Ahnfeltia plicata* is a broadly distributed species across a wide temperature range in the temperate and arctic regions of the Atlantic and Pacific (Lüning 1984); hence, some other local factor must be limiting this species in Camden Bay. This may not have a large effect on the overall biodiversity considerations in these two regions, but it would be informative for our understanding of the region if the bottleneck in Camden Bay is in dispersal, settlement, or growth.

Invertebrate assemblages in Camden Bay differed distinctly between the Boulder Patch and Camden Bay. Overall average invertebrate biomass in Camden Bay was only about a third of the average biomass in the Boulder Patch. Given that the macroalgal assemblage was distinct but composed of largely the same taxa, the differences in invertebrate assemblages may not be due to physical habitat differences provided by macroalgae but may be more related to other environmental factors (substrate composition, food availability, disturbance, etc.). On the phylum level, Boulder Patch invertebrate assemblages were dominated by Porifera, Bryozoa, and Cnidaria (Hydrozoa), while in Camden Bay they were dominated by Arthropoda and Mollusca. Maybe most striking was the complete absence of some groups in Camden Bay, such as all Echinodermata, Polyplacophora, Decapoda (i.e., *Pagurus*). Some of these differences are almost certainly driven by the much lower sampling effort in Camden bay as, for example, echinoderms in the Boulder Patch occurred infrequently but then with high biomass (e.g., a large sea star), which these taxa with a more clumped distribution can easily be missed with lower sampling effort. Other taxa, such as chitons, seem to indicate at a more

reliable difference between the two regions and may be related to possible differences in the abundance of encrusting coralline red algae. Higher biomass of some taxa (e.g., the amphipod *Atylus carinatus* and the barnacle *Balanus crenatus*, or the bivalve *Musculus* spp. and the gastropod *Boreocingula martyni*) accounted for the high presence of Arthropoda and Mollusca, respectively, but also explained the lower invertebrate Shannon diversity index than at the Boulder Patch. Overall, these findings seem to indicate that the Camden Bay boulder fields provide excellent habitat for some species, which then thrive, but that a possible lack of microhabitat or challenging environmental challenges limit the diversity of invertebrate taxa in Camden Bay. A detailed study of environmental conditions in Camden Bay, as has been done in the Boulder Patch, could possibly provide some indication of these environmental limitations.

3. Patterns and drivers of benthic community structure and early succession in an estuarine Arctic kelp bed

Christina E. Bonsell and Kenneth H. Dunton

INTRODUCTION

Kelp bed communities in the Arctic are expected to change dramatically as climate warming reduces ice cover and warms temperatures. Boreal species are expected to shift distributions poleward into the Arctic realm and contribute to predicted increases in primary productivity and biomass in rocky nearshore habitats (Müller et al. 2009, Krause-Jensen et al. 2012, Krause-Jensen and Duarte 2014). However, the future of kelp beds adjacent to erosional coasts and rivers may be more uncertain than those along stable, rocky coasts (Filbee-Dexter et al. 2019). In these inner shelf areas, salinity stress from augmented freshwater inputs can reduce kelp photosynthetic capacity and recruitment (Karsten et al. 2001, McClelland et al. 2006, Fredersdorf et al. 2009). Increased sediments (Gordeev 2006, Lantuit et al. 2012, Fritz et al. 2017) that attenuate light (Van Duin et al. 2001, Aumack et al. 2007) and hinder recruitment (Devinny and Volse 1978, Zacher et al. 2016, Lind and Konar 2017, Traiger and Konar 2017) may further obstruct persistence of local kelps. As these habitats characterize a considerable portion of Arctic kelp beds, especially in Alaska and Russia (Lantuit et al. 2012, Filbee-Dexter et al. 2019), baseline data on the physical environment and biological patterns of shallow, river influenced areas is vital to assess and evaluate the redistribution of Arctic biota and ecosystems.

The Boulder Patch is the largest of the discrete kelp beds scattered along the Alaskan Beaufort Sea coast, located in shallow (~4-7 m), nearshore waters of Stefansson Sound, east of Prudhoe Bay and adjacent to the Sagavanirktok River delta (Fig. 3.1). Influence from the Sagavanirktok River, and other large rivers (including the Mackenzie River) along the Beaufort Sea coast, make Stefansson Sound considerably estuarine in character (Section 1.1). Boulder and cobble substrates that characterize the Boulder Patch support a rich epibenthic community with greater diversity than the surrounding soft sediment habitat (Dunton et al. 1982, Dunton and Schonberg 2000). Diversity and structure of this community varies across the kelp bed (Martin and Gallaway 1994). The community is dominated by the Arctic endemic kelp, *Laminaria solidungula*. The kelps *Saccharina latissima* and *Alaria esculenta* are also present, though the latter is rare. Foliose red algae, including *Phyllophora truncatus*, *Dilsea socialis*, and *Phycodrys rubens* form a dense turf community throughout much of the Boulder Patch. Nestled amongst the turf are filter feeders: sponges (such as *Halichondria panacea* and *Semisuberites cribrosa*), bryozoans (such as *Eucratea loricata*), and hydroids (*Sertularia* spp.). The soft coral *Gersemia rubiformis* is a charismatic community member, and common in certain areas. At some sites, crustose coralline algae (likely *Leptophytum laeve* and *L. foecundum*) coats much of the rock surface unoccupied by the preceding groups, though it is completely absent in other areas. While the relationship between

underwater light levels and kelp growth in the Boulder Patch is well established (Dunton 1990, Aumack et al. 2007, Dunton et al. 2009, Bonsell and Dunton 2018), the causes of these spatial variations in community structure are unknown.

The Arctic coastal ocean is distinctively seasonal, with strong influence from the cycles of terrestrial freshwater inflow and sea ice extent, the physiochemical marine environment transforms considerably from ice covered winter, to spring melt, to open water summer. The range of conditions experienced over the year could have strong effects on ecosystem characteristics and processes. It is especially pertinent to establish linkages between abiotic variability and biological ecosystem characteristics because seasonal patterns are rapidly shifting in the Arctic due to increased surface air temperatures (~1^{o}C/decade, Christiansen et al. 2013) and the expansion of the summer open water season (Markus et al. 2009, Parkinson, 2014). These changes have already altered community structure and ecosystem function in Arctic marine habitats (e.g., Wassmann 2011, Kortsch et al. 2012). Shifts in sea ice extent and sea surface temperature – which can be measured remotely – have demonstrable effects on benthic community composition (Beuchel et al. 2006, Grebmeier et al. 2006, Kortsch et al. 2012). Linkages between year-round *in situ* environmental conditions and ecosystem characteristics, such as community structure and recruitment, allows for stronger predictions of Arctic ecosystem change in the face of climactic warming and increased industrial activity.

Additionally, the drivers and spatiotemporal patterns of benthic recruitment and succession are currently understood via a handful of studies carried out in Svalbard and Eastern Greenland (Beuchel and Gulliksen 2008, Fricke et al. 2008, Kuklinski et al. 2013, Meyer et al. 2017), and one in the Beaufort Sea (Konar 2013). In some habitats, recruitment can occur relatively quickly, such as in shallow, Atlantic influenced Svalbardian fjords (Meyer et al. 2017), while in other areas, recruitment and succession can proceed very slowly, taking over a decade for cleared experimental plots to resemble the benthic community (Beuchel and Gulliksen 2008, Konar 2013). Kortsch et al. (2012) hypothesized that climate driven shifts in temperature and ice cover had reduced the resilience of benthic communities in Svalbard by altering patterns of recruitment and succession. These processes are a key component in the future persistence of Arctic kelp beds.

The goal of the present study is to determine how seasonal variation in the physiochemical environment, spatial variation in benthic community structure, and community development are related in a shallow (< 9 m), river influenced Arctic kelp bed. We paired long-term environmental data (Section 1.1) with benthic surveys to assess how benthic community composition may reflect spatial environmental variability. We also used in situ settlement tiles to evaluate whether community structure was simply an effect of larval supply. We examined if recruited community composition was different from established benthic community composition but became more similar to the benthic community over time. The progression of ecological succession can reveal mechanisms that relate abiotic differences to community dissimilarity (Kroeker et al. 2012, Kroeker et al. 2013).

Additionally, we were interested in the timescale of community development. Previous work indicates that recovery from disturbance can take a decade or more in the Boulder Patch (Konar 2013). However, climax community composition could be determined early on in succession due to abiotic restraints on species composition. This would especially be the case if the strength of competitive biotic interactions is low due to abiotic stress (Bertness and Callaway 1994). Therefore, this study also indirectly addresses the role of abiotic versus biotic variables in determining community structure in Arctic nearshore ecosystems.

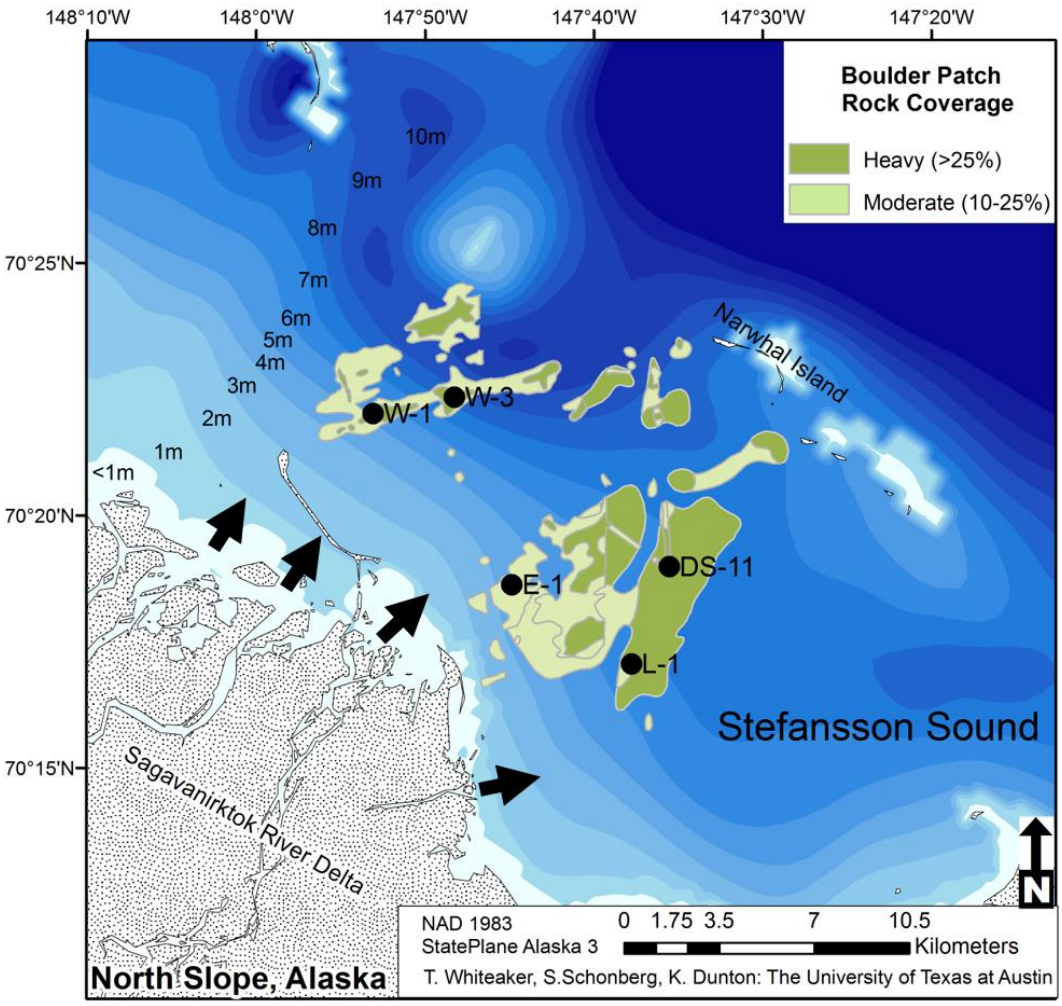

Figure 3.1. Map of study sites (W1, W3, E1, L1, and DS11) in the Boulder Patch with rock cover indicated in green. Adapted from Bonsell and Dunton 2018. Arrows indicate channel inputs from the Sagavanirktok River

METHODS

Study sites and environment

We used five long-term study sites that vary in their depth, distance to shore, and proximity to the mouth of the Sagavanirktok River. (Fig. 3.1). Three sites (DS11, E1, L1) lie between a set of barrier islands (including Narwhal Island) and the mainland, while the other two sites (W1 and W3) are more exposed, located near deep channels between a shoal and barrier islands (Fig. 3.1).

Annual and seasonal means of temperature, salinity, underwater light levels (photosynthetically active radiation, PAR), and current velocity at each site were derived from Section 1.1. Briefly, in situ benthic loggers were deployed at each site for multiple years, bounded by the period of August 2011-August 2017 (methods described in Section 1.1). Distance from each site to nearest river input (Fig. 3.1) was estimated in ArcGIS by drawing a line between each site and the nearest land boundary associated with a river channel mouth. Depth per site is from Aumack et al. (2007) and Bonsell and Dunton (2018).

Benthic community structure and succession

To characterize established benthic community structure at each site, 0.05 m^2 photoquadrats were taken by a diver using a Nikon 1 AW1 waterproof digital camera in July and August 2016 and 2017. Due to the predominantly poor visibility and heterogeneous rock cover in the Boulder Patch, the diver would take the photos haphazardly while working in a spiral pattern by rising above the benthos, kicking twice and 'landing' with the photoquadrat. If rock cover within the photoquadrat appeared to be >75%, a photo was taken. Photos were analyzed for benthic percent cover to the lowest possible taxonomic group using point intercept of 56 stratified random points using the online program CoralNet (coralnet.ucsd.edu). Photos with >25% soft sediment or >20% unclear points were removed from the analysis, with 24 to 43 photos used in final analysis for each site (n: E1=36, DS11=31, L1=24, W1=43, W3=35). All data were normalized to percent rock cover in each photoquadrat.

To assess recruitment and succession patterns at each site, settlement tiles (10x10 cm fiber cement) were deployed in July 2015. Each subsequent year, a subset of these tiles was removed, and a new set was deployed by divers. This gave us data from plates that had been deployed for durations of one (2015-2016, 2016-2017, and 2017-2018), two (2015-2017 and 2016-2018), and three years (2015-2018), with each plate representing an independent unit. Not all deployed plates were recovered due to loss by ice scour or adverse diving conditions (Supp. Table 3.1). After retrieval by divers, plates were placed in individual sealed containers with seawater and transported live to the lab where they were examined under a dissecting microscope. Organisms were identified to the lowest taxonomic level possible and counted.

Five functional groups were used to evaluate differences in community structure among sites: kelp, crustose coralline algae (hereafter abbreviated as CCA), fleshy red algae, filter feeders, and suspension feeders (Table 3.1). There are various definitions for "filter" and "suspension" feeding, and the two are sometimes used synonymously. Here, these terms are used to separate bryozoans, corals, and hydroids (suspension feeders) from sponges and ascidians (filter feeders). For the species present in this study, the former extends appendages (cilia or tentacles) into the water column to acquire food particles, while the latter actively pump water through their bodies to feed. These groups also differ in their gross morphology: the filter feeders are generally robust while the suspension feeders are more filamentous. Differences in feeding behavior and morphology may lead to differing responses to variation in flow and suspended sediments, and use of multiple traits to group biota leads to higher sensitivity when assessing differences in community composition (Bremner et al. 2003).

Data analysis

To determine differences in established benthic communities among sites, a Bray-Curtis matrix was calculated from square-root transformed percent cover data, then analyzed statistically using PERMANOVA as well as visually using an nMDS plot. Square root transformation decreased the number of pairwise differences in homogeneity, but the transformation did not change PERMANOVA results. Differences in total abundance of biota on settlement tiles within sites and within ages (one, two, and three years) was assessed with Welsh one-way tests, or Welsh two-sample t-test, depending on the number of groups. To compare the benthic community to settlement tile communities, percent cover (photoquadrats) and abundance (tiles) data were transformed into proportional abundance of each functional group, then square-root transformed, and a Bray-Curtis matrix was calculated. The trajectory of community development on the tiles was evaluated using NMDS plots that grouped mean benthic community and means of each age of tile community, as well as by plotting the Bray-Curtis dissimilarity to the benthic community over time at each site. Additionally, mean and variance in Bray-Curtis dissimilarity between one- and two-year old tiles for each site was plotted.

The relationship between mean environmental variables and percent cover by each functional group was assessed with Spearman's rank-correlations. The use of correlations to connect the physical environment to biological characteristics is meant to springboard future field studies and experiments. While low sample number (five sites) prevents more rigorous statistical tests, we aim to characterize broad patterns which link abiotic factor to community structure and present a baseline in the growing field of Arctic kelp bed ecology.

Table 3.1. Common species and genera from the Boulder Patch associated with each functional group category used in community analysis.

Functional group	Common Boulder Patch examples
Foliose red algae	*Phyllophora truncata* *Dilsea socialis* *Phycodrys rubens*
Crustose coralline algae (CCA)	*Leptophytum foecundum* *Leptophytum laevae*
Kelp	*Laminaria solidungula* *Saccharina latissima* *Alaria esculenta*
Suspension feeders	**Phylum Bryozoa** *Alcyonidium* sp. *Eucratea loricata* **Phylum Cnidaria** *Sertularia* sp. *Calicella* sp. *Obelia* sp. *Gersemia rubiformis* **Phylum Crustacea** *Balanus* sp.
Filter feeders	**Phylum Porifera**: *Semisuberites cribrosa* *Halichondria panicea* **Phylum Urochordata** *Rhizomogula* sp.

RESULTS

Benthic community structure

Benthic community composition (%), as recorded by photoquadrats, varied among sites (Figs. 3.2-3.4, Tables 3.2 and 3.3). The community at the deep, offshore site DS11 prominently featured kelp (mostly *Laminaria solidungula*, though *Saccharina latissima* and *Alaria esculenta* were common) and CCA (Figs. 3.3 and 3.4, Table 3.2). The foliose red *Dilsea socialis* was more common at this site than at the shallower sites. *D. socialis* was also relatively common at the other deep site, W3, along with *Phyllophora truncata* and CCA. *Gersemia rubiformis* was also present in at W3, though other invertebrate groups were rare (Figs. 3.3 and 3.4, Table 3.2). This contrasts with and adjacent but shallow site (W1), where *G. rubiformis*, sponges, hydroids, and bryozoans were relatively common, though the community was

dominated by foliose reds (especially *Phycodrys rubens*) (Figs. 3.3 and 3.4, Table 3.2). The shallowest site, E1, exhibited the highest cover by foliose reds, dominated by *P. rubens*, though *P. truncata* was also abundant (Figs. 3.3 and 3.4, Table 3.2). This was the only site where barnacles were recorded in photoquadrats. Neither CCA nor *G. rubiformis* were recorded at this site. *Gersemia rubiformis* was also absent from L1 and DS11 photoquadrats, though it was observed at DS11. As with the other shallow sites, L1 was dominated by foliose reds, but also had the second-highest kelp cover (Figs. 3.3 and 3.4, Table 3.2). CCA was present, but rare at this site. All sites had >10% cover by bare rock, with sites W3 and W1 having over 30% bare rock coverage (Table 3.2).

For E1 and W1, where photoquadrats were taken over two consecutive years, community structure did not vary by year (PERMANOVA, $p>0.05$), so analysis was done by site only. Benthic community structure based on functional groups was significantly different among sites (Table 3.3, Fig. 3.2). Pairwise comparisons demonstrated that all sites were unique from each other, except E1 and L1 (Supp. Table 3.2).

Relationship to environmental variables

Comparisons between functional group percent cover and environmental variables at each site (Supp. Table 3.3) revealed only one significant relationship – a positive correlation between cover of CCA and distance from Sagavanirktok River channels ($\rho = 1.0$, $p<0.05$; Fig. 3.5A-B). Distance from river channels had stronger correlations with functional group percent cover than depth (Fig. 3.5A). There were negative, but non-significant, relationships between mean salinity and cover by both invertebrate groups (Fig. 3.5A). Temperature and velocity had no strong correlations with any functional group (Fig. 3.5A). Interestingly, PAR also had no strong correlations with any algal group but was negatively related to filter feeder cover (Fig. 3.5A).

Settlement tiles and comparisons to benthic community

Abundance of individual biota could be extremely variable among settlement tiles (Table 3.4). In general, mean overall abundance increased over time (Table 3.4). Deployment duration had a significant effect on total abundance of tile biota at sites W1 (Welch one-way test, $F_{2,19}=21.033$, $p<0.05$) and W3 (Welch two-sample t-test, $t_{17.38} =-2.67$, $p<0.05$). Mean abundance was greatest for tiles deployed at DS11, though not significant due to high variability (Table 3.4).

Settlement tile communities significantly varied by site and age (PERMANOVA, $p>0.05$). Within each site, tile communities significantly differed among specific years of deployment (e.g. at DS11, the community on one-year-old tiles from 2015-2016 was significantly different from one year-old tiles from 2016-2017) as well as age (Pairwise PERMANOVAs, $p>0.05$; Fig 3.6A-E). Within durations, communities were also different among sites (PERMANOVA, $p>0.05$), except for

one-year-old tiles from L1 and W1. Microscopic red algae recruits and juveniles were common on many of the tiles, though they were too small to identify species (Fig. 3.4). CCA recruits and juveniles were also common on tiles at most sites and were even present at E1 (on tiles deployed in 2017-2018 only) despite the absence of this group from the adjacent established benthic community (Fig. 3.4). Notably, no juvenile kelp ever recruited to the tiles.

At DS11, tiles were numerically dominated by CCA, while other sites were dominated by both CCA and/or red algae and suspension feeders (Fig. 3.4). Many filter feeders also recruited to W3 tiles in year one (Fig. 3.4). Comparison of tile communities (proportional abundance) to the benthic community (proportional percent cover) demonstrates that tile communities were generally dissimilar to the benthic community, and only became more similar to the benthic community in year two at site W3, and in year three at W1 (Fig. 3.6F). Of all the sites, tiles at DS11 were the most like the benthic community and had the least change between ages (Figs. 3.6A and F and 7). Tile communities at W1 and W3 were very dissimilar between years one and two, with high variation in how the community developed (Figs. 3.6D-F and 7).

Table 3.2. Mean and standard deviation of each functional group in the established benthic community at each site.

Site	CCA	Red algae	Kelp	Filter feeders	Suspension feeders	Rock
E1	0 ± 0	79.31 ± 0.51	2.9 ± 0.25	0.77 ± 0.11	6.12 ± 0.21	10.91 ± 0.34
L1	0.64 ± 0.06	71.67 ± 1.19	9.85 ± 0.93	0.48 ± 0.05	2.79 ± 0.21	14.57 ± 0.82
W1	0.48 ± 0.03	47.32 ± 0.76	4.4 ± 0.24	2.12 ± 0.12	14.87 ± 0.39	30.81 ± 0.59
W3	4.67 ± 0.15	58.01 ± 0.63	1.65 ± 0.14	0.77 ± 0.05	0.24 ± 0.02	34.66 ± 0.61
DS11	18.67 ± 0.46	38.01 ± 0.78	19.03 ± 0.75	0.44 ± 0.03	4.08 ± 0.19	19.77 ± 0.59

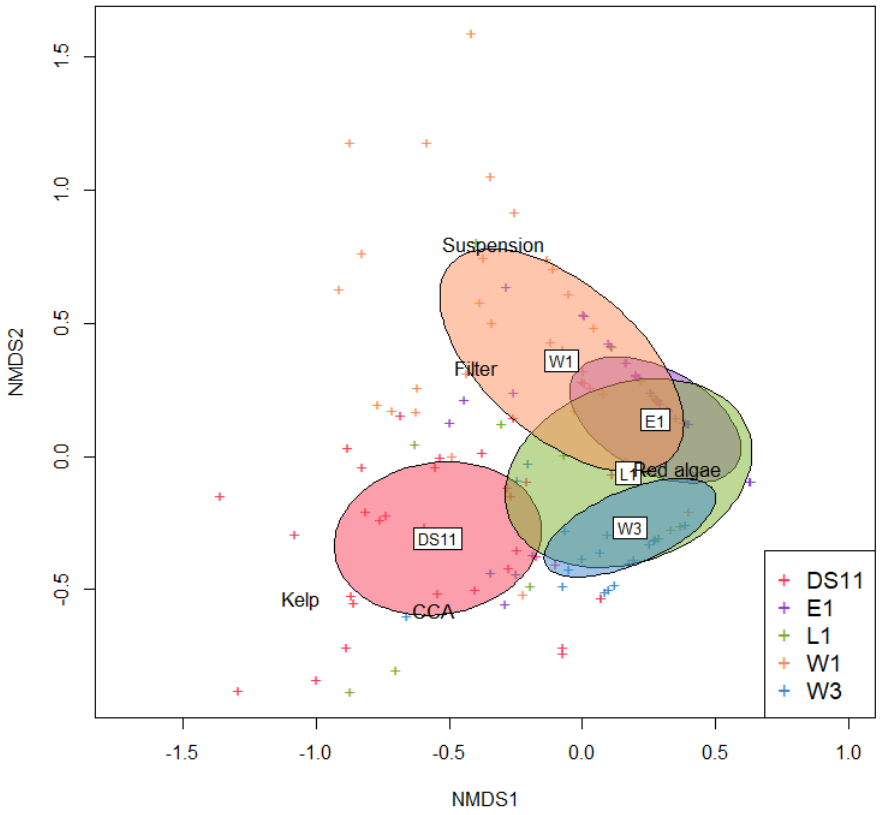

Figure 3.2. Non-metric multidimensional scaling plot (Bray-Curtis matrix, square root transform) of benthic community structure by functional group at each site. Center of ellipses indicate median community structure; ellipse area indicates standard deviation. Crosses indicate individual photoquadrats. 2D stress=0.14.

Table 3.3. PERMANOVA summary table for comparing benthic community structure by site (square root transformed data).

	Df	**Sums of Sqs**	**Mean Sqs**	**F. Model**	**R^2**	**Pr(>F)**
Site	4	6.01	1.50	23.45	0.36	0.01
Residuals	164	16.51	0.06		0.64	

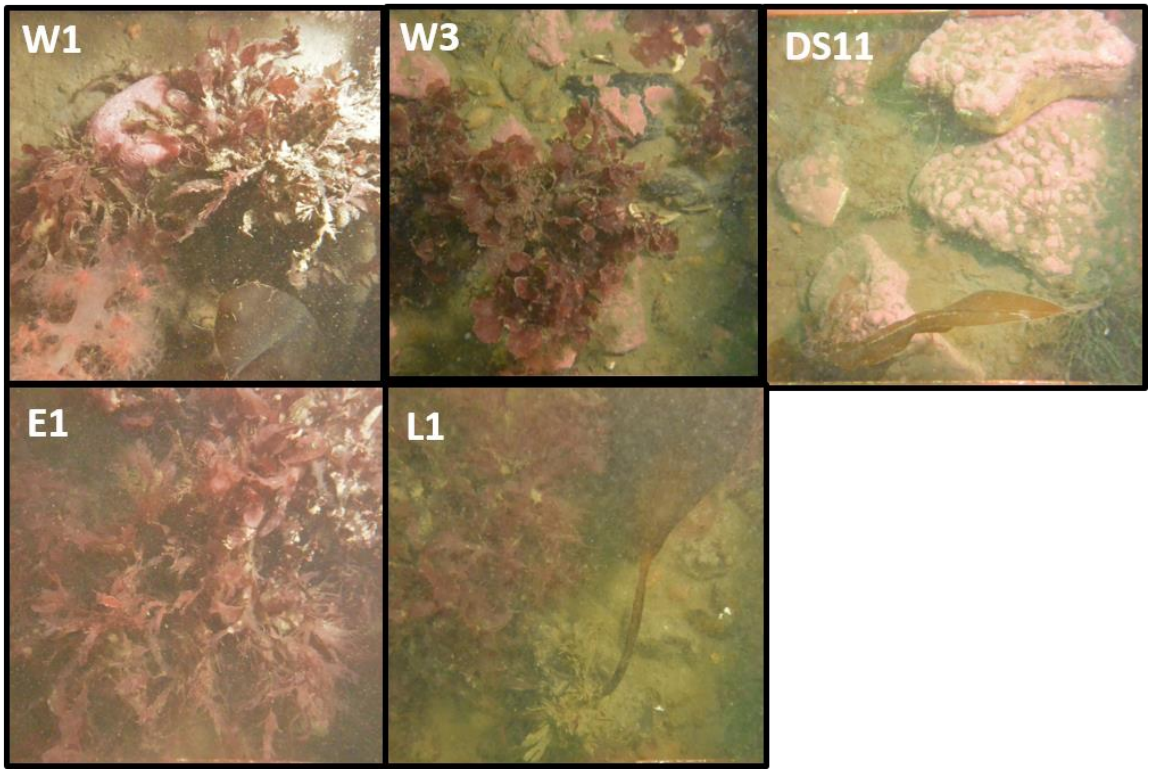

Figure 3.3. Example photoquadrats from each site.

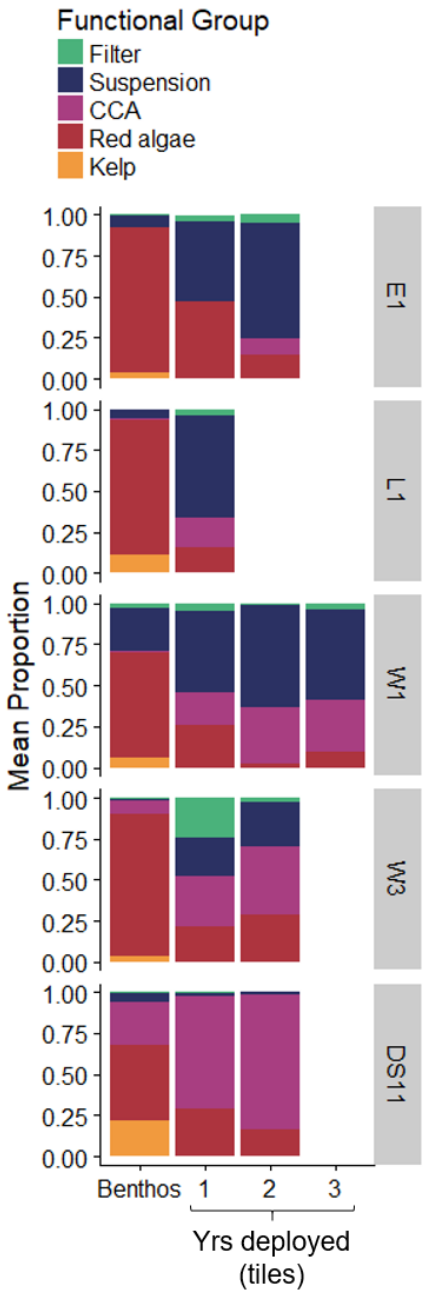

Figure 3.4. Mean proportion of each functional group at each site recorded for benthic photoquadrats and settlement tiles. This value represents proportion of total biotic percent cover for the benthic community and proportional abundance for tile communities. Note that no kelp recruited to settlement tiles.

Table 3.4. Mean total abundance (± standard deviation) of individual biota per 100 cm^2 settlement tile and number of tiles per deployment duration. * Indicates that abundances were significantly different between or among deployment durations for that site.

Site	1 Year		2 Years		3 Years	
	Mean ± SD	N	Mean ± SD	N	Mean ± SD	N
DS11	69.9 ± 61.7	24	233.0 ± 316.3	16	-	-
E1	17.8 ± 17.8	24	61.6 ± 108.5	16	-	-
L1	3.3 ± 2.1	16	-	-	-	-
W1*	15.0 ± 18.9	24	14.1 ± 4.7	8	35.9 ± 8.2	8
W3*	22.3 ± 19.6	16	42.0 ± 15.6	16	-	-

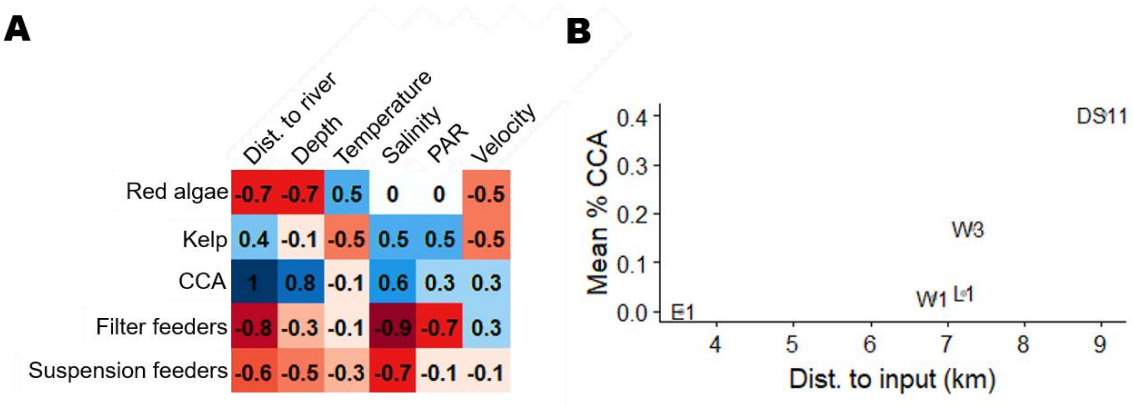

Figure 3.5. A) Correlation matrix between percent cover of functional groups and mean environmental variables at each site. Number denotes Spearman rank correlation (ρ), with ρ=1 being statistically significant in these cases (p<0.05). Color indicates correlation value, with deeper blue meaning more positively correlated and deeper red meaning more negatively correlated. B) Mean percent cover of crustose coralline algae (CCA) in the benthic community at each site compared to distance to nearest river input. See Fig. 3.1 for site locations.

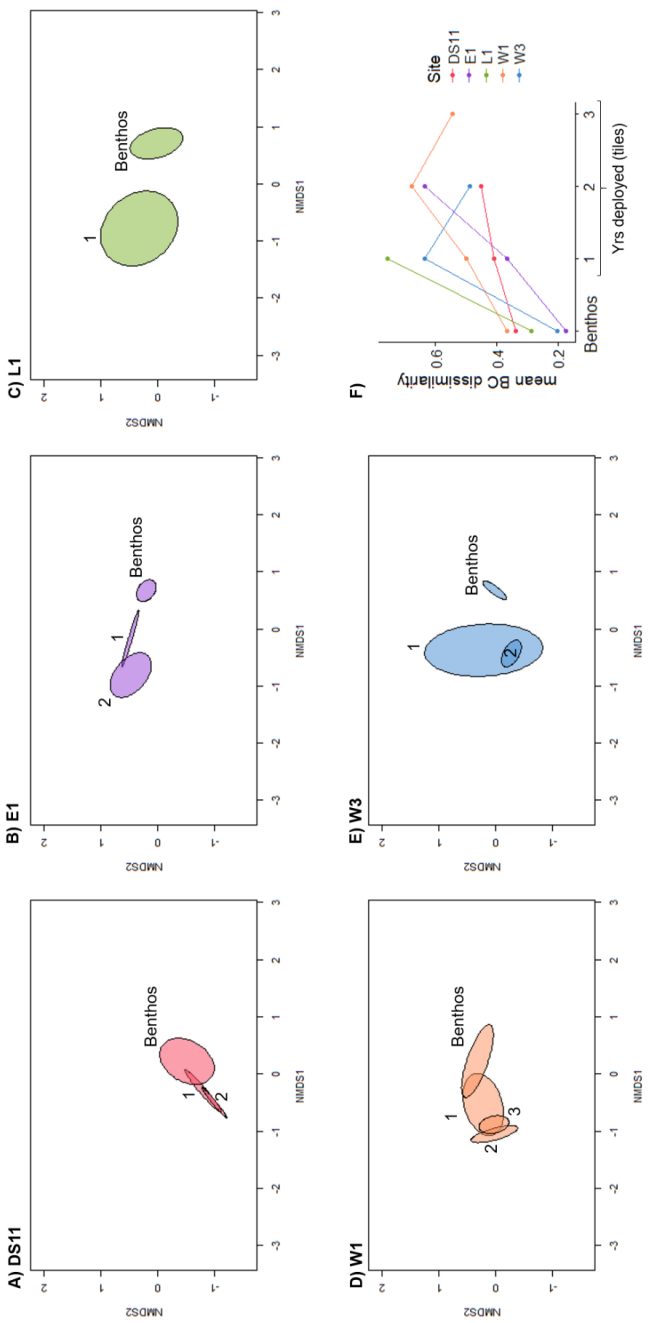

Figure 3.6. Development on tile communities over time as compared to the benthic community at each site. A-E) Non-metric multidimensional scaling plot of benthic and tile communities (from Bray-Curtis matrix on square-root transformed proportional data) broken up by site showing the trajectory of community development over time. Ellipses represent the mean and standard deviation of each community. 2D stress=0.11. F) Mean development of settlement tile communities over time compared to benthos, represented as mean BC dissimilarity. The leftmost points represent the mean dissimilarity between photoquadrats within the benthic community at each site.

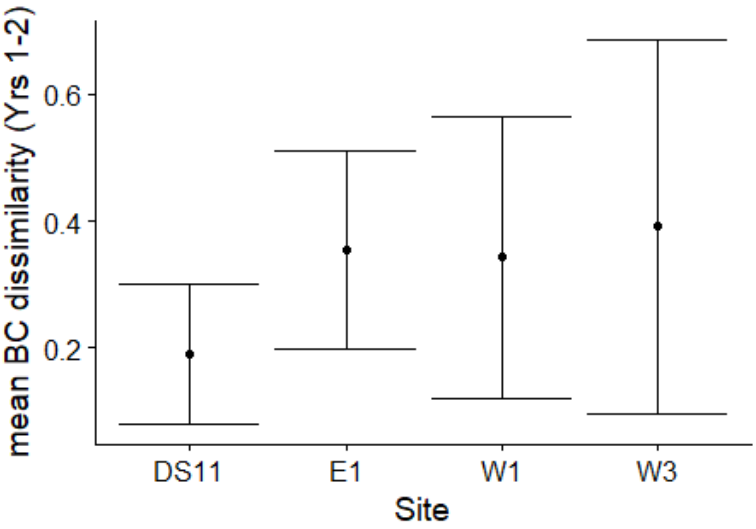

Figure 3.7. Development of settlement tile communities at each site between years one and two represented as mean (± standard deviation) Bray-Curtis dissimilarity. Standard deviation increased with distance to inter-island passes (Fig. 3.1).

DISCUSSION

Spatial heterogeneity in benthic community structure

Freshwater that flows from the Sagavanirktok River in the spring and early summer strongly influences Boulder Patch benthic community structure. In general, there were more invertebrates closer to the river and at lower mean salinities, while kelp and CCA showed the opposite pattern (Fig. 3.5A). This relationship was strongest with cover by CCA, which increased with distance from river inputs (Fig. 3.5B). During the spring freshet, Stefansson Sound can become extremely stratified (Weingartner et al. 2017), with shallow, inshore sites above the halocline (Section 1.1). The site closest to the river (E1) is distinct in its lack of CCA, relatively high cover by foliose red algae (79%), and low cover by kelp (3%) relative to the other sites. CCA are ecologically important members of subtidal habitats (Steneck 1986, Mccoy and Kamenos 2015) and are competitive dominants in the Boulder Patch (Konar and Iken 2005) and other Arctic epilithic communities (Beuchel and Gulliksen 2008, Kuklinski 2009), so their complete absence at E1 represents an significant ecological pattern. Although CCA are usually dominant in low light environments (Vadas and Steneck 1988), the lack of CCA at E1 does not seem to be related to light levels, as this site is comparable, or darker than other sites (Dunton et al. 2009, Bonsell and Dunton 2018, Section 1.1). The environmental data indicate that freshwater influence may preclude the establishment of CCA at this site (Fig. 3.5A and B). While CCAs are prone to low pH, Sagavanirktok River water is considerably basic (Craig and McCart 1975, A. Muth pers. comm.). Instead, low

salinities may be responsible for the absence of macroscopic CCA (King and Schramm 1982, Schoenrock et al. 2018). Settlement tile data demonstrates that recruitment is not limiting, as CCA can recruit to E1 in certain years (Fig. 3.4). Furthermore, the low rate of growth of all recruited taxa prevents competitive exclusion early in succession. Instead, osmotic stress and mortality caused by exposure to the buoyant freshwater layer in certain years prevent slow growing CCA from becoming part of the established community.

Salinity stress may also explain the low kelp abundance at E1. Karsten (2008) demonstrated that *L. solidungula* exhibits decreased photosynthetic performance after two days of exposure to salinities less than 20, conditions that often occur at E1 during the freshet (Section 1.1). Salinity gradients structure kelp forests globally (e.g., Sundene 1953, Buschmann et al. 2004, Spurkland and Iken 2011), and low salinities resulted in the first published instance of kelp habitat deforestation (Yendo 1914, Steneck and Erlandson 2002). In Stefansson Sound, warmer, fresher waters during the spring and summer may give a competitive advantage to red algae over CCA and kelp (King and Schramm 1982, Harley et al. 2012, Schoenrock et al. 2018), and thereby amplify the negative effect of foliose red algae on kelp (Filbee-Dexter and Wernberg 2018). This relationship is also implied by the high kelp cover observed at the site with the lowest foliose red algae cover (DS11, Table 3.2).

Current dynamics are an important structuring mechanism for benthic communities because they alter the delivery of propagules, food, and nutrients, and can cause mechanical stress or removal of entire organisms. Current direction also determines the source of propagules delivered to any particular area. W1 had a large percent bare rock cover (31%) and a greater abundance of invertebrates (Fig. 3.4, Table 3.2). The greater current velocities from the nearby passes (Section 1.1) may favor filter and suspension feeders by providing higher delivery rates of particulate food (e.g., Pequegnat 1964, Sebens 1984), though further investigation is needed. Community composition at L1 was not statistically different from that at E1, with both sites dominated by foliose red algae (Figs. 3.2 and 3.4, Table 3.2, Supp. Table 3.2). Although these locations experience different regimes of temperature and salinity, their seasonal current dynamics are very similar (Section 1.1). These sites may be protected from strong currents due to their shallow position between barrier islands and the shore, which may provide a competitive advantage to algae over invertebrates (Fig. 3.1). W3 and DS11 both exhibit relatively elevated mean light levels and current speeds (Section 1.1), but have dissimilar benthic communities, with less CCA and kelp at W3 (Figs. 3.2 and 3.4, Supp. Table 3.2). Prominent bare rock cover at W3 (average 35%) implies that this difference may be due to more frequent disturbance. The proximity of this site to a deep channel pass into Stefansson Sound may expose it not only to stronger currents, but also to more frequent ice scour, a common disturbance in benthic polar habitats (Conlan et al. 1998, Beuchel and Gulliksen 2008) that has been observed extensively at W3 (Section 1.1). This would preclude dominance by slow growing, but competitively

dominant Arctic CCA (Konar and Iken 2005, Kuklinski 2009, Schoenrock et al. 2018) and slow to establish kelp (this study).

The influence of light levels on benthic community composition are not straight forward, likely due to interactions between environmental variables influencing benthic biota. The most nearshore site (E1) and the most offshore site (DS11) had similar light levels, but disparate salinity regimes over the time period of data collection (Section 1.1). Elevated light levels at DS11 in the absence of low salinities (Section 1.1) may contribute to the abundance of kelp at this site. It is well established, and confirmed by our results, that elevated underwater irradiance at this site supports large kelp biomass (Dunton 1990, Aumack et al. 2007, Dunton et al. 2009, Bonsell and Dunton 2018). Kelp are well known foundation species which alter patterns of water motion (e.g., Kitching et al. 1934) and chemistry (e.g., Krause-Jensen et al. 2016), so community structure at this site could reflect the direct and indirect interspecific effects of high *L. solidungula* biomass. The negative relationship between light levels and filter feeders (Fig. 3.5A) similarly indicates that invertebrates are outcompeted by macroalgae in locations with elevated light levels. Suspended sediments in the water column, the main source of underwater light variability in the Boulder Patch, can also have strong negative effects on filter feeders by reducing feeding efficiency and pumping rate (e.g., Bell et al. 2015).

Patterns of recruitment and succession

Recruitment varied both spatially and interannually. The benthic community seems to recruit from a propagule pool generally derived from adjacent biota at certain locations (E1, W1, and DS11; Fig. 3.6F). At sites towards the edges of the main Boulder Patch area (L1 and W3; Fig. 3.6F), propagule input from other locations could result in a community of recruits that is substantially different from the established epilithic community. These spatial differences likely derive from the influence of hydrodynamic patterns across Stefansson Sound on larval transport and retention, as locations at the edge of the Boulder Patch may receive proportionally greater propagule input from adjacent soft bottom habitats (so-called “edge effects”). Abundant recruits and juveniles at DS11 may result from elevated local propagule production due to advantageous environmental conditions, or simply enhanced priority effects (numerical dominance of local propagules leading to local recruits) due to the overall high epilithic cover at this site.

Rhodophytes dominated tile communities (Fig. 3.4). Foliose red algae, which readily settled in great numbers, appear to be key early successional species in this community. Investigations of overgrowth interactions in the Boulder Patch demonstrated that foliose red algae often act as a substrate for bryozoan, hydroid, and sponge growth (Konar and Iken 2005). Consequently, the interactions between this group and other functional groups, including its negative effect on kelps (Filbee-Dexter and Wernberg 2018), may shape the trajectory of community development. CCA was also numerically dominant on tiles, and was even present at E1 where adults were absent, indicating that these algae produce abundant propagules, as has been found in shallow areas of Arctic fjords (Meyer et al. 2017). Also similar for

these two habitats is dominance by algal recruits compared to invertebrates (Meyer et al. 2017).

Although kelp is a dominant benthic biota at these sites and readily recruits to tiles in large numbers in the lab (C. Bonsell, pers. obs.), it did not recruit to settlement tiles at all during the study period. In a previous study from the Boulder Patch, the first kelp to recruitment to bare boulders only occurred after seven years (Martin and Gallaway 1994). The low apparent recruitment of kelps does not prove that kelp are not present on the tiles, a "seed bank" of gametophytes may be present that have not formed sporophytes yet due to lack of some environmental cue (Carney and Edwards 2010, Carney et al. 2013;). Alternatively, kelp spore chemotaxis may lead to settlement on alternative habitats in the environment (Amsler et al. 1992, Reed et al. 1992). However, if kelp are slow to recruit, establishment may be inhibited by faster growing foliose red algae and benthic invertebrates in habitats where these groups are abiotically favored, such as turbid or high flow areas (Witman and Dayton 2001, Filbee-Dexter and Wernberg 2018).

Tile communities only become more similar to the benthic community over time at two sites, W1 and W3. However, both sites were still 40% dissimilar to the benthic community at the end of the study (Fig 3.6F). Community development at these two sites was also highly variable (Fig. 3.7). Their location adjacent to a deep pass connecting Stefansson Sound and the Beaufort Sea, and the associated strong currents at these sites (Section 1.1.) may lead to temporal patchiness in the propagule pool, contributing to the variability in the recruited community. Tiles at DS11 were the most like the benthic community, with the smallest shift in community between years one and two (Figs. 3.6 and 3.7), again indicating the importance of priority effects at this site. These results overall indicate that propagule pressure resulting from the interaction between local production and hydrodynamics leads to initial recruited community, then environmental filtering shapes the trajectory of early succession.

Succession occurred very slowly, in agreement with past studies in the Boulder Patch (Martin and Gallaway 1994, Konar 2013). Even after three years in situ, the large majority of individuals on the tile remained <1 mm. Consequentially, very few instances of overgrowth were observed, unlike similar studies in Arctic fjords (Beuchel and Gulliksen 2008, Meyer et al. 2017). Overall, community development in the Boulder Patch appears to be very slow, which makes it difficult to parse out successional patterns over timescales less than a decade (Martin and Gallaway 1994, Beuchel and Gulliksen 2008, Konar 2013, Meyer et al. 2017). These results bolster conclusions that the Boulder Patch community would be very sensitive to any catastrophic disturbance event (Konar 2013).

Scaling up: links to Arctic climate

Understanding the links between climatic changes and shifts in Arctic kelp bed community structure and distribution requires knowing the connections between climate, the abiotic environment, and biota. The body of research

surrounding Arctic kelp ecology is small compared to that of lower latitudes but drawing upon knowledge of the physical environment of Arctic coasts can illuminate relationships between climate and community structure (Fig. 3.8). The majority of the proposed relationships shown in Figure 3.8B have not been empirically tested. Rather, we present them as hypotheses for future scientific inquiry.

First, coastal salinity reflects freshwater inputs from both Arctic rivers and sea ice melt. Downwelling winds entrain freshwater along Arctic inner shelves, while upwelling winds advect it offshore and bring in cool, salty oceanic water (Sellmann et al. 1992, Weingartner et al. 2017). Low salinities exert considerable influence on community structure by causing osmotic stress in certain algal groups, particularly CCA (King and Schramm 1982, Schoenrock et al. 2018), which is reflected in Boulder Patch community structure (Fig. 3.4). Through the negative effect of CCAs on invertebrate groups and foliose red algae (Konar and Iken 2005, Beuchel and Gulliksen 2008, Kuklinski 2009, Kortsch et al. 2012), low salinity can give a competitive advantage to these groups. The adverse effects of salinity on kelp (Fredersdorf et al. 2009, Karsten 2007) is amplified by the negative effects of red algae on kelp (Filbee-Dexter and Wernberg 2018). As the Arctic Ocean freshens due to runoff and sea ice melt (McClelland et al. 2006, McPhee et al. 2009, Morison et al. 2012), kelp beds in shallow, river influenced areas may face increasingly adverse conditions for kelps and CCA to persist. However, intensification of easterly winds, such as what is occurring along the Beaufort Sea coast (Wood et al. 2013, 2015) may ameliorate salinity conditions through upwelling.

Second, fluvial inputs and coastal erosion introduce suspended sediments to nearshore habitats, which increases light attenuation (Van Duin et al. 2001, Aumack et al. 2007, Fritz et al. 2017). Wind driven currents and mixing in the open water season resuspend benthic sediments on Arctic inner shelves, and further degrade the underwater light environment (Aumack et al. 2007 Bonsell and Dunton 2018). While all algae need light to grow, Arctic kelps are particularly sensitive to low light conditions caused by sediment resuspension (Dunton 1990, Aumack et al. 2007, Bartsch et al. 2016, Bonsell and Dunton 2018), while red algae are generally more tolerant of low-light conditions (Vadas and Steneck 1988). Sediments also have a negative effect on filter feeders (Fig. 3.4B), such as sponges (Bell et al. 2015). Identical to freshwater inputs, downwelling winds entrain water masses with high concentrations of suspended sediments along the coastal margin (Dunton et al. 2006). Climate driven lengthening of the open water season, intensified coastal erosion, and increased fluvial sediment inputs would thereby have a negative effect on abundance and persistence of nearshore kelps and filter feeders (Fig. 3.8).

Finally, wind dynamics can considerably impact patterns of benthic recruitment by altering the speed and direction of prevalent current flow. Faster currents and currents that advect water masses out of the coastal zone decrease local propagule retention (e.g., Gaylord et al. 2012). The community of recruits would potentially be more varied (Fig. 3.6), and the established community would

reflect the relative ability of each individual to withstand the local environment (Leibold et al. 2004). The resultant decrease in priority effects (wherein current community composition strongly influences future composition by dominating the propagule pool) would strengthen the importance of abiotic effects on benthic community structure (Fig. 3.8).

The community structure of Arctic kelp beds reflects an integration of local environmental conditions over decadal timescales due to the long successional cycle and longevity of many of the taxa. While this study highlights the effects of seasonal abiotic variation on benthic community structure, it also demonstrates that variability within a single year (or even >5 years) cannot account for the spatial distribution of taxa. Researchers must account for long-term environmental variability to fully comprehend and predict the impact of climate variation on kelp bed structure and distribution.

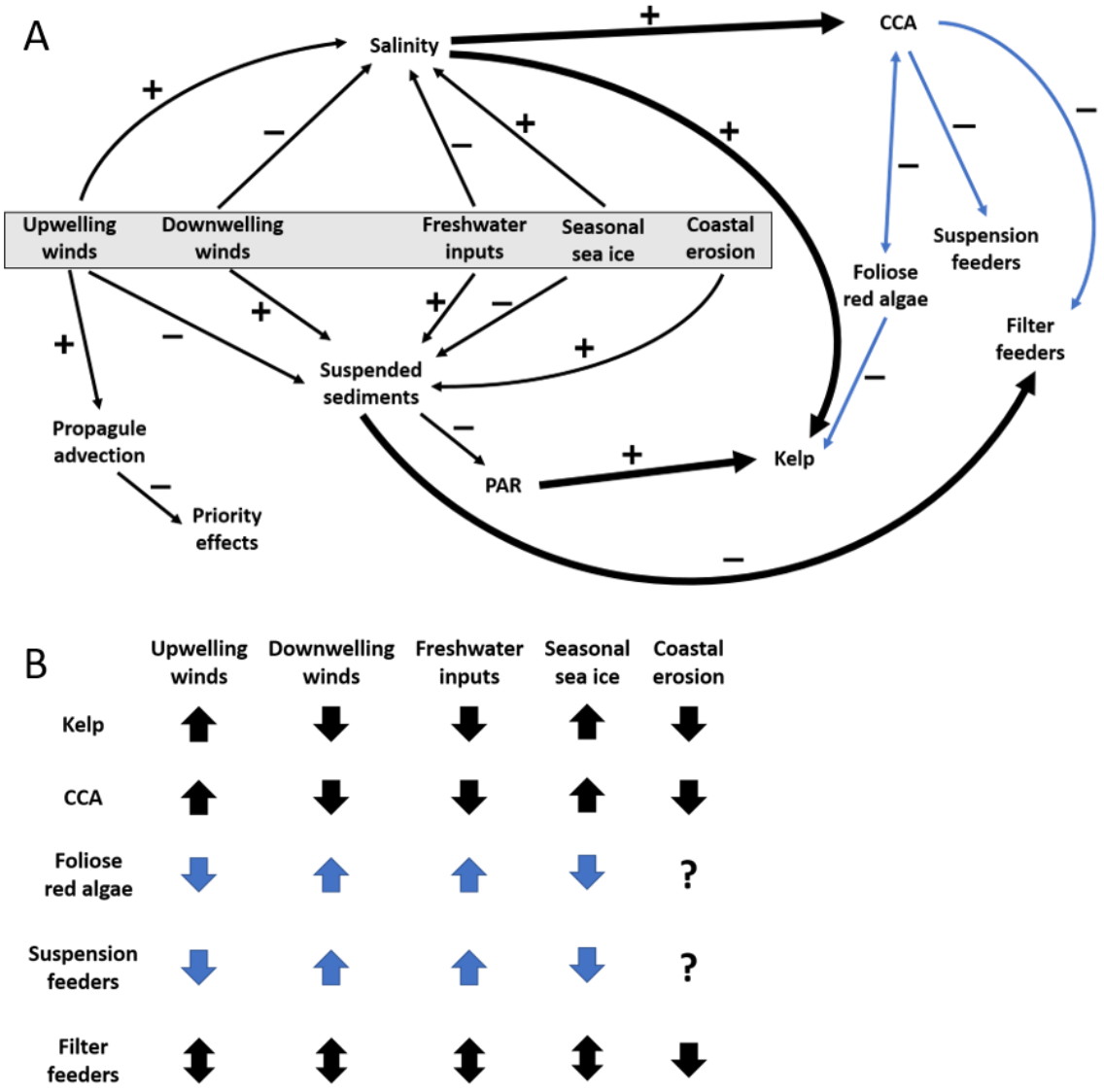

Figure 3.8. A) Positive and negative impacts (represented as arrows) of climatic drivers (in grey box) on environmental parameters/processes and functional groups on Arctic inner shelves. Biotic interactions are represented by blue arrows. A decrease in priority effects would strengthen the impacts of abiotic variables on functional group abundance (bolded arrows). See in-text citations (p 80). B) Overall effect of climatic drivers on functional group abundance. Indirect effects that occur through biological interactions are in blue.

Appendix

Supplemental Table S3.1. Number of tiles (and tile pieces) retrieved from each site for each deployment period. *indicates plates lost to ice scour.

Site	One year			Two years		Three years
	2015-2016	2016-2017	2017-2018	2015-2017	2016-2018	2015-2018
DS11	10	8	8	8	8	0*
E1	8	8	8	8	8	0
L1	0	0	8	0	0	0
W1	8	8	8	8	0	8
W3	0*	8	8	0*	8	0*

Supplementary Table S3.2. Pairwise PERMANOVA summary table for comparing benthic community structure at each site (square root transformed data). *Denotes significant difference.

	Df	SS	MS	F. Model	R2	Pr(>F)
DS11|E1* N:31|36						
Site	1	3.23	3.23	69.59	0.52	0.01
Residuals	65	3.02	0.05		0.48	
DS11|L1* N:31|24						
Site	1	1.91	1.91	26.83	0.34	0.01
Residuals	53	3.76	0.07		0.66	
DS11|W1* N:31|43						
Site	1	2.67	2.67	29.80	0.29	0.01
Residuals	72	6.45	0.09		0.71	
DS11|W3* N:31|35						
Site	1	1.71	1.71	30.45	0.32	0.01
Residuals	64	3.58	0.06		0.68	

E1|L1 N:36|24						
Site	1	0.11	0.11	2.42	0.04	0.12
Residuals	58	2.57	0.04		0.96	
E1|W1* N:36|43						
Site	1	0.89	0.89	12.98	0.14	0.01
Residuals	77	5.26	0.07		0.86	
E1|W3* N:36|35						
Site	1	0.98	0.98	28.23	0.29	0.01
Residuals	69	2.40	0.03		0.71	
L1|W1* N:24|43						
Site	1	0.82	0.82	8.91	0.12	0.01
Residuals	65	6.00	0.09		0.88	
L1|W3* N:24|35						
Site	1	0.44	0.44	8.06	0.12	0.01
Residuals	57	3.14	0.06		0.87	
W1|W3* N:43|35						
Site	1	2.00	2.00	26.14	0.26	0.01
Residuals	76	5.83	0.08		0.74	

Supplementary Table S3.3. Environmental characteristics of each site (Section 1.1). Values for physiochemical parameters represent mean±SD.

Site	Lat. (DD)	Long. (DD)	Depth (m)	Dist. to river input (km)	Temp. (°C)	Salinity	Current velocity (cm s^{-1})	PAR (mol photons m^{-2} day^{-1})
DS11	70.32228	-147.579	6.1	9.03	-0.78 ±1.96	32 ±3	4.4 ±5.3	0.271 ±1.013
E1	70.31495	-147.732	4.4	3.54	-0.41 ±2.50	31 ±4	2.8 ±3.2	0.208 ±0.925
L1	70.28993	-147.613	5.5	7.20	-0.82 ±1.89	33 ±4	1.9 ±2.7	0.194 ±0.756
W1	70.37003	-147.873	6.0	3.54	-0.95 ±1.84	30 ±4	4.3 ±5.4	0.102 ±0.236
W3	70.37627	-147.794	6.6	7.31	-0.80 ±1.88	32 ±3	4.8 ±4.6	0.184 ±0.700

DIRECTED EXPERIMENTAL AND OBSERVATIONAL STUDIES

4. Within- and between-basin population connectivity in the Arctic endemic kelp *Laminaria solidungula*

Christina E. Bonsell and Kenneth H. Dunton

GLOSSARY

Microsatellites: DNA loci containing repeated short sequences of nucleotides. In genetic studies, comparisons are made using microsatellite length.
LSU: The ribosomal large sub-unit. In Phaeophyceae, the LSU has a size of 26S. In genetics studies, comparisons are made between LSU ribosomal DNA sequences (which code for the ribosomal RNA that makes up the LSU).
H_O: Observed heterozygosity.
H_E: Expected heterozygosity.
F_{ST}: Fixation index. The mean reduction in heterozygosity of subpopulations compared to the total population. Subpopulations that are not differentiated have a value close to zero and subpopulations that are completely differentiated have a value closer to 1. If F_{ST} is significantly different from 0, then there is significant (sub)population differentiation.
G_{ST}: Similar to F_{ST}, but explicitly developed for >2 alleles. However, G_{ST} can never reach 1 if there are >2 alleles.
F_{IS}: Inbreeding coefficient. Mean reduction of individual heterozygosity due to inbreeding within a subpopulation. Has a value of 1 if all individuals are homozygous (an indication of inbreeding), and -1 if all individuals are heterozygous.
G_{IS}: Similar to F_{IS}, but explicitly developed for >2 alleles.

INTRODUCTION

Contemporary dispersal pathways and post-glacial recolonization into and across the Arctic are not well understood (Hardy et al. 2010), but are necessary to quantitatively forecast Arctic ecosystem changes (Krause-Jensen and Duarte 2014). The Arctic is warming at a faster rate than any other region in the world (IPCC 2014). As a result, a suite of ecosystem changes are occurring, including changes in species distributions (Bluhm et al. 2011, Grebmeier 2012, Michel et al. 2012). The northward range expansion of species of diatoms (Reid et al. 2007), bivalves (Berge, et al. 2005), and fish demonstrate that "the coming Arctic invasion" (Vermeij and Roopnarine 2008) is occurring across many taxonomic groups. These changes reflect increases in suitable habitats for subpolar species, but invasion success also requires adequate vectors to disperse individuals to new areas (Sakai et al. 2001). These vectors are changing as well, since ships traversing the increasingly navigable Northwest Passage transport non-native species into Arctic waters (Smith and Stephenson 2013, Chan et al. 2016). The spatial spread of species moving poleward as the Arctic warms will likely reflect the dispersal pathways used by contemporary

Arctic species (Vermaij and Roopnarine 2008). Understanding how populations are connected through the region allows for accurate prediction and sound management of species' persistence and the borealization of polar ecosystems.

In the changing Arctic, dispersal among populations and the resultant genetic connectivity can determine a population's capacity to withstand change or recover from disturbance. Healthy populations, with enough genetic diversity, can be self-sustaining (Hamilton 2009). However, immigration from outside populations may play an important role in 'rescuing' populations dwindled by ecosystem change or decimated by disturbance (Brown and Kodric-Brown, 1977). Persistence of foundation species (sensu Dayton 1972), such as kelps, in the face of warmer temperatures, increased turbidity, and lower salinities is central to the redistribution of habitats and ecosystem functions in the emerging Arctic.

In rocky subtidal Arctic areas, kelps provide habitat and a source of primary production that can increase local biodiversity and production, and alter local biogeochemistry (Dunton et al. 1982, Dunton and Schell 1987, Krause-Jensen et al. 2016, Filbee-Dexter et al. 2019). Shifts in kelp distributions are occurring globally (Krumhansl et al. n.d.), and are recorded in a few Arctic areas (Bartsch et al. 2016). Sub-polar kelps are expected to expand their range northward due to increasing temperatures and alleviated underwater light conditions (Müller et al. 2009, Krause-Jensen and Duarte 2014). However, baseline understanding of Arctic kelp biology and ecology is limited, making it challenging to predict and anticipate change under future climate and development scenarios (Filbee-Dexter et al. 2019). Currently, fourteen species of kelp inhabit the Arctic region (Filbee-Dexter et al. 2019). Only one of these species, *Laminaria solidungula*, is defined as an "Arctic endemic" due to its evolutionary history and its association with dark, freezing temperature waters. This species is also common in deep waters of cold, subarctic areas, including Svalbard (Lüning 1990). Consequently, the distributional pattern of *L. solidungula* provides a valuable opportunity to examine mechanisms of physical dispersal and kelp evolutionary history, due to the trans-Arctic spread of Laminariales into the Atlantic Ocean from the North Pacific (Stam et al. 1988). Furthermore, as this species represents the most cold tolerant kelp (tom Dieck 1993), it is of interest for comparative biogeography studies and predicting future kelp distributions.

Due to their requirement of rocky substrate, *L. solidungula* can exist in patches separated by 100s of kms, as they do in the Alaskan Beaufort Sea (Dunton et al. 1982; Fig. 4.1). Genetic data indicate that marine macroalgae disperse on scales of 100s to 1000s of m $year^{-1}$ on average, either through their free swimming microscopic stage or their macroscopic stage via drift (Kinlan and Gaines 2003). A lack of habitat continuity may limit the amount of genetic exchange between *L. solidungula* patches, and decreased within patch genetic diversity, as shown in other kelp species (Alberto et al. 2010, Durrant et al. 2018). Genetic diversity of a population can be linked to the probability that a declining population could be "rescued" by migration from other populations, as well as linked to the capacity of a

population to adapt to change or disturbance (Brown and Kodric-Brown, 1977, Sakai et al. 2001). Recently, work by Wernberg et al. (2018) highlighted the link between higher genetic diversity (expected heterozygosity) in temperate kelp populations and their resilience to extreme climatic events – kelp forests with higher genetic diversity showed greater capacity to regrow after experimental disturbance and a marine heatwave. Genetic diversity, therefore, may then provide an important measure to evaluate the vulnerability of Beaufort Sea *L. solidungula* populations to the environmental perturbations associated with climate change and coastal development.

Spatial genetic data can be used to infer information about dispersal and population connectivity. Closely related populations of individuals are generally characterized by having higher connectivity through propagule dispersal. The timescale of connectivity conferred by genetic data varies by genetic marker. For example, microsatellite markers, which evolve relatively quickly, are used to infer population connectivity over scales of decades to thousands of years while mitochondrial cytochrome C oxidase subunit I gene (COI), internal transcribed spacer (ITS), and other ribosomal markers are used to infer population connectivity and species relationships over longer periods, from tens of thousands to millions of years. Mitochondrial and ribosomal markers have been used to infer the recolonization history of the Arctic by macroalgae after the Last Glacial Maximum (McDevit and Saunders 2010, Coyer et al. 2011, Bringloe and Saunders 2018). However, data from more than a few high Arctic sites within these studies are rare (but see Nieva et al. 2018).

The aim of this study is to evaluate genetic connectivity of *Laminaria solidungula* populations across two different scales in the Arctic: 1) among stations within the Alaskan Beaufort Sea, including six stations within the Stefansson Sound Boulder Patch, Camden Bay, and Barter Island, and 2) among sites in the Western Arctic Basin, including the Beaufort Sea, Arctic Canada, Newfoundland, and Svalbard. We used two different markers, corresponding to each scale. For the regional scale study, we used microsatellite markers to infer population connectivity and genetic diversity in the Alaskan Beaufort Sea. These are putatively neutral and rapidly evolving, often used to determine population differentiation across geographic scales of 10s-1000s of m. For the basin scale assessment, we sequenced the D1/D2 region of the large subunit (26S) ribosomal RNA gene (rDNA). The 26S rDNA sequence is generally highly conserved in Phaeophyceae and has been used in combination with other molecular markers to resolve taxonomic relationships in brown algae at the level of order and above (Phillips et al. 2008, Lane 2006), but its use in determining genetic divergence within kelp species is limited. However, the more divergent D1/D2 hypervariable regions within the LSU rDNA gene, which have been excluded from large phylogenetic analysis of Phaeophyceae due to high variability (Draisma et al. 2001), are often used to barcode species of taxa such as dinoflagellates (Scholin et al. 1994) and ciliates (Stoeck et al. 2014) and have been suggested as a barcode gene for all metazoans (Sonnenberg et al. 2007). We therefore expected subspecies level variability in the

D1/D2 region within Laminariales, reflecting population differentiation over longer timescales than microsatellites.

METHODS

Adult sporophytes of *L. solidungula* were collected from six sites: Stefansson Sound Boulder Patch (Beaufort Sea), Camden Bay (Beaufort Sea), Barter Island (Beaufort Sea), Finlayson Islands (Canadian Archipelago), Bonne Bay (Newfoundland), and Kongsfjorden (Svalbard; Fig. 4.1). Within the Beaufort Patch there were six distinct sampling stations: B1, DS11, E1, L1, W1, and W3 (Fig. 4.1). Therefore, there were eight Beaufort Sea stations total, among three sites. Stefansson Sound, Bonne Bay, and Kongsfjorden samples were collected by divers. Camden Bay samples were obtained by dragging for plant material. Barter Island samples were collected from fresh drift algae. Finlayson Island samples were acquired incidentally via benthic trawl. Tissue samples were collected from the meristem (when possible), then dried in silica desiccant and frozen at -80°C.

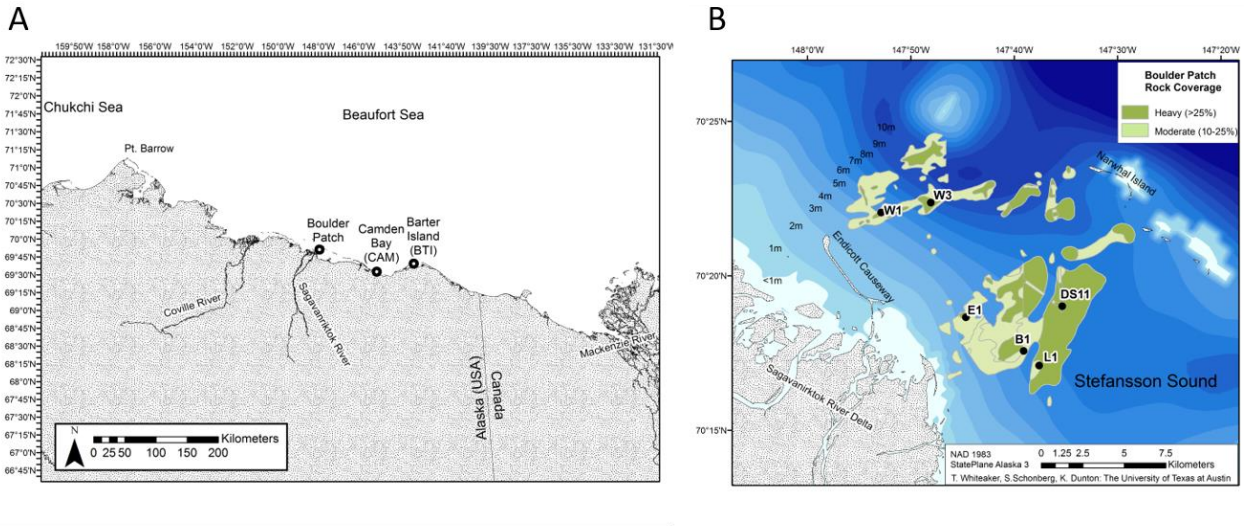

Figure 4.1. A) Location of three Beaufort Sea sampling sites. B) Location of sampling stations within the Boulder Patch. Benthic cover and long-term environmental data exist for sites DS11, E1, L1, W1, and W3.

For DNA extraction, ~10-20 mg of dry material from each sporophyte was ground using an MPBio FastPrep tissue lyser (Lysing Matrix A). Extraction was carried out using a cetyltri-methylammonium bromide (CTAB) protocol (Zuccarello and Lokhorst 2005). Briefly, ground kelp material was added to a microcentrifuge tube with 500-700 µL of CTAB extraction buffer and incubated overnight at 65 °C with gentle shaking. Chloroform: isoamyl alcohol (24:1) was added then briefly

vortexed, and the phases were separated by centrifugation at 12000*g* for 10 min. The aqueous phase was removed to a new centrifuge tube, and the extraction step was repeated in that tube. The twice extracted aqueous phase was again placed in a new tube along with an equal volume of 100% isopropanol, then mixed by inversion. The sample was incubated at room temperature for 30 min to 1 hr. Precipitated nucleic acids were collected by centrifugation for 30 min at 12000*g* at 20°C, after which the supernatant was decanted. The DNA pellet was washed in 70% ethanol, concentrated by centrifugation for 5 min at 12000*g*, drained, and air-dried. Depending on the size of the pellet, we added 50-150 µL of 0.1 X TE buffer (145 M Tris, 1 µM EDTA). Samples were frozen at -20°C.

Microsatellite analysis

From population genetic studies in other kelp species, we selected five primer pairs that amplified microsatellite sequences in *L. solidungula* sampled in the Boulder Patch (Table 4.1, Supp. Table 4.1). PCR reactions consisted of 0.25 mM dNTPs, 0.5 mM MgCl, 1X Dream Taq buffer, 2U Dream Taq polymerase, 0.4 µM of each reverse primer and fluorescently labeled forward primer, and 1 µL DNA template (10-20 ng) in 20µL total volume. Capillary electrophoresis fragment analyses were performed at Texas A&M University Corpus Christi Genomics Core Lab on an Advanced Analytical Fragment Analyzer. Peaks were scored in Geneious (http://geneious.com).

Table 4.1. Information for loci used in this study. *Marker development reference

Locus	AT	Sequence motif	*L. solidungula* fragment length	Cross amplification species	References
Ld-3	51	(aag)6	251-263	*S. japonica*, *L. hyperborea*	Liu et al. 2012*
Ld-13	54	(ggaa)10	159-231	*S. japonica*	Liu et al. 2012*
Ld2/520	53	(at)6(gt)7	366-388	*L. digitata*, *L. nigrecens*	Billot et al. 1998*, Martinez et al. 2015
LolVVIV-15	60	(aac)21	102-144	*L. hyperborea*, *L. ochroleuca*	Coelho et al. 2014*
LolVVIV -23	60	(aac)14	105-111	*L. digitata*, *L. hyperborea*, *L. ochroleuca*	Coelho et al. 2014*

Microsatellite loci only amplified consistently for samples collected in Beaufort Sea, so this analysis excluded the other sites. Data were filtered to only include samples with one or fewer missing loci. We used MICRO-CHECKER (Van Oosterhout et al. 2004) to scan for evidence of null alleles and scoring errors. Per

locus F_{ST} and F_{IS} were determined in GENEPOP (Rousset 2008), along with tests for linkage disequilibrium, deviations from Hardy Weinberg equilibrium, and heterozygote excess. We used Fisher's exact test in GENEPOP to determine pairwise population differentiation on genotypes. Per population F statistics and AMOVA were analyzed using GENODIVE (Meirmans and Van Tienderen 2004). All other data analysis and visualization for microsatellite DNA variation was carried out in R (R Core Team 2016).

To assess the role of environmental factors on genetic differentiation among stations within the Boulder Patch, we compared biotic and abiotic environmental variables (Section 1.1. and 1.2) to genetic diversity using a distance based redundancy analysis (db-RDA; Legendre and Anderson 1999). Benthic percent cover data of functional groups (kelp, crustose coralline algae, foliose red algae, filter feeders, suspension feeders) were arcsine transformed. To homogenize the mean and standard deviation for all environmental data for the db-RDA, including benthic cover, raw values were normalized by subtracting the grand mean and dividing by the standard deviation. Dissimilarity between kelp stations based on microsatellite data were calculated using a principal coordinate analysis (PCoA, R package adgenet; Jombart 2008). The relationship between PCoA coordinates and normalized environmental variables was determined using a db-RDA, with a stepwise model building approach (R package vegan; Oksanen et al. 2016). Differences among stations were assessed using one-way ANOVAs on each environmental variable, with posthoc Tukey HSD tests.

Ribosomal large subunit (LSU) DNA

The lack of microsatellite amplification in individuals collected outside of the Beaufort Sea necessitated the use of a different marker to investigate population differences among geographic regions in the Western Arctic Ocean Basin. Partial sequences of LSU ribosomal RNA genes covering the D1/D2 region (~550 bp) were acquired for samples from Boulder Patch stations DS11 (n=4) and B1 (n=5), Barter Island (n=3), Camden Bay (n=8), Newfoundland (n=3), Svalbard (n=7), and the Finlayson Islands (n=4). Amplification was carried out in 20 µL total volume using 0.4 µM D1R/D2C primers (Scholin et al. 1994), 1X Myfi mix (Bioline), and 10-20 ng DNA. Cycling conditions consisted of 2 min at 94°C, then 30 cycles of 1 min at 94 °C, 40 sec at 51 °C, 1.5 min at 72 °C, with a final elongation step of 5 min at 72 °C.

Sequences were visually inspected, trimmed, and aligned using Geneious. To assess the relative phylogenetic significance of variation in the LSU, we aligned *L. solidungula* sequences with other sequences from the Order Laminariales available on GenBank (Table 4.2). A neighbor-joining algorithm was used to visualize LSU variation within and between species.

Table 4.2. List of samples used for LSU analysis and accession numbers.

Species	Collection information	No. samples	LSU Genbank and reference
Laminaria solidungula	Boulder Patch, AK, USA (collector: C. Bonsell)	9	
	Camden Bay, AK, USA (collectors: J. Dunton and T. Dunton)	8	
	Barter Island, AK, USA (collector: C. Bonsell)	3	
	Bonne Bay, NL, Canada (collector: G. Bishop)	3	
	Hansneset, Svalbard, Norway (collector: I. Bartsch)	7	
	Finlayson Islands, NU, Canada (collector: B. Bluhm)	4	
Laminaria yezoensis	L. Druehl culture	1	AY851518 (Lane et al. 2006)
Laminaria sinclarii	Mud Cove, Bamfield, BC, Canada	1	AY851516 (Lane et al. 2006)
Laminaria ochroleuca	Roscoff, Brit., France	1	AF071154 (Rousseau et al. 2000)
Laminaria digitata	Roscoff, Brit., France	1	AF071153 (Rousseau and De Reviers 1999)
	Green Pt., Lepreau, NB, Canada	1	AY851517 (Lane et al. 2006)
	Hornbaek, Sjaelland, Denmark	1	AY441778 (Erting et al. 2004)
Laminaria hyperborea	Roscoff, Brit., France	1	AF071155 (Rousseau and De Reviers 1999)
	Deget, Denmark	1	AY441779 (Erting et al. 2004)
Saccharina sessilis	Cape Beale, Bamfield, BC, Canada	1	AY851513 (Lane et al. 2006)
Saccharina nigripes	Green Pt., Lepreau, SB, Canada	1	AY851514 (Lane et al. 2006)
Saccharina latissima	Helsinborg, Denmark	1	AY441780 (Erting et al. 2004)
	Hirsholm, Denmark	1	AY441781 (Erting et al. 2004)
	Drelnes, Denmark	1	AY441782 (Erting et al. 2004)
Saccharina gyrate	L. Druehl culture	1	AY851526 (Lane et al. 2006)
Saccharina augustata	L. Druehl culture	1	AY851515 (Lane et al. 2006)
Cymathaere triplicate	Wiffen Spit, Sooke, BC Canada	1	AY851519 (Lane et al. 2006)
Egregia menziezii	Boiler Bay, OR, USA	1	AY851506 (Lane et al. 2006)
Lessonia corrugata	Gov. Is. Reserve, Tas., Australia	1	AY851532 (Lane et al. 2006)
Lessonia flavicans	Rookery Bay, Falkland Islands	1	AY851531 (Lane et al. 2006)
Lessonia nigrescens	Las Cruces, Chile	1	AY851530 (Lane et al. 2006)

RESULTS

Microsatellite analyses: Beaufort Sea populations

For the 119 individuals analyzed, the five polymorphic loci had a total of 49 alleles, ranging from 5 to 13 alleles per locus (Table 4.3). No significant linkage disequilibrium was detected ($p<0.05$). Heterozygosity varied among loci, and overall heterozygosity was moderate (H_o=0.67, Table 4.3). No difference between observed and expected heterozygosity was observed (Bartlett's K^2=0.217, $p>0.05$). Three out of five loci deviated significantly from Harvey-Weinberg Equilibrium ($p<0.05$, Table 4.3). Genetic diversity (number of alleles per individual) varied among sites, depending on sample size (Table 4.4).

Table 4.3. Summary statistics for microsatellite loci. Bold indicates significant deviance from Harvey-Weinberg Equilibrium ($p<0.05$). * indicates significant deviance from HWE after Bonferroni correction.

Locus	**# alleles**	**H_o**	**H_e**	**F_{is}**	**F_{st}**
Ld-3	8	0.75	0.66	**-0.132**	0.001
Ld-13	13	0.25	0.24	-0.018	0.016
Ld2/520	12	0.85	0.72	**-0.188**	0.006
LolVVIV-15	11	0.82	0.68	**-0.208***	0.017
LolVVIV -23	5	0.80	0.49	-0.636	0.013
Global		0.69	0.56	**-0.244***	0.010

Table 4.4. Summary statistics for samples from each location. Bold indicates sig after Bonferroni correction.

Site or Station	**N**	**# alleles/ind**	**Effective # of alleles**	**H_o**	**H_e**	**F_{is}**	***p* (Heterozygote excess)**
BTI	12	2.083	2.61	0.627	0.533	**-0.138**	0.766
CAM	2	6.000	2.47	0.625	0.425	0.167	1.000
Boulder Patch Stations:							
B1	16	1.438	2.66	0.689	0.537	-0.240	0.091
DS11	19	1.421	2.45	0.800	0.571	**-0.378**	**0.000**
E1	13	1.692	2.40	0.662	0.517	-0.243	0.258
L1	18	1.389	2.71	0.696	0.569	**-0.198**	0.741
W1	20	1.450	2.39	0.667	0.530	-0.227	0.010
W3	19	1.421	2.50	0.703	0.547	-0.260	**0.004**

The likely total number of alleles per individual for these stations and loci is ~1.5. Overall heterozygosity at each station (H_o) was moderate to high (0.625-0.800, Table 4.4). There were significant departures from Hardy-Weinberg Equilibrium at three out of the eight sampling stations, and overall ($F_{IS} \neq 0$; Tables 4.4 and 4.5). Chi-squared tests demonstrated that heterozygote excess was present at two sites, as well as within the global population (Table 4.4). There was no significant population structure given by sites (AMOVA, $p<0.05$). Similarly, overall population differentiation (F_{ST} = 0.010, 0.006 excluding Camden Bay samples, Table 4.5) and pairwise F_{ST} (0-0.107, Table 4.6) were low, meaning that populations are not well differentiated by site. However, some pairwise genetic differentiation was statistically significant, with site DS11 showing the most consistent genetic differentiation from the other sites (Table 4.6). DS11 had significantly higher kelp cover than the other sites (α=0.05; one way ANOVA: $F_{(1,4)}$=9.70, Supp. Tables 4.2 and 4.3) and comparison to environmental parameters via dbRDA revealed that benthic cover by kelp significantly influenced the genetic differences between sites (Table 4.7, Fig. 4.2).

Table 4.5. Overall differentiation statistics for Beaufort Sea stations. Values in brackets include the two Camden Bay individuals. *statistically significant.

F_{st}	0.006 (0.010*)
F_{is}	-0.248 (-0.243)
G_{st}	0.005 (0.028*)
G_{is}	-0.200* (-0.241*)

Table 4.6. Pairwise F_{ST} values between Beaufort Sea sampling locations. Sampling sites are in bold, sampling stations within the Boulder Patch site are in normal font. * indicates significant differentiation ($p<0.05$). **indicates significant differentiation after Bonferroni correction.

	CAM	B1	DS11	E1	L1	W1	W3
BTI	0.059	0	0.019*	0.009	-0.008	-0.002	0
CAM		0.18*	0.1*	0.107*	0.052	0.089	0.069
B1			0.022*	0.014	-0.003	-0.004	0
DS11				0.031**	0.003	0.019*	0.016**
E1					0.009	0.005	-0.006
L1						-0.003	-0.001
W1							-0.01

Table 4.7. Stepwise model building results for the effect of environmental variables on the distance between stations given by PCoA on genetic data. **Bold** indicates significance. Units: Temperature, daily mean (ºC); Light (photons m^{-2} day^{-1}); Salinity, daily mean; Current velocity, daily mean (cm sec^{-1})

	Df	AIC	F	*p*
% Kelp cover	1	-15.705	4.7264	0.025
% CCA cover	1	-13.585	2.057	0.15
Temperature (Ice cover)	1	-13.131	1.6179	0.2333
Temperature (Year-round)	1	-13.355	1.829	0.2417
Light (Open water)	1	-12.64	1.1858	0.3833
Temperature (Open water)	1	-12.9	1.4095	0.3917
% Red algae cover	1	-12.573	1.1298	0.4167
Light (Year-round)	1	-12.617	1.1664	0.425
Salinity (Open water)	1	-12.157	0.8	0.5417
Salinity (Year-round)	1	-12.173	0.8124	0.575
% Filter feeder cover	1	-11.957	0.6516	0.6167
Salinity (Ice break-up)	1	-12.048	0.7185	0.6333
Temperature (Ice break-up)	1	-11.914	0.6202	0.6583
Salinity (Ice freeze-up)	1	-11.608	0.4055	0.75
Salinity (Ice cover)	1	-11.517	0.3436	0.7833
Current velocity (Ice break-up)	1	-11.339	0.227	0.8083
Current velocity (Ice cover)	1	-11.341	0.2282	0.825
Current velocity (Ice freeze-up)	1	-11.301	0.2021	0.9
Temperature (Ice freeze-up)	1	-11.037	0.0377	0.9083
% Suspension feeder cover	1	-11.135	0.0978	0.9167
Current velocity (Open water)	1	-11.108	0.0811	0.9417
Current velocity (Year-round)	1	-11.023	0.0292	1

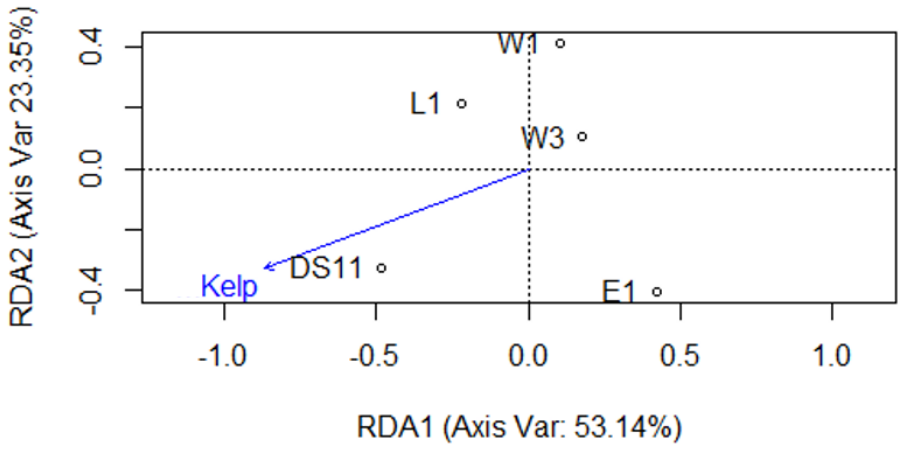

Figure 4.2. Ordination plot of stations within the Boulder Patch based on genetic distance compared to kelp cover.

LSU analysis: *Laminaria solidungula* across the Western Arctic Ocean Basin and comparisons to other Laminariales

LSU rDNA sequences were ~550 bases long after trimming, with two variable sites: C-T polymorphism and a G-A polymorphism. All individuals had either the C and G or T and A combination, resulting in two genotypes. One genotype was found exclusively in the Beaufort Sea individuals, and the other was restricted to the Canadian/Atlantic Arctic, with a single exception in Camden Bay (Fig 4.3). The Beaufort Sea genotype was 1 base different from the *L. yezoensis* genotype (Fig. 4.4). These two species had fewer deviations from *Saccharina* species and *C. triplicata* than from other Laminaria species (Fig. 4.4).

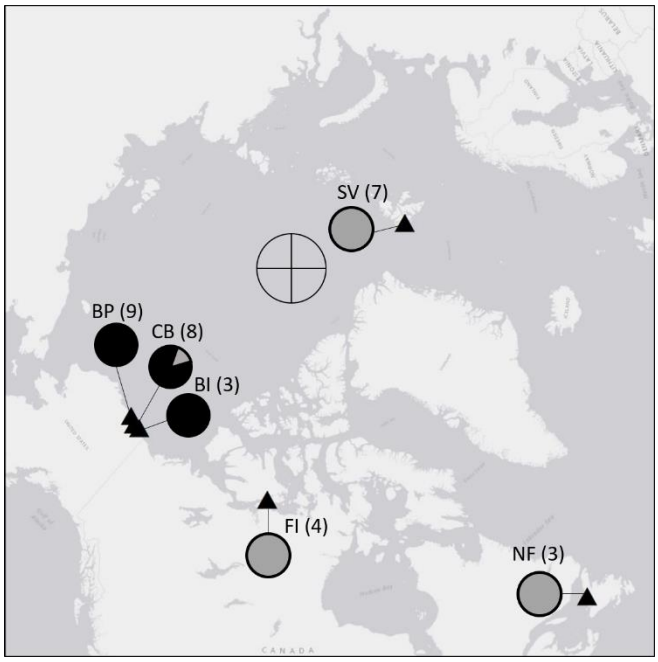

Figure 4.3. Map of *L. solidungula* sampling locations (triangles) and percent of LSU genotypes, represented as pie graphs. Black = "Beaufort" genotype, grey = "Atlantic Arctic" genotype. Number of samples in parentheses. Cross shows location of the pole.

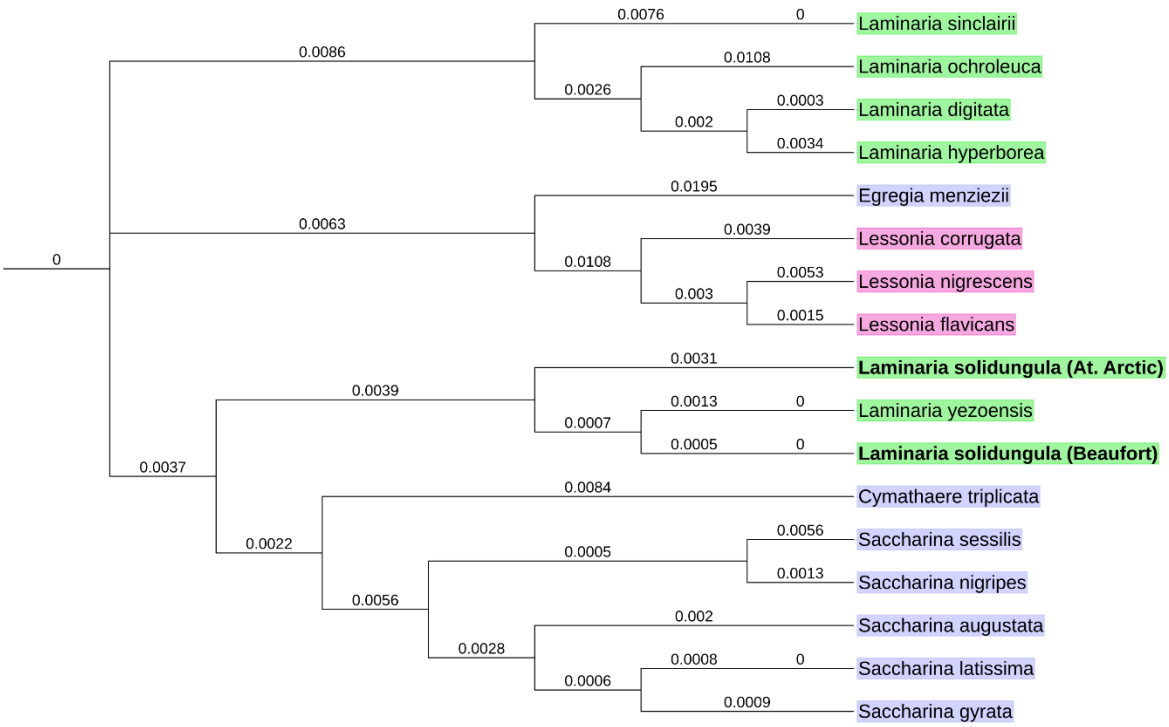

Figure 4.4. Topology of LSU sequences from kelps in the families Arthromenceae (blue), Lessonaceae (pink), and Laminaraceae (green). *Laminaria solidungula* sequences, generated in this study are bolded. All other sequences from GenBank (Table 4.2). Branch numbers indicate percent difference between sequences. Adding the differences along the path between any two species will give the total percent difference in sequence between those two species. This tree does not represent a phylogeny.

DISCUSSION

Evidence for panmixia in the Beaufort Sea

When compared to other microsatellite studies on kelps, the level of population differentiation (F_{ST}) we found in the Beaufort Seas corresponds to the low end of differentiation found over scales of <20 km (Billot et al. 2003, Alberto et al. 2010, Brennan et al. 2014, Robuchon et al. 2014). As the majority of our samples came from within the Boulder Patch, our results fit into the model of weak differentiation over smaller scales for most kelp species (Billot et al. 2003, Coleman et al. 2011, Brennan et al. 2014). However, we found that drift kelp on Barter Island

were not differentiated from attached kelp within the Stefansson Sound Boulder Patch, approximately 150 km away. This indicates that the Beaufort Sea population of *Laminaria solidungula* has the capacity for panmixia (random mating within the region), despite the lack of habitat continuity. Other studies have reported strong differentiation over similar spatial scales, which was attributed to complex coastline or hydrographic barriers (Billot et al. 2003, Breton et al. 2018, Durrant et al. 2018). Coleman et al (2011) demonstrated that genetic connectivity of kelps is related to the strength of currents that connects those systems. The lack of genetic structure in the Beaufort Sea indicates high connectivity among habitats, which may be assisted by the regional circulation regime.

Kelp dispersal in the nearshore Beaufort Sea is likely enhanced by fall storm events, which can transport large numbers of reproductive individuals, as evidenced by the extensive biomass that can wash onshore after a large wind event (Fig. 4.5). Experiments with seabed drifters show that neutrally buoyant, near bottom drift (which would transport kelp), can transport materials alongshore by 10s of km under ice cover and 100s of km in the summer (Barnes and Reimnitz 1982). Summer circulation patterns along the Alaska Arctic coast, including over the Boulder Patch, are wind driven and primarily alongshore, with dominant westward flows (Barnes and Reimnitz 1982, Weingartner et al. 2017, Section 1.1). In the Beaufort Sea, *L. solidungula* releases meiospores under the cover of 1.8 m thick landfast sea ice in late winter or early spring (K. Dunton, pers.comm.). Currents are minimal during this time, so the transport of mature adults during the summer and fall is more important for maintaining population connectivity, since kelp meiospores, whose small size exposes them to boundary layer effects, can only travel 10s of m without the aid of strong currents (Gaylord et al. 2006). The low pairwise genetic differentiation demonstrates that each sampling site is highly connected to the others. The fact that this population exhibits low genetic differentiation among geographically distinct locations suggests that range expansion by boreal species may occur rather quickly within the Beaufort Sea, given suitable habitat.

Additional evidence of a panmictic *L. solidungula* population in the Beaufort Sea is high observed heterozygosity, as well as heterozygote excess at two Boulder Patch stations (DS11 and L1, Table 4.4), and negative inbreeding coefficients ($F_{IS}<0$, Tables 4.4 and 4.5). Outbreeding is rare in kelps (Valero et al. 2001) and isolated kelp patches should display prominent selfing and inbreeding (Gaylord et al. 2012). However, despite the habitat isolation of the Boulder Patch, the kelp are apparently not isolated genetically. While connectivity to a wider kelp population is not unexpected, the level of heterozygosity in the Beaufort Sea population is unusual. Interestingly, this suggests that very little sexual reproduction occurs within the Boulder Patch itself; in other words, the Boulder Patch is not self-recruiting. Concurrent observations in the Boulder Patch show that sporophyte recruitment happens over spans of >5 yrs. (Martin and Gallaway 1994, Konar 2013, Section 1.2). Furthermore, kelp establishment on hard substrate, rather than to algae or invertebrates that will become dislodged, is extraordinarily rare considering the

relative availability of rock surface (Bonsell and Muth unpub. data). Additionally, *L solidungula* in the Boulder Patch can be considerably long lived: Dunton (1990) was able to relocate individuals more than two decades after they had been tagged for growth measurements. The genetic structure may reflect establishment in the Boulder Patch by drift kelp from various sources and breeding populations followed by little to no self-recruitment. Submergence of the Beaufort Sea coast after the last glacial maximum, and subsequent recruitment of kelp to the Boulder Patch, may have effectively occurred relatively recently compared to the apparent long *L. solidungula* generation time. As a result, Boulder Patch genetic structure may show heterozygote excess associated with recent population mixing (i.e., isolate breaking). This may act in combination with a selective benefit to heterozygosity, as seen in other kelp species (Raimondi et al. 2004, Johansson et al. 2013).

Heterozygote excess and high variability in inter-locus F_{IS} (Table 4.3) are also an indicator of clonal reproduction (Balloux et al. 2003). However, the kelp haploid-diploid life cycle would require apomeiosis and the production of diploid zoospores instead of the normal haploid to increase population heterozygosity. Regular production of diploid zoospores has only been reported from a single wild subpopulation of *L. digitata* (Oppliger et al. 2014). In that case, the irregular zoospores did not significantly contribute to population dynamics. Therefore, it would be extremely unusual if our results reflected *L. solidungula* clonal reproduction.

Smaller scale differentiation within the Beaufort Sea mainly consisted of pairwise differentiation of the Boulder Patch station DS11 compared to other stations. This station has the highest kelp density (Supp. Table 4.2; Dunton and Iken unpubl. data), and high annual kelp growth (Bonsell and Dunton 2018; K. H. Dunton et al. 2009). It is notable that there was significant differentiation between kelps from DS11 and W3, which have comparable depths and environmental regimes (Section 1.2), similar levels of genetic diversity, and similarly high heterozygosity (Fig. 4.2, Table 4.4). Ordination analysis also revealed high dissimilarity among three spatially adjacent stations: E1, L1, and DS11 (Figs. 4.1 and 4.2). These stations all have distinct environmental regimes (Section 1.2); however, ordination analysis indicated that genetic dissimilarity between sites was related to kelp cover rather than to any particular abiotic factor (Table 4.7). Given the long-lived nature of *L. solidungula*, our multi-year environmental data may not have covered enough timespan to capture selective forces, such as multidecadal disturbance and environmental variability. Furthermore, spatial patterns in benthic cover are related to environmental variables in the Boulder Patch (Section 1.2). Significant outbreeding at DS11 and at W3 suggest that these areas may exhibit high genetic exchange. These two sites exhibit especially strong along shore currents during the open water season (Section 1.2). Flow patterns demonstrate regular physical connectivity with areas outside the Boulder Patch. The deeper, offshore areas of the Boulder Patch could therefore function as sources of *L. solidungula* propagules or entrap kelp drift from the eastern Beaufort Sea and act as sinks.

Divergence between Arctic basins: outcome of glacial cycles

Despite the high connectivity within the Beaufort Sea, LSU sequences indicated that there is far less gene flow occurring between the Canadian Arctic and the U.S. Arctic. Two distinct genotypes were identified, which occurred almost exclusively in different basins except for one Canadian genotype present in Camden Bay. The dominance of one genotype in each basin indicates long-term evolutionary divergence between *L. solidungula* lineages from the Canadian and Alaskan Artic. This observation is supported by results from sequencing for COI in the same species collected from the North American Arctic (McDevit and Saunders 2009, Bringloe 2018 Fig. E58). It also resembles the pattern in *Saccharina latissima*, a circumpolar species, which shows strong population differentiation between Pacific and Atlantic populations, with the Canadian Arctic as an area of interbreeding (McDevit and Saunders 2010). Based on various lines of genetic evidence, *S. latissima* recolonized the Arctic after the Last Glacial Maximum from at least two different populations, likely from a Pacific and Atlantic population, or a local refuge population (McDevit and Saunders 2010, Bringloe and Saunders 2018). We propose that a similar process occurred for *L. solidungula,* recolonization from allopatric source populations, with mixing between the two occurring in the eastern Beaufort. The population structure of *S. latissima* displays within basin admixture at high Arctic sites (Neiva et al. 2018). This reflects our microsatellite analysis findings of admixture within the Beaufort population of *L. solidungula* and suggests that cross basin range expansion by boreal species will occur much more slowly than within basin.

Polymorphism within *L. solidungula* LSU is interesting given the lack of within species variation in other investigated kelp species (*L. digitata*, *S. latissima*), and the overall low genetic divergence among kelp species. Whole LSU sequences are <3% divergent among species in the Laminariales, while other markers (ITS, RUBISCO, mitochondrial) are much more variable (Lane et al. 2006). Significant divergence, beyond the LSU locus, may also explain why microsatellite markers developed from Boulder Patch samples failed to amplify in all samples from outside the Beaufort Sea, and most samples from Camden Bay. The degree of genetic (COI) differentiation in *S. latissima* among Arctic basins led Nieva et al. (2018) to conclude that the phylogenetic lineages represented incipient species. Although our work only involves one genetic marker, the scale of genetic differentiation within the Laminariales suggests similar emerging divergence for *L. solidungula. L. solidungula* is hypothesized to have first colonized the Arctic after the opening of the Bering Strait ~ 5.32 mya (Rothman et al. 2017). Glacial growth and retreat then lead to allopatric divergence and phylogeographic population structure (McDevit and Saunders 2010, Neiva et al. 2018).

Relationship to other kelp species

LSU topology grouped *L. solidungula* with *L. yezoensis*, separate from other Laminaria, in agreement with the findings of Rothman et al. (2017) for concatenated

alignment of rbcL and ITS. McDevit and Saunders (2010) also found high relatedness of *L. solidungula* and *L. yezoensis* based on COI sequences, though neither study included Beaufort Sea samples. Interestingly, the divergence between Beaufort *L. solidungula* and *L. yezoensis* is less than the divergence between Beaufort and Atlantic Arctic genotypes of *L. solidungula* (Fig. 4.4). The rbcL topology of Rothman et al. (2017) placed Canadian *L. solidungula* between *L. yezoensis* from Japan and *L. yezoensis* from British Columbia. Their time calibrated phylogeny indicated that these two species started diverging 16.4 to 5.6 mya, but these species are not monophyletic for LSU (this study) or rbcL (Rothman et al. 2017). These two species may have continued to interbreed during glacial maxima when *L. solidungula* would have been pushed south of the Arctic basin. The genetic relationships within and between these two species would be an interesting investigation based on the priorities to resolve kelp phylogenies with molecular data (e.g., Lane et al. 2006; McDevit and Saunders 2009; Jackson et al. 2016; Rothman et al. 2017). Taxonomic investigation of *L. solidungula* and *L. yezoensis* may uncover hidden diversity in the Arctic and North Pacific and unravel Pacific-Atlantic migration histories in Laminaria.

CONCLUSIONS

The phylogeographic history of kelp and the origin of kelp in the Arctic remains highly debated (Adey et al. 2008, Bolton 2010, Rothman et al. 2017). Our LSU results reveal significant and previously unknown subspecies diversity in *L. solidungula*, the only Arctic endemic kelp. Further investigation via multiple genetic markers may uncover whether the two genotypes require taxonomic consideration. *Laminaria solidungula*, an Arctic endemic with relatively wide distribution, but distinct substrate requirements, is a model organism for testing the various hypothesis of recolonization and potential glacial refugia. Significant subspecies differentiation, tied to geography, demonstrate the substantial impact of glacial cycles on current Arctic diversity. While our results shed some light upon those processes, additional details of trans-Arctic population connectivity could be elucidated with further genetic investigation.

Kelp are thought to be poor dispersers in their zoospore stage (Santelices 1990, Norton 1992, Gaylord et al. 2006), but as sporophytes they can dislodged by storms carried long distances (e.g., Saunders 2014). In the Alaskan Beaufort Sea, fall storm cause large masses of kelp to wash ashore along exposed area of the coast, from Pt. Barrow to Demarcation Bay (Fig. 4.4). These storms coincide with the time that the local kelp develop reproductive structures and become fecund and may therefore be a key mechanism for kelp dispersal within the Beaufort Sea and contribute to the high gene flow shown in this study. As the timing of sea ice freeze-up becomes later due to warming, dislodgement by waves and transport by storm driven currents will become more frequent (Thomson et al. 2016). This would enhance the connectivity of existing Arctic benthic populations, as well as potentially assist the spread of boreal species.

The genetic structure of *Laminaria solidungula* in the Beaufort Sea suggests that this area is one of high gene flow and genetic diversity. However, it also indicates that the Boulder Patch kelps are not self-seeding, but are instead a part of a large, mixed population in the Beaufort Sea. This may be connected to relatively recent population mixing in the current inter glacial period compared to long *L. solidungula* generation times. Along with the low apparent recruitment of kelps (Dunton et al. 1982, Konar 2013, Section 1.2), it appears that kelp removal or die off would be followed by a decade or more of recovery, with kelp recruiting from the larger regional population. While the recovery time of a disturbed local kelp population would take many years (Konar 2013, Section 1.2), the high rates of genetic exchange indicate that population connectivity ultimately lends resilience to the *L. solidungula* population of the Boulder Patch. The Boulder Patch is the largest kelp bed in the Beaufort Sea, and kelp inhabiting alternative habitats are clearly important to regional genetic patterns and population persistence. In the face of further development in the nearshore Beaufort Sea, more work is needed to investigate the spatial distribution, size, and mating patterns of the regional kelp population to accurately assess the consequences of anthropogenic modification to kelp habitats such as the Boulder Patch.

Figure 4.5. Reproductive *Laminaria solidungula* (main species), *Saccharina latissima*, and *Alaria esculenta* drift algae on the northwest side of Endicott Causeway. 15 August 2017.

Supplemental Table S4.1. All primers tested, species for which there are multiple alleles at that locus, and citations.

Primers	**Species**	**Citation**
Lo4-24	*L. ochroleuca, L. hyperborea*	Coelho et al. 2014
LoIVVIV-13 F	*L. ochroleuca, L. hyperborea, L. digitata*	Coelho et al. 2014
LoIVVIV-15 F	*L. ochroleuca, L. hyperborea*	Coelho et al. 2014
LoIVVIV-17 F	*L. ochroleuca, L. hyperborea, L. digitata*	Coelho et al. 2014
LoIVVIV-23 F	*L. ochroleuca, L. hyperborea, L. digitata*	Coelho et al. 2014
LoIVVIV-24 F	*L. ochroleuca, L. hyperborea, L. digitata*	Coelho et al. 2014
LoIVVIV-27 F	*L. ochroleuca*	Coelho et al. 2014
LoIVVIV-28 F	*L. ochroleuca, L. hyperborea, L. digitata*	Coelho et al. 2014
Ld1-124 F	*L. digitata, Lessonia nigrescens*	Billot et al 1998, Martinez et al. 2005
Ld2-148 F	*L. digitata, L. hyperborea, Lessonia nigrescens*	Billot et al. 1998, Martinez et al. 2005, Robuchon et al. 2014
Ld2-158 F	*L. digitata, L. hyperborea, Lessonia nigrescens*	Billot et al. 1998, Martinez et al. 2005, Robuchon et al. 2014
Ld2-167 F	*L. digitata, L. hyperborea, Lessonia nigrescens*	Billot et al. 1998, Martinez et al. 2005, Robuchon et al. 2014
Ld2-371 F	*L. digitata, Lessonia nigrescens*	Billot et al. 1998, Martinez et al. 2005
Ld2-520 F	*L. digitata, Lessonia nigrescens*	Billot et al 1998, Martinez et al 2005
Ld2-531 F	*L. digitata, Lessonia nigrescens*	Billot et al. 1998, Martinez et al 2005
Ld2-704 F	*L. digitata, Lessonia nigrescens*	Billot et al 1998, Martinez et al. 2005
Ld-2 F	*S. japonica*	Liu et al. 2012
Ld-3 F	*S. japonica, L. hyperborea*	Liu et al. 2012, Evankow 2015
Ld-6 F	*S. japonica, L. hyperborea*	Liu et al. 2012, Evankow 2015
Ld13-F	*S. japonica*	Liu et al. 2012

Supplementary Table S4.2. Daily, year-round mean (±SD) benthic environmental conditions (originally from Bonsell 2019) and mean benthic percent cover of functional groups (originally from Bonsell 2019) at each site. Bold indicates significant differences between sites (Supp. Table 4.3). Superscripts indicate grouping from Tukey HSD test.

Site	Temp. (°C)	Sal.	Current vel. (cm s^{-1})	PAR (mol photons m^{-2} day^{-1})	Crus-tose coral-line algae	Foliose red algae	Kelp	Filter feeders	Suspen-sion feeders
DS11	**-0.78 ±1.96^{a}**	**32 ±3^{a}**	**4.4 ±5.3^{a}**	0.271 ±1.013	**18.67 ± 0.46^{a}**	**38.01 ± 0.78^{a}**	**19.03 ± 0.75^{a}**	**0.44 ± 0.03^{ab}**	**4.08 ± 0.19^{a}**
E1	**-0.41 ±2.50^{b}**	**31 ±4^{b}**	**2.8 ±3.2^{b}**	0.208 ±0.925	**0± 0^{b}**	**79.31 ± 0.51^{b}**	**2.9 ± 0.25^{b}**	**0.77 ± 0.11 ^{b}**	**6.12 ± 0.21^{a}**
L1	**-0.82 ±1.89 ^{a}**	**33 ±4^{a}**	**1.9 ±2.7^{c}**	0.194 ±0.756	**0.64 ± 0.06^{c}**	**71.67 ± 1.19^{bc}**	**9.85 ± 0.93^{b}**	**0.48 ± 0.05 ^{ab}**	**2.79 ± 0.21^{ab}**
W1	**-0.95 ±1.84^{a}**	**30 ±4^{c}**	**4.3 ±5.4^{a}**	0.102 ±0.236	**0.48 ± 0.03^{d}**	**47.32 ± 0.76^{ad}**	**4.4 ± 0.24^{b}**	**2.12 ± 0.12 ^{a}**	**14.87 ± 0.39^{d}**
W3	**-0.80 ±1.88^{a}**	**32 ±3^{b}**	**4.8 ±4.6^{a}**	0.184 ±0.700	**4.67 ± 0.15^{a}**	**58.01 ± 0.63^{cd}**	**1.65 ± 0.14^{b}**	**0.77 ± 0.05 ^{ab}**	**0.24 ± 0.02^{c}**

Supplementary Table S4.3. Results table for comparing benthic cover by each functional group among sites via ANOVA. *Indicates significant differences among sites (α=0.05).

Variable: Crustose coralline algae % cover*			
	Sum Sq.	**DF**	**F**
Intercept	5.55	1	472.18
Site	4.00	4	84.99
Residuals	1.93	164	
Variable: Foliose red algae % cover*			
	Sum Sq.	**DF**	**F**
Intercept	2.06	1	199.01
Site	0.51	4	12.43
Residuals	1.70	164	
Variable: Kelp % cover*			
	Sum Sq.	**DF**	**F**
Intercept	4.16	1	74.30
Site	2.17	4	9.70
Residuals	9.19	164	
Variable: Filter feeder % cover*			
	Sum Sq.	**DF**	**F**
Intercept	0.031	1	3.65
Site	0.085	4	2.49
Residuals	1.393	164	
Variable: Suspension feeder % cover*			
	Sum Sq.	**DF**	**F**
Intercept	0.20	1	22.40
Site	0.64	4	17.78
Residuals	1.48	164	

5. Long-term patterns of benthic irradiance and kelp production in the central Beaufort Sea reveal implications of warming for Arctic inner shelves

Christina E. Bonsell and Kenneth H. Dunton

INTRODUCTION

Seasonal sea ice cover plays a prominent role in marine primary productivity in high latitude ecosystems, as it can set the timing of peak production and determine annual light budgets (Clark et al. 2013, Ji et al. 2013, Kahru Manzano et al. 2011, Post et al. 2013). In the Arctic Ocean, there has been a striking decline in sea ice extent since the onset of observations via satellite measurements, at a rate of approximately 13.3% loss in area per decade (Serreze and Stroeve 2015). Despite on-going efforts by scientists to investigate the effects of sea ice loss on pelagic production (reviewed in Wassmann and Reigstad 2011), only a few studies to date have addressed the direct consequences on benthic production (Krause-Jensen et al. 2012, Clark et al. 2013, Krause-Jensen and Duarte 2014). In coastal Arctic systems, benthic primary production by macro- and microalgae in Arctic waters is important to ecosystem production, elemental cycling, and food web dynamics, especially during times of limited pelagic production (Dunton and Schell 1987, Glud et al. 2009, McMeans et al. 2015, Renaud et al. 2015). Additionally, biophysical processes in shallow, nearshore Arctic areas, where much of this production takes place, remain understudied due to logistical constraints (e.g., Fritz et al. 2017). Changes to production in these areas would have broad consequences for Arctic ecosystem function.

Because of the strong annual cycle of solar irradiance in polar regions, seasonal sea ice and solar energy models predict that earlier dates of ice break-up will result in exponential increases in benthic light budgets (Clark et al. 2013). For instance, Krause-Jensen et al. (2012) and Clark et al. (2013) used existing gradients in seasonal ice cover in Greenland and Antarctica, respectively, to link lengthened ice free seasons with increases in macroalgal production and hypothesized that future warming driven reductions in seasonal sea ice extent and duration will enhance annual production by benthic macrophytes. These predictions contribute to the idea that Arctic coastal habitats will become increasingly macrophyte-dominated as Arctic warming continues, with consequences for Arctic food webs and seawater chemistry (Clark et al. 2013, Krause-Jensen and Duarte 2014, Krause-Jensen et al. 2016). However, variations in underwater optical properties, which have a profound influence on light transmittance to the benthos and demonstrable impacts on benthic primary production (Van Duin et al. 2001), are largely overlooked in these analyses. Bartsch et al. (2016) hypothesized that enhanced sediment inputs from glacial melt caused a narrower euphotic zone during the open water season, leading to observed shallowing of peak biomass and shallower depth limit of kelps in Svalbard over the past two decades. The links between ice loss,

irradiance at depth, and primary production appear to be multifaceted and warrant further investigation.

While ice cover determines irradiance at the water's surface, irradiance at depth under an ice-covered ocean also depends on light attenuation of the water column. In the coastal Arctic Ocean, summer water transparency is influenced by concentrations of phytoplankton and sediments suspended in the water column. Concentrations of suspended sediments during the open water summer in the coastal Beaufort Sea have been directly linked to increased light attenuation and decreased annual production by benthic macroalgae (Aumack et al. 2007). Many Arctic inner shelf areas (depth <10 m), such as the Alaskan Beaufort Sea coast, have particularly high suspended sediment concentrations due to shallow depth, persistence of unconsolidated sediments, and significant inputs by numerous rivers and streams (notably, the Arctic Ocean receives 11% of global river discharge, but only constitutes 1% or global ocean volume; McClelland et al. 2011). These sediments originate from coastal erosion, resuspension due to water motion, and fluvial inputs by Arctic rivers, which discharge the large majority of their annual suspended sediments loads by the end of the spring melt (O'Brien et al. 2006, Walker et al. 2008, Wegner et al. 2003). Because most river fluxes occur before the end of ice break-up, changes in wind direction and/or speed during the open water period are the main drivers of temporal variability in underwater irradiance in the nearshore areas, as they are in other shallow aquatic systems (Van Duin et al. 2001). Annual benthic light budgets may consequently have a negative relationship with wind speeds during the ice-free season.

The primary objective of this paper is to examine how sea ice extent and wind dynamics affect variation in the annual benthic light budget and production by the Arctic endemic kelp *Laminaria solidungula* in the central Beaufort Sea. Since 1979, sea ice duration in the Beaufort Sea has decreased at an accelerating rate, while summertime easterly winds have increased in speed and frequency across the coastal region (Frey et al. 2015, Wood et al. 2013, 2015). These long-term environmental changes may have significant, but opposing, effects on long-term primary production patterns. Although lengthened ice-free season results in increased irradiance at the waters' surface, enhanced summer winds may degrade the underwater light climate. Frond elongation in *L. solidungula*, is entirely dependent on the utilization of photosynthetically derived carbon reserves produced the previous summer (Dunton and Schell 1986). The resulting annual growth has a strong correlation with the light budget of the preceding ice free season (Dunton 1990). This species is ideal for assessing the biological effects of changes to the Arctic underwater light environment due to its enhanced capacity to respond to small changes in irradiance compared to other kelp species, particularly evident in its low saturating irradiance for photosynthesis (38 μmol photons sec^{-1}; Dunton and Jodwalis 1988).

Multidecadal time series that document biological responses to variations in regional climate in Arctic marine systems are rare, but critical for the development

of accurate projections of future ecosystem change (Wassmann et al. 2011). Here, we synthesize a multidecadal dataset (collected from 1977-1992 and 2002-2008) and incorporate previously unpublished data (2012-2016), on benthic irradiance and kelp growth from Stefansson Sound in the central Beaufort Sea (Dunton 1990, Aumack et al. 2007, Dunton et al. 1992, Dunton et al. 2009) to demonstrate the combined influence of seasonal ice extent and wind dynamics on the annual light budget, and annual kelp production. Additionally, we assess whether annual variations in *L. solidungula* growth relate to seasonal ice extent and summer wind dynamics. In doing so, this work highlights the importance of including factors that affect underwater light transmittance in projecting changes in primary productivity and ecosystem structure in Arctic marine ecosystems.

METHODS

Study Site

The Stefansson Sound Boulder Patch (hereafter 'the Boulder Patch') is an isolated rocky zone of boulders and cobbles covering an area of approximately 63 km^2 in a region dominated by soft sediment (Barnes and Reimnitz 1974; Fig. 5.1). Located in relatively shallow water (4-8 m) within 15 kilometers of the coast, and directly adjacent and north of the Sagavanirktok River Delta, the Boulder Patch remains a non-depositional environment. Geologists have long maintained that the Boulder Patch, which lies within the Gubik Formation, is an erosional environment that is largely free of Pleistocene sediment accumulation. High wind-driven water currents that persist throughout the summer open-water period are thought to transport sediments to deeper inner shelf areas, especially during the 1-2 week period of peak discharge from the Sagavanirktok in late May and early June (Dunton et al. 1982, Rember and Trefry 2004).

The epilithic community in the Boulder Patch is dominated by the kelp *L. solidungula* and represents a regional biodiversity hotspot. Research conducted in the area since the 1970s has focused primarily on characterizing the underwater light environment and the biological production of *L. solidungula* (Dunton 1985, Dunton and Schell 1986, Dunton and Schell 1987, Dunton et al. 1992, Henley and Dunton 1995, Aumack et al. 2007, Dunton et al. 2009). Field studies have been nearly continuous since 1978 except for a single seven-year lapse (1993-2000), with ten long-term study sites occupied since 1984 (Fig. 5.1).

Kelp production

Laminaria solidungula individuals from long-term study sites were collected by SCUBA divers at one- or two-year intervals. The thallus of this species consists of a single blade with multiple ovate growth sections, each representing one year of production. The blade section closest to the stipe represents production from the most recent year and the immediate distal section represents growth from the

previous year. Because multiple years of production can be measured from a single individual, this dataset spans from 1976 to 1990 and 1996 to 2015.

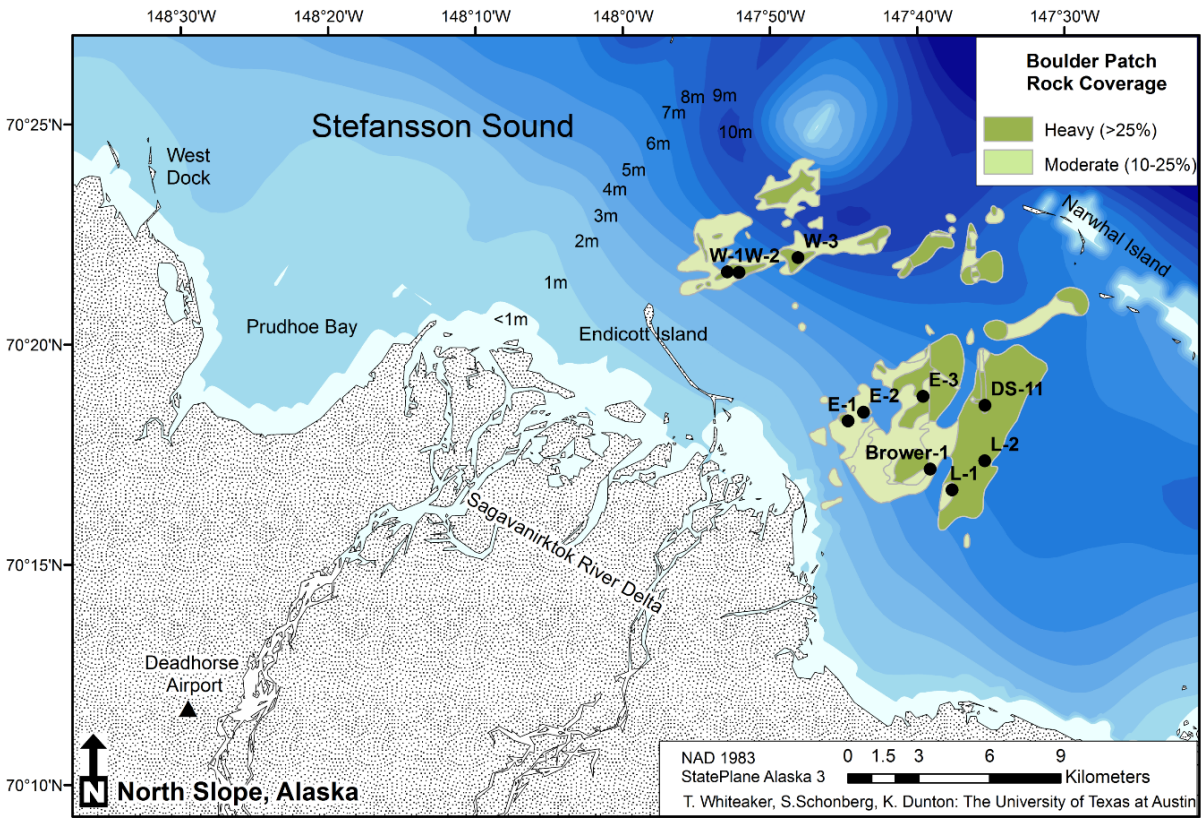

Figure 5.1. The Stefansson Sound Boulder Patch, showing location of long-term study sites in relation to percent rock cover in Stefansson Sound. Inset shows location of Stefansson Sound (blue star) in reference to Alaska.

Benthic and surface irradiance

Spherical quantum sensors (LI-193SA, LI-COR Inc.), placed ~0.5 m above the benthos, were deployed for measurements of photosynthetically active radiation (PAR) at sites across the Boulder Patch (Fig. 5.1, Supp. Table 5.1). Sensors were deployed in conjunction with either CR21 (Campbell Scientific), LI-1000, LI-1400, or LI-1500 dataloggers (LI-COR Inc.), depending on the site and study year (Supp. Table 5.1). Cosine PAR sensors (LI-192SA, LI-COR Inc.) deployed in line with a LI-1000 datalogger collected continuous surface light measurements at East Dock in Prudhoe Bay (1986-1987) and Endicott Island (1987-2016; Fig. 5.1). Sensors were cleaned between deployments (once a year), as biofouling in this environment is negligible. Sensors made instantaneous measurements every minute and logged the average every 1 or 3 hours, depending on site and study year (Supp. Table 5.1). All PAR measurements were converted into total daily photon flux rate (mol m^{-2} day^{-1})

for analysis. Daily hours of saturating irradiance for *L. solidungula* (H_{sat}: hours with average photon flux rate ≥38 µmol photon m^{-2} sec^{-1}; Dunton and Jodwalis 1988) were also calculated, as this metric is more closely related to annual production than photon flux rate (Dunton 1990). For years with irradiance data for >90% of the year, annual H_{sat} was calculated at each site.

Sea Ice

Sea ice concentration from 1979-2016, measured via passive microwave data, was obtained from the National Sea Ice Data Center via the Arctic Data Integration Portal (http://portal.aoos.org) for the two 25 km^2 grid areas that contain the Boulder Patch. Values from the two areas mirrored each other closely over time and were therefore averaged daily. Dates of key events in the ice season (break-up start, break-up end, freeze-up start, and freeze-up end) were calculated using the algorithms described by Johnson and Eicken (2016). These events define the seasonality of direct incident solar radiation to the sea surface. The length of the ice-free season was calculated as freeze-up start minus break-up end.

Wind

Wind speed and direction for West Dock in western Stefansson Sound (National Climate Data Center ID 9497645), spanning 1993-2016, were obtained from the National Weather Service Cooperative Observer Program (COOP) via the R package "r-noaa" (Chamberlain et al. 2016). Wind speed and direction for Deadhorse Airport, spanning 1973-2016, were obtained from the Alaska Airport Weather Observations Network (mesonet.agron.iastate.edu/ASOS/) and underwent quality control procedures before analysis. Coastal wind speed was estimated from the Deadhorse data using the linear relationship between wind speed at Deadhorse and West Dock (see *Results*). For consistency, we only use the estimated coastal wind speed in analyses relating to irradiance and kelp growth. To examine changes in summer winds over time, we used data confined by the dates of start of break-up and start of freeze-up for each year; for analyses relating wind to benthic light or kelp growth, we focused on wind data confined by the dates of end of break-up and start of freeze-up for each year. In concurrence with other studies in the region, storm events were defined as >6 consecutive hours of average wind speeds over 10 m s^{-1}, with direction defined by primary cardinal direction (e.g., winds from NNE were defined as N winds; Manson and Solomon 2007).

To assess the effect of wind speed on underwater light transmittance, we plotted the relationship between mean daily coastal wind speed (as estimated from Deadhorse) and daily percent surface irradiance. Due to noisy data, wind speeds were binned by rounding to the nearest whole number.

Production model

To assess the effects of ice extent and wind speed on annual kelp production, we used the model developed by Aumack et al. (2007) to calculate daily production

rates under given depth and suspended sediment concentrations. Briefly, this model uses incident radiation and a suspended sediment concentration specific light attenuation coefficient to estimate benthic irradiance to calculate *L. solidungula* production over the open water season. We estimated incident radiation on each day of the year by averaging values for each day from all the years of surface irradiance measurements. We incorporated daily wind speeds by using estimates of suspended sediment concentrations under given wind speeds obtained in this region (Trefry et al. 2009, Aumack and Dunton unpublished data; Supp. Table 5.2). We confined the model to ice free dates only and used daily average coastal wind speed. Annual carbon production was estimated for the average size of individuals from our long-term dataset (22.5 cm basal blade length). Modelled carbon production was compared to the long-term kelp growth dataset, with measured kelp growth converted into g C yr^{-1} based on previously derived relationships (Dunton and Jodwalis 1988, Aumack 2003).

Statistical analysis

Trends in ice events, wind speed, and kelp growth over time were assessed using linear regression analyses. The relative effects of year and site, and the interaction between the two terms, on kelp growth were determined using ANOVA. We tested the relationships between kelp growth (linear elongation in centimeters) and date of ice break-up and length of ice-free season by linear regression.

For years and sites with irradiance data for >90% of the summer period (July-September), we tested if ice break-up date and length of ice-free season predicted the annual benthic irradiance budget using linear models. For these data, cumulative H_{sat} was calculated for each day by inclusively summing H_{sat} from all previous days to determine the seasonality of potential kelp production.

For all years of irradiance data, the longest portion of the year with representative data for multiple sites and years from multiple decades is 27 July – 31 August. There were not adequate redundancies in sites across years for these dates, so separate one-way ANOVAs were conducted to test the individual effects of site and year on three irradiance variables: a) total annual irradiance, b) mean irradiance, and c) total H_{sat}. The relative effects of mean daily sea ice concentration and mean daily maximum wind speed, and the interaction between the two terms, on the three irradiance variables for this 36-day period were determined by linear regressions. As westerly winds entrain turbid coastal water in the nearshore in this region, we also tested the effects of wind direction and proportion of westerly winds on the three irradiance variables using linear regression. We defined westerly wind as within 45^{o} of due west (270^{o}). To test the relative importance of this period of time to annual kelp production, the relationships between site specific annual kelp growth and total irradiance, as well as between site specific annual kelp growth and total H_{sat}, were each tested by linear regression.

All analyses were carried out using R (R Core Team, 2016). Directional data was analyzed and plotted using the R package "circular" (Lund and Agostinelli 2015).

RESULTS

Physical drivers: sea ice and winds

We found that the ice-free season in Stefansson Sound (end of break-up to start of freeze-up) lengthened during the period of this study. Dates between ice break-up and freeze-up increased from 74 days in 1979 to 132 days in 2016 (Fig. 5.2-5.3, Supp. Table 5.3). Duration of ice break-up, however, does not show any change (Fig. 5.3, Supp. Table 5.3).

Coastal wind speeds directly measured at West Dock and estimated from Deadhorse show no trends over time (linear regressions on daily summer wind speed and fraction of hours with wind speeds > 10 m/s, $p>0.05$, $R^2<0.1$). We also did not find evidence for a strengthening of easterly or westerly winds over time (linear regressions, $p>0.05$, $R^2<0.1$). From the 1993-2016 data, we calculated the linear relationship between West Dock and Deadhorse daily wind speeds as

(Eq. 1) $$Speed_{West\ Dock} = 1.40 + 1.04 * Speed_{Deadhorse}$$

where speeds are in m s^{-1} (linear regression, $p<0.05$, $R^2=0.63$). Wind direction data for both stations are not vonMises distributed and therefore could not be analyzed statistically for trends over time. We discerned that mean wind direction at each station varies between years (particularly at Deadhorse), but typically originates from the east at West Dock and from the northeast at Deadhorse (Fig. 5.4).

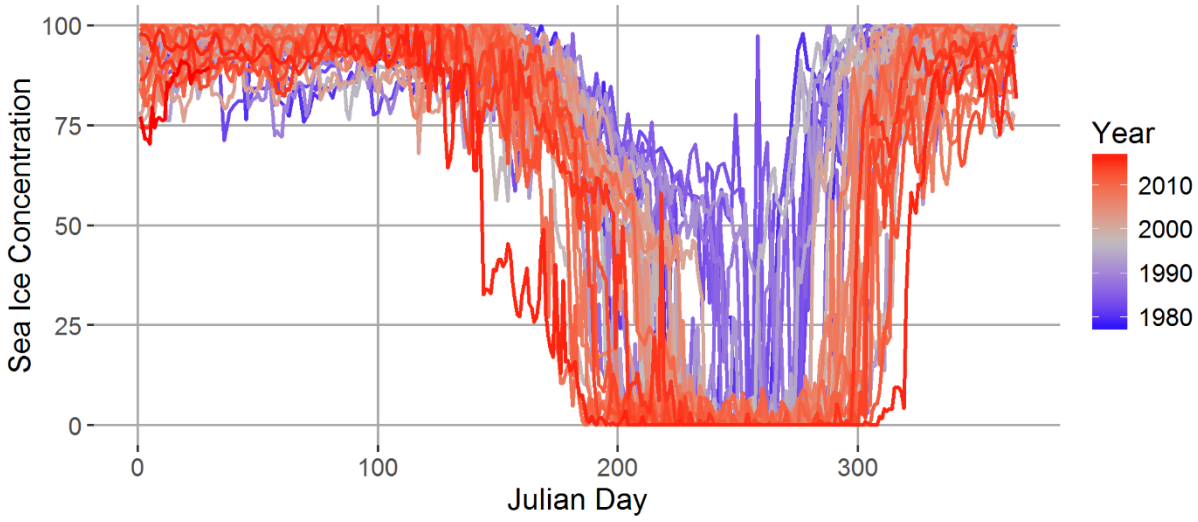

Figure 5.2. Sea ice concentration by Julian Day in Stefansson Sound over a 38-year period (January 1979-2017) illustrates the lengthening of the open water season and the decrease in summer ice concentration over time.

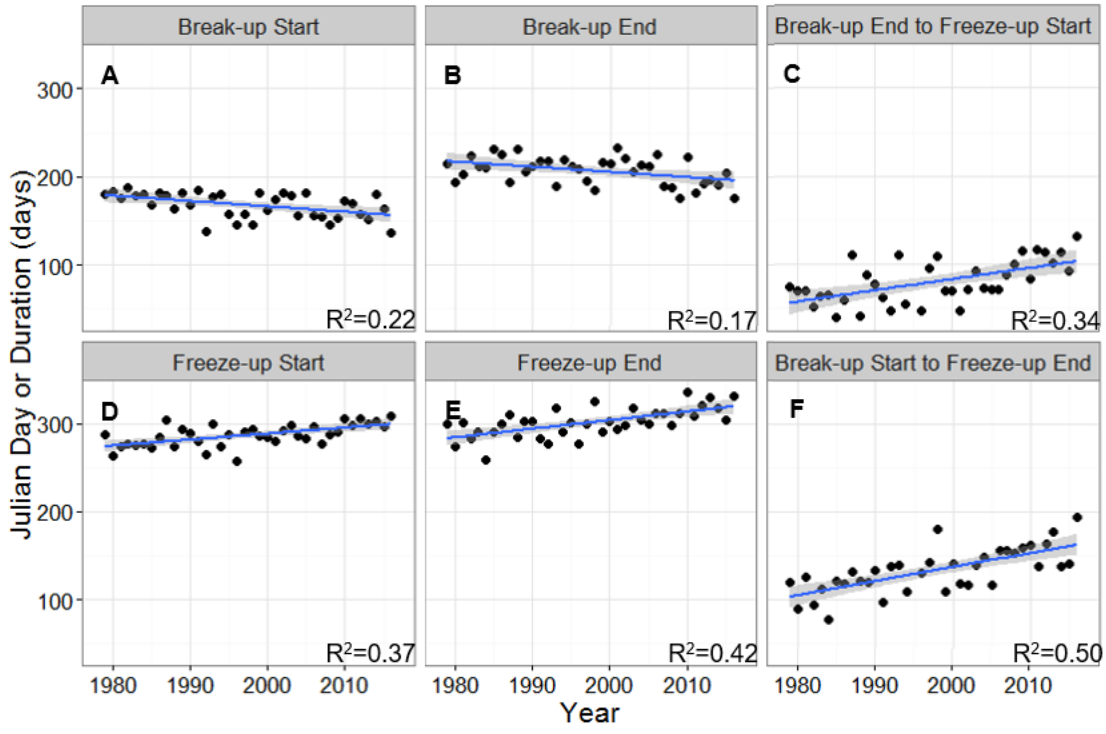

Figure 5.3. Key events related to freeze-up and break-up by Julian Day (A-B, D-E) or duration of event in days (C, F). Generally, break-up is occurring earlier and freeze-up later over the 38-year period. Blue line represents the linear relationship ±SE (grey shading).

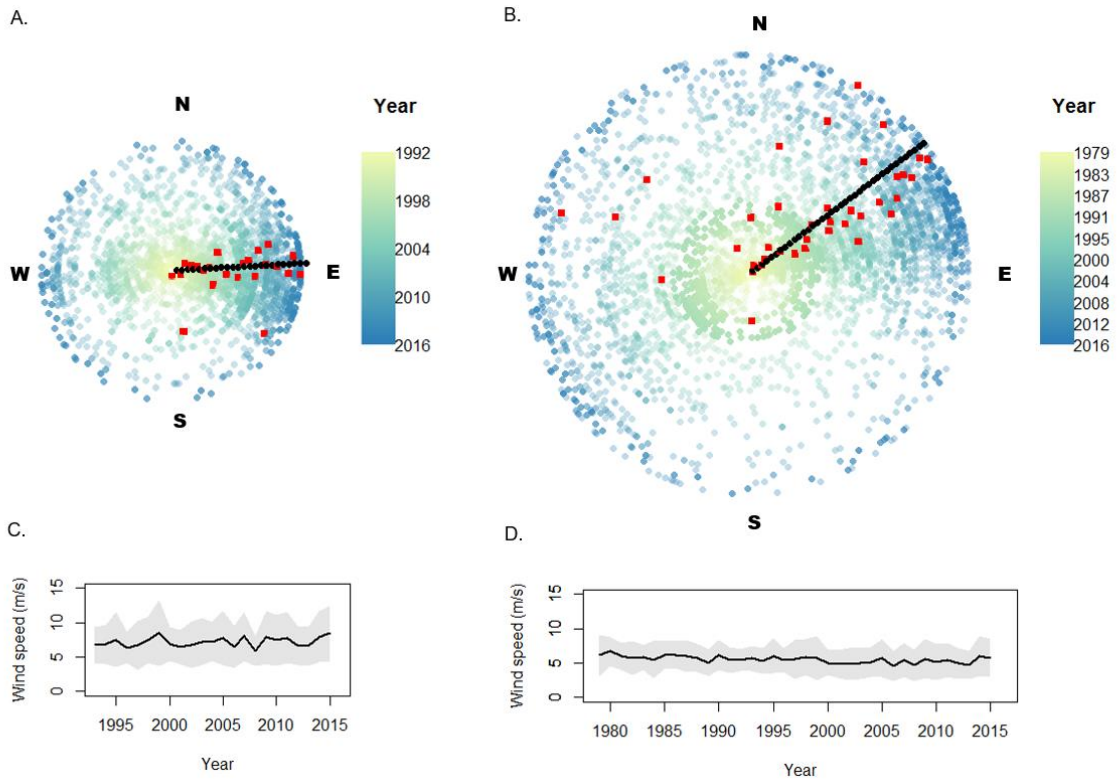

Figure 5.4. Daily summer wind variables over time for West Dock (A, C) and Deadhorse Airport (B, D). The distributions of daily mean wind direction (A, B) show that winds tend to originate from the east. The earliest year of measurement is the most interior circle of points, the latest year is the most exterior. Semi-transparent points indicate daily average wind direction, colored by year. Opaque red squares indicate annual mean direction. Black line indicates overall mean direction for all years. Daily wind speeds (C, D) are shown as annual means ±SD (black line and grey shading). Wind speed varies between summers but shows no long-term trends.

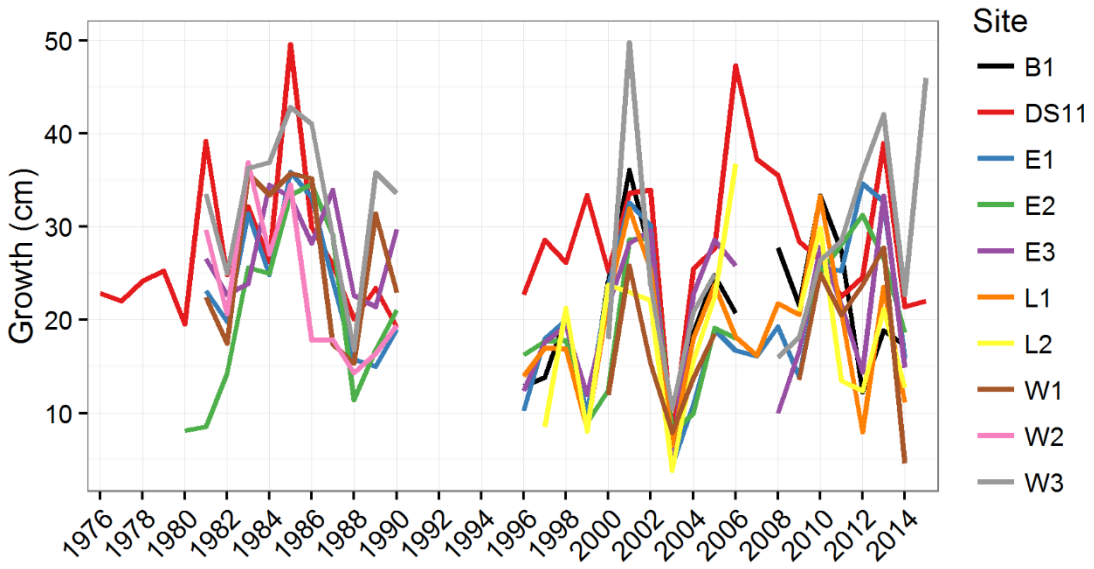

Figure 5.5. Mean *Laminaria solidungula* growth (cm) varies between sites and years, with some years showing strong annual patterns (e.g. 2001 and 2003).

In situ kelp growth and benthic irradiance: relationships to sea ice and wind

Analysis of the long-term data shows that kelp growth (as measured by blade elongation) in the Boulder Patch fluctuates over time and between sites (Fig. 5.5), although there is more variation in growth between sites than between years (SS_{Site}=80127, $F_{Site}(9,8936)$=105, p<0.01 SS_{Year}=442890, $F_{Year}(34,8936)$=153, -p<0.01). The relationship between annual kelp growth across the Boulder Patch and the length of the open water season is not significant (linear regression, p>0.05, R^2<0.1).

Benthic irradiance at all sites displays strong seasonality, with some variation in maximum daily photon flux per year (Fig. 5.6). We only have data for the entire summer for a couple of years, confined mostly to the late 1980s and early 1990s, but we did not find any trends over time in the annual maximum daily photon flux rate (linear regressions performed for each site, p>0.05, R^2<0.1). Under ice cover, no measurable light occurs except at some sites in some years in the spring under "clean ice" (Dunton 1984), until around the time of the freshet when irradiance levels return to zero (Fig. 5.6). The first significant light transmittance occurs after ice break-up has begun (Figs. 5.6 and 5.7). Overall summer light levels are low, with most days lacking light levels that approach saturation irradiance for *Laminaria solidungula* (Table 5.1). Interestingly, these data show that the days surrounding ice break-up contribute strongly to annual H_{sat} for a given site, sometimes over 50% of the annual value (Fig. 5.7).

Our analysis of data from 27 July – 31 August showed no significant differences between sites for mean daily benthic irradiance (MDI), total benthic

irradiance (TBI), or total H_{sat} (TH). However, we detected significant differences between years for this period ($SS_{MDI\sim Year}$=10.58, $F_{MDI\sim Year}$ (6,18)=9.95, p <0.01; $SS_{TBI\sim Year}$=12102, $F_{TBI\sim Year}$ (6,18)=10.54, p<0.01; $SS_{TH\sim Year}$=85591, $F_{TH\sim Year}$ (6,18)=11.8, p<0.01). TBI and TH from this period do not predict annual kelp growth (linear regressions, p>0.05, R^2<0.1). We did not find significant effects of mean daily sea ice concentration, or the interaction between ice concentration and mean daily maximum wind speed on MDI, TBI, or TH. However, mean daily maximum wind speed alone significantly affects MDI (linear regression, p<0.05, R^2=0.24), TBI (linear regression, p<0.05, R^2=0.24), and TH (linear regression, p<0.05, R^2=0.19). This effect of wind is always negative. Plots of binned mean daily wind speed compared to percent surface irradiance for all ice-free dates at each site echo this negative relationship (Fig. 5.8). In contrast, there is no linear relationship between daily percent surface irradiance and sea ice concentration in the summer, with high irradiance values possible at high ice concentrations (Fig. 5.9). Although there is no relationship between mean wind direction and MDI, TBI, or TH for the 27 July – 31 August data, the proportion of westerly winds has a significant, negative effect on each of these irradiance variables (linear regressions, p<0.05, R^2_{MDI}=0.21, R^2_{TBI}=0.20, R^2_{TH}=0.19).

Modelled kelp production based on wind during the ice-free summer is more variable between sites than measured production and shows a general increase over time in annual production (Fig. 5.10). Compared to measured production, the model is conservative, often underestimating annual kelp production, and has a high incidence of predicting zero production, especially for shallower sites.

Table 5.1. Summary of underwater daily light values for ice free summer (end of break-up to the start of freeze-up). Differences in mean daily surface irradiance between sites are due to differences in benthic light data coverage over time (Supp. Table 5.1).

Site	Depth (m)	Mean daily surface irradiance (mol photons m^{-2} day^{-1})	Mean daily percent surface irradiance ±SD	Mean light attenuation, k (m^{-1})	Percent of days with benthic photon flux of 0	Mean daily hours H_{sat}	Percent of days with 0 hours H_{sat}
DS11	6.1	15.5	4.1±6.2	0.52	20.9	1.9±4.0	77.8
E1	4.4	15.1	3.2±6.4	0.78	29.9	1.7±4.0	81.5
E2	4.3	13.8	3.1±6.2	0.81	38.1	1.5±3.6	82.8
E3	5.5	12.7	3.6±6.6	0.60	35.4	1.7±3.9	78.8
L1	5.5	17.0	1.9±3.8	0.72	35.3	1.4±3.7	82.7
W1	6.0	12.5	1.9±3.7	0.66	39.3	0.8±2.5	87.0
W2	6.2	13.3	2.2±4.2	0.62	41.2	0.9±2.9	87.9
W3	6.6	12.2	2.3±4.3	0.57	43.9	1.1±2.8	84.2

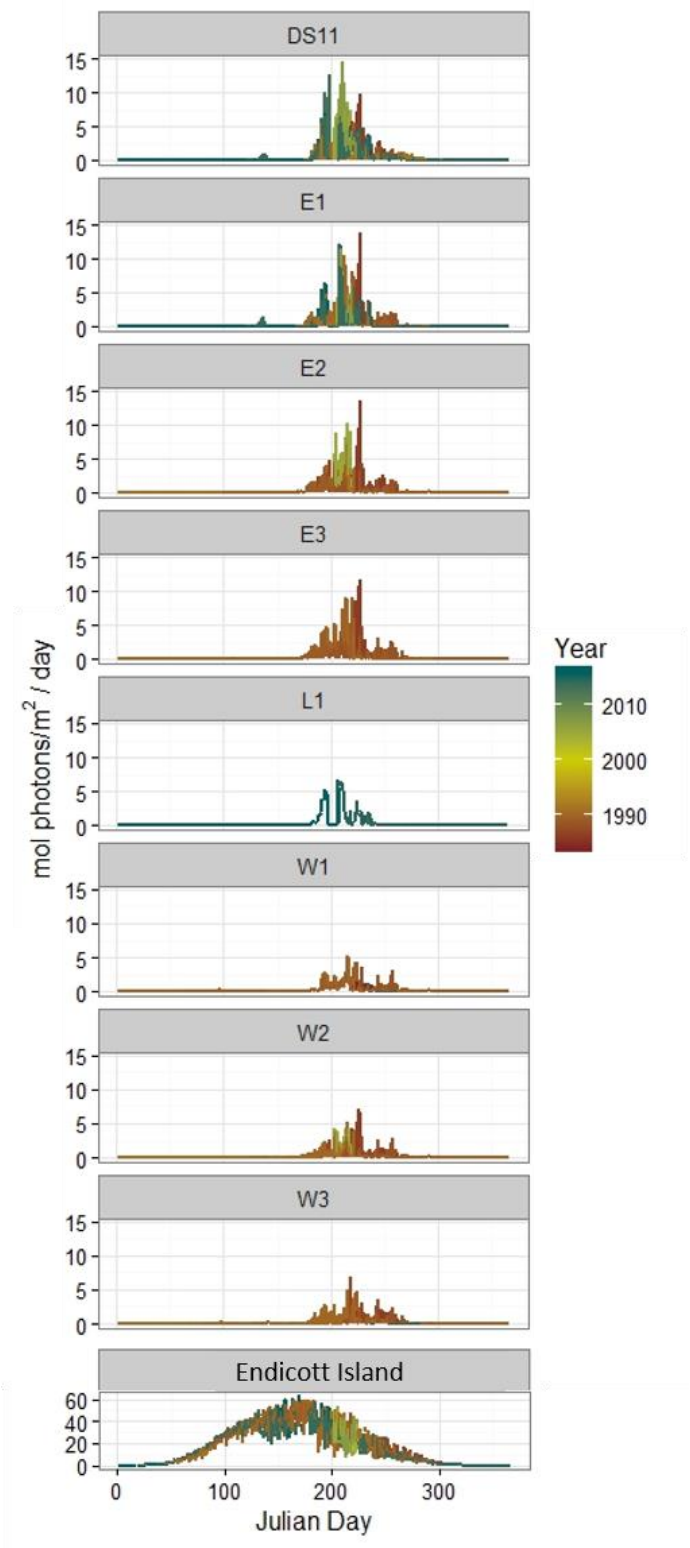

Figure 5.6. Seasonal pattern of both incident (Endicott Island) and underwater irradiance (mol photons m^{-2} day^{-1}) on the seabed at eight locations in Stefansson Sound by year. Note change in scale for surface irradiance.

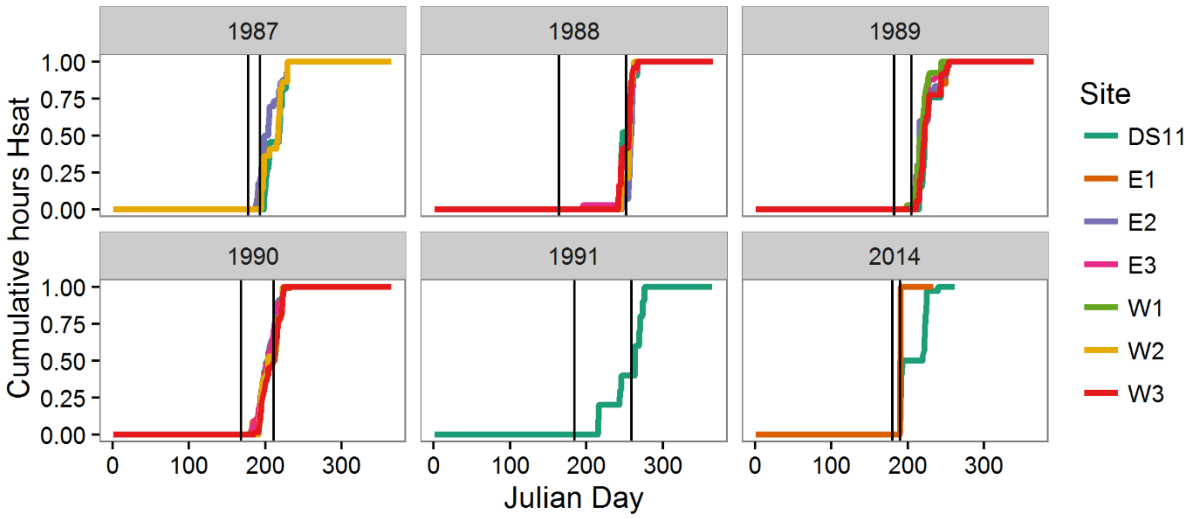

Figure 5.7. Cumulative H_{sat}, as proportion of annual H_{sat}, illustrates the rapid accumulation of hours of saturating irradiance during and directly following the period of ice break-up, based on available in situ irradiance data from each site from July through September. Pairs of black vertical lines frame the period between start of break-up and when sea ice concentration reaches 15%.

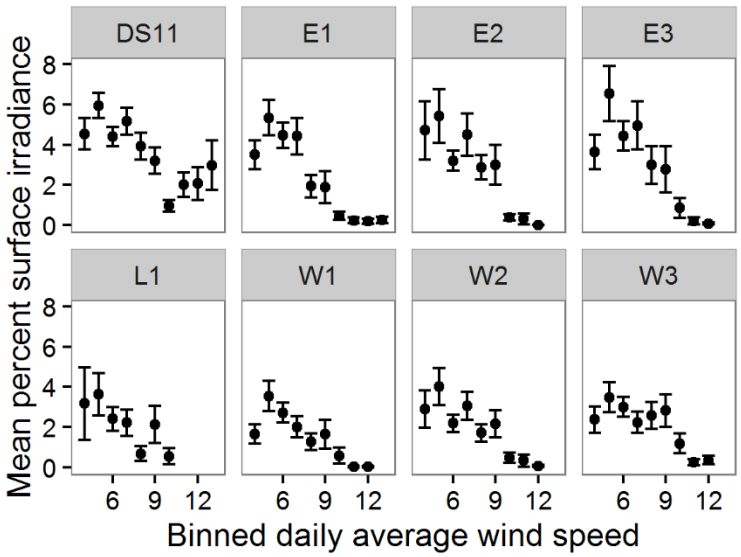

Figure 5.8. Mean daily underwater irradiance, as percent surface irradiance, at each site in relation to coastal wind speed calculated from the Deadhorse Airport station (Eq. 1).

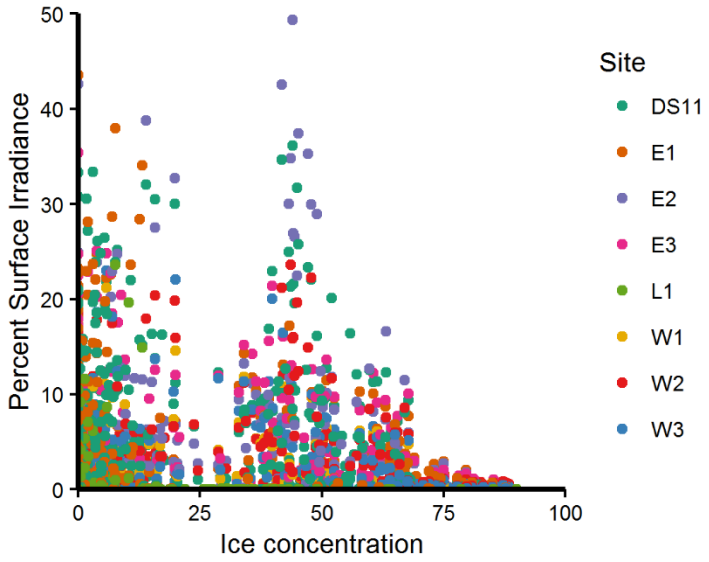

Figure 5.9. Distribution of daily underwater irradiance values (as percent of surface irradiance) as a function of ice concentration during the period from the start of ice break-up to the start of freeze-up. Note that high irradiance values are possible at relatively high ice concentrations.

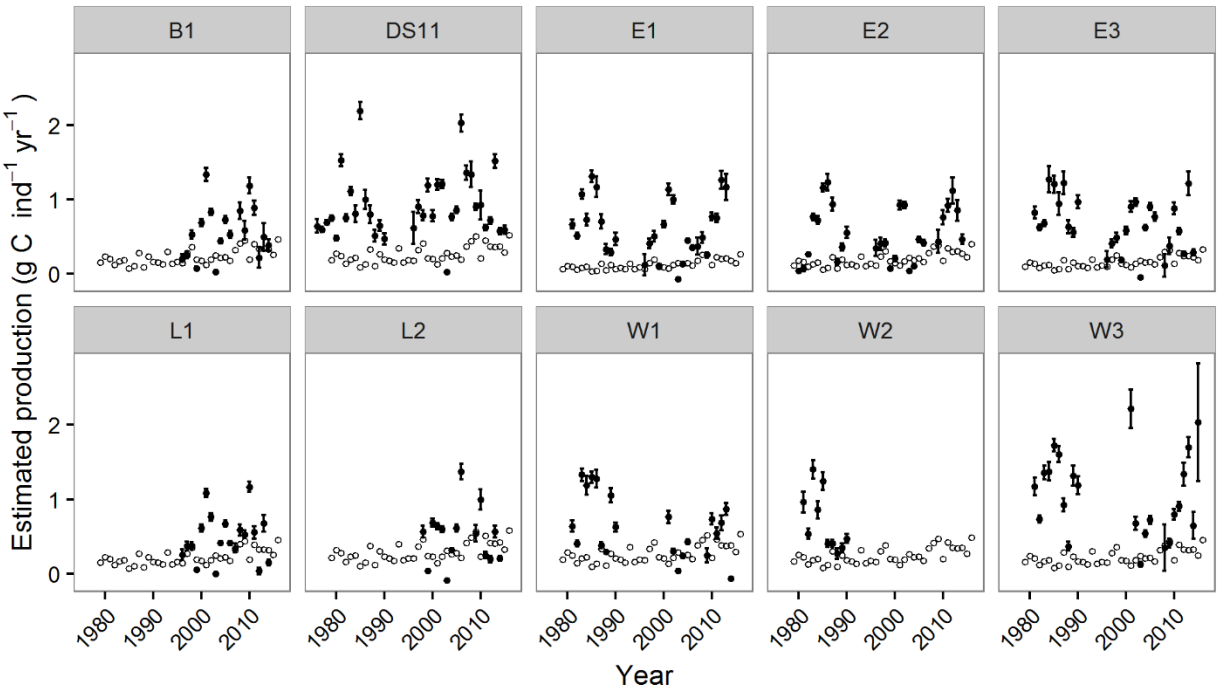

Figure 5.10. Modelled kelp production (white circles), calculated for an average sized individual (22.5 cm basal blade length) based on the relationship between wind velocity, total suspended solids, and light attenuation during the ice free period, compared to measured mean kelp production (black circles ±SE) calculated from blade elongation.

DISCUSSION

Although the ice-free season has lengthened over time in Stefansson Sound, we found no evidence of increased kelp production. Low light conditions prevail during the summer, suggesting that suspended sediments, often derived from wind driven water motion, are integral in controlling light transmittance in shallow, nearshore regions of the Arctic. However, annual kelp production and long-term trends were not accurately predicted by our model, which relied on established relationships between wind speed and light attenuation during the ice-free summer. Instead, annual benthic light budgets – and therefore annual kelp production – appear to rely heavily on enhanced light transmittance in the days surrounding ice break-up. Overall, our results suggest that sea ice presence in these systems has a net positive effect on underwater light transmittance and marine primary production by attenuating swell and wave action.

Laminaria solidungula in Stefansson Sound survive at impressively low quantum budgets, reported previously by Dunton et al. (1990) at 45 mol photons m^{-2} yr^{-1}, the lowest measured for any kelp population (Lüning and Dring 1979 reported boreal *Laminaria hyperborea* at 71 mol photons m^{-2} yr^{-1}). In addition, *L. solidungula* exhibits saturation (E_k) and compensation (E_c) irradiance at 38 µmol photons m^{-2} sec^{-1} and 0.5-3 µmol photons m^{-2} sec^{-1}, respectively (Chapman and Lindley 1980,

Dunton and Jodwalis 1988), among the lowest reported for marine macroalgae (Wiencke et al. 2006), and well below that of other cold water kelp species (*Laminaria digitata*: E_k and E_c =150 µmol photons m^{-2} sec^{-1} and 6 µmol photons m^{-2} sec^{-1}, respectively; *Saccharina latissima*: E_k and E_c =150 µmol photons m^{-2} sec^{-1} and 5 µmol photons m^{-2} sec^{-1}, respectively; *L. hyperborea* E_k and E_c =90 µmol photons m^{-2} sec^{-1} and 9 µmol photons m^{-2} sec^{-1}, respectively; Lüning 1971, King and Schramm 1976). Consequently, because *L. solidungula* is very responsive to the low irradiance with an annual growth pattern strongly linked to summer open water conditions (Dunton 1990), the species is an excellent indicator of interannual variations in the underwater light climate.

Ice concentration, wind dynamics, benthic irradiance, and kelp growth

Summer sea ice concentrations in Stefansson Sound have declined considerably since the 1980s (Fig. 5.2). Our analysis indicates that the open water season (break-up end to freeze-up start) of the Boulder Patch area has gained approximately 17 days between 1979 and 2016 (Fig. 5.3). This rate of change is considerably less than that measured for the western coastal Beaufort Sea (~54 days over 34 years, Johnson and Eicken 2016) and the Beaufort Sea as a whole (~36 days over 30 years, Markus et al. 2009; ~31 days over 34 years, Stroeve et al. 2014; ~41 days over 33 years Frey et al. 2015). However, the Beaufort Sea is a region characterized by considerable variability compared to other Arctic regions (Markus et al. 2009, Stroeve et al. 2014), and the rate of change for Stefansson Sound is similar to the trend for the entire Arctic (~20 days over 30 years, Markus et al. 2009; ~15 days over 34 years, Parkinson 2014). While some of these differences may be attributed to varied definitions of "ice covered", geomorphology is likely the main cause of disparity. Stefansson Sound is largely protected by a chain of barrier islands, which affects the dynamics of landfast ice compared to pack ice. Landfast ice forms first in protected areas, such as lagoons and sheltered bays, and the timing of its freeze and melt are closely tied to the onset of freezing and thawing temperatures, respectively (Barry et al. 1979, Mahoney et al. 2014). As a result, ice presence in sheltered coastal waters such as Stefansson Sound may respond to different forcing and exhibit more moderate long-term trends than in exposed and offshore waters.

One expected outcome of decreased seasonal ice is an increase in underwater light and annual production in *L. solidungula* over time (i.e., Krause-Jensen et al. 2012, Clark et al. 2013), as demonstrated by our productivity model (Fig. 5.10). Our data, however, do not show such a trend (Figs. 5.4 and 5.10). Previous research has demonstrated that while there is a strong correlation between annual benthic irradiance and *L. solidungula* production, there is no correlation between daily surface and underwater irradiance in Stefansson Sound (1990). Additionally, the timing of ice dynamics has no direct impact on annual kelp production. Instead, annual benthic light budgets in Stefansson Sound are primarily limited by resuspension of sediments by wind induced water motion (Aumack et al. 2007). This is partially demonstrated by the considerable accumulation of H_{sat} during the

dates surrounding ice break-up (Fig. 5.7), when wind driven water motion is limited by high sea ice concentrations. The negative relationship between wind speed and benthic irradiance over month long periods, and the prevalence of low light conditions during the ice-free season (Table 5.1), further emphasize the link between wind and light attenuation.

The lack of a significant relationship between ice concentration and benthic light during late July through August indicates that the negative effects of wind outweigh the potentially remediating effects of any sea ice that lingers in the nearshore area after the open water season is underway. As in other shallow aquatic systems, rates of particle settlement and transport of suspended sediments confound the connection between benthic irradiance and wind (Van Duin et al. 2001). The effect of wind direction on the entrainment or advection of turbid coastal waters adds additional complexity to this relationship. It appears that the frequency of short-term increases in underwater light transmittance, under favorable wind and ice conditions ultimately determine the annual benthic light budget in this system.

The temporal accumulation of H_{sat} suggests that the days surrounding ice break-up contribute significantly (as much as 75-100%; Fig. 5.7) to annual benthic light budgets and annual kelp production. Underwater irradiance during this time depends on the amount of sediments contained within the ice (Dunton et al. 1982; Kempema et al. 1989), as well as ice dynamics during break-up, which are difficult to predict, and therefore not included in our production model. The omission of the break-up period may explain why the ice and wind-based production model often underestimated kelp growth (Fig. 5.10). The drastically reduced light levels during the ice-free summer and the lack of relationship to annual kelp growth demonstrate that light conditions during the ice-free summer are usually poor. Consequently, contracted sea ice extent may simply contribute to wind driven mixing of the water column and increased suspended sediments earlier in the year, effectively diminishing benthic irradiance and kelp production during the ice-free summer.

Reduced sea ice coverage in the coastal Beaufort Sea has increased wave fetch and intensified wave energy (Thomson and Rogers 2014, Thomson et al. 2016) that can substantially increase suspended sediments (Trefry 2009). Other studies in this region show that wave height is related to wind speed, as well as ice concentration (Manson and Solomon 2007). Therefore the strengthening of easterly winds in the region since the mid-2000s may also contribute to enhanced sediment resuspension (Wood et al. 2013, 2015), though this trend was not reflected in the wind measurements recorded at the Prudhoe Bay weather stations.

Current projections for macrophyte communities in Arctic marine systems assume that benthic irradiance will increase as sea ice extent contracts (i.e., Clark et al. 2013, Krause-Jensen and Duarte 2014). The long-term data presented here show that this assumption may not apply to inner shelf regions, especially marginal Arctic seas that receive substantial river inputs during the summer open water period.

This also agrees with results from a glacially influenced site, where sediment laden glacial meltwater is thought to have shrunk the euphotic zone over time (Bartsch et al. 2016). Light attenuation by suspended sediments demonstrably affects irradiance available for primary production, both in the water column (Van Duin et al. 2001) and in the benthos (Anthony et al. 2004, Aumack et al. 2007), and should be considered for Arctic ecosystem change scenarios.

The Arctic inner shelf under future climate change

Shallow inner shelf zones make up 20% of the area of Arctic shelves (Fritz et al. 2017). Outside of Greenland and the Canadian Archipelago, these systems experience considerable inputs from Arctic rivers during the melt season that contribute to total suspended sediment (TSS) concentrations (Gordeev et al. 1996, Gordeev 2006; Holmes et al. 2002, McClelland et al. 2012). Coastal erosion also significantly contributes to elevated TSS levels in inner shelf zones (Reimnitz et al. 1988, Hill and Nadeau 1989), which are often maintained by wind events that resuspend unconsolidated sediments on shallow shelves (Hill and Nadeau 1989). The reduction in water transparency in response to increased TSS, which is accentuated by expanded fetch and diminished ice extent, demonstrates the effects of a warming Arctic on primary production, especially on the coast and inner shelf. Consequently, we should expect that coastal ecosystems will respond differently to climate change than deeper, offshore seasonal ice zones.

As warming continues, multiple environmental factors in nearshore Arctic areas will cause average summer light attenuation to surpass current levels (~0.8 m^{-1}; Table 5.1). The persistence of these high attenuation conditions, which match the turbid conditions previously measured in Stefansson Sound (Dunton 1990, Dunton et al. 2009), will alter regimes of underwater light transmittance and primary productivity (Fig. 5.11). First, the reduction of sea ice will increase the incident sunlight to the ocean, leading to enhanced capacity for primary productivity at the surface. However, this reduction in sea ice will also lead to lengthened fetch, larger swell, stronger wave activity in the nearshore, and higher incidence of sediment resuspension (Wegner et al. 2003, Walker et al. 2008, Thomson and Rogers 2014, Thomson et al. 2016). Nearshore wave activity also intensifies coastal erosion, aided by melting permafrost and sea level rise (ACIA 2005, Overeem et al. 2011). Currently, both sheltered mainland lagoon and open ocean exposed coastlines of the Beaufort Sea are eroding at rates of 0.9 to 1.8 m y^{-1}, respectively (Gibbs and Richmond 2015). Globally, rates have been measured as high as 25 m y^{-1} (Jones et al. 2009, Gunther et al. 2015). Beaufort Sea Coast erosion rates appear to have increased, or even doubled over the past five decades (Jones et al. 2008, Jones et al. 2009). As the climate continues to warm, most Arctic coastlines are expected to experience accelerated coastal erosion (ACIA 2005, Fritz et al. 2017). River discharge to the Arctic Ocean is also increasing, with measured increase of ~11% from 1964-2000 (McClelland et al. 2006). This will contribute to intensified fluvial sediment flux, estimated to rise by 30-122% for the six largest Arctic rivers by the end of the century (Gordeev 2006).

The additive effects of sea ice loss, coastal erosion, and enhanced fluvial inputs will ultimately increase suspended sediments in Arctic inner shelf waters during the open water season (Fig. 5.11). Our research suggests that as summer ice concentrations continue to decrease, the annual benthic light budget in nearshore areas will progressively depend on light transmitted through the ice and water before and during break-up. It also shows that primary production may shift in unexpected ways in the future, depending on local characteristics. In areas with high suspended sediments, benthic production may not be enhanced by ice loss, but will increasingly rely on light transmittance during break-up. Phytoplankton productivity in the nearshore Arctic will also depend on the balance between light attenuation by suspended sediments and nutrient concentrations in the upper water column, which are similarly determined by sediment resuspension, erosion, and fluvial inputs. Decreased light transmission during summer will shallow the critical depth of growth, altering depth distributions of benthic and planktonic primary producers. Our work demonstrates that environmental factors that characterize Arctic inner shelves, particularly suspended sediments, should be considered in projections that evaluate the response of Arctic ecosystems to climate change.

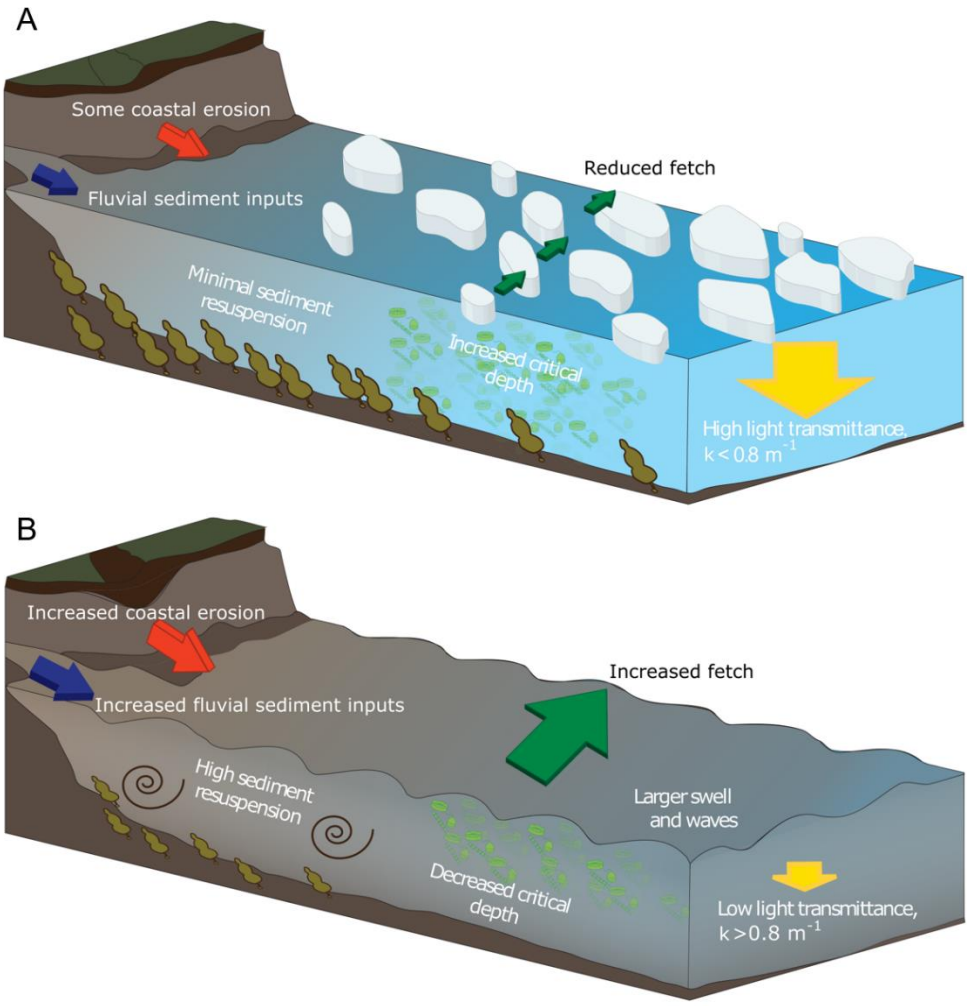

Figure 5.11. Conceptual diagram of the effects of a) summer ice cover versus b) reduced summer ice cover on processes affecting the underwater light environment in shallow inshore (<10 m) Arctic ecosystems. Reduced ice will increase coastal erosion, lead to larger swell, and increase sediment resuspension, which will combine with enhanced fluvial sediment inputs to ultimately increase light attenuation (k). This will decrease annual growth of benthic macrophytes, and shift depth distributions of pelagic and benthic primary producers by shallowing the critical depth.

6. Physiological responses of an Arctic crustose coralline alga (*Leptophytum foecundum)* within variations of salinity

Arley F. Muth and Kenneth H. Dunton

INTRODUCTION

Dissolution of marine calcifying organisms is of broad and current interest in ocean climate change studies. Lower pH levels, driven by carbon dioxide (CO_2) uptake into ocean water, causes a reduction in calcium carbonate (also other carbonate minerals e.g., aragonite and calcite) saturation levels leading to increased dissolution rates of calcifying species. However, pH is only one parameter of the saturation level equation and other mechanisms and factors have the potential to affect calcium carbonate saturation levels. At high latitudes, aragonite saturation levels are low (~2) when compared to ocean averages (~3.5) or low latitude values (~4; Gangstø et al., 2008; Jiang et al., 2015) due to processes such as freshwater input, rapid seasonal ice melt, upwelling, and relatively high respiration rates of organic matter (Mathis et al., 2015a). In the Arctic Ocean, natural factors in addition to anthropogenic factors have the potential to decrease aragonite saturation levels below natural variations ($\mathbf{\Omega}_{\text{aragonite}}$ 3.5-0.8) by 2025 (Mathis et al. 2015a).

Decreased rates of productivity, growth, and net calcification have been shown to occur when coralline algal species are exposed to lower than ambient pH conditions for short time periods (~21 days; Diaz-Pulido et al. 2012, Mccoy 2013, Büdenbender et al. 2015). CCA species are often the first species affected by lower pH because they precipitate magnesium calcite, which is about 20% more soluble than aragonite (Kamenos et al. 2008). CO_2 vents in Italy decrease pH locally and coralline species disappeared near the vents while turf algal biomass increased 60%, including certain invasive species (Hall-Spencer et al. 2008). Low salinities also decrease calcification rates and productivity in CCA species (King and Schramm 1982). Schoenrock et al. (2018) saw decreased calcification rates, photosynthetic efficiency, and density in *Lithothamnion glaciale* in southwest Greenland as waters became fresher in fjord environments. Marine invertebrates are also susceptible to dissolution as juvenile oysters cultured under decreased salinity and pH conditions showed increased rates of mortality in response to both factors, but that low salinities alone had the most impact (Dickinson et al. 2012).

Within the Beaufort Sea, a diverse benthic community attached to boulders and cobbles occurs in an area known as the Boulder Patch (for a detailed description see (Dunton et al. 1982, Wilce & Dunton 2014). Three kelp species (*Laminaria solidungula*, *Saccharina latissima* and *Alaria esculenta*) and various red

algal species (e.g., *Phycodrys fimbriata* and *Coccotylus truncatus*) are common on rock surfaces (Wilce and Dunton 2014). CCA species, including *Leptophytum foecundum* and *L. lavae*, cover 77% of the hard substratum in some areas and are completely absent in others (see section 1.2 and 1.3). Arctic species are adapted to high seasonal changes but in a relatively small geographic area (~ 6 km) within the Boulder Patch. Benthic surveys show patterns of decreasing CCA coverage at inshore areas as well as changes to algal diversity, composition and biomass. Within the Boulder Patch, a complete loss of CCA can be seen at inshore sites, and this study aims to understand the mechanisms preventing CCA from occurring at inshore locations.

The goals of this study were to understand the role of salinity and related abiotic parameters (pH, total alkalinity) on CCA physiology and distribution. Do changes in salinity affect CCA physiology independent of pH? Are seawater chemistry conditions influencing CCA distributions? Laboratory experiments were used to focus on short-term changes to CCA physiological mechanisms in response in alterations in water chemistry, and field studies allowed for real time, long-term observations of recruitment and persistence in natural conditions.

METHODS

Study site and species background

Within the Boulder Patch, Stefansson Sound, Alaska, there are varying distributions of CCA and the most striking of these patterns is between an inshore site, located near the mouth of the Sagavanirktok River (E-1) and an offshore site (DS-11; Fig. 6.1). The substrate of cobbles and boulders at the offshore site is covered with CCA (*Leptophytum foecundum,* determined by Paul Gabrielson of University of North Carolina Chapel Hill), while CCA is absent at the inshore site. Salinity measurements throughout the study area from past years have shown that salinity can drop to 15-20 at both sites but can reach as low as 0 at the inshore site (see section 1.1). Total alkalinity (A_T) is often lower in fresh and brackish waters, which reduces pH buffering capacities and results in lower pH values, leading to dissolution of the calcium carbonate skeletons of calcifying organisms. However, continuous pH_T for the Boulder Patch show consistently higher pH values at the inshore site, where CCA are absent. A_T values did decrease with lower salinity measurements as expected, and mesocosm experiments were conducted to observe if changes in salinity and A_T, with a constant pH, could drive dissolution and/or lower photosynthetic efficiency in *L. foecundum.*

Mesocosm Experiments

Culture conditions

Cobbles were collected in July of 2016 at DS-11 and transported to the

University of Texas Marine Science Institute (UTMSI) and kept in a 0°C chamber until experiments began. *Leptophytum foecundum cobbles* were cultured in complete darkness at three salinities (10, 20 and 30) and 0°C. A no-specimen control treatment (salinity of 30) was also monitored to determine the effect of the medium on water chemistry. Samples (n=4) were placed in salinity treatments for 5 weeks, after which all samples recovered at 30 for 5 weeks. Growth media (pH 8) was created using Gulf of Mexico (GOM) offshore water (low in nutrients) and distilled water, and all treatments were supplemented with Provasoli's Enriched Seawater, ensuring sufficient supply of macro and micronutrients. Media was replaced weekly and water quality parameters (pH, temperature, salinity) were recorded before and after each water change using a data sonde (YSI 6920V2-2). Water samples were also taken before and after each water change for titratable alkalinity measurements (values were log transformed to meet ANOVA assumptions of normality and equal variances).

Photosynthetic efficiency

Samples were monitored weekly for photosynthetic efficiency, dark-adapted yield values (F_v/F_m) using a pulse amplitude modulation (PAM) fluorometer (Walz, diving-PAM model). Three areas per cobble (n=4 for each salinity treatment) were measured for yield values each week at the same location on the cobble and time of day.

Calcium carbonate dissolution

Calcium carbonate dissolution was estimated by analyzing culture medium A_T when the medium was first replaced (initial) and after one week (final). An automated open cell Gran titration system (ASALK2; Apollo SciTech) coupled to a thermostated water bath was used to measure A_T (Lonthair et al. 2017) at experimental temperature. A_T values were combined with temperature, pH and salinity measurements to estimate aragonite saturation levels using the software program CO_2SYS. Saturation levels equal to one are at equilibrium, greater than one indicate precipitation and less than one indicates dissolution.

Pigments

Cobble photographs were taken at the start of the experiment, after 5 weeks in salinity treatments and after the 5-week recovery period, then analyzed using ImageJ to estimate percent pigment.

CCA recruit survivorship

In July 2017, fiber cement tiles (10 x 10 cm) were retrieved from DS-11 (Fig. 6.1) following a 12-month deployment on the seabed. Tiles/samples were transported to UTMSI and kept in a 0°C chamber until experiments began. CCA recruit (1-2 yr. old individuals) survivorship was monitored in salinity treatments of 10, 20 and 30. Tiles (n=5) were placed in each salinity treatment (10, 20 and 30) and five CCA recruits were identified and marked to ensure the same individuals were monitored throughout the experiment. Tiles were kept within the salinity

treatments for three months (Sept. 27 – 23 Dec. 23, 2017) and monitored weekly for survivorship.

In situ field experiments

Adults

To observe natural effects of abiotic factors and spatial changes in carbonate chemistry on *L. foecundum* in situ, reciprocal transplants between the inshore (E-1) and offshore site (DS-11) were conducted. Cobbles from offshore (n=6) with CCA present were photographed and transferred to the inshore site and remained on the seabed from July 2016 – July 2017. Cobbles were retrieved and kept in cool, dark conditions while transferred to the laboratory on Endicott Island, Alaska. In addition to the transplanted cobbles, control cobbles from each site were also collected for comparison in July 2017. In the laboratory, all cobbles with CCA present were measured for dark-adapted yield using PAM fluorometry (same methods as above). Tissue samples of the transplanted and control CCA were collected for pigment analysis, stored at -80°C and analyzed using the methods described above.

Recruits

Fiber-cement settlement tiles deployed in the Boulder Patch seafloor in July 2016 (see section 1.3) were retrieved from sites E-1 and DS-11 in July 2018 were transported to UTMSI and kept in a 0°C chamber prior to quantifying and comparing estimates of density and size of CCA recruits between sites. Tiles analyzed from E-1 the previous year had no CCA recruits present at the inshore (E-1) site, however, in July 2017, recruits were observed on the inshore settlement tiles (Section 1.2). Using a uniform grid, density of CCA individuals was counted for 50 FOV per tile at 40x. Pictures were taken at 40x, capturing 5 individuals per tile and ImageJ was used to analyze the size of the recruits from both sites.

Statistics

Mesocosm parameters were compared by calculating differences in A_T and pH in new media and week-old media, using 2-way ANOVAs (salinity treatment and treatment/recovery period) and values were log transformed in order to meet test normality and equal variance assumptions. Fv/Fm among treatments were compared using repeated measures 2-way ANOVAs (salinity and time) while cobbles were in salinity treatments and after all cobbles had been placed in recovery conditions. Changes in visual pigments were compared using 2-way ANOVAs (salinity treatment and treatment/recovery period) and ANOVAs were used to compare recruit size (values were square root transformed in order to meet ANOVA assumptions of normality and equal variances and density (values were log transformed in order to meet ANOVA assumptions of normality and equal variances) between sites. All statistics were run using R Version 3.3.1.

RESULTS

Culture Conditions

Salinity and temperature treatments remained consistent over the 5-week treatment period (control: 30.9 ± 0.2; 30: 31.5 ± 0.2; 20: 20.9 ± 0.1; 10: 10 ± 0.1) and salinity values in the recovery treatments were 31.2 ± 0.1. pH values decreased in all treatments over each week (start pH 8.06 ± 0.02, end pH 7.84 ± 0.02), but the changes did not differ among treatments or between periods (treatment/recovery; 2-way ANOVA: period F_1=0.004, p=0.949; salinity treatment F_4=1.07, p=0.388; interaction F_4=0.661, p=0.623).

Mesocosm Experiments

Photosynthetic Efficiency

Yield values were significantly different between the salinity of 10 treatment and the salinity of 20 and 30 treatments and interaction of time and salinity was also significant, as yield values dropped in the 10 salinity treatment throughout the 5 week period, specifically weeks 3 and 5 (Fig. 6.1; Repeated measures 2-way ANOVA: salinity F_1=23.60, p<0.001, time F_5=44.33, salinity*time F_5=5.47, p<0.001). After cobbles were all placed in a recovery salinity of 30, the previous salinity treatments did not affect yield values, however yield values for all treatments did decrease initially and then recover over time (Fig. 6.1; Repeated measures 2-way ANOVA: salinity F_1=0.50, p=0.49, time F_4=56.88, p<0.001, salinity*time F_4=2.14, p=0.07).

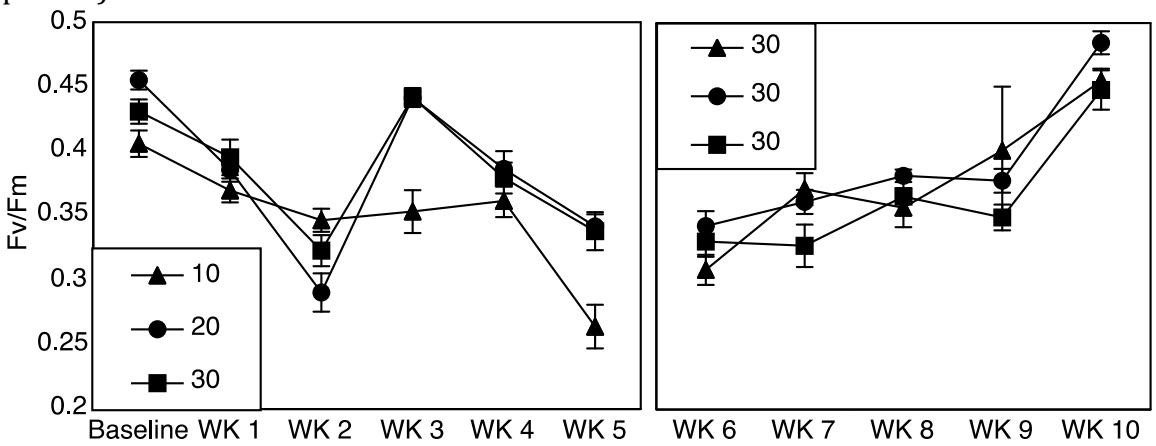

Figure 6.1. Fv/Fm values across 5 weeks of salinity treatments (10, 20 and 30) and 5 weeks in a recovery treatment of 30. Error bars represent SE.

Calcium Carbonate Parameters

Discrete water samples analyzed for A_T fluctuations each week of the experiment showed a significant increase in A_T in the salinity of 10 treatment

compared to the control, and salinity of 20 and 30 treatments during the 5-week period. Samples placed in a recovery salinity of 30 showed not significant differences in A_T (Fig. 6.3; 2-way ANOVA period F_1=5.39, p=0.027; treatment F_4=6.39, p<0.001; interaction F_4=4.50, p=0.006). Media aragonite saturation levels for each treatment (Table 6.1), showed only the salinity of 10 treatment was under saturation (Ω aragonite = 0.5), with 20 and 30 treatments at equilibrium and 1.6 respectively. The 20 and 30 treatments also did not differ in respect to A_T (Fig. 6.2).

Table 6.1. Carbonate chemistry parameters for salinity treatments used in laboratory experiments. When Ω = 1, the seawater is exactly in equilibrium (saturation) with respect to aragonite. Values in parentheses are SE.

Salinity Treatment	pH (NBS scale)	HCO3 in (mmol/kgSW)	CO3 in (mmol/kgSW)	CO2 in (mmol/kgSW)	W Ca out	W Ar out
10	8.07 (0.05)	1131.1 (107.2)	32.4 (9.3)	17.2 (3.1)	0.9 (0.3)	0.5 (0.1)
20	8.07 (0.04)	1711.8 (100.1)	64.9 (13.0)	21.7 (3.6)	1.7 (0.3)	1.0 (0.2)
30	8.06 (0.03)	2293.0 (65.9)	105.4 (2.4)	25.9 (1.1)	2.6 (0.1)	1.6 (0.1)

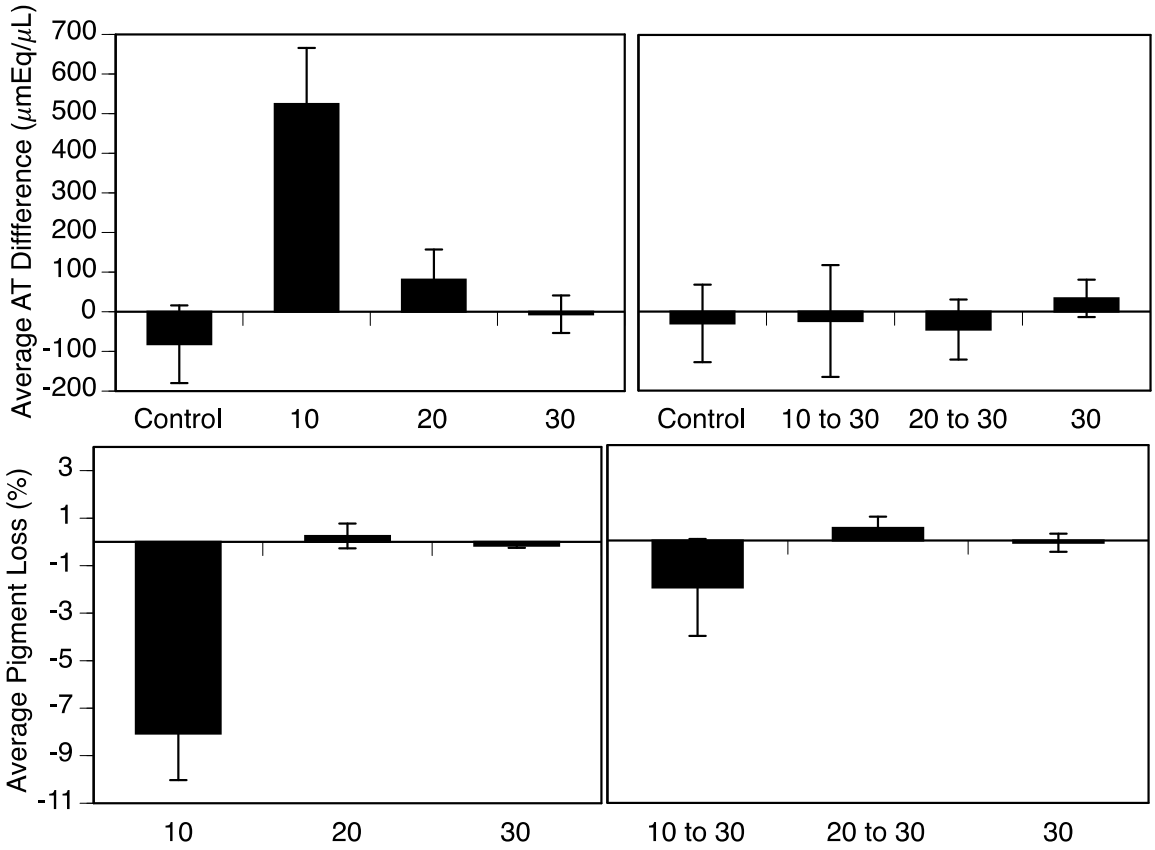

Figure 6.2. Top: Average A_T differences over 5 weeks at varying salinities (10, 20, 30 and control without any cobbles) and 5 weeks of recovery, all treatments at salinity of 30. Bottom: Average pigment loss over 5 weeks of salinity treatments (10, 20 and 30) and 5 weeks of recovery, all treatments at a salinity of 30. Error bars are SE.

Pigments

Percent changes in visual pigments of the cobbles in the salinity of 10 treatment lost significantly more pigments during the treatment period (Fig. 6.3; 2-way ANOVA: period F_1=4.4, p=0.046; salinity treatment F_3=15.56, p<0.001, interaction F_4=5.92, p=0.024) while the salinity of 20 and 30 cobbles remained unaffected and lost little to no pigmentation throughout the experiment (Fig. 6.3).

Recruit survivorship

CCA recruits (n=25) were monitored for 3 months in salinity treatments of 10, 20 and 30. Throughout the study recruits were lost (salinity of 10 = 5 lost, salinity of 20 = 2 lost and salinity of 30 = 2 lost), however the number of individuals lost did not significantly differ among treatments (ANOVA $F_{1,13}$ = 1.09, p=0.31).

Field Experiments

Adults

Photosynthetic efficiency and Pigments

Field transplants with adult CCA showed high amounts of variability. Yield (Fv/Fm) values were not significantly different, however, non-pigmented areas had yield values as high or higher than pigmented areas, likely due to endolithic algal species (transplanted 0.45 ± 0.01, control 0.43 ± 0.01, ANOVA $F_{1,34}$=2.79, p=0.103). Transplanted cobbles from the offshore to the inshore site pigmentation, but percent lost was highly variable (Fig. 6.4, a-d; 23.03% ± 15.0%).

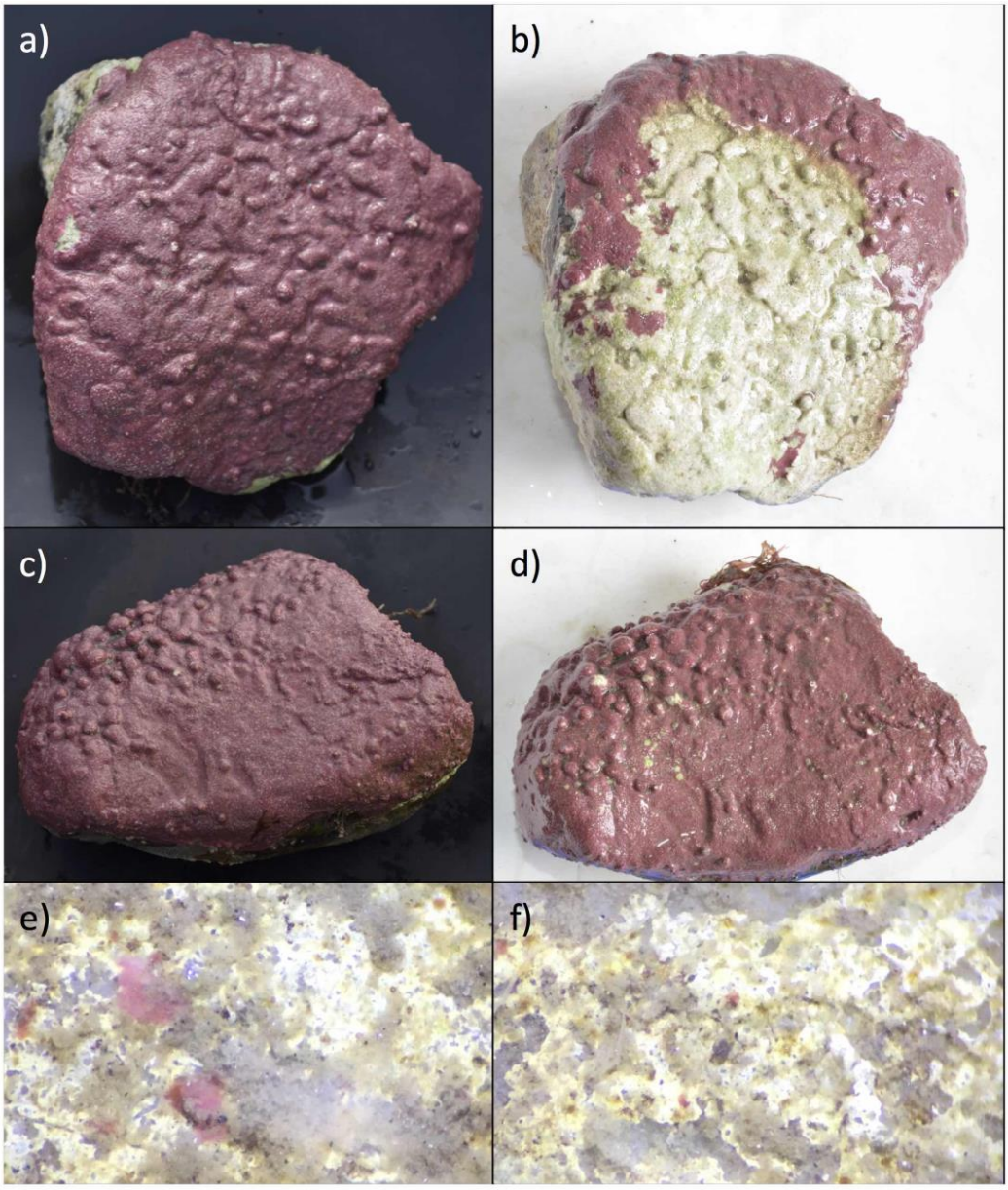

Figure 6.3. a) cobble photographed in 2016 pre-transplant b) same cobble as a, photographed in 2017 after a one year transplant to an inshore site, high pigment loss c) cobble photographed in 2016 pre-transplant d) same cobble as c, photographed in 2017 after a one year transplant to an inshore site, low pigment loss e) one year recruits at the offshore site at 40x f) one year recruits at the inshore site at 40x.

Recruits

Size and Density

Recruit size and density were compared between the offshore and nearshore site. Recruits were present at both sites but were significantly larger at the offshore

site (Fig. 6.3, e and f; offshore size 12.89 ± 1.91 mm^2, inshore size 1.35 ± 0.209 mm^2; ANOVA $F_{1,78}$=64.91, p<0.001). Densities of CCA recruits were significantly higher at the offshore (site offshore density 1.16 ± 0.40 per cm^2, inshore density 9.02 ± 3.76 per cm^2; ANOVA $F_{1,14}$=7.02, p=0.01).

DISCUSSION

Arctic coralline algae survive in an environment of high seasonal variability and drastic water chemistry changes (see section 2.4). Within the Boulder Patch of Stefansson Sound, Alaska, CCA distributions vary from dominant benthic space holders to complete absence. Influence of the Sagavanirktok River and associated freshwater input into the sound drives carbonate chemistry parameter changes, causing seawater variations that affect CCA and their ability to persist (section 2.4).

Results from mesocosm laboratory experiments illustrate that *Leptophytum foecundum,* the dominant CCA species at the offshore site (DS-11), was able to tolerate salinities in the range of 20 without any significant physiological impacts. Photosynthetic efficiency (Fig. 6.1), visual pigments and dissolution of calcium carbonate (Fig. 6.2) were not significantly different between the 20 and 30 salinity treatments. However, at a salinity of 10, CCA experienced reduced photosynthetic efficiency, decreased visual pigments and increased calcium carbonate dissolution (Figs. 6.1 and 6.2). Interestingly, all parameters measured (Fv/Fm, pigments and A_T) were able to recover very quickly once specimens were placed in a recovery salinity of 30. These results highlight that *L. foecundum* is likely very resilient to lower salinities and changes in carbonate chemistry and has acclimated to periods of stress, occurring each year during break-up.

The significant increase in A_T in the 10-salinity treatment is most likely driven by the 0.5 $\boldsymbol{\Omega}$ aragonite value. When the saturation level is below one, dissolution of calcium carbonate is favored and in the closed systems of the mesocosms, dissolution is the only process that would affect A_T. CCA precipitate magnesium calcite, which is 20% more soluble than aragonite, therefore CCA are likely susceptible to dissolution when $\boldsymbol{\Omega}$ aragonite levels are less than one.

Cobbles transplanted in the field were extremely variable in their response to transferring to the inshore site (Fig. 6.3, a-d). On average, 23% of the visual pigments were lost, but the error associated with that value was 15%. During the year the cobbles were transplanted (2016-2017), salinity levels at the inshore site did not fall below 20, while the following year (2017-2018), salinity at the inshore site was near zero (see section 2.4). These annual variations and periods of low salinity likely affect CCA attempting to recruit to the inshore sites, and extreme low salinity events prevent CCA from persisting.

Recruits of CCA were not shown to be more susceptible to lower salinities

than adults in mesocosm studies and after 3 months in salinity treatments of 10, 20 and 30 there was no significant difference in recruit survivorship. However, within the 3-month period we may not have been able to detect difference in growth or calcification rates due to the small size of the individuals tracked. Recruits size and density were significantly larger and denser at the offshore site than the inshore site (Fig. 6.3, e and f). The recruitment of CCA onto settlement tiles was observed at the inshore site (Section 1.2), which shows that the absence of CCA at the inshore site is not due to propagule dispersal limitations. CCA propagules are reaching the inshore site, but they are unable to persist and grow into adults, likely due to water chemistry changes associated with low salinity.

During the years of this study (2016-2018), **Ω** aragonite saturation levels were found to remain around one for much of the year (see section 2.4), even at the offshore site where CCA cover the benthos. Studies have predicted that Arctic waters could reach **Ω** aragonite levels of one by 2100 (Gangstø et al. 2008), however, these levels are currently occurring in nearshore environments. CCA species in the Boulder Patch survive at **Ω** aragonite levels near one, but during break-up, **Ω** aragonite levels drastically drop and these events drive CCA distributions.

Corallines are known to grow laterally rather than vertically when colonizing space, allowing them to cover the benthos (Airoldi 2000). However, the roles, which corallines play in algal and sessile invertebrate succession, vary drastically across communities. Studies have shown that corallines enhance biodiversity (Asnaghi et al. 2015), while other work has focused on the lack of further algal recruitment once coralline secure dominance (Bulleri et al. 2002). Johnson and Man (1986) found *Phymatolithon* in Nova Scotia to suppress the recruitment of turf algal species. A similar pattern has been observed in the Boulder Patch of Stefansson Sound, however, a few algal species seem to possess the ability to recruit to the CCA species present (*Leptophytum foecundum* and *L. lavae*). The mechanism that allows for this recruitment is unknown, but slower growing crusts (e.g., *Lithothamnion phymatodeum*; (Dethier and Steneck 2001) have shown resilience to turf overgrowth and shading. In Stefansson sound, red algal biomass is reduced when CCA are present, but kelp biomass increases (see section 1.2 and 1.3). The mechanism driving this pattern needs to be explored; but as CCA coverage varies, algal and invertebrate assemblages co-vary.

Due to susceptibility of CCA to variations in carbonate chemistry, these species also serve as bioindicators for changes in ocean chemistry in nearshore environments. As freshwater input into the Arctic Ocean increases, areas devoid of CCA could increase, causing changes to the epilithic communities. CCA are conspicuous benthic species, and their presence and absence could serve as an effective tool for assessing water quality and changes in the nearshore Arctic that will affect not only CCA, but also other marine calcifying organisms.

7. Carbonate chemistry of the nearshore Arctic: shifts and future implications

Arley F. Muth and Kenneth H. Dunton

INTRODUCTION

Arctic marine species are tolerant to extreme seasonal shifts in environmental conditions, but high latitude systems are also predicted to be the most impacted by climate change. These impacts include increased temperature, freshwater input, changes in ice coverage and higher susceptibility to ocean acidification. As carbon dioxide (CO_2) increases in the atmosphere, more CO_2 is absorbed by the world's ocean, causing a decrease in pH. High latitude waters are colder; making CO_2 more soluble and prolonged periods of time dominated by heterotrophy (respiration) cause higher amounts of carbon dioxide partial pressure (pCO_2) within the water column and decrease ocean pH. In the Arctic, this process is exacerbated by large amounts of freshwater input, decreasing nearshore salinities and total alkalinity (A_T; Mathis et al., 2015)

The Arctic Ocean receives 11% of the world's freshwater run-off, but only comprises 1% of the world's oceans (McClelland et al. 2012). Furthermore, most of this water is released during a short period each spring during break-up, causing drastic changes to the nearshore water composition and chemistry. The Sagavanirktok River, which is the second largest river draining the North of Alaska (1.6 km^3 annual discharge; McClelland et al. 2014), drains the Brooks Range into Stefansson Sound. These rapid and drastic changes to nearshore waters directly affect the saturation level of aragonite (Ω aragonite), the most commonly reported calcium carbonate mineral, and calcifying organisms ability to persist (Gangstø et al. 2008, Diaz-Pulido et al. 2012).

The goal of this study was to capture the first continuously measured ocean total pH (pH_T) for the nearshore Arctic Ocean. Spatial placement of sensors in varying proximity to freshwater input allowed for comparisons to be made between areas of differing water masses (marine dominated vs. seasonal freshwater influenced). This seasonally dynamic region of the coast is of great interest and has ecological implications for fisheries, subsistence hunting, and is under great flux due to anthropogenic climate change. Additionally, by capturing pH_T, salinity, temperature and A_T from discrete water samples, aragonite saturation levels Ω aragonite were estimated in order to further understand water chemistry effects on calcifying organisms. Benthic species (invertebrate and algal) were catalogued and compared between sites in order to assess water chemistry effects on species composition.

METHODS

Study Sites and Background

Sea-bird (Satlantic) SeaFETs and SBE 37-SM MicroCATs C-T (P) were deployed July 2016-July 2018 at two sites within the Boulder Patch, Stefansson Sound, Alaska (Fig. 7.1); Site E1 (70º18.8665 N, 147º44.0413 W; 4 m depth) and site DS-11 (70º19.3248 N, 147º34.8816; 7 m depth). Sites varied in proximity to the Sagavanirktok River, as such, we expected marked spatial and temporal gradients in salinity and carbonate chemistry moving from near shore of the Sagavanirktok River to offshore in open Beaufort
Sea.

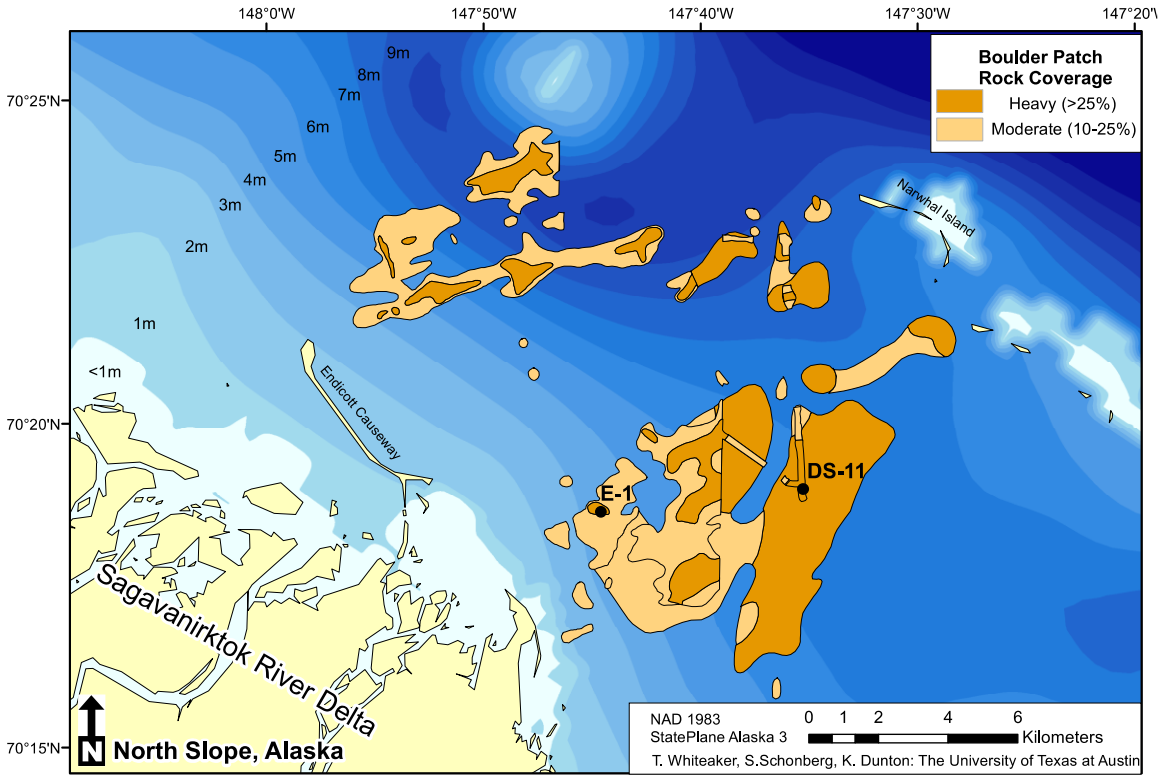

Figure 7.1. Map of the Boulder Patch and instrument deployment sites.

Calibration

Water samples were collected when instruments were deployed and retrieved. Single point calibration techniques were used to ensure sensor accuracy throughout deployment period. Samples were preserved with mercuric chloride and stored as directed by Dickson et al. (2007) for pH total (pH_T) and total alkalinity (A_T) analysis. Spectrophotometric pH was measured at 25ºC for 2016 deployment samples and 20ºC for 2017 retrieval and deployment samples, using m-cressol purple. An automated open cell Gran titration system (ASALK2; Apollo SciTech) was used to measure A_T (Lonthair et al. 2017). Due to logistical constraints, water

samples were taken at time of deployment and applied to values the following day, keeping time of day consistent. Sensors were conditioned before deployment; however, values became steady after one day on the seafloor, and applying calibration values the following day was more accurate to the data.

Error Calculations

Retrieval water samples were used to calculate sensor error over the year-long deployment for the 2016-2017 dataset. New sensors were deployed in 2018, and retrieval samples were not collected, however, several pH (NBS) values were measured at the retrieval sites. In order to estimate a conversion factor between pH_{NBS} and pH_T, spectrophotometric pH was measured at 25ºC from a certified reference material (CRM, Dickson Laboratory, UC Scripps, Batch 171) that was diluted to create five salinity samples (33.43, 20, 15, 10, 5). pH_T was corrected using A_T, temperature and salinity of the samples. A calibrated PRO DSS YSI sonde (same model used in original field measurements) was then used to measure pH_{NBS} for each salinity sample created. Although there is greater error associated with the data sonde (pH ± 0.01), this calibration protocol allowed the use of the pH_{NBS} values to estimate sensor error (pH_{NBS} + 0.118 = pH_T).

Data processing and carbonate chemistry parameter calculations

pH values reported are all calibrated pH_T values. Internal pH was reported for both 2016-2017 datasets and 2017-2018 E-1, while external pH was reported for 2017-2018 DS-11. Aragonite saturation levels were estimated for each data set using pH, salinity, and temperature values, and estimated A_T from several discrete water samples taken throughout the Boulder Patch in July of 2018 (n=13; CO_2Calc, USGS). A_T was measured using the techniques described above and regressed against salinity values ($y=31.032x + 1653.3$; $r^2=0.61$).

Temperature and salinity values were plotted against the water freeze line to ensure the values were valid measurements. Any values that fell below the freeze line were not included in the analysis.

Cobble Analysis

In 2016, cobbles were collected haphazardly along ordinal direction transects (180˚) at dive sites DS-11, E-1 and W-3. Cobbles were photographed with and without algal biomass, image analysis software ImageJ was used to estimate percent cover of encrusting algal and rock surface area. Algal species were separated and wet weight of each was recorded. A *t*-test was used to compare red algal biomass wet weights between DS-11 and E-1. Invertebrate species were identified, catalogued and preserved for further identification and biomass measurements at the University of Texas at Austin, Marine Science Institute.

RESULTS

pH_T values were recorded hourly for 2016 deployments, however, upon retrieval both pH sensors had failed (E-1: July 2016-June2017; DS-11: July 2016-February 2017). Sensors were reset for the 2017 deployments to record pH_T every two hours and were actively recording when retrieved in July 2018. Values and trends were similar between sites for each year, but drastic variations were seen between years.

2016 Results

Coastal ocean pH_T, salinity, and temperature follow seasonally distinct transitions that relate to four main events: the summer open water, fall freeze-up, the winter ice covered season, and the spring freshet. All variables were stable when ice forms in the fall but become more variable during the open water period (Fig. 7.2). However, for the 2016-2017 deployment, pH_T during the freshet was not captured due to sensor failure. Ranges in temperature (E1: -1.87 – 7.08°C; DS-11: -1.88 – 6.08°C) and salinity (E1:19.07 – 34.35; DS-11: 21.93 – 34.51) were similar between sites (Fig. 7.3), especially when compared to 2017 data (see below). While pH_T varied from 7.83 – 8.70 at E1 (error 0.042) and 7.79 – 8.69 at DS-11 (0.046), both sites showed a unique pH spike during freeze-up (Fig. 7.2).

The temporal separation of the salinity/pH relationships showed two distinct "water masses" or "chemistry regimes" that occur before and after Oct 25 (for EI) and Nov 5 (for DS-11). These anomalous shifts are likely associated with changes in the physicochemical environment with the freezing of coastal waters and/or the influence freshwater discharge from the Sagavanirktok River (Fig. 7.2). These dates also correspond to the first spike in pH_T seen at each site (E1: ~October 25; DS-11: ~November 5th). Both sites show a slight decrease in pH November through February as heterotrophy and respiration increase pCO_2 in the water column, and an increase from March until break-up (only seen at E-1), due to the presence of light and primary production (Fig. 7.2).

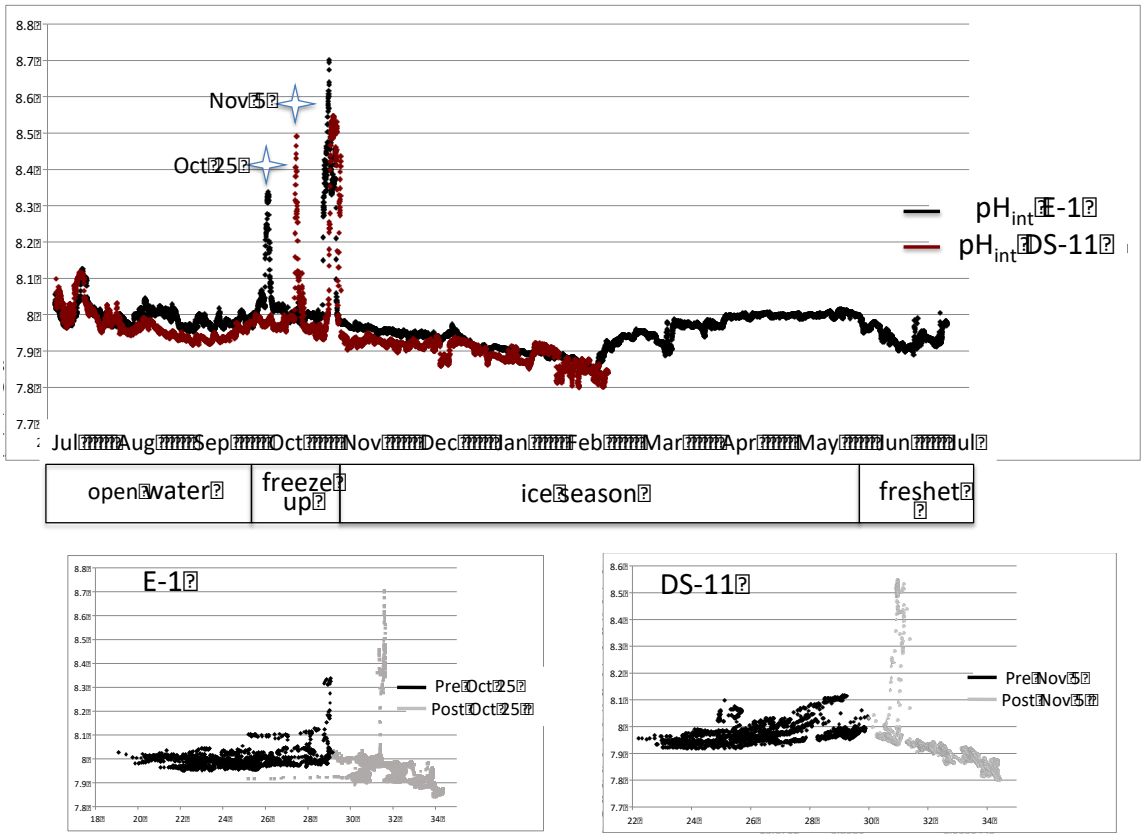

Figure 7.2. pH_T for DS-11 (red) and E-1 (black) 2016-2017 as ocean conditions vary from open water, freeze-up, ice season and the spring freshet. Spikes of pH in Oct-Nov correspond to freeze-up. Bottom graphs show salinity vs. pH relationships for each site before and after Oct 25, 2016 (E-1) and Nov 5, 2016 (DS-11). Dates correspond to freeze-up, peaks in pH and a change in the relationship of pH and salinity.

Temperature and salinity measurements also followed temporal patterns as seen in pH_T that correspond to open water, freeze-up, ice cover, and the spring freshet (Fig. 7.3). The 2016 dataset highlighted (more exaggerated in the 2017 dataset below) the influence of the Sagavanirktok River on changes in pH_T, salinity and temperature. Although salinity levels were lower at E-1, the inshore site, during times in the spring, salinity ranges between sites were similar (E1: 19.07 – 34.35; DS-11 21.93-34.51).

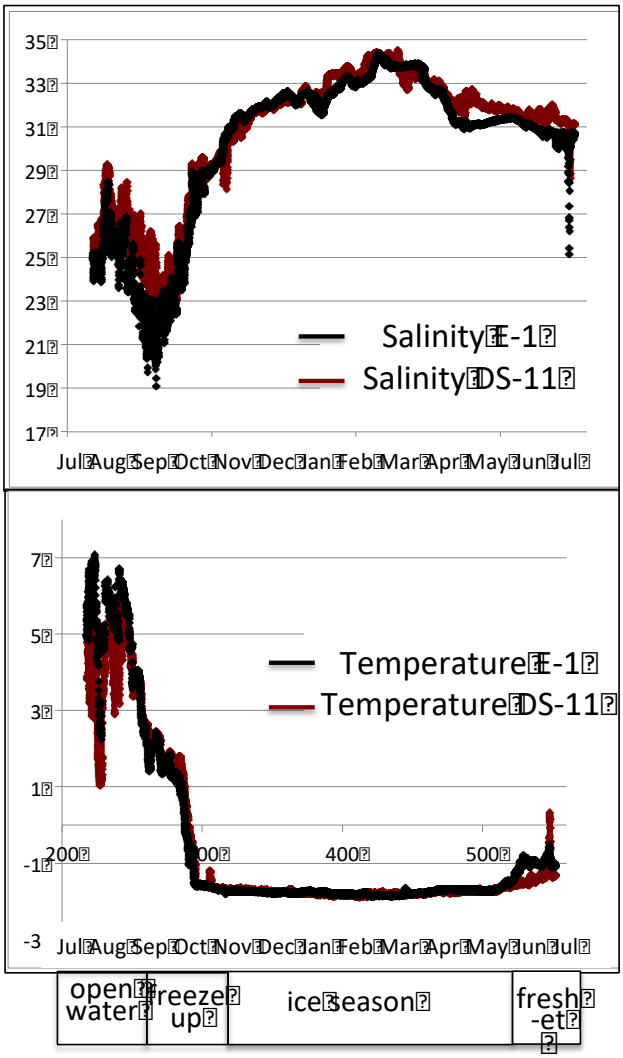

Figure 7.3. Salinity (top) and temperature (bottom) for 2016-2017, E-1 (black) and DS-11 (red) as ocean conditions vary from open water, freeze-up, ice season and the spring freshet.

2017 Results

Annual variations of pH_T, salinity, and temperature were apparent between 2016-2017 and 2017-2018 datasets. The 2017-2018 values also centered on ice formation and the spring freshet. As in 2016-2017, factors stabilized during the ice season and temperature (E1: -1.86 – 9.73°C; DS-11: -1.91 – 9.05°C) and salinity (E1:0.001 – 34.02; DS-11: 12.72 – 34.86) varied drastically during July 2017 and July of 2018, between sites, but did follow seasonal patterns (Fig. 7.4).

pH_T varied from 7.67 – 8.67 at E1 (error 0.085) and 7.75 – 8.34 at DS-11 (0.028), both sites showed pH spikes when salinity declined due to run-off from the Sagavanirktok River; open water season (DS-11-July 2017) and the spring freshet (E1-July 2018), but spikes were not detected during freeze-up as they were in 2016

for both sites (Fig. 7.5). Heterotrophy during the ice season and low light season likely increased pCO_2 and caused a slight decrease in pH as seen in 2016-2017. Salinity/pH relationships continued to be temporally separated for both sites, however, they were not related to freeze-up, but rather related to freshwater input, and ice cover. These chemical signatures were seen at both sites for both years and signaled a change between ice covered stabilized ocean water and ocean water mixed with freshwater from the Sagavanirktok River.

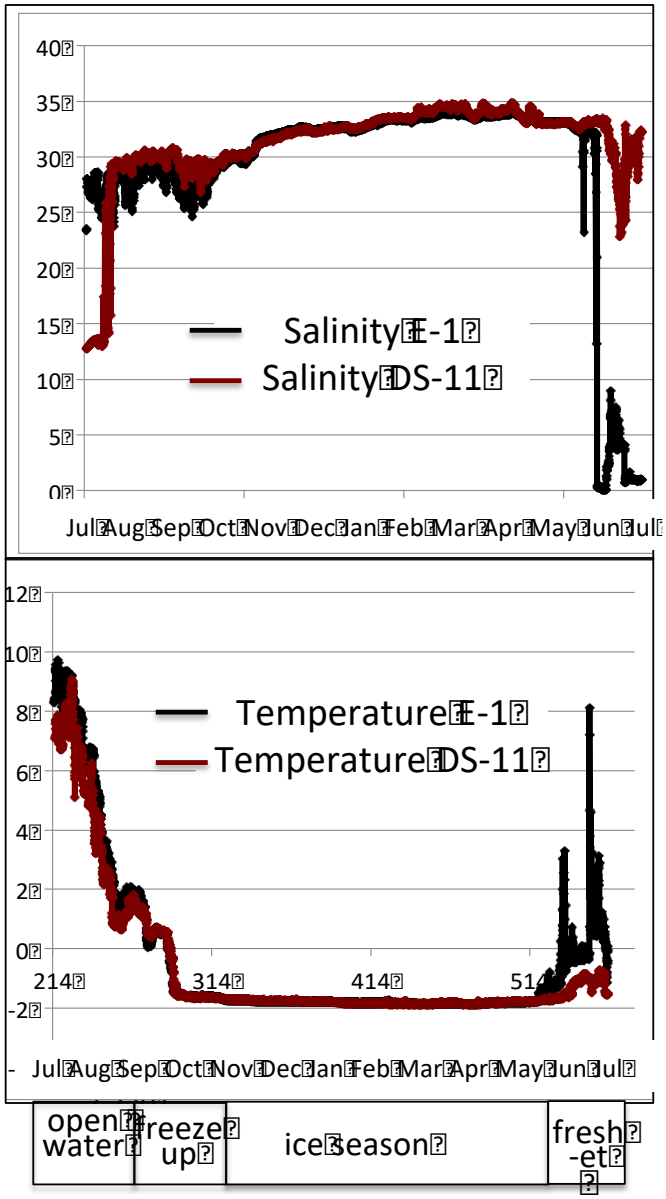

Figure 7.4. Salinity (top) and temperature (bottom) for 2017-2018, E-1 (black) and DS-11 (red) as ocean conditions vary from open water, freeze-up, ice season and the spring freshet. Note the salinity declines in July 2017 at DS-11 and Jun/Jul 2018 at E-1.

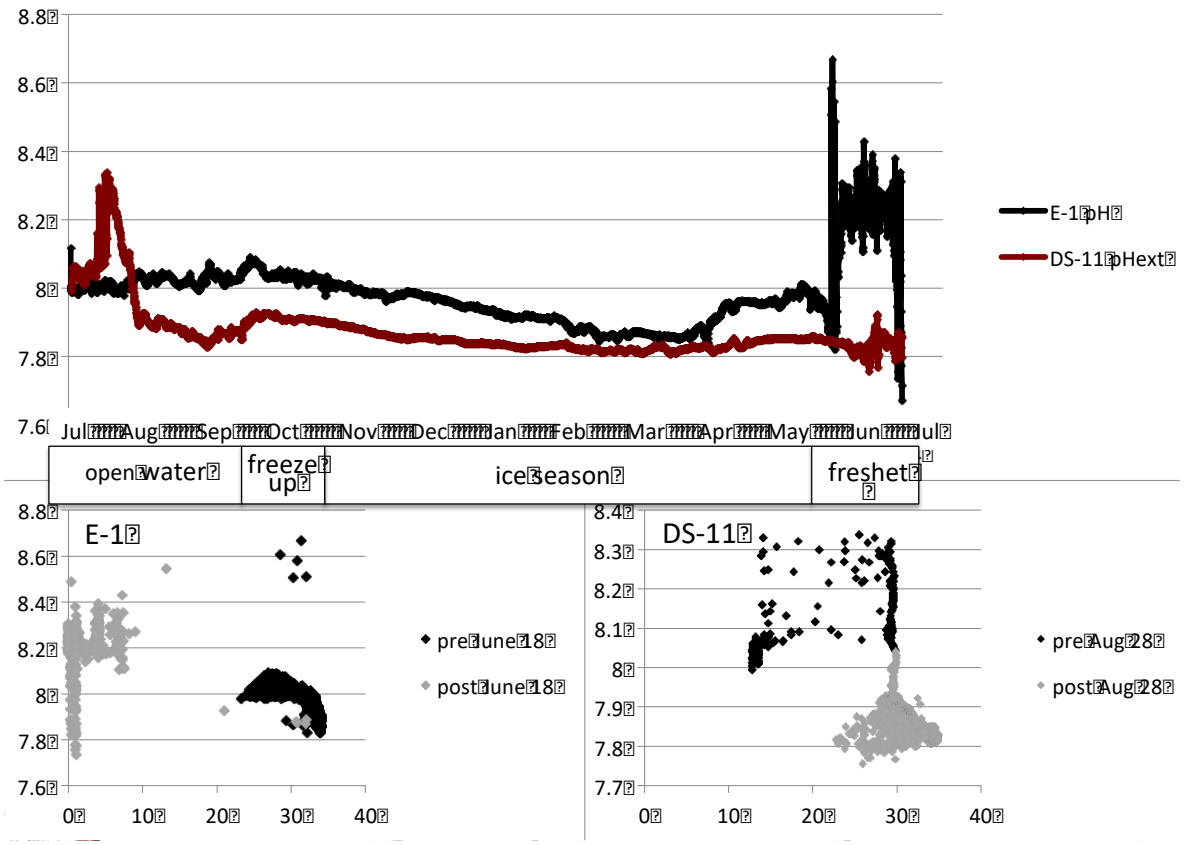

Figure 7.5. pH_T for DS-11 (red) and E-1 (black) 2017-2018 as ocean conditions vary from open water, freeze-up, ice season and the spring freshet. Spikes of pH in Jun/Jul of 2018 at E-1 correspond to low salinity levels and the spring freshet. Bottom graphs show salinity vs. pH relationships for each site before and after June 18th, 2018 for E-1 and before and after August 28th, 2017 for DS-11.

Ω Aragonite Levels

Estimated **Ω** aragonite levels ranged from 0.91 – 4.96 at E-1 and 0.91 to 4.88 at DS-11 for 2016-2017, with values near equilibrium (Fig. 7.6a, blue line) for much of the ice season at both sites. Peaks in **Ω** aragonite levels corresponded to peaks in pH_T (Fig. 7.2). The 2017-2018 dataset exhibited more variability in **Ω** aragonite levels between sites than 2016-2017 (Fig. 7.6b) and this was also reflected in other parameters measured (as seen in Figs. 7.4 and 7.5). DS-11 2017-2018 **Ω** aragonite levels fluctuated from 0.56 – 3.14 and 0.00 - 4.66 at E-1. Lowest levels for both sites were reached during the spring freshet in July of 2018.

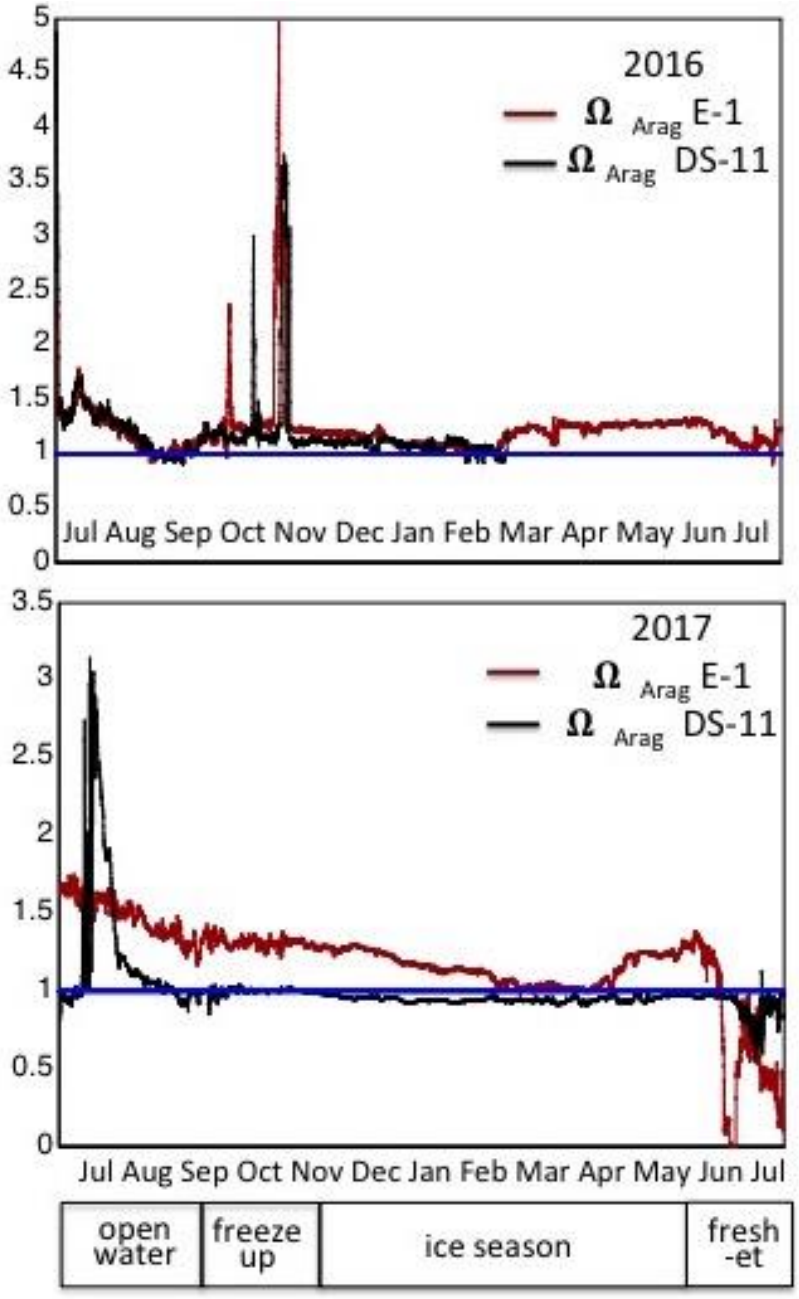

Figure 7.6. **Ω** aragonite levels for 2016-2017 (top) and 2017-2018 (bottom). The blue line shows equilibrium with respect to aragonite, values in June/July of 2018 fell well below equilibrium.

Cobble Analysis

Crustose coralline algae (CCA) covered on average of 77.5% (±3.8%) of the cobbles at DS-11 and was not present at E-1. DS-11 was dominated by one CCA species, *Leptophytum foecundum*, but samples of *Leptophytum leave* were also found. When CCA were absent (E-1), red algal biomass was significantly greater (T-test: $t_{20.72}$=-2.2762, p=0.03; Fig. 7.7), but was dominated by two species (Fig. 7.8). Overall,

red algal species on the cobbles from DS-11 and E-1 are similar (Table 7.1), but DS-11 was more diverse and more species contributed to the overall biomass (Fig. 7.8). Branching invertebrates also showed a conspicuous pattern in the presence and absence of CCA.

Invertebrate species differed between sites (Table 7.2). *Sertularia cupressoides* (hydroid) was only found at DS-11 and recruited to the edges of the CCA (~0.0009 g per cm^2). *Eucratea loricata* (bryozoan) covered the tops of the cobbles along with red algae species at E-1 where CCA was not present (0.01 g cm^{-2}).

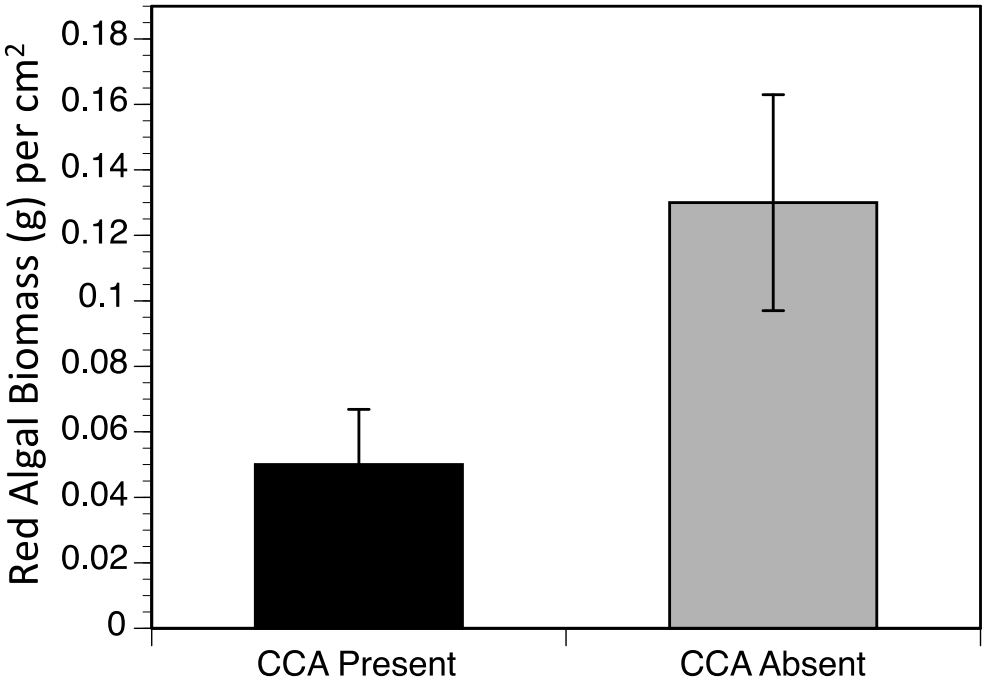

Figure 7.7. Red algal biomass per cm^2 of cobble surface at DS-11 with CCA present and E-1 with CCA absent. Error bars represent SE.

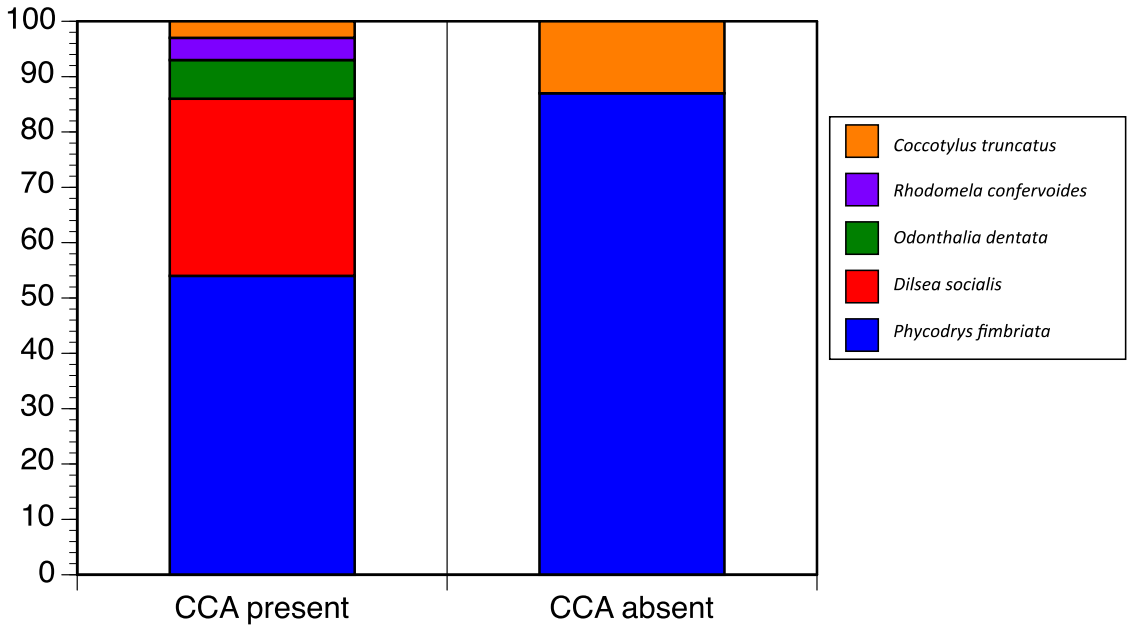

Figure 7.8. Red algal biomass composition at DS-11 with CCA present and E-1 with CCA absent.

Table 7.1. Red algal species present on cobbles collected at DS-11 with CCA present and E-1 with CCA absent.

		CCA	No CCA
Rhodophyta	*Phycodrys fimbiata*	x	x
	Coccotylus truncatus	x	x
	Rhodomela confervoides	x	x
	Odonthalia dentata	x	x
	Dilsea socialis	x	x
	Ahnfeltia borealis		x
Chlorophyta	*Chaetomorpha* sp.		x
Ochrophyta	*Laminaria solidungula*	x	x
	Sphacelaria plumosa		x
	Ecotocarpus siliculosus		x

Table 7.2. Invertebrate species present at DS-11 and E-1

	E-1	DS-11
Bryozoa	*Eucratea loricata* *Alcyonidium gelatinosum*	*Eucratea loricata* *Carbasea carbasea* *Flustrella gigantea* *Crisiidae* sp. Unknown Bryozoan
Hydrozoa	*Lafoniа maxima* *Abietinaria* sp. *Sertularia albimaris*	*Lafoniа maxima* *Sertularia cupressoides* *Sertularia albimaris*
Polychaeta	*Nereimyra aphroditoides* *Exogone* sp. *Harmothoe imbricata*	unknown Nereis *Exogone* sp. unknown Serpulidae unknown Polydora unknown Spionidae
Porifera		*Haliclona rufescens*
Nematoda	unknown Nematoda	unknown Nematoda
Foraminifera		unknown Foramnifera
Chiton		*Stenosemus albus*
Amphipoda	*Caprella* sp. *Atylus carinatus*	
Cirripedia	*Balanus crenatus*	
Ascidian	unknown Ascidian *Chelysoma* sp. *Dendrodoa aggregata*	

DISCUSSION

Due to environmental factors in the Arctic (e.g., cold water, respiration, freshwater influence), low aragonite saturation levels have been reported for these waters (Yamamoto-Kawai et al. 2009); however, values for near shore areas are unknown. Capturing the first continuous pH_T dataset with associated carbonate chemistry parameters is critical for the nearshore Arctic, in order to obtain baseline values, and to disseminate factors or interactions of factors affecting water chemistry.

Annual variability in pH_T corresponded to distinct time periods associated with open water, freeze-up, ice cover, and the spring freshet. Other parameters measured (salinity, temperature) also have specific patterns within these time periods (Figs. 7.3 and 7.4). In 2016, pH increases were observed at E-1 and DS-11 (Fig. 7.2), near freeze-up. Additional work is needed to describe the exact reason for

these spikes, but likely the spikes are driven by an increase in primary production, drawing down water pCO_2, and causing pH to rise. These increases can occur due to several factors, but because the spikes were seen at both sites, roughly around the same time as freeze-up, the increases could be a result of brine formation and water column turnover. As ice forms, high salinity waters form at the surface below the ice, however, this water is dense and it ultimately migrates to the bottom, causing an overturn of the water column. This process can disturb the bottom, increase sedimentation, and re-suspend benthic phytoplankton. We also see conductivity sensors fail during this time period, and it is believed that this is due to an increase in sedimentation that obstructs the sensors. Further work needs to be done (chl *a* data, exact ice formation, etc.) in order to be sure this is the process causing pH changes. Before freeze-up pH was variable (Fig. 7.2), however, once freeze-up occurred and ice formed, values stabilized. There was a slight reduction in pH during the winter months, possibly due to the lack of photosynthesis and an increase in CO_2 production due to heterotrophic processes. This decrease was seen at both sites for 2016 and 2017 (Figs. 7.2 and 7.5), and as spring approached pH increased. For 2016, sensor failure resulted in no data for the spring freshet, however this data was captured in the 2017 dataset.

The 2017 dataset patterns were different than 2016 and the sites also differed from one another (Fig. 7.5). The fall pH anomalies related to freeze-up were not detected in 2017, but there was a very strong signal for E-1 during the spring freshet and pH increased dramatically with the associated freshwater pulse from the Sagavanirktok River.

There was a distinct temporal separation with the relationship between salinity and pH before and after freeze-up from both sites in 2016 (Fig. 7.2). Separations were seen in 2017 as well, but due to timing of the separation, it appears different events, other than freeze-up, caused the separation. DS11, the offshore site separated very soon after deployment, and this is likely driven by the reduction of river water into the system after late summer and this water shows a different pH and salinity relationship than under ice seawater. The inshore site, E-1, has the opposite pattern, the separation happens during the spring freshet. Although a number of processes can drive these water mass changes, the differences likely represent ocean water that is mixed with run-off from the Sagavanirktok River (lower salinity, higher pH vs. higher salinity, lower pH) and ocean water that is stable and static under the ice. Aragonite saturation levels were calculated in order to understand how these seasonal water chemistry variations affect benthic assemblages.

By calculating $\boldsymbol{\Omega}$ aragonite, salinity, pH, A_T and temperature are integrated and calcification process of biological organisms is better understood. Saturation level patterns for aragonite showed that for much of the year, the saturation levels were at equilibrium (=1), but during the spring freshet of 2018, the levels dropped to zero at the inshore site. A value below one causes dissolution of aragonite, and experimentally this was observed with the crustose coralline algae (CCA) species

found in the Boulder Patch, *Leptophytum foecundum* (section 2.3). Low **Ω** aragonite levels associated with the near shore site, likely drive crustose coralline algae distribution (see section 2.3) and cause the absence of this species at the near shore sites (see sections 1.2 and 1.3).

Other systems under saturated with respect to aragonite, CCA are also absent. Studies of CO_2 vents in the Mediterranean show a simplification, less canopy-forming algal species, and an increase in turf algae in areas of close proximity to the vents, where saturation levels are low (Kroeker et al., 2013). We see similar patterns in the Boulder Patch, in areas where CCA are not present, there was greater red algal biomass (Fig. 7.7), and the biomass was dominated by two species (Fig. 7.8). From this study, we see that the near shore site, that is under saturated in respect to aragonite, especially during spring break-up, is devoid of CCA and the benthic assemblage was distinct from the offshore site where CCA are present.

Further investigation is needed to understand the changes in invertebrate distributions, but there were different assemblages seen at each site. One striking pattern was the dominance of *Eucratea loricata* (bryozoan) at the in-shore site. This bryozoan, along with a few red algal species covered the rocks and cobbles at this site but was found in very low densities at the offshore site and only in areas where CCA were not present.

There are many factors that may cause a decrease in **Ω** aragonite and many of these factors naturally occur in the Arctic Ocean (cold temperatures, heterotrophy, freshwater input etc.; Mathis et al. 2015). In addition, these waters are susceptible to ocean acidification, a process caused by the anthropogenic increase in CO_2 in the atmosphere. These processes combined have the potential alter the benthic states that are now present in the Boulder Patch offshore sites to resemble the inshore sites without CCA and a less diverse benthic community. In addition, *Laminaria solidungula* densities are lower at the inshore sites (sections 1.2 and 1.3) and it is unclear if this deficiency is due to changes in the benthic structure (i.e., presence or absence of CCA) or if some other abiotic factor (see section 2.5). Independent of the cause, a benthic shift of species in the Boulder Patch would affect the biodiversity and productivity of the system and the myriad organisms these systems sustain.

8. Freshwater input effects on *Laminaria solidungula* microscopic stages (short report)

Arley F. Muth, Christina E. Bonsell and Kenneth H. Dunton

INTRODUCTION

Brown seaweeds of the order Laminariales (kelps) play important roles in the ecosystems they inhabit. *Laminaria solidungula*, the only Arctic endemic kelp, provides a food source and habitat for benthic communities along the north coast of Alaska. This kelp species is perennial and persists beneath the ice in polar night light conditions, providing the basis of the food chain when phytoplankton is unable to survive. In winter months, up to 50% of mysid body carbon was derived from *L. solidungula* detritus (Dunton and Schell 1987).

Kelps use a diplohaplontic life history strategy for reproduction. Macroscopic sporophytes release microscopic zoospores at a 50:50 male to female ratio. Zoospores settle onto the substrate, undergo gametogenesis and once gametophytes are formed, gametes are released. Male gametophytes produce spermatozoids that are released and fertilize eggs that protrude from the female gametophytes. Once fertilization occurs, a microscopic sporophyte is produced (Fig. 8.1). Often, microscopic stages are more vulnerable to changes in environmental conditions (Deysher and Dean 1986a, reviewed in Graham et al. 2007, Harley et al. 2012), which ultimately affects adult population persistence (Graham et al. 2007).

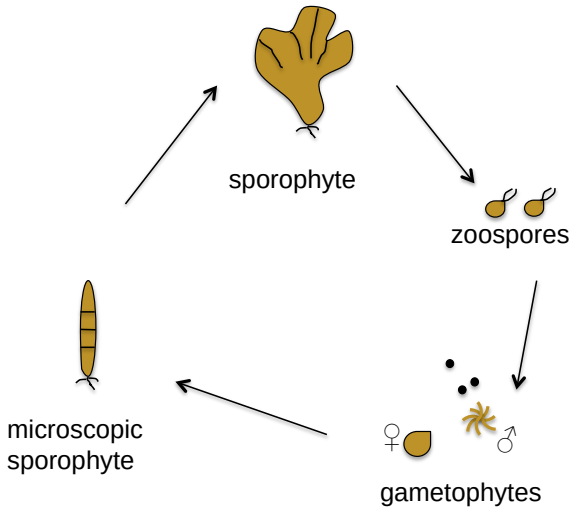

Figure 8.1. *Laminaria solidungula* (general kelp) life history. Macroscopic sporophytes (2n) release zoospores (1n) at a 50:50 sex ratio. Zoospores develop into male and female gametophytes, and the female egg is fertilized by the male spermatozoids, producing a microscopic sporophyte (2n).

Many abiotic factors affect reproductive success in kelps, such as temperature (Deysher and Dean 1986b, Matson and Edwards 2007), nutrients (Santelices and Ojeda 1984), light (Lüning and Dring 1979, Lüning 2018) and settlement densities of zoospores (Reed et al. 1991, Muth 2012). In the U.S. Arctic, salinity and light levels differ drastically among seasons (section 1.1), but interactive effects on *L. solidungula* are unknown.

The Stefansson Sound Boulder Patch is an area of rocky substrate composed of boulders and cobbles that creates an ideal habitat for kelp populations. Kelp densities within this area decrease with proximity to the Sagavanirktok River (see sections 1.2 and 1.3) and we were interested in exploration of potential mechanisms affecting kelp density and distributions within the Boulder Patch. Light levels and salinity levels are reduced at sites closer to the Sagavanirktok River (see section 1.1) due to river run-off and increased sedimentation. This experiment was designed to explore the effects of salinity and light separately and interactively on *L. solidungula* microscopic stages and sporophyte production.

METHODS

Reproductive *Laminaria solidungula* individuals were collected from Endicott Island, Alaska and shipped to the University of Texas Marine Science Institute. Samples were kept at 0°C in aerated filtered seawater. Reproductive sori were placed in between layers of damp paper towels and kept in darkness for 24 h. Then sori were placed in 10°C seawater to induce sporulation (Dec. 7th, 2017). After sporulation, 10 mL of the solution was placed in 50 x 10 mm Petri Dishes. The zoospore solution remained in the dishes for 1 week to allow for maximum settlement, the medium was then replaced with Gulf of Mexico seawater and RO water to attain salinity treatments of 10, 20 and 30, and Provasoli's Enriched Seawater (PES) to ensure all micro and macro nutrients were available. After settlement, dishes were divided into 3 light treatments within the salinity treatments (10, 20 and 40 μmol photons m^2 s^{-2}), creating nine salinity/light treatments and each treatment was replicated 5 times. Medium was changed weekly. Dishes were kept at 0°C in a 10:14 light:dark regime.

Dishes were monitored weekly for microscopic stage development. Initial settlement densities were quantified (Dec. 15th, 2017) to ensure all treatments initially had similar settlement. Gametophyte densities were quantified Jan. 26th, 2018 and finally sporophyte densities over one month (Feb. 28th, Mar. 16th and Mar. 27th), in order to track any delays in sporophyte production. Each dish was observed under 400x magnification for 10 fields of view.

Densities at each stage (settlement and gametophytes) were compared using 2-way ANOVAs among light and salinity levels. Sporophyte densities were compared using a repeated measures 2-way ANOVA (time, light, salinity, and light x salinity) to assess sporophyte densities over time. The interaction of light and salinity was not significant and was removed from the model. All statistics were run

using R Version 3.3.1.

RESULTS

Zoospore settlement densities were not significantly different among salinity and light treatments (2-way ANOVA, light vs. salinity $F_{3,41} = 0.3293$, p=0.80; Table 8.1, Fig. 8.2). Any differences in gametophyte or sporophyte densities were a result of environmental conditions after settlement. Gametophyte densities were significantly different among salinity treatments, however, there was no significant difference among light treatments or the salinity light interactions (2-way ANOVA, salinity $F_{3,41} = 21.67$, p<0.001).

Table 8.1. Treatments (salinity:10, 20, 30 and light: 10, 20, 40) and average densities for zoospores, gametophytes and sporophytes.

Salinity	Light (umol photons m-2 s-2)	zoospores (mm2) Dec. 15th, 2017	zoospore standard error	gametophytes (mm2) Jan. 26th, 2018	gametophyte standard error	sporophytes (mm2) Feb. 28th, 2018	sporophyte standard error	sporophytes (mm2) Mar. 16th, 2018	sporophyte standard error	sporophytes (mm2) Mar. 27th, 2018	sporophyte standard error
10	10	1.05	0.34	0.13	0.13	-	-	-	-	-	-
10	20	1.05	0.16	-	-	-	-	-	-	-	-
10	40	1.18	0.86	-	-	-	-	-	-	-	-
20	10	1.32	0.36	1.58	0.16	0.01	0.00	0.03	0.01	0.01	0.00
20	20	0.79	0.48	0.66	0.29	0.02	0.00	0.03	0.01	0.03	0.01
20	40	1.18	0.25	0.66	0.21	0.04	0.01	0.04	0.02	0.07	0.03
30	10	1.45	0.64	2.37	0.49	0.02	0.00	0.02	0.01	0.04	0.01
30	20	1.32	0.21	1.45	0.44	0.03	0.01	0.06	0.02	0.04	0.01
30	40	1.32	0.21	2.37	0.34	0.04	0.01	0.04	0.01	0.03	0.01

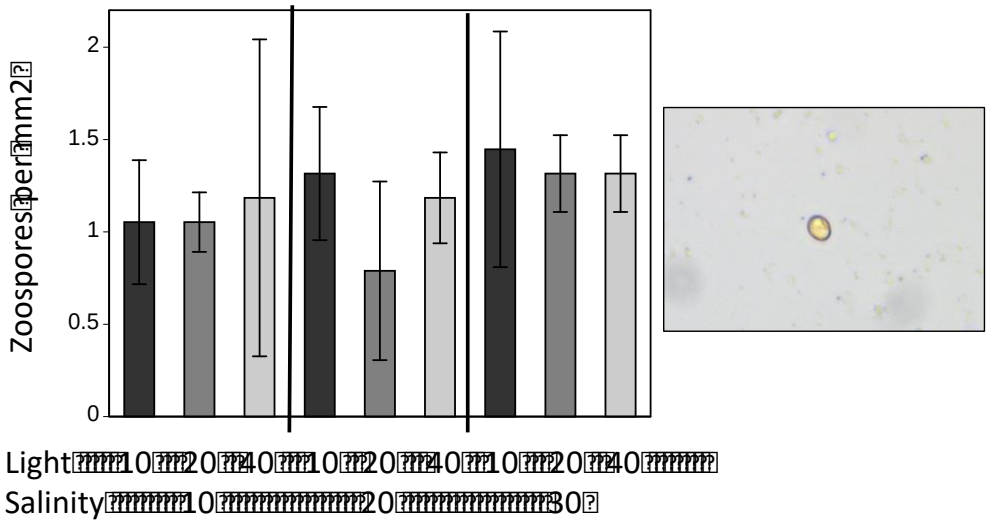

Figure 8.2. Zoospores per mm² after a 1-week settlement period. No significant difference among salinity or light treatments.

Gametophytes were the first stage to show an effect of salinity. The low salinity treatment (10) was significantly lower than the 20 and 30 treatments, however, light was not significant and the interaction between light and salinity was not significant either.

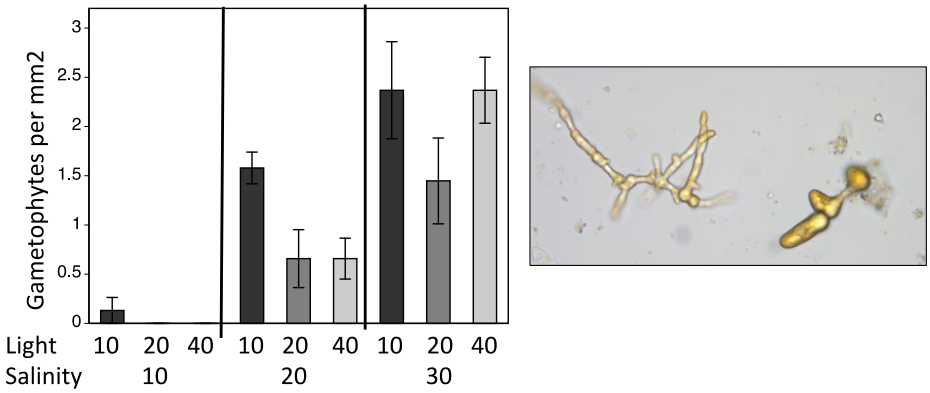

Figure 8.3. Gametophytes per mm^2. Salinity treatments (10 vs. 20 and 30) were significantly different. Light and salinity x light interaction were not significant.

Sporophytes densities were quantified over one month, but time was not significant (p=0.127). Sporophyte densities between 40 and 10 µmol photons m^{-2} s^{-1} light treatments were significantly different (Fig. 8.4, Table 8.1) and densities between the salinity of 10 treatment and the 20 and 30 were significantly different (repeated measures ANOVA: light p=0.01, salinity p<0.001).

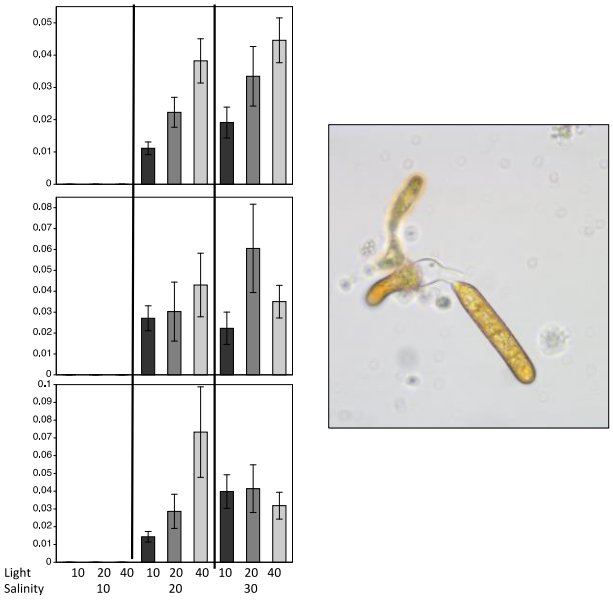

Figure 8.4. Sporophyte densities per mm^2 over 1 month. Top (Feb. 28th, 2018), center (March 16th, 2018) bottom (Mar. 27th, 2018). Densities were significantly lower in the 10 vs. 40 µmol photons m^2 s^{-1}. Sporophytes were not detected in the low salinity treatment (10), and densities were not significantly different between the 20 and 30 treatments.

DISCUSSION

Laminaria solidungula is a conspicuous kelp species that occurs on the north coast of Alaska and dominant seaweed in the Boulder Patch of Stefansson sound (see sections 1.2 and 1.3). Understanding population and distribution dynamics of this species is an integral, if not primary goal of our Boulder Patch monitoring program. Through this preliminary experiment, we were able highlight the effects variable salinity and light play on *L. solidungula* microscopic stages that are critical for adult population persistence.

Data from the Boulder Patch has shown that light and salinity values are lowest at sites in closer proximity to the Sagavanirktok River (E-1, see section 1.1). These sites also have lower kelp abundances (see section 1.2 and 1.3), even when standardized to less available substrate (i.e., rock cover). This data illustrates how light and salinity can affect successful kelp recruitment (sporophyte production), but that low salinity levels (10) prevent sporophytes from forming. The current experiment did introduce salinity treatments at the settlement stage, so although settlement was equal at the start of the experiment, salinity and light lowered gametophyte densities in certain treatments (Fig. 8.3, Table 8.1). A lack of mature gametophytes would also contribute to lower sporophyte densities.

Microscopic stages were cultured under optimal temperature and nutrient regimes; however, settlement densities were very close to one (Fig. 8.2; Reed et al. 1991). Lower settlement densities resulted in lower gametophyte and sporophyte densities but were high enough for fertilization to occur and sporophytes to form. Because settlement density did not differ among treatments from day one of the experiment, initial densities did not affect results.

In addition, *L. solidungula* microscopic stages develop at a much slower pace than most other kelps (Reed et al. 1991, Muth et al. 2019). Using *Macrocystis pyrifera* as a guide, settlement is counted after 24 h, germination after 48 h, gametophytes after 7 days and sporophytes within 2-5 weeks (Reed et al. 1991). However, *L. solidungula* was left to settle for one week in the dishes, germinated zoospores may take up to 3 weeks to observe, gametophytes in general were seen after 6 weeks and sporophytes after 10 weeks. *Laminaria solidungula* from the Canadian Arctic had similar developmental times, but in general produces reproductive material earlier and zoospore release is later than the populations of the Boulder Patch (Roleda 2016). This slower process may be due to the timing of zoospore release (January-March) and the timing of break-up and light availability (June-July). This delayed recruitment process subjects the sensitive microscopic stages to abiotic conditions for longer periods of time than most kelp species, but might also be an adaptation for commencing their macroscopic form under the ice.

Future studies will explore how each stage (settlement, gametophytes, and sporophytes) respond to variations in salinity. Pin pointing stages that are more

vulnerable to low salinity events will allow us to predict how earlier spring break-up events and increased periods of freshwater flow may affect future *L. solidungula* populations.

References

Adey, W. H., Lindstrom, S. C., Hommersand, M. H., & Müller, K. M. (2008). The biogeographic origin of Arctic endemic seaweeds: a thermogeographic view 1. *Journal of Phycology*, *44*(6), 1384–1394.

Airoldi, L. (2000). Effects of disturbance , life histories , and overgrowth on coexistence of algal crusts and turfs. *Ecology*, *81*(3), 798–814.

Alberto, F., Raimondi, P., & Reed, D. (2010). Habitat continuity and geographic distance predict population genetic differentiation in giant kelp. *Ecology*, *91*(1), 49–56.

Alkire, M. B., & Trefry, J. H. (2006). Transport of spring floodwater from rivers under ice to the Alaskan Beaufort Sea. *Journal of Geophysical Research: Oceans*, *111*(12), 1–12.

Amsler, C., Reed, D., & Neushul, M. (1992). The microclimate inhabited by macroalgal propagules. *British Phycological Journal*, 37–41.

Anthony, K. R. N., Ridd, P. V, Orpin, A. R., Larcombe, P., Lough, J., Connolly, S., & Anthony, D. (2004). Temporal variation of light availability in coastal benthic habitats: Effects of clouds, turbidity, and tides. *Limnology and Oceanography*, *49*(6), 2201–2211.

Asnaghi, V., Thrush, S. F., Hewitt, J. E., Mangialajo, L., Cattaneo-Vietti, R., & Chiantore, M. (2015). Colonisation processes and the role of coralline algae in rocky shore community dynamics. *Journal of Sea Research*, *95*, 132–138.

Aumack, C. F., Dunton, K. H., Burd, A. B., Funk, D. W., & Maffione, R. A. (2007). Linking light attenuation and suspended sediment loading to benthic productivity within an Arctic kelp-bed community 1. *Journal of Phycology*, *43*(5), 853–863.

Balloux, F., Lehmann, L., & De Meeûs, T. (2003). The population genetics of clonal and partially clonal diploids. *Genetics*, *164*(4), 1635–1644.

Barnes, D.K.A. (2002) Polarization of competition increases with latitude. *Proceedings of the Royal Society of London B* 269: 2061–2069.

Barnes, D.K.A., Kuklinski, P. (2004) Scale-dependent variation in competitive ability among encrusting Arctic species. *Marine Ecology Progress Series* 275: 21–32.

Barry, R. G., Moritz, R. E., & Rogers, J. C. (1979). The fast ice regimes of the Beaufort and Chukchi Sea coasts, Alaska. *Cold Regions Science and Technology*, *1*(2), 129–152.

Bartsch, I., Wiencke, C., Bischof, K., Buchholz, C.M., Buck, B.H., Eggert, A., Feuerpfeil, P., Hanelt, D., Jacobsen, S., Karez, R., Karsten, U. (2008). The genus *Laminaria* sensu lato: recent insights and developments. *European Journal of Phycology* 43(1): 1-86.

Bartsch, I., Paar, M., Fredriksen, S., Schwanitz, M., Daniel, C., Hop, H., & Wiencke, C. (2016). Changes in kelp forest biomass and depth distribution in Kongsfjorden, Svalbard, between 1996–1998 and 2012–2014 reflect Arctic warming. *Polar*

Biology, *39*(11), 2021–2036.

Bell, J. J., McGrath, E., Biggerstaff, A., Bates, T., Bennett, H., Marlow, J., & Shaffer, M. (2015). Sediment impacts on marine sponges. *Marine Pollution Bulletin*, *94*(1–2), 5–13.

Berge, J., Johnsen, G., Nilsen, F., Gulliksen, B., & Slagstad, D. (2005). Ocean temperature oscillations enable reappearance of blue mussels *Mytilus edulis* in Svalbard after a 1000 year absence. *Marine Ecology Progress Series*, *303*, 167–175.

Bertness, M. D., & Callaway, R. (1994). Positive interactions in communities. *Trends in Ecology & Evolution*, *9*(5), 27–29.

Beuchel, F., & Gulliksen, B. (2008). Temporal patterns of benthic community development in an Arctic fjord (Kongsfjorden, Svalbard): Results of a 24-year manipulation study. *Polar Biology*, *31*(8), 913–924.

Beuchel, F., Gulliksen, B., & Carroll, M. L. (2006). Long-term patterns of rocky bottom macrobenthic community structure in an Arctic fjord (Kongsfjorden, Svalbard) in relation to climate variability (1980–2003). *Journal of Marine Systems*, *63*(1–2), 35–48.

Borum, J., Pedersen, M., Krause-Jensen, D., Christensen, P., Nielsen, K. (2002) Biomass, photosynthesis and growth of *Laminaria saccharina* in a high-arctic fjord, NE Greenland. *Marine Biology* 141(1):11-19.

Billot, C., Engel, C. R. C., Rousvoal, S., Kloareg, B., & Valero, M. (2003). Current patterns, habitat discontinuities and population genetic structure: the case of the kelp *Laminaria digitata* in the English Channel. *Marine Ecology Progress Series*, *253*, 111–121.

Bluhm, B., Gebruk, A., & Gradinger, R. (2011). Arctic marine biodiversity: an update of species richness and examples of biodiversity change. *Oceanography*, *24*(3), 232–248.

Bolton, J. J. (2010). The biogeography of kelps (Laminariales, Phaeophyceae): a global analysis with new insights from recent advances in molecular phylogenetics. *Helgoland Marine Research*, *64*(4), 263–279.

Bonsell, C., & Dunton, K. H. (2018). Long-term patterns of benthic irradiance and kelp production in the central Beaufort sea reveal implications of warming for Arctic inner shelves. *Progress in Oceanography*, *162*(February), 160–170.

Bremner, J., Rogers, S., & Frid, C. (2003). Assessing functional diversity in marine benthic ecosystems: a comparison of approaches. *Marine Ecology Progress Series*, *254*, 11–25.

Brennan, G., Kregting, L., Beatty, G. E., Cole, C., Elsasser, B., Savidge, G., & Provan, J. (2014). Understanding macroalgal dispersal in a complex hydrodynamic environment: a combined population genetic and physical modelling approach. *Journal of The Royal Society Interface*, *11*(95), 20140197–20140197.

Breton, T. S., Nettleton, J. C., O'Connell, B., & Bertocci, M. (2018). Fine-scale population genetic structure of sugar kelp, *Saccharina latissima* (Laminariales, Phaeophyceae), in eastern Maine, USA. *Phycologia*, *57*(1), 32–40.

Bringloe, T. T., & Saunders, G. W. (2018). Mitochondrial DNA sequence data reveal

the origins of postglacial marine macroalgal flora in the Northwest Atlantic. *Marine Ecology Progress Series*, *589*, 45–58.

Brown, J. H. J. H., & Kodric-Brown, A. (1977). Turnover rates in insular biogeography: effect of immigration on extinction. *Ecology*, *58*(2), 445–449.

Bulleri, F., Bertocci, I., & Micheli, F. (2002). Interplay of encrusting coralline algae and sea urchins in maintaining alternative habitats. *Marine Ecology Progress Series*, *243*, 101–109.

Buschmann, a. H., Vasquez, J. a., Osorio, P., Reyes, E., Filun, L., Hernandez-Gonzalez, M. C., & Vega, A. (2004). The effect of water movement, temperature and salinity on abundance and reproductive patterns of Macrocystis spp. (Phaeophyta) at different latitudes in Chile. *Marine Biology*, *145*(5), 849–862.

Buschmann, A., Graham, M., & V√°squez, J. (2007). Global Ecology of the Giant Kelp Macrocystis, 39–88.

Cacabelos, E., Olabarria, C., Incera, M., Troncoso, J.S. (2010) Effects of habitat structure and tidal height on epifaunal assemblages associated with macroalgae. *Estuarine and Coastal Shelf Science* 89(1): 43-52.

Campana, G.L., Zacher, K., Fricke, A., Molis, M., Wulff, A., Quartino, M.L., Wiencke, C. (2009) Drivers of colonization and succession in polar benthic macro- and microalgal communities. *Botanica Marina* 52: 655–667.

Carmack, E., & Macdonald, R. (2002). Oceanography of the Canadian Shelf of the Beaufort Sea: a setting for marine life. *Arctic*, *55*(2002), 29–45.

Carney, L. T., Bohonak, A. J., Edwards, M. S., & Alberto, F. (2013). Genetic and experimental evidence for a mixed-age, mixed-origin bank of kelp microscopic stages in southern California. *Ecology*, *94*(9), 1955–1965.

Carney, L. T., & Edwards, M. S. (2010). Role of nutrient fluctuations and delayed development in gametophyte reproduction by *Macrocystis pyrifera* (Phaeophyceae) in Southern California. *Journal of Phycology*, *46*(5), 987–996.

Chan, F. T., MacIsaac, H. J., & Bailey, S. A. (2016). Survival of ship biofouling assemblages during and after voyages to the Canadian Arctic. *Marine Biology*, *163*(12), 1–14.

Chapman, A., & Lindley, J. (1980). Seasonal growth of *Laminaria solidungula* in the Canadian High Arctic in relation to irradiance and dissolved nutrient concentrations. *Marine Biology*, *5*, 1–5.

Christie H, Jørgensen NM, Norderhaug KM, Waage-Nielsen E (2003) Species distribution and habitat exploitation of fauna associated with kelp (*Laminaria hyperborea*) along the Norwegian Coast. J Mar Biol Assoc UK 83: 687–699.

Christie H, Jørgensen NM, Norderhaug KM (2007) Bushy or smooth, high or low; importance of habitat architecture and vertical position for distribution of fauna on kelp. J Sea Res 58(3): 198-208.

Clark, G. F., Stark, J. S., Johnston, E. L., Runcie, J. W., Goldsworthy, P. M., Raymond, B., & Riddle, M. J. (2013). Light-driven tipping points in polar ecosystems. *Global Change Biology*, *19*(12), 3749–3761.

Clarke KR, Gorley RN, Somerfield PJ, Warwick RM (2014). Change in marine communities: an approach to statistical analysis and interpretation. 3rd edition. PRIMER-E, Plymouth, UK.

Coleman, M. a., Roughan, M., Macdonald, H. S., Connell, S. D., Gillanders, B. M., Kelaher, B. P., & Steinberg, P. D. (2011). Variation in the strength of continental boundary currents determines continent-wide connectivity in kelp. *Journal of Ecology*, *99*(4), 1026–1032.

Conlan, K. E., Lenihan, H. S., Kvitek, R. G., & Oliver, J. S. (1998). Ice scour disturbance to benthic communities in the Canadian High Arctic. *Marine Ecology Progress Series*, *166*, 1–16.

Cowen, R. K., & Sponaugle, S. (2009). Larval Dispersal and Marine Population Connectivity. *Annual Review of Marine Science*, *1*(1), 443–466.

Coyer, J. a., Hoarau, G., Van Schaik, J., Luijckx, P., & Olsen, J. L. (2011). Trans-Pacific and trans-Arctic pathways of the intertidal macroalga *Fucus distichus* L. reveal multiple glacial refugia and colonizations from the North Pacific to the North Atlantic. *Journal of Biogeography*, *38*, 756–771.

Craig, P. C., & McCart, P. J. (1975). Classification of stream types in Beaufort Sea drainages between Prudhoe Bay , Alaska , and the Mackenzie Delta, N. W. T., Canada. *Arctic and Alpine Research*, *7*(2), 183–198.

Dethier, M. N., & Steneck, R. S. (2001). Growth and persistence of diverse intertidal crusts : survival of the slow in a fast-paced world, *223*, 89–100.

Devinny, J., & Volse, L. (1978). Effects of sediments on the development of Macrocystis pyrifera gametophytes. *Marine Biology*, *348*, 343–348.

Deysher, L. E., & Dean, T. A. (1986). In situ recruitment of sporophytes of the giant kelp, *Macrocystis pyrifera* (L.) C.A. Agardh: Effects of physical factors. *Journal of Experimental Marine Biology and Ecology*, *103*(1–3), 41–63.

Deysher, L. E., & Dean, T. A. (1986). Interactive effects of light and temperature on sporophyte production in the giant kelp *Macrocystis pyrifera*. *Marine Biology*, *93*, 17–20.

Diaz-Pulido, G., Anthony, K. R. N., Kline, D. I., Dove, S., & Hoegh-Guldberg, O. (2012). Interactions between ocean acidification and warming on the mortality and dissolution of coralline algae. *Journal of Phycology*, *48*(1), 32–39.

Dickinson, G. H., Ivanina, A. V., Matoo, O. B., Portner, H. O., Lannig, G., Bock, C., … Sokolova, I. M. (2012). Interactive effects of salinity and elevated CO2 levels on juvenile eastern oysters, *Crassostrea virginica*. *Journal of Experimental Biology*, *215*(1), 29–43.

Dunton, K. H. (1985). Growth of Dark-exposed *Laminaria saccharina* (L.) Lamour. and *Laminaria solidungula* J. Ag. (Laminariales : Phaeophyta) in the Alaskan Beaufort Sea. *Journal of Experimental Marine Biology and Ecology*, *94*(1–3), 181–189.

Dunton, K. H. (1990). Growth and production in Laminaria solidungula: relation to continuous underwater light levels in the Alaskan High Arctic. *Marine Biology*.

Dunton, K. H., & Jodwalis, C. M. (1988). Photosynthetic performance of *Laminaria solidungula* measured in situ in the Alaskan High Arctic. *Marine Biology*, *98*(2),

277–285.

Dunton, K. H., Reimnitz, E. R. K., & Schonberg, S. (1982). An Arctic Kelp Community in the Alaskan Beaufort Sea. *Arctic*, *35*(4), 465–484.

Dunton, K. H., Reimnitz, E., Schonberg, S., Dunton, K. H., Reimnitz, E. R. K., & Schonberg, S. (1982). An Arctic Kelp Community in the Alaskan Beaufort Sea. *35*(4), 465–484.

Dunton, K. H., & Schell, D. M. (1987). Dependence of consumers on macroalgal (*Laminaria solidungula*) carbon in an arctic kelp community: δ13C evidence. *Marine Biology*, *93*(4), 615–625.

Dunton, K. H., Schonberg, S. V., & Funk, D. W. (2009). Interannual and spatial variability in light attenuation: evidence from three decades of growth in the arctic kelp, *Laminaria solidungula*. In *Smithsonian at the Poles/Contributions to*

Dunton, K. H., Schonberg, S. V, Martin, L. R., & Mueller, G. S. (1992). Seasonal and annual variations in the underwater light environment of an Arctic kelp community. *Diving for Science*.

Dunton, K. H., Weingartner, T., & Carmack, E. C. (2006). The nearshore western Beaufort Sea ecosystem: Circulation and importance of terrestrial carbon in arctic coastal food webs. *Progress in Oceanography*, *71*(2–4), 362–378. https://doi.org/10.1016/j.pocean.2006.09.011

Dunton, K., & Schell, D. (1986). Seasonal carbon budget and growth of Laminaria solidungula in the Alaskan High Arctic. *Marine Ecology Progress Series*, *31*(1977), 57–66. https://doi.org/10.3354/meps031057

Durrant, H. M. S., Barrett, N. S., Edgar, G. J., Coleman, M. A., & Burridge, C. P. (2018). Seascape habitat patchiness and hydrodynamics explain genetic structuring of kelp populations. *Marine Ecology Progress Series*, *587*, 81–92.

Erting, L., Daugbjerg, N., & Pedersen, P. M. (2004). Nucleotide diversity within and between four species of Laminaria (Phaeophyceae) analysed using partial LSU and ITS rDNA sequences and AFLP. *European Journal of Phycology*, *39*(3), 243–256.

Filbee-Dexter, K., & Wernberg, T. (2018). Rise of Turfs: A new battlefront for globally declining kelp forests. *BioScience*, *68*(2), 64–76.

Filbee-Dexter, K., Wernberg, T., Fredriksen, S., Norderhaug, K. M., & Pedersen, M. F. (2019). Arctic kelp forests: Diversity, resilience and future. *Global and Planetary Change*, *172*, 1–14.

Fredersdorf, J., Müller, R., Becker, S., Wiencke, C., & Bischof, K. (2009). Interactive effects of radiation, temperature and salinity on different life history stages of the Arctic kelp Alaria esculenta (Phaeophyceae). *Oecologia*, *160*(3), 483–492.

Frey, K. E., Moore, G. W. K., Cooper, L. W., & Grebmeier, J. M. (2015). Divergent patterns of recent sea ice cover across the Bering, Chukchi, and Beaufort seas of the Pacific Arctic Region. *Progress in Oceanography*, *136*, 32–49.

Fricke, A., Molis, M., Wiencke, C., Valdivia, N., & Chapman, A. S. (2008). Natural succession of macroalgal-dominated epibenthic assemblages at different water depths and after transplantation from deep to shallow water on Spitsbergen. *Polar Biology*, *31*(10), 1191–1203.

Fritz, M., Vonk, J. E., & Lantuit, H. (2017). Collapsing Arctic coastlines. *Nature Clim. Change*, *7*(1), 6–7.

Gangstø, R., Gehlen, M., Schneider, B., Bopp, L., Aumont, O., & Joos, F. (2008). Modeling the marine aragonite cycle: Changes under rising carbon dioxide and its role in shallow water CaCO3dissolution. *Biogeosciences*, *5*(4), 1057–1072.

Gaylord, B., Nickols, K. J., & Jurgens, L. (2012). Roles of transport and mixing processes in kelp forest ecology. *Journal of Experimental Biology*, *215*(6), 997–1007.

Gaylord, B., Reed, D. C., Raimondi, P. T., & Washburn, L. (2006). Macroalgal spore dispersal in coastal environments: Mechanistic insights revealed by theory and experiment. *Ecological Monographs*, *76*(4), 481–502.

Gibbs, A. E., & Richmond, B. M. (2015). *National assessment of shoreline change—Historical shoreline change along the north coast of Alaska, U.S.–Canadian border to Icy Cape: U.S. Geological Survey Open-File Report 2015–1048,*.

Glud, R. N., Woelfel, J., Karsten, U., Ku, ¨hl, M., & Rysgaard, S. (2009). Benthic microalgal production in the Arctic: Applied methods and status of the current database. *Botanica Marina*, *52*(6), 559–571.

Gordeev, V. V. (2006). Fluvial sediment flux to the Arctic Ocean. *Geomorphology*, *80*(1–2), 94–104.

Gordeev, V. V., Martin, J. M., Sidorov, I. S., & Sidorova, M. V. (1996). A reassessment of the Eurasian river input of water, sediment, major elements, and nutrients to the Arctic Ocean. *American Journal of Science*, *296*, 664–691.

Grebmeier, J. M. (2012). Shifting Patterns of Life in the Pacific Arctic and Sub-Arctic Seas. *Annual Review of Marine Science*, *4*(1), 63–78.

Grebmeier, J. M., Overland, J. E., Moore, S. E., Farley, E. V, Carmack, E. C., Cooper, L. W., … Mcnutt, S. L. (2006). A major ecosystem shift in the Northern Bering Sea. *Science*, *311*(March), 1461–1465.

Gunther, F., Overduin, P. P., Yakshina, I. A., Opel, T., Baranskaya, A. V., & Grigoriev, M. N. (2015). Observing Muostakh disappear: permafrost thaw subsidence and erosion of a ground-ice-rich island in response to arctic summer warming and sea ice reduction. *Cryosphere*, *9*, 151–178.

Hall-Spencer, J. M., Rodolfo-Metalpa, R., Martin, S., Ransome, E., Fine, M., Turner, S. M., … Buia, M. C. (2008). Volcanic carbon dioxide vents show ecosystem effects of ocean acidification. *Nature*, *454*(7200), 96–99. https://doi.org/10.1038/nature07051

Hardy, S. M., Carr, C. M., Hardman, M., Steinke, D., Corstorphine, E., & Mah, C. (2010). Biodiversity and phylogeography of Arctic marine fauna: insights from molecular tools. *Marine Biodiversity*, *41*(1), 195–210.

Harley, C. D. G., Anderson, K. M., Demes, K. W., Jorve, J. P., Kordas, R. L., Coyle, T. A., & Graham, M. H. (2012). EFfects Of Climate Change On Global Seaweed Communities. *Journal of Phycology*, *48*(5), 1064–1078.

Harris, C. M., McTigue, N. D., McClelland, J. W., & Dunton, K. H. (2018). Do high Arctic coastal food webs rely on a terrestrial carbon subsidy? *Food Webs*, *15*.

Henley, W., & Dunton, K. (1995). A seasonal comparison of carbon, nitrogen, and pigment content in Laminaria solidungula and L. saccharina (Phaeophyta) in the Alaskan Arctic. *Journal of Phycology*, *331*, 325–331.

Hill, P. R., & Nadeau, O. C. (1989). Storm-dominated Sedimentation on the Inner Shelf of the Canadian Beaufort Sea. *Journal of Sedimentary Petrology*, *59*(3), 455–468.

Holmes, R. M., McClelland, J. W., Peterson, B. J., Shiklomanov, I. A., Shiklomanov, A. I., Zhulidov, A. V, … Bobrovitskaya, N. N. (2002). A circumpolar perspective on fluvial sediment flux to the Arctic ocean. *Global Biogeochemical Cycles*, *16*(4), 14–45.

Holmes, R. M., McClelland, J. W., Raymond, P. A., Frazer, B. B., Peterson, B. J., & Stieglitz, M. (2008). Lability of DOC transported by Alaskan rivers to the Arctic Ocean. *Geophysical Research Letters*, *35*(3), 3–7.

Jackson, C., Salomaki, E. D., Lane, C. E., & Saunders, G. W. (2016). Kelp transcriptomes provide robust support for interfamilial relationships and revision of the little know Arthrothamnaceae (Laminariales). *Journal of Phycology*, 1–6.

Ji, R., Jin, M., & Varpe, Ø. (2013). Sea ice phenology and timing of primary production pulses in the Arctic Ocean. *Global Change Biology*, *19*(3), 734–741.

Jiang, L., Feely, R. A., Carter, B. R., Greeley, D. J., Gledhill, D. K., & Arzayus, K. M. (2015). Global Biogeochemical Cycles saturation state in the global oceans. *Global Biogeochemical Cycles*, *29*(10), 1656–1673.

Johansson, M. L., Raimondi, P. T., Reed, D. C., Coelho, N. C., Serrão, E. a, & Alberto, F. a. (2013). Looking into the black box: simulating the role of self-fertilization and mortality in the genetic structure of Macrocystis pyrifera. *Molecular Ecology*, *22*(19), 4842–4854.

Johnson, M., & Eicken, H. (2016). Estimating Arctic sea-ice freeze-up and break-up from the satellite record: A comparison of different approaches in the Chukchi and Beaufort Seas. *Elementa: Science of the Anthropocene*, *4*(1), 000124.

Jones, B. M., Arp, C. D., Jorgenson, M. T., Hinkel, K. M., Schmutz, J. A., & Flint, P. L. (2009). Increase in the rate and uniformity of coastline erosion in Arctic Alaska. *Geophysical Research Letters*, *36*(3), 1–5.

Jones, B. M., Hinkel, K. M., Arp, C. D., & Eisner, W. R. (2008). Modern erosion rates and loss of coastal features and sites, Beaufort Sea coastline, Alaska. *Arctic*, *61*(4), 361–372.

Kahru, M., Brotas, V., Manzano-Sarabia, M., & Mitchell, B. G. (2011). Are phytoplankton blooms occurring earlier in the Arctic? *Global Change Biology*, *17*(4), 1733–1739.

Karsten, U. (2007). Research note: Salinity tolerance of Arctic kelps from Spitsbergen. *Phycological Research*, *55*(4), 257–262.

Karsten, U., Bischof, K., & Wiencke, C. (2001). Photosynthetic performance of arctic macroalgae after transplantation from deep to shallow waters. *Oecologia*, *127*(1), 11–20.

Kasper, J. L., & Weingartner, T. J. (2015). The Spreading of a Buoyant Plume Beneath

a Landfast Ice Cover. *Journal of Physical Oceanography*, *45*(Reimnitz 2002), 478–494.

Kempema, E. W., Reimnitz, E., & Barnes, P. W. (1989). Sea Ice Sediment Entrainment and Rafting in the Arctic. *Journal of Sedimentary Petrology*, *59*(2), 308–317.

King, R. J., & Schramm, W. (1976). Photosynthetic Rates of Benthic Marine Algae in Relation to Light Intensity and Seasonal Variations. *Marine Biology*, *37*(3), 215–222.

King, R. J., & Schramm, W. (1982). Calcification in the Maerl Coralline Alga Phymatolithon-Calcareum - Effects of Salinity and Temperature. *Marine Biology*, *70*(2), 197–204.

Kinlan, B., & Gaines, S. (2003). Propagule dispersal in marine and terrestrial environments: a community perspective. *Ecology*, *84*(8), 2007–2020.

Kitching, J. A., Macan, T. T., & Gilson, H. C. (1934). Studies in Sublittoral Ecology. I. A Submarine Gully in Wembury Bay, South Devon. *Journal of the Marine Biological Association of the United Kingdom*, *19*(2), 677–705.

Konar, B. (2013). Lack of recovery from disturbance in high-arctic boulder communities. *Polar Biology*, *36*(8), 1205–1214.

Konar, B. (2007) Recolonization of a high latitude hard-bottom nearshore community. *Polar Bio*logy 30(5): 663-667.

Konar, B., & Iken, K. (2005). Competitive dominance among sessile marine organisms in a high Arctic boulder community. *Polar Biology*, *29*(1), 61–64.

Kortsch, S., Primicerio, R., Beuchel, F., Renaud, P. E., Rodrigues, J., Lønne, O. J., & Gulliksen, B. (2012). Climate-driven regime shifts in Arctic marine benthos. *Proceedings of the National Academy of Sciences of the United States of America*, *109*(35), 14052–14057.

Krause-Jensen, D., & Duarte, C. M. (2014). Expansion of vegetated coastal ecosystems in the future Arctic. *Frontiers in Marine Science*, *1*(December), 1–10.

Krause-Jensen, D., Marbà, N., Olesen, B., Sejr, M. K., Christensen, P. B., Rodrigues, J., … Rysgaard, S. (2012). Seasonal sea ice cover as principal driver of spatial and temporal variation in depth extension and annual production of kelp in Greenland. *Global Change Biology*, *18*(10), 2981–2994.

Krause-Jensen, D., Marbà, N., Sanz-Martin, M., Hendriks, I. E., Thyrring, J., Carstensen, J., … Duarte, C. M. (2016). Long photoperiods sustain high pH in Arctic kelp forests. *Science Advances*, *2*(December), e1501938.

Kroeker, K. J., Gambi, M. C., & Micheli, F. (2013). Community dynamics and ecosystem simplification in a high-CO2 ocean. *Proceedings of the National Academy of Sciences of the United States of America*, *110*(31), 12721–12726.

Kroeker, K. J., Micheli, F., & Gambi, M. C. (2012). Ocean acidification causes ecosystem shifts via altered competitive interactions. *Nature Climate Change*, *2*(10), 1–4.

Krumhansl, K. A., Okamoto, D. K., Rassweiler, A., Novak, M., Bolton, J. J., Cavanaugh, K. C., … Conceptualized Research, J. E. K. B. (n.d.). Global patterns of kelp forest change over the past half-century, 1–6.

Kuklinski, P., Barnes, D.K. (2008) Structure of intertidal and subtidal assemblages in Arctic vs temperate boulder shores. *Polish Polar Research* 29(3): 203-218.

Kuklinski, P., Gulliksen, B., Lønne, O.J., Weslawski, J.M. (2006) Substratum as a structuring influence on assemblages of Arctic bryozoans. *Polar Biology* 29(8): 652-661.

Kuklinski, P. (2009). Ecology of stone-encrusting organisms in the Greenland Sea-a review. *Polar Research*, *28*(2), 222–237.

Kuklinski, P., Berge, J., McFadden, L., Dmoch, K., Zajaczkowski, M., Nygård, H., … Tatarek, A. (2013). Seasonality of occurrence and recruitment of Arctic marine benthic invertebrate larvae in relation to environmental variables. *Polar Biology*, *36*(4), 549–560.

Lane, C. E., Mayes, C., Druehl, L. D., & Saunders, G. W. (2006). A multi-gene molecular investigation of the kelp (Laminariales, Phaeophyceae) supports substantial taxonomic re-organization. *Journal of Phycology*, *42*(2), 493–512.

Lantuit, H., Overduin, P. P., Couture, N., Wetterich, S., Aré, F., Atkinson, D., … Vasiliev, A. (2012). The Arctic Coastal Dynamics Database: A New Classification Scheme and Statistics on Arctic Permafrost Coastlines. *Estuaries and Coasts*, *35*(2), 383–400.

Legendre, P., & Anderson, M. J. (1999). Distance-Based Redundancy Analysis: Testing Multispecies Responses in Multifactorial Ecological Experiments. *Ecological Monographs*, *69*(1), 1.

Leibold, M. a., Holyoak, M., Mouquet, N., Amarasekare, P., Chase, J. M., Hoopes, M. F., … Gonzalez, a. (2004). The metacommunity concept: a framework for multi-scale community ecology. *Ecology Letters*, *7*(7), 601–613.

Lind, A. C., & Konar, B. (2017). Effects of abiotic stressors on kelp early life-history stages. *Algae*, *32*(3), 223–233.

Lippert, H., Iken, K., Rachor, E., Wiencke, C. (2001) Macrofauna associated with macroalgae in the Kongsfjord (Spitsbergen). *Polar Biol*ogy 24(7): 512-522.

Lüning, K. (2018). Critical levels of light and temperature regulating the gametogenesis of three *Laminaria* species (Phaeophyceae)1. *Journal of Phycology*, *16*(1), 1–15.

Lüning, K., & Dring, M. J. (1979). Continuous underwater light measurement near Helgoland (North Sea) and its significance for characteristic light limits in the sublittoral region. *Helgolander Wiss. Meeresunters*, *32*, 403–424.

Lüning, K. (1984) Temperature tolerance and biogeography of seaweeds: the marine algal flora of Helgoland (North Sea) as an example. *Helgoland Marine Research* 38(2): 305-317.

Macdonald, R. W., & Yu, Y. (2006). The Mackenzie Estuary of the Arctic ocean. *Handbook of Environmental Chemistry, Volume 5: Water Pollution*, *5*(PART H), 91–120.

Mahoney, A. R., Eicken, H., Gaylord, A. G., & Gens, R. (2014). Landfast sea ice extent in the Chukchi and Beaufort Seas: The annual cycle and decadal variability. *Cold Regions Science and Technology*, *103*, 41–56.

Manson, G. K., & Solomon, S. M. (2007). Past and future forcing of Beaufort Sea coastal change. *Atmosphere-Ocean*, *45*(2), 107–122.

Markus, T., Stroeve, J. C., & Miller, J. (2009). Recent changes in Arctic sea ice melt onset, freezeup, and melt season length. *Journal of Geophysical Research: Oceans*, *114*(12), 1–14.

Martin, L., & Gallaway, B. (1994). The effects of the Endicott Development Project on the Boulder Patch, an arctic kelp community in Stefansson Sound, Alaska. *Arctic*, *47*(1), 54–64.

Mathis, J., Cross, J., Evans, W., & Doney, S. (2015). Ocean Acidification in the Surface Waters of the Pacific-Arctic Boundary Regions. *Oceanography*, *25*(2), 122–135.

Mathis, J. T., Cooley, S. R., Lucey, N., Colt, S., Ekstrom, J., Hurst, T., … Feely, R. A. (2015). Ocean acidification risk assessment for Alaska's fishery sector. *Progress in Oceanography*, *136*, 71–91.

Matson, P. G., & Edwards, M. S. (2007). Effects of ocean temperature on the southern range limits of two understory kelps, Pterygophora californica and *Eisenia arborea*, at multiple life-stages. *Marine Biology*, *151*(5), 1941–1949.

Matthews, J. B. (1981a). Observations of surface and bottom currents in the Beaufort Sea near Prudhoe Bay, Alaska. *Journal of Geophyisical Research*, *86*(C7), 6653–6660.

Matthews, J. B. (1981b). Observations of under-ice circulation in a shallow lagoon in the Alaskan Beaufort Sea. *Ocean Management*, *6*(2–3), 223–234.

McClelland, J. W., Déry, S. J., Peterson, B. J., Holmes, R. M., & Wood, E. F. (2006). A pan-arctic evaluation of changes in river discharge during the latter half of the 20th century. *Geophysical Research Letters*, *33*(6), 2–5.

Mcclelland, J. W., Holmes, R. M., & Dunton, K. H. (2012). The Arctic Ocean Estuary, 353–368.

McClelland, J. W., Townsend-Small, A., Holmes, R. M., Pan, F., Stieglitz, M., Khosh, M., & Peterson, B. J. (2014). River export of nutrients and organic matter from the North Slope of Alaska to the Beaufort Sea. *Water Resources Research*, *50*(2),

Mccoy, S. J. (2013). Morphology of the crustose coralline alga *Pseudolithophyllum muricatum* (Corallinales, Rhodophyta) responds to 30 years of ocean acidification in the Northeast Pacific. *Journal of Phycology*, *49*(5), 830–837.

Mccoy, S. J., & Kamenos, N. A. (2015). Coralline algae (Rhodophyta) in a changing world: Integrating ecological, physiological, and geochemical responses to global change. *Journal of Phycology*, *51*(1), 6–24.

McDevit, D. C., & Saunders, G. W. (2009). On the utility of DNA barcoding for species differentiation among brown macroalgae (Phaeophyceae) including a novel extraction protocol. *Phycological Research*, *57*(2), 131–141.

McDevit, D., & Saunders, G. (2010). A DNA barcode examination of the Laminariaceae (Phaeophyceae) in Canada reveals novel biogeographical and evolutionary insights. *Phycologia*, *49*(May), 235–248.

McMeans, B. C., McCann, K. S., Humphries, M., Rooney, N., & Fisk, A. T. (2015). Food web structure in temporally-forced ecosystems. *Trends in Ecology and*

Evolution, *30*(11), 662–672.

McPhee, M. G., Proshutinsky, A., Morison, J. H., Steele, M., & Alkire, M. B. (2009). Rapid change in freshwater content of the Arctic Ocean. *Geophysical Research Letters*, *36*(10), 1–6.

Meirmans, P. G., & Van Tienderen, P. H. (2004). GENOTYPE and GENODIVE: Two programs for the analysis of genetic diversity of asexual organisms. *Molecular Ecology Notes*, *4*(4), 792–794.

Meyer, K. S., Sweetman, A. K., Kuklinski, P., Leopold, P., Vogedes, D., Griffiths, C., … Renaud, P. E. (2017). Recruitment of benthic invertebrates in high Arctic fjords: relation to temperature, depth, and season. *Limnology and Oceanography*, *in press*(Diamond 1975).

Michel, C., Bluhm, B., Gallucci, V., Gaston, a. J., Gordillo, F. J. L., Gradinger, R., … Nielsen, T. G. (2012). Biodiversity of Arctic marine ecosystems and responses to climate change. *Biodiversity*, *13*(3–4), 200–214.

Morison, J., Kwok, R., Peralta-Ferriz, C., Alkire, M., Rigor, I., Andersen, R., & Steele, M. (2012). Changing Arctic Ocean freshwater pathways. *Nature*, *481*(7379), 66–70.

Müller, R., Laepple, T., Bartsch, I., & Wiencke, C. (2009). Impact of oceanic warming on the distribution of seaweeds in polar and cold-temperate waters. *Botanica Marina*, *52*(6), 617–638.

Muth, A. F. (2012). Effects of zoospore aggregation and substrate rugosity on kelp recruitment success. *Journal of Phycology*, *48*(6), 1374–1379.

Muth, A. F., Graham, M. H., Lane, C. E., & Harley, C. D. G. (2019). Recruitment tolerance to increased temperature present across multiple kelp clades. *Ecology*, *100*(3), e02594.

Neiva, J., Paulino, C., Nielsen, M. M., Krause-Jensen, D., Saunders, G. W., Assis, J., … Serraõ, E. A. (2018). Glacial vicariance drives phylogeographic diversification in the amphi-boreal kelp *Saccharina latissima*. *Scientific Reports*, *8*(1), 1–12.

Norton, T. (1992). Dispersal by macroalgae. *British Phycological Journal*, *27*(3), 293–301. https://doi.org/10.1080/00071619200650271

O'Brien, M. C., Macdonald, R. W., Melling, H., & Iseki, K. (2006). Particle fluxes and geochemistry on the Canadian Beaufort Shelf: Implications for sediment transport and deposition. *Continental Shelf Research*, *26*(1), 41–81.

Overeem, I., Anderson, R. S., Wobus, C. W., Clow, G. D., Urban, F. E., & Matell, N. (2011). Sea ice loss enhances wave action at the Arctic coast. *Geophysical Research Letters*, *38*(17), 1–6.

Parkinson, C. L. (2014). Spatially mapped reductions in the length of the Arctic sea ice season. *Geophysical Research Letters*, *41*(12), 4316–4322.

Pequegnat, W. E. (1964). The epifauna of a California siltstone reef. *Ecology*, *45*(2), 272–283.

Post, E., Bhatt, U. S., Bitz, C. M., Brodie, J. F., Fulton, T. L., Hebblewhite, M., … Walker, D. a. (2013). Ecological consequences of sea-ice decline. *Science (New York, N.Y.)*, *341*(6145), 519–524.

Raimondi, P. T. P. T., Reed, D. C. C., Gaylord, B., & Washburn, L. (2004). Effects of self-

fertilization in the giant kelp, Macrocystis pyrifera. *Ecology*, *85*(12), 3267–3276.

Reed, D., Amsler, C., & Ebeling, A. (1992). Dispersal in kelps: factors affecting spore swimming and competency. *Ecology*, *73*(5), 1577–1585.

Reed, D. C., Neushul, M., & Ebeling, A. W. (1991). Role of settlement density on gametophyte growth and reproduction in the kelps *Pterygophora californica* and *Macrocystis pyrifera* (Phaeophyceae). *Journal of Phycology*.

Reid, P. C., Johns, D. G., Edwards, M., Starr, M., Poulin, M., & Snoeijs, P. (2007). A biological consequence of reducing Arctic ice cover: arrival of the Pacific diatom *Neodenticula seminae* in the North Atlantic for the first time in 800 000 years. *Global Change Biology*, *13*(9), 1910–1921.

Reimnitz, E. (2000). Interactions of river discharge with sea ice in proximity of arctic deltas: A review. *Polarforschung*, *70*(1–2), 123–134.

Reimnitz, E., Graves, S. M., & Barnes, P. W. (1988). *Beaufort Sea coastal erosion, shoreline evolution, and sediment flux. US Department of the Interior, Geological Survey.*

Rember, R. D., & Trefry, J. H. (2004). Increased concentrations of dissolved trace metals and organic carbon during snowmelt in rivers of the Alaskan Arctic. *Geochimica et Cosmochimica Acta*, *68*(3), 477–489.

Renaud, P. E., Løkken, T. S., Jørgensen, L. L., Berge, J., & Johnson, B. J. (2015). Macroalgal detritus and food-web subsidies along an Arctic fjord depth-gradient. *Frontiers in Marine Science*, *2*(June), 1–15.

Rigby, P.R., Iken, K., Shirayama, Y. (2007) Sampling Biodiversity in Coastal Communities: NaGISA Protocols for Seagrass and Macroalgal Habitats. Kyoto University Press, Japan.

Robuchon, M., Le Gall, L., Mauger, S., & Valero, M. (2014). Contrasting genetic diversity patterns in two sister kelp species co-distributed along the coast of Brittany, France. *Molecular Ecology*, *23*(11), 2669–2685.

Roleda, M. Y. (2016). Stress physiology and reproductive phenology of Arctic endemic kelp Laminaria solidungula J. Agardh. *Polar Biology*, *39*(11), 1967–1977.

Rothman, M. D., Mattio, L., Anderson, R. J., & Bolton, J. J. (2017). A phylogeographic investigation of the kelp genus *Laminaria* (Laminariales, Phaeophyceae), with emphasis on the South Atlantic Ocean. *Journal of Phycology*, *53*(4), 778–789.

Rousseau, F., de-Reviers, B., Leclerc, M. C., Asensi, A., & Delepine, R. (2000). Adenocystaceae fam. nov. (Phaeophyceae) based on morphological and molecular evidence. *European Journal of Phycology*, *35*, 35–43.

Rousseau, F., & De Reviers, B. (1999). Phylogenetic relationships within the fucales (phaeophyceae) based on combined partial ssu + lsu rdna sequence data. *European Journal of Phycology*, *34*(1), 53–64.

Sakai, A. K., Allendorf, F. W., Holt, J. S., Lodge, D. M., Molofsky, J., With, K. A., … Weller, S. G. (2001). The Population Biology of Invasive Species. *Annual Review of Ecology and Systematics*, *32*(2001), 305–332.

Santelices, B., & Ojeda, F. P. (1984). *Lessonia nigrescens*, *19*(1973), 73–82.

Saunders, G. W. (2014). Long distance kelp rafting impacts seaweed biogeography in the Northeast Pacific: the kelp conveyor hypothesis. *Journal of Phycology*, *50*(6), 968–974.

Scheschonk, L., Becker, S., Hehemann, J.H., Diehl, N., Karsten, U., Bischof, K. (2019) Arctic kelp eco-physiology during the polar night in the face of global warming: a crucial role for laminarin. *Marine Ecology Progress Series* 611: 59-74.

Schoenrock, K. M., Bacquet, M., Pearce, D., Rea, B. R., Schofield, J. E., Lea, J., … Kamenos, N. (2018). Influences of salinity on the physiology and distribution of the Arctic coralline algae, *Lithothamnion glaciale* (Corallinales, Rhodophyta). *Journal of Phycology*, *702*, 690–702.

Schoschina, E.V. (1996) Seasonal and age dynamics of growth and reproduction of *Phycodrys rubens* (Rhodophyta) in the Barents and White Seas. *Aquatic Botany* 55(1): 13-30.

Scholin, C. A., Herzog, M., Sogin, M., & Anderson, D. M. (1994). Identification of group - and strain - specific genetic markersfor globally distributed *Alexandrium* (Dinophyceae) II. Sequenceanalysis of a fragment of the LSU rRNA gene. *J. Phycol.*, *30*, 999–1011.

Sebens, K. P. (1984). Water flow and coral colony size: Interhabitat comparisons of the octocoral Alcyonium siderium. *Proceedings of the National Academy of Sciences*, *81*(17), 5473–5477.

Sellmann, P. V., Delaney, A. J., Chamberlain, E. J., & Dunton, K. H. (1992). Seafloor temperature and conductivity data from Stefansson Sound, Alaska. *Cold Regions Science and Technology*, *20*(3), 271–288.

Serreze, M. C., & Stroeve, J. C. (2015). Arctic sea ice trends, variability and implications for seasonal ice forecasting. *Philosophical Transactions of the Royal Society A: Mathematical, Physical and Engineering Sciences*, *373*(2045), 20140159.

Smith, L. C., & Stephenson, S. R. (2013). New Trans-Arctic shipping routes navigable by midcentury. *Proceedings of the National Academy of Sciences of the United States of America*, *110*(13), E1191-5.

Sonnenberg, R., Nolte, A., & Tautz, D. (2007). An evaluation of LSU rDNA D1-D2 sequences for their use in species identification. *Frontiers in Zoology*, *4*, 1–12.

Spurkland, T., & Iken, K. (2011). Kelp Bed Dynamics in Estuarine Environments in Subarctic Alaska. *Journal of Coastal Research*, *275*, 133–143.

Stam, W. T., Bot, P. V. M., Boele-Bos, S. A., van Rooij, J. M., & van den Hoek, C. (1988). Single-copy DNA-DNA hybridizations among five species of *Laminaria* (Phaeophyceae): Phylogenetic and biogeographic implications. *Helgoländer Meeresuntersuchungen*, *42*(2), 251–267.

Steneck, R. (1986). The ecology of coralline algal crusts: Convergent patterns and adaptative strategies. *Annual Review of Ecology and Systematics*, *17*(1), 273–303.

Steneck, R.S., Graham, M.H., Bourque, B.J., Corbett, D., Erlandson, J.M., et al. (2002) Kelp forest ecosystems: biodiversity, stability, resilience and future. *Environmental Conservation* 29: 436–459.

Stoeck, T., Przybos, E., & Dunthorn, M. (2014). The D1-D2 region of the large subunit

ribosomal DNA as barcode for ciliates. *Molecular Ecology Resources*, *14*(3), 458–468.

Stroeve, J. C., Markus, T., Boisvert, L., Miller, J., & Barrett, A. (2014). Changes in Arctic melt season and implifications for sea ice loss. *Geophysical Research Letters*, *41*, 1216–1225.

Thomson, J., Fan, Y., Stammerjohn, S., Stopa, J., Rogers, W. E., Girard-Ardhuin, F., … Bidlot, J. R. (2016). Emerging trends in the sea state of the Beaufort and Chukchi seas. *Ocean Modelling*, *105*, 1–12.

Thomson, J., & Rogers, W. E. (2014). Swell and sea in the emerging Arctic Ocean. *Geophysical Research Letters*, *41*(9), 3136–3140.

tom Dieck, I. (1993). Temperature tolerance and survival in darkness of kelp gametophytes (Laminariales, Phaeophyta) - Ecological and biogeographical implications. *Marine Ecology Progress Series*, *100*(3), 253–264.

Torres, A.C., Veiga, P., Rubal, M., Sousa-Pinto, I. (2015). The role of annual macroalgal morphology in driving its epifaunal assemblages. *Journal of Experimental Marine Biology and Ecology* 464: 96-106.

Traiger, S. B., & Konar, B. (2017). Supply and survival: Glacial melt imposes limitations at the kelp microscopic life stage. *Botanica Marina*, *60*(6), 603–617.

Vadas, R. L., & Steneck, R. S. (1988). Zonation of Deep Water Benthic Algae in the Gulf of Maine. *Journal of Phycology*, *24*(3), 338–346.

Valero, M., Engel, C., Billot, C., Kloareg, B., & Destombe, C. (2001). Concepts and issues of population genetics in seaweeds. *Cahiers de Biologie Marine*, *42*(1–2), 53–62.

Van Duin, E. H. S., Blom, G., Los, F. J., Maffione, R., Zimmerman, R., Cerco, C. F., … Best, E. P. H. (2001). Modeling underwater light climate in relation to sedimentation, resuspension, water quality and autotrophic growth. *Hydrobiologia*, *444*, 25–42.

Van Oosterhout, C., Hutchinson, W. F., Wills, D. P. M., & Shipley, P. (2004). MICRO-CHECKER: Software for identifying and correcting genotyping errors in microsatellite data. *Molecular Ecology Notes*, *4*(3), 535–538.

Van Oppen, M.J., Draisma, S.G., Olsen, J.L., Stam, W.T. (1995). Multiple trans-Arctic passages in the red alga *Phycodrys rubens*: evidence from nuclear rDNA ITS sequences. *Marine Biology* 123(1): 179-188.

Vermeij, G., & Roopnarine, P. (2008). The coming Arctic invasion. *Science*.

Walker, T. R., Grant, J., Cranford, P., Lintern, D. G., Hill, P., Jarvis, P., … Nozais, C. (2008). Suspended sediment and erosion dynamics in Kugmallit Bay and Beaufort Sea during ice-free conditions. *Journal of Marine Systems*, *74*(3–4), 794–809.

Wassmann, P. (2011). Arctic marine ecosystems in an era of rapid climate change. *Progress in Oceanography*, *90*(1–4), 1–17.

Wassmann, P., Duarte, C. M., Agustí, S., & Sejr, M. K. (2011). Footprints of climate change in the Arctic marine ecosystem. *Global Change Biology*, *17*(2), 1235–1249.

Wassmann, P., & Reigstad, M. (2011). Future Arctic Ocean Seasonal Ice Zones and

Implications for Pelagic-Benthic Coupling. *Oceanography*, *24*(3), 220–231.

Wegner, C., Hölemann, J. A., Dmitrenko, I., Kirillov, S., Tuschling, K., Abramova, E., & Kassens, H. (2003). Suspended particulate matter on the Laptev Sea shelf (Siberian Arctic) during ice-free conditions. *Estuarine, Coastal and Shelf Science*, *57*(1–2), 55–64.

Weingartner, T. J., Danielson, S. L., Potter, R. A., Trefry, J. H., Mahoney, A., Savoie, M., … Sousa, L. (2017). Circulation and water properties in the landfast ice zone of the Alaskan Beaufort Sea. *Continental Shelf Research*, *148*(March), 185–198.

Wiencke, C., Clayton, M. N., Gómez, I., Iken, K., Lüder, U. H., Amsler, C. D., … Dunton, K. (2006). Life strategy, ecophysiology and ecology of seaweeds in polar waters. *Reviews in Environmental Science and Bio/Technology*, *6*(1–3), 95–126.

Wilce, R. T., & Dunton, K. H. (2014). The Boulder Patch (North Alaska, Beaufort Sea) and its benthic algal flora. *Arctic*, *67*(1), 43–56.

Wood, K. R., Bond, N. A., Danielson, S. L., Overland, J. E., Salo, S. A., Stabeno, P. J., & Whitefield, J. (2015). A decade of environmental change in the Pacific Arctic region. *Progress in Oceanography*, *136*, 12–31.

Wood, K. R., Overland, J. E., Salo, S. a., Bond, N. a., Williams, W. J., & Dong, X. (2013). Is there a "new normal" climate in the Beaufort Sea? *Polar Research*, *32*, 1–9.

Yamamoto-Kawai, M., McLaughlin, F. A., Carmack, E. C., Nishino, S., & Shimada, K. (2009). Aragonite Undersaturation in the Arctic. *Science*, *326*(November), 1098–1100.

Zacher, K., Rautenberger, R., Hanelt, D., Wulff, A., Wiencke, C. (2009) The abiotic environment of polar marine benthic algae. *Botanica Marina* 52: 483–490.

Zacher, K., Bernard, M., Bartsch, I., & Wiencke, C. (2016). Survival of early life history stages of Arctic kelps (Kongsfjorden, Svalbard) under multifactorial global change scenarios. *Polar Biology*, *39*(11), 2009–2020.

Zuccarello, G., & Lokhorst, G. (2005). Molecular phylogeny of the genus Tribonema (Xanthophyceae) using rbc L gene sequence data: monophyly of morphologically simple algal species. *Phycologia*, *44*(July), 384–392.